CRANFIELD INSTITUTE OF TECHNOLOGY
DEPERTMENT OF ELECTRONIC SYSTEM DESIGN

PhD Thesis

Academic year 1989-1990

ALI ABBAS ALI

THEORY AND ASSESSMENT OF AN IMPROVED POWER SPECTRAL DENSITY ESTIMATOR

Supervisor : *Prof. H.W.Loeb*

June 1990

This Thesis is submitted in partial submission for the degree ofDoctor of Philosophy

To my wife Eman
my two doughters Hind and Ragad
and my boy Ahmed
with love.

ABSTRACT

This thesis is concerned with the processing of time domain signals received by a single sensor. An example of such signals is the radar return, which is used in one way or another to estimate the power spectral density - a frequency representation of the power of the signal - in order that we can pick up and track the moving targets. Since the *POWER SPECTRAL DENSITY ESTIMATION* is a fundamental tool in digital signal processing, the theory of the different approaches to *PSDE* is given in the Literature review chapter.

The aim of this research is to develop a technique for the Power Spectral Density Estimation *(PSDE)* of multiple signals in white noise, which has high resolution capability and less frequency estimation errors. Hence, the various techniques mentioned above are tested for their detection, resolution capabilities and performance.

Finally the different parameters affecting the resolution and detection capabilities of the Eigen Vector Decomposition Techniques *(EVDT)* for *PSDE* are studied in some depth.

ACKNOWLEDGEMENT

All the praises and thanks be to *GOD*, the most beneficient, the most merciful.

I would like to extend my sincere gratitude to my supervisor *Prof. H.W.LOEB* for his constant advice and encouragement during this research.

My thanks also to the Government and People of the Republic of Iraq for the financial support during my stay in England.

Many thanks also to the staff of the Department of Electronic System Design and in particular to *Dr. D.Russell* for reading the draft of this thesis, *Mr. K.Bowdler* for his help with the mathematics and *Mrs. M.B.Shield, Mrs. J.S.Hornsby* and *Mr. G.M.Young* for their help in getting the laser copy of this thesis.

Finally I would like to thank my beloved *wife Eman* and my lovely *childrens Hind, Ragad and Ahmed* for whom I own my life.

LIST OF SYMBOLS

a_k	*AR model parameters.*
b_k	*MA model parameters.*
$a_{pk} \ldots a_{pp}$	*Prediction parameters.*
σ_p^2	*Prediction error power.*
e_{pn}	*Forward prediction parameters.*
b_{pn}	*Backward prediction parameters.*
B_{EV}	*Covariance Matrix with unity eigen values.*
B_{WEV}	*NCM with unity eigen values.*
B_{SEV}	*SCM with unity eigen values.*
C,F	*Frequency search vector.*
$E[.]$	*Expectation operator.*
E_p	*Prediction error energy.*
f	*Linear frequency.*
I	*Identity matrix.*
L_n	*Symmetric data window.*
N	*Number of data samples.*
T	*Observation length;* $T=N\Delta t$.
$P(f)$	*PSD.*
$R_{xx}(m)$	*Autocorrelation function.*
R_{xx}	*Covariance matrix.*
$R_{xx}(l,k)$	*Element of the covariance matrix.*
$x(t)$	*Deterministic analoge signal.*
x_n	*Discrete (sampled) signal.*
$X(f)$	*Fourier Transform of* $x(t)$.
$X_m(f)$	*Discrete Fourier Transform.*
w_n	*White Gaussian noise.*
$\delta(t)$	*Dirac Delta function.*
Δt	*Sampling Interval.*
Δf	*Frequency separation.*
ω	*Radian frequency.*

LIST OF ABREVIATIONS

AIC	*Akaike Criterion.*
AN	*Additive Noise.*
ANDGS	*Additive Noise DGS.*
AR	*Auto Regressive.*
ARMA	*Auto Regressive Moving Average.*
ASP	*Array Signal Processing.*
BT	*Blackman-Tukey.*
CM	*Covariance Matrix.*
CN	*Convolutive Noise.*
DFT	*Discrete FT.*
DGS	*Data Generating System.*
DOA	*Direction Of Arrival.*
DSP	*Digital Signal Processing.*
EV	*Eigen Values.*
EVDM	*Eigen Vector Decomposition Method.*
EVDT	*Eigen Vector Decomposition Technique.*
EVM	*Eigen Vector Method.*
FIR	*Finite Impulse response.*
FT	*Fourier Transform.*
FFT	*Fast FT.*
FRL	*Fourier Resolution Limit.*
GFC	*General Form Criterion.*
GLDE	*General LDE.*
GTF	*General Transfer Function.*
ICM	*Inverse Covariance Matrix.*
IIR	*Infinite Impulse Response.*
LDE	*Linear Difference Equation.*
MA	*Moving Average.*
MDL	*Schwartz and Ressanen Criterion.*
MEM	*Maximum Entropy Method.*
ML	*Maximum Likelihood.*

MLM	*Maximum Likelihood Method.*
MLSE	*Maximum Likelihood Spectral Estimation.*
MPCM	*Modified PCM.*
MUSIC	*Multiple Signal Classification.*
NCM	*Noise CM.*
NDDGS	*Noise Driven DGS.*
NEV	*Noise EV.*
NFAP	*Number of Free Adjustable Parameters.*
NICM	*Inverse NCM.*
NSS	*Noise Subspace.*
PC	*Principal Components.*
PCM	*Principal Components Method.*
PER	*Periodogram.*
PHD	*Pisarenko Harmonic Decomposition.*
PICM	*Power Inverse Constraint Method.*
PMFT	*Parametric Model Fitting Technique.*
PSD	*Power Spectral Density.*
PSDE	*PSD Estimation.*
SEV	*Signal EV.*
SCM	*Signal CM.*
SICM	*Inverse SCM.*
SLF	*Source Location Finding.*
SLS	*Spontaneous Line Splitting.*
SOT	*Sub-Optimum Technique.*
SSP	*Signal Subspace.*
TCM	*Total CM.*
TEV	*Total EV.*
TICM	*Inverse TCM.*

NOTE: The following words and abreviations which appeared in the text and many figures are supposed to stand for :

1) Exact Covariance Matrix for True Covariance Matrix.

2) Simulated Covar. Matrix for Estimated Covar. Matrix.

3) EVDM for EVM.

4) TCM for CM.

CONTENTS

Chapter One

INTRODUCTION

CHAPTER ONE

INTRODUCTION

We are currently facing an industrial revolution of high technology in which digital signal processing plays a fundamental role. The final objective of this field - where ideas and methodologies from system theory, statistics, numerical analysis, computer science and very large scale integrated circuits (VLSI) technology have been combined -, is to process a finite set of data *(time or space domain)* and to extract important information which is hidden in it.

Among the most fundamental and useful tools in digital signal processing *(DSP)* has been the estimation of the Power Spectral Density *(PSD)* of a discrete time deterministic and stochastic process. The advances achieved so far in communication, radar, sonar, speech, biomedical and image processing systems are related to the expansion of new power spectrum estimation techniques.

One of the earliest and most popular techniques for power spectral density estimation is the *Fourier Transform,* which became very efficient and more popular after the invention of the Fast Fourier Transform *(FFT)* in the midsixties. But the lack of resolution - which depends mainly upon the data length - and the sidelobe-leakage, are the main limitations to the use of this technique.

Over the last two decades, or so, there has been considerable interest in so-called modern techniques for PSDE -see *Kay* and *Marple [33]*, *Ulrych* and *Clayton [54]*,

Cadzow [7] and *Haykin [23]*-, their works and others form good references for consultation. The new techniques offer high resolution and less frequency bias.

Recent work shows a great interest in a group of techniques which depend upon the Eigen vector Eigen value Decomposition of the data covariance matrix and the so-called signal subspace and noise subspace .This group of techniques, pioneered by *Pisarenko [45]*, offers the best resolution achieved to-date.

So, the available power spectral density estimation techniques may be considered in a number of separate classes namely, *Conventional Techniques (or 'Fourier type')*, *Modelling Techniques* (Auto Regressive Moving Average *(ARMA)*, Auto Regressive *(AR)* and Moving Average *(MA)* modelling), *Nonparametric Techniques* (such as Maximum Likelihood Method *(MLM)*, Pisarenko Harmonic Decomposition *(PHD)*, and *Eigen Vector Decomposition Techniques (EVDT)*). Research in this area has extended to *Multidimensional, Multichannel,* and *Array Signal Processing* problems.

Each one of the above mentioned approaches to power spectral density estimation has certain advantages and limitations, not only in terms of estimation performance, but also in terms of estimation complexity, cost of implementation, finite data length effects and resolution capabilities.

1.1 PROBLEM FORMULATION and SOLUTION :

Suppose we have a segment *x(t)*, of a sample function from a zero mean stationary random process and we wish to generate an estimate of the power spectral density.

When it is desired to distinguish between sharply peaked components of the spectrum at some minimal separation , then the choice of a particular estimate is largely dependent on the time of observation *(data length T)*, *-i.e* the total sampling time $N\Delta t$, where N, is the number of samples and Δt is the sampling interval-. Now when N is large and Δf (the frequency separation between the two peaks to be resolved) is larger than the resolution limit $(1/N\Delta t)$, then any of the large number of schemes will achieve the desired resolution with reasonably small estimate variance. In many situations however, the observation interval (and hence the number of samples N) is constrained to be relatively short (*e.g.* when $x(t)$ may only be considered stationary over a short time interval) and one must choose an estimate subject to the requirement

$$i.e \qquad \Delta f \leq (1/N\Delta t) \qquad (1.1.1)$$

which is not satisfied using most of the available approaches, and this will be the requirement upon which we will depend in testing the different algoritms.

The solution to this problem is the use of Eigen Vector Decomposition Techniques *(EVDT)* which were pioneered by *Pisarenko (1973)* and *Ligget (1973)* and improved by *Schmidt (1979)* and *Bienvenu* and *Koop (1980)*. It is a high resolution technique which is based on the underlying orthogonality relation existing between the *'noise subspace'*, spanned by the eigen vectors corresponding to the smallest eigen values of the random process covariance matrix and the *'signal subspace'* spanned by the eigen vectors corresponding to the largest eigen values.

1.2 THESIS LAY OUT :

The thesis is comprised of seven chapters in addition to three appendices and an attachment. It is organized as follows :

Chapter one is the Introduction chapter, and *Chapter two* presents the Literature review -summary of the theory of the different approaches to the power spectral density estimation -.

Chapter three contains the Simulation results of most of the aforementioned approaches and an objective comparison study to show the disability of most of the algorithms to resolve closely separated sinusoids contaminated by white Gaussian noise, when Δf is less than the resolution limit.

The theory of the high resolution techniques -*Maximum Likelihood Method (MLM), Maximum Entropy Method (MEM) and Eigen Vector Decomposition Technique (EVDT)*- are given in *Chapter four*, in which the new proposed algorithm is developed. In addition, the Partitioning problem (*or the problem of separating the signal eigen values from the noise eigen values)* will be dealt with in this chapter, and a new method for this process is suggested.

Chapter five contains the Simulation results of the proposed algorithm together with those of the most widely used algorithms -*Maximum Likelihood Method, Maximum Entropy Method* and *Eigen Vector Method*-, for the purpose of comparison.

The Parameters affecting the resolution capability of the Eigen Vector Decomposition Technique are dealt with in *Chapter six,* while conclusions and suggestions for further work are given in *Chapter seven.*

Appendix One contains the representation of the Covariance Matrix in terms of its Eigen vectors and Eigen valueas, *Appendix Two* contains the derivation of the Optimum Weight for the *MLM* filter and *Appendix Three* contains two data records as an example of the data generated and used to test the different *PSDE* approaches.

The list of the *Fortran 77* Programs and Subroutines, written to simulate and test the different Power Spectral density Approaches is given in *Attachment One*.

Chapter Two

LITERATURE REVIEW

CHAPTER TWO

LITERATURE REVIEW

2.1. INTRODUCTION :

Spectral estimation has progressed through several stages since *FOURIER* established the basis for defining a spectrum of a function. Fourier analysis has played a primary role in much of the earlier as well as more recent efforts in spectral estimation of and frequency retrieval from experimentally collected data.

The Fourier Transform *(FT)* is an excellent method of obtaining an estimate of the spectrum of a time domain signal. So, if we have $x(t)$ as a deterministic analog waveform, then its Fourier transform will be :

$$X(f) = \int_{-\infty}^{\infty} x(t)\exp(-j2\pi ft)dt \qquad (2.1.1)$$

and the power spectrum estimation at frequency f is :

$$\hat{P}(f) = |X^2(f)| \qquad (2.1.2)$$

Now, if the signal $x(t)$ is sampled at constant rate of Δt's intervals to produce a discrete sequence $x_n = x(n\Delta t)$ for $-\infty \leq n \leq \infty$, then the sampled sequence can be obtained by multiplying the original time function $x(t)$ by an infinite set of equispaced Dirac delta function $\delta(t)$. The Discrete Fourier Transform *(DFT)* of this sampled sequence can be written, using distribution theory, *[5]*, as :

$$X(f) = \int_{-\infty}^{\infty} \left[\sum_{n=-\infty}^{\infty} [x(t)\delta(t-n\Delta t)\Delta t] exp(-j2\pi ft)dt \right]$$

$$= \Delta t \sum_{-\infty}^{\infty} x_n exp(-j2\pi fn\Delta t) \qquad (2.1.3)$$

But in the practical spectral estimation problems, it is desired to estimate the *PSD* with this estimate being based on only a finite set of data samples (observations) *N*, and the transform is discretized also for *N* values by taking samples at the frequencies $f=m\Delta f$, for $m=0,1,2,.....,N-1$, where $\Delta f=1/N\Delta t$ *[33]*, then

$$X_m(f) = \Delta t \sum_{n=0}^{N-1} x_n exp(-j2\pi m\Delta fn\Delta t)$$

$$= \Delta t \sum_{n=0}^{N-1} x_n exp(-j2\pi mn/N) \qquad (2.1.4)$$

equation *(2.1.4)* is the familiar discrete fourier transform *(DFT)*.

Now, let us consider a more practical case, where it has applications, such as in Radar, Doppler processing, Adaptive filtering, Speech processing, Spectral estimation, Array processing,.....,etc, it is desired to estimate the statistical characteristics of a wide-sence stationary, stochastic process rather than a deterministic, finite energy waveform. The energy of such process is infinite, so that the quantity of interest is the *Power Spectral Density*

The Autocorrelation function of such process is given by,

$$R_{xx}(m) = E\left[x_{n+m}\, x_n^*\right]$$

where E and $*$ denote the expectation operator and the complex conjugate respectively.

$$\text{Or} \quad \hat{R}_{xx}(m) = \frac{1}{N-m} \sum_{n=0}^{N-m-1} x_{n+m}\, x_n^* \qquad (2.1.5)$$

for $m = 0,1,\ldots\ldots,M$, and $M \leq N-1$. Equation $(2.1.5)$ is called the unbiased estimator.

This autocorrelation function possesses the following properties [44] :

$$(1) \quad |R_{xx}(m)| \leq R_{xx}(0)$$

$$(2) \quad R_{xx}(-m) = R_{xx}^*(m)$$

$$(3) \quad R_{xx}(0) = E\left[x_n^2\right]$$

The first property states that $R_{xx}(m)$ is bounded by its value at the origin, the third property states that this bound is equal to the mean squared value called the power in the process.

The negative lag estimates are determined from the positive ones in accordance with the conjugate symmetric property (2) of the autocorrelation function.

Jenkins-Watts [26] and *Parzen [42]* and *[43]* provided arguments for the use of the autocorrelation lag estimate which tends to have less mean square error than the estimate expressed by equation *(2.1.5)*. This new estimate is called the biased estimate and written as follows :

$$\hat{R}_{xx}(m) = \frac{1}{N} \sum_{n=0}^{N-m-1} x_{n+m}\, x_n^* \qquad (2.1.6)$$

Current methods for *PSDE* can be classified into four categories as follows :

(1) Conventional PSD estimation methods.
(2) Parametric PSD estimation methods.
(3) Non-Parametric PSD estimation methods.
(4) Multidimentional PSD estimation methods.

2.2. CONVENTIONAL PSDE methods :

In *1959*, *Blackman* and *Tukey [4]* presented a generalized procedure for estimating the *PSD - see Fig(2.1) -*. This procedure involves two steps, *(1)* determining the autocorrelation lags estimates $R_{xx}(m)$ using the available data samples and *(2)* taking the Fourier Transform of these estimates as follows :

$$\hat{P}_{BT}(f) = \sum_{n=-M}^{M} L_n \hat{R}_{xx}(m)\, exp(-j2\pi fm\Delta t) \qquad (2.2.1)$$

where $(-1/2\Delta t) \leq f \leq (1/2\Delta t)$, and L_n is a symmetric data window that is chosen to achieve various desirable effects such as side lobe reduction. This window is sometimes selected to be rectangular in which case $L_n=1$.

This power spectral density estimate is in fact the discrete-time version of the *Wiener-Khinchine* expression which relates the autocorrelation function via the *FT* to the *PSD [33]*, which states that :

$$P(f) = \int_{-\infty}^{\infty} R_{xx}(\tau)\, exp(-j2\pi f\tau)d\tau \qquad (2.2.2)$$

In *Blackman-Tukey - Equ.(2.2.1)* above - it is seen that only a finite number of autocorrelation terms *(2M+1)* are involved in the spectral estimate, which is a direct consequence of the fact that only a finite set of autocorrelation lag estimates are obtainable from the observation set if a standard lag estimation method is used.

Alternatively the *PSD* can be calculated directly from the data set $x_0,.....,x_{N-1}$ through the Fourier Transform as follows :

$$\hat{P}_{PER}(f) = \frac{1}{N\Delta t} \left| \Delta t \sum_{n=0}^{N-1} x_n\, exp\,(-j2\pi fn\Delta t) \right|^2 \qquad (2.2.3)$$

for $(-1/2\Delta t) \leq f \leq (1/2\Delta t)$

Equation *(2.2.3)* is called the Periodogram expression *(or estimate)* for the power spectral density estimation, *-see Fig(2.1) -*, which is computationally inefficient - the same can be said for *BT* estimate -. But the advent of the Fast Fourier Transform *(FFT)* in the mid sixties popularised these two methods. It permits the evaluation of equ. *(2.2.3)* at the discrete set of *N* equally spaced frequencies $f_m = m\Delta f$ *Hz*, for $m = 0,1,.....,N-1$ and $\Delta f = 1/N\Delta t$.

$$\hat{P}_m(f) = \hat{P}_{PER}(f) = \frac{1}{N\Delta t} \left| X_m(f) \right|^2 \qquad (2.2.4)$$

where

$$X_m(f) = \Delta t \sum_{n=0}^{N-1} x_n \, exp(-j2\pi mn/N) \qquad (2.2.5)$$

The *Periodogram* by itself is not a good power spectral density estimation since its variance does not satisfy statistical criteria, and it can be viewed as a special case of *BT* estimate since it will yield identical numerical results to that of *BT* estimate when the biased autocorrelation estimate is used and as many lags as data samples *(M=N-1)* are computed.

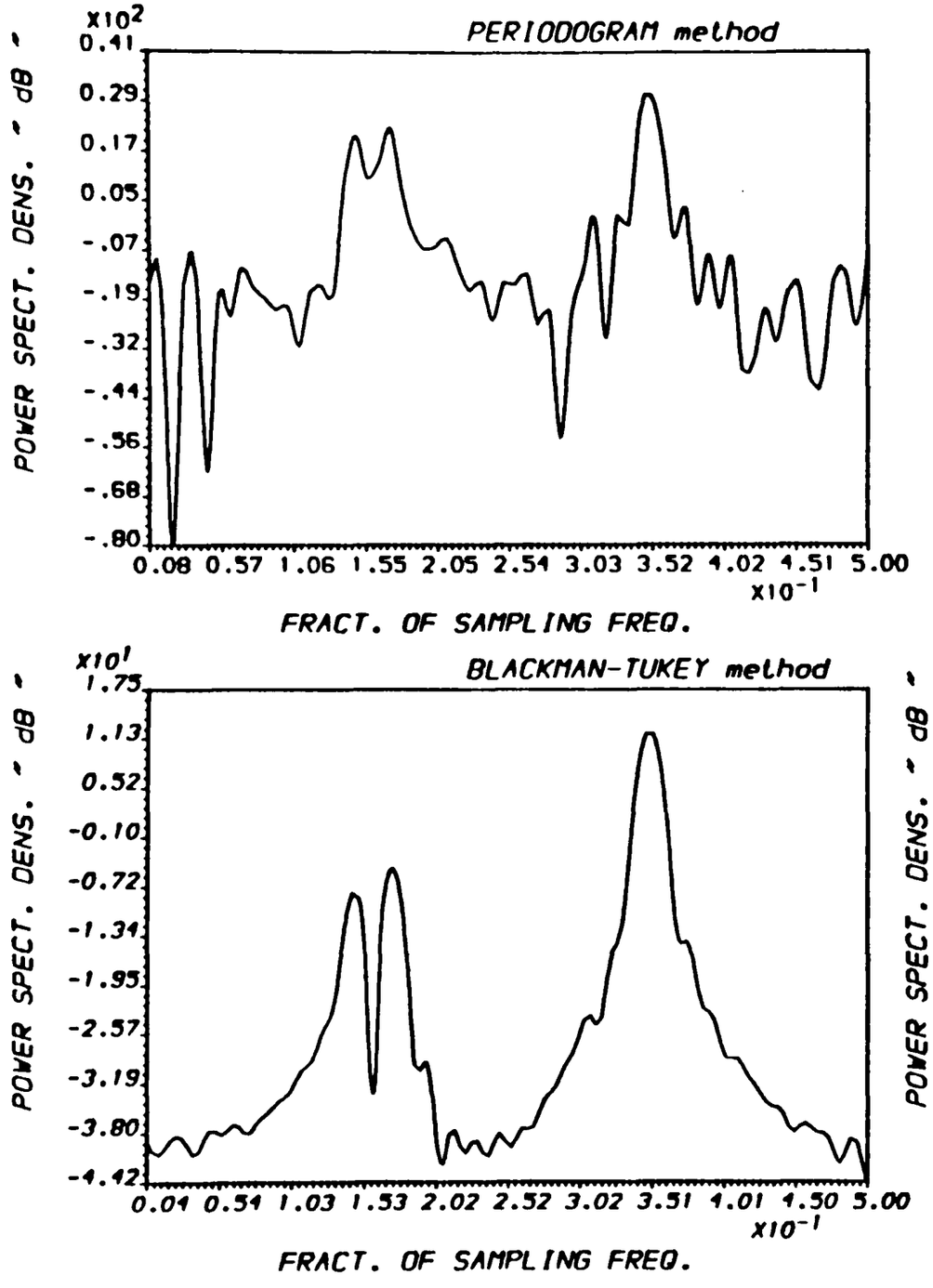

RP : Noisy sinusoid

NMAX : 64

SAMP.FR. : 1.000

AMPLITUDS : 1.00 1.00 2.00

FREQS. : 0.1500 0.1700 0.3500

Init.Phase : 0.00 0.00 0.00

SNRs (dB): 10.000 10.000 16.021

STAND.DEV. : 0.3162277660168379

RESOL. LINIT :0.0156

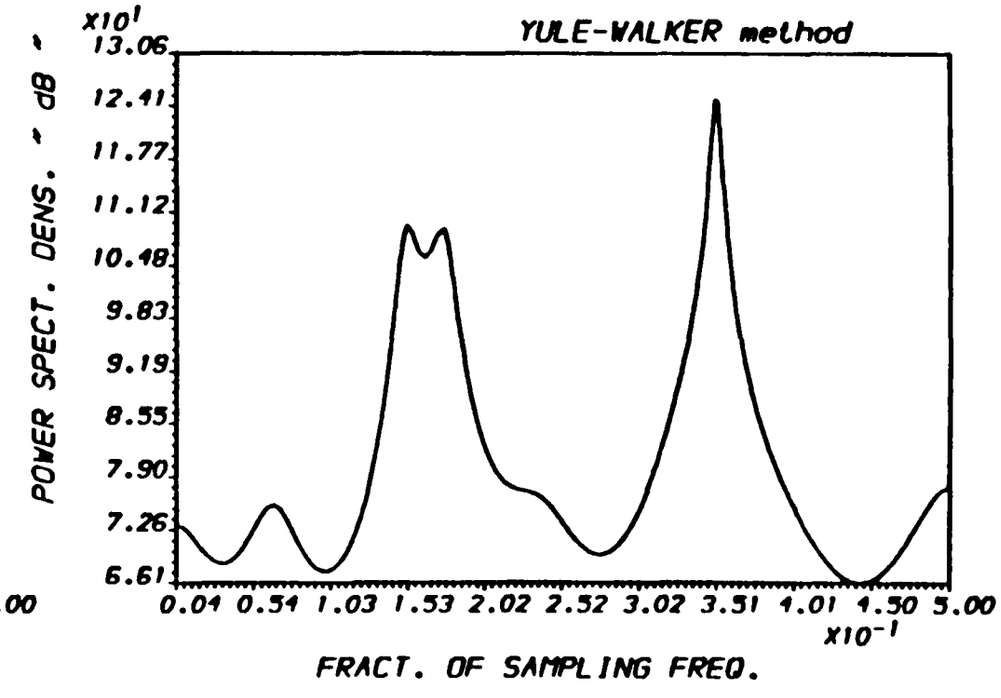

OUTPUT A.ALI -"PLOT2MT- Ex.(4/ 64) RUN :23-FEB-90 12:46:24

FIG.(2.1) POWER SPECTRAL DENSITY ESTIMATES
* For different PSDE methods *

These approaches to *PSD* estimation normally suffer from some inherent limitations. Such limitations are, first the distortion caused by the side lobe effect -*side lobes from strong frequency components can mask the main lobe of weak frequency components*-, which is in turn caused by the tacit windowing of the data, (the assumptions made about the data outside the measurement interval to be equal to zero). The second limitation is that of frequency resolution, *i.e* its ability to distinguish between two closely separated signals. The resolution is always limited to the main lobe width of the window transform *[22]*, which is proportional to the observation length *($T=N\Delta t$)*.

Zero padding the data sequence before transforming will not improve the resolution of the periodogram, but it will smooth the appearance of its estimate by interpolating additional *PSD* values between those that could be obtained with a non-zero padding, see Fig.*(2.2)*.

2.3. PARAMETRIC PSDE methods :

In this type of power spectral density estimation, the observed data are considered to be the output of a model whose parameters are sought as equivalent to the spectrum, *i.e* we try to fit a model to the data in hand, then solving for the model parameters. Hence this type of spectral estimation becomes a three steps approach :-

a) Select the time series model.

b) Estimate the model parameters using the available data samples or autocorrelation lags (*known or estimated*).

c) Then as a last step, obtain the spectral estimate by substituting the estimated model parameters into the model theoretical *PSD* implied by the model.

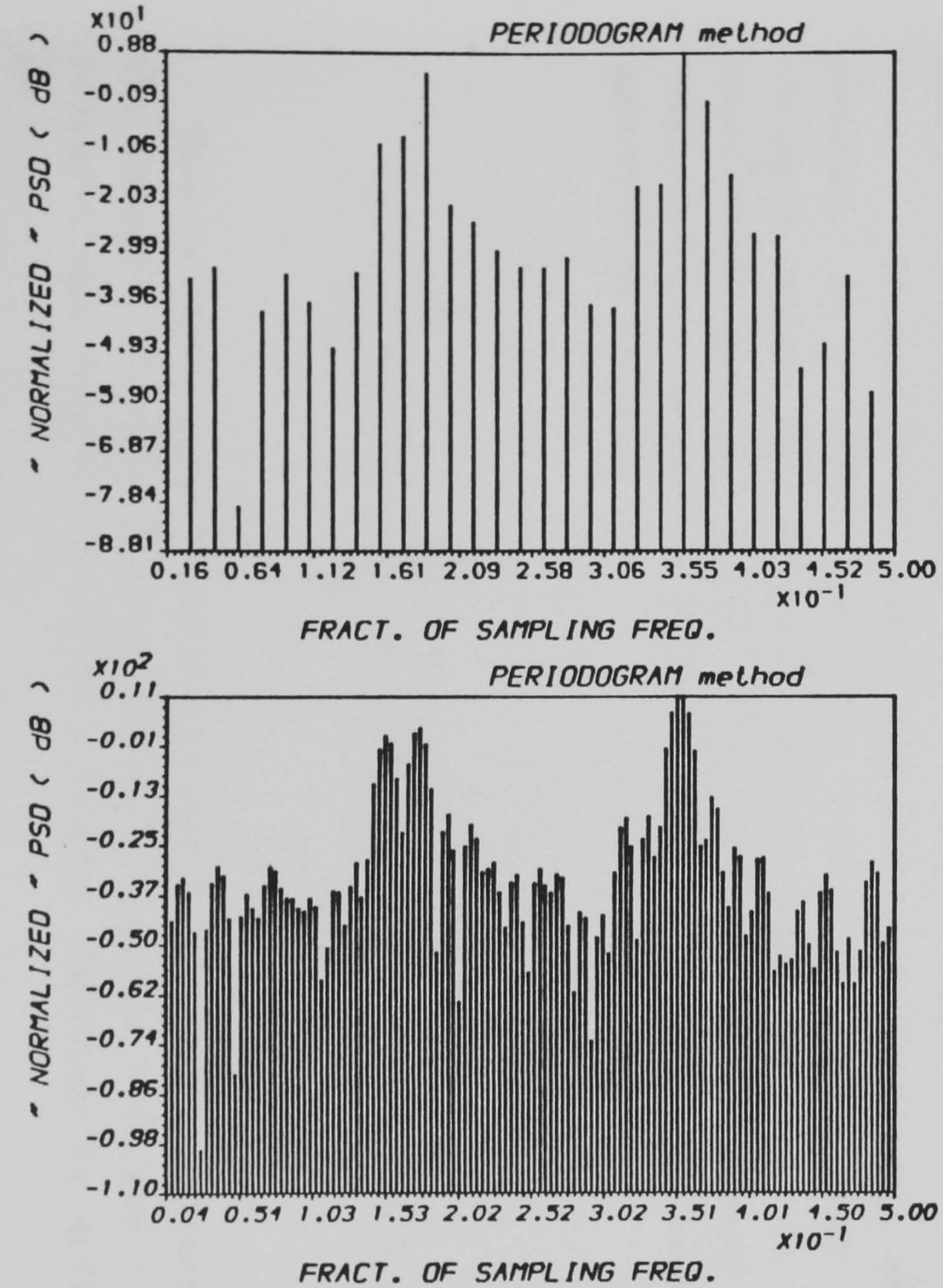

RP : Noisy sinusoid

NMAX : 64

SAMP.FR. : 1.000

AMPLITUDS : 1.00 1.00 2.00

FREQS. : 0.1500 0.1700 0.3500

Init.Phase : 0.00 0.00 0.00

SNRs (dB): 10.000 10.000 16.021

STAND.DEV. : 0.3162277660168379

RESOL. LIMIT :0.0156

OUTPUT A.AL1 -"PLOT2M"- Ex.(1/ 64) RUN :19-APR-90 13:44:50

FIG.(2.2) POWER SPECTRAL DENSITY ESTIMATES
* For different PSDE methods *

Now, in the following, each type of the Parametric Model Fitting Technique *(PMFT)* will be discussed together with its advantages and disadvantages starting with the General Transfer Function *(GTF)*.

2.3.1. MODELLING TECHNIQUES :

A common approach to characterising the spectrum of a stationary random process is to model the process as the output of a rational linear system excited by white Gaussian noise. The model may be purely descriptive, or it may be structurally identified with an actual system whose unknown parameters are to be estimated; in either case, the model is fully defined by the locations of the system's poles and zeros in the complex plane.

2.3.1.1. AUTO REGRESSIVE MOVING AVERAGE model :

In this model, the input driving sequence w_n, as we proceed, is a white Gaussian noise, of zero mean and variance equal σ_w^2, and the output sequence x_n, is the observation sequence which needs to be modelled. These two sequences are related to each other by the linear difference equation as follows :

$$x_n = \sum_{i=0}^{q} b_i w_{n-i} - \sum_{j=1}^{p} a_j x_{n-j} \qquad (2.3.1)$$

This General Linear Difference Equation *(GLDE)* represents the general rational filter -*Infinite Impulse Responce (IIR) filter-*, see *Fig.(2.3)*, whose transfer function is written as :

$$H(z) = \frac{B(z)}{A(z)} \qquad (2.3.2)$$

where

$$B\ (z) = \sum_{i=0}^{q} b_i\ z^{-i} \qquad (2.3.3)$$

which represents the transfeer function of the Finite Impulse Response *(FIR)* filter, and

$$A\ (z) = \sum_{i=0}^{p} a_i\ z^{-i} \qquad (2.3.4)$$

is the transfeer function of the recursive filter (some times called all pole filter).

Now, relating the output power of the filter, through the *TF, Equ.(2.3.2)*, to the power of the input driving process $P_w(z)$ as follows :

$$P_x(z) = H(z)\ H^*(1/z^*)\ P_w(z)$$

$$= \frac{B\ (z)\ B^*(1/z^*)}{A\ (z)\ A^*(1/z^*)}\ P_w(z) \qquad (2.3.5)$$

The power of the input driving process *(white Gaussian noise)* is $P_W(z) = \sigma_W^2 \Delta t$, hence the *PSD* formula *-Equ.(2.3.5)-* implied by the Auto Regressive Moving Average *(ARMA)* model will be as follows :

$$P_{ARMA}(z) = P_X(z) = \sigma_W^2 \, \Delta t \left| \frac{B(z)}{A(z)} \right|^2 \qquad (2.3.6)$$

Evaluating *Equ.(2.3.6)* along the unit circle $z=exp(j\omega\Delta t)$ where $\omega = 2\pi f$, and $(-1/2\Delta t) \leq f \leq (1/2\pi\Delta t)$, equation *(2.3.6)* will be :

$$P_{ARMA}(e^{j\omega}) = \sigma_W^2 \Delta t \left| \frac{b_0 + b_1 e^{-j\omega\Delta t} + \ldots\ldots + b_q e^{-jq\omega\Delta t}}{1 + a_1 e^{-j\omega\Delta t} + \ldots\ldots + a_p e^{-jp\omega\Delta t}} \right|^2$$

$$= \sigma_W^2 \Delta t \left| \frac{b_0 + \sum_{k=1}^{q} b_k exp\,(-j2\pi fk\Delta t)}{1 + \sum_{k=1}^{p} a_k exp\,(-j2\pi fk\Delta t)} \right|^2$$

or simply $$P_{ARMA}(f) = \sigma_W^2 \Delta t \left| \frac{B(f)}{A(f)} \right|^2 \qquad (2.3.7)$$

which represents the *PSD* of the *ARMA* model whose a_k and b_k parameters need to be estimated.

2.3.1.2. AUTO REGRESSIVE model :

The Auto Regressive *(AR)* model can be easily deduced from the *ARMA* model simply by assuming that all the b_i terms in equation *(2.3.1)*, except $b_0=1$, are zeros, see *Fig.(2.3)*,then :

$$x_n = -\sum_{k=1}^{p} a_k x_{n-k} + w_n \qquad (2.3.8)$$

Inspecting equation *(2.3.8)*, we can conclude that the present value of the process equals the weighted sum of the past values plus a noise term.

The Auto Regressive *(AR)* spectra can be deduced from tha *ARMA* spectra -equation *(2.3.7)*- as well, so :

$$P_{AR}(f) = \frac{\sigma_w^2 \Delta t}{|\ A\ (f)\ |^2}$$

$$= \frac{\sigma_w^2 \Delta t}{\left|\ 1 + \sum_{k=1}^{p} a_k exp\ (-j2\pi f k \Delta t)\ \right|^2} \qquad (2.3.9)$$

where the *AR* a_k's parameters are needed to be estimated.

2.3.1.3. MOVING AVERAGE *model :*

Now, let us assume that all the a_i terms, except $a_0=1$, are zero, and see what will happen. Equation *(2.3.1)* will become :

$$x_n = \sum_{k=0}^{q} b_k w_{n-k} \qquad (2.3.10)$$

The resultant equation, *equ.(2.3.10)* above, represents the Moving Average *(MA)* model *-see Fig.(2.3)-*. *MA* spectra can be deduced from *equ.(2.3.7)* to be equal :

$$P_{MA}(f) = \sigma_w^2 \Delta t \left| B(f) \right|^2$$

$$= \sigma_w^2 \Delta t \left| 1 + \sum_{k=1}^{q} b_k \exp(-j2\pi f k \Delta t) \right|^2 \qquad (2.3.11)$$

Again, in order to have an estimate to the *MA* spectra, we need to estimate its model parameters, b_k's.

2.3.2. ESTIMATION OF THE MODEL SPECTRA :

In all the three types of modelling approaches to Power Spectral Density Estimation *(PSDE)* mentioned earlier in this chapter, one need only to know the model parameters and the noise variance in order to use either of the three equations for the estimation of the process *PSD.* Hence a lot of estimation methods have been developed so far to estimate the model parameters,and one of the major motivations for the current interest in the modelling approaches is the higher frequency resolution they can achieve over those

which can be obtained using the Conventional Techniques which were discussed previously.

2.3.2.1. AR spectra :

The process is said to be an *AR (p)* process if it is generated (or can be modelled) using equation *(2.3.8)* and its spectra can be estimated using equation *(2.3.9)*.

So, the present task is to determine the *(p+1)* parameters (a_k, σ_w^2) of th *AR* model which can be achieved using the first well known relationship between the *AR* parameters and the autocorrelation function. This relationship is known as the *Yule-Walker normal equations,* which can be derived simply by multiplying *Equ.(2.3.8)* by x^*_{n+k} and taking the expected value as follows :

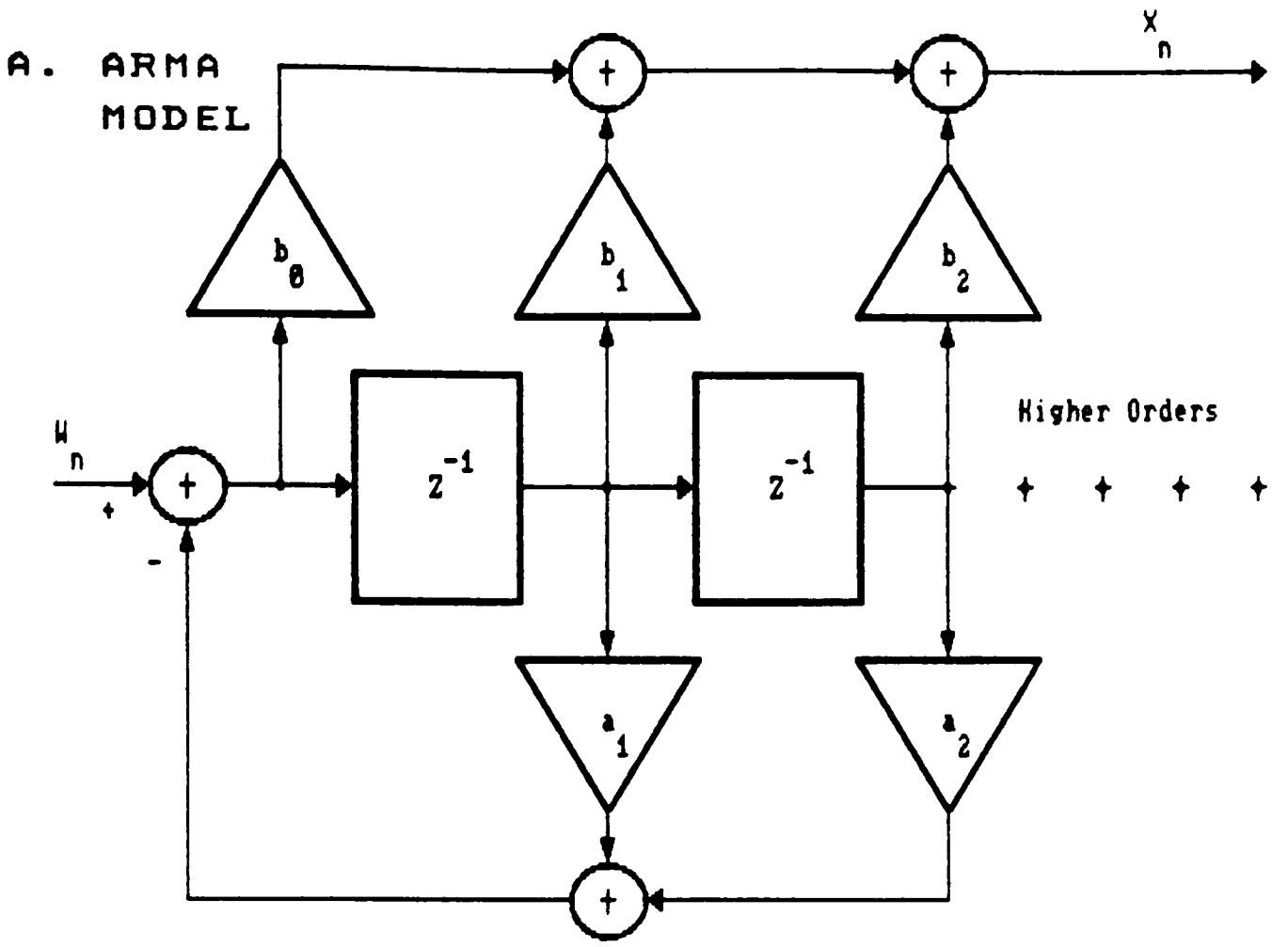

Fig.(2.3) MODEL CONFIGURATIONS

$$E\ (x_{n+k}x_n^*) = E\left[\ x_n^*\ (\ -\sum_{l=1}^{p} a_l x_{n-l+k}\ +\ w_{n+k})\ \right]$$

$$R_{xx}(k) = \begin{cases} -\sum_{l=1}^{p} a_l R_{xx}(k-l) & \text{for } k>0 \\ -\sum_{l=1}^{p} a_l R_{xx}(-l) + \sigma_w^2 & \text{for } k=0 \end{cases} \qquad (2.3.12)$$

Equation *(2.3.12)* can be put in a more compact form *(matrix form)* as follows :

$$\begin{bmatrix} R_{xx}(0) & R_{xx}(-1) & \ldots\ldots & R_{xx}(-p) \\ R_{xx}(1) & R_{xx}(0) & \ldots\ldots & R_{xx}(-p+1) \\ \vdots & \vdots & & \vdots \\ R_{xx}(p) & R_{xx}(p-1) & \ldots\ldots & R_{xx}(0) \end{bmatrix} \begin{bmatrix} 1 \\ a_1 \\ \vdots \\ a_p \end{bmatrix} = \begin{bmatrix} \sigma_w^2 \\ 0 \\ \vdots \\ 0 \end{bmatrix} \qquad (2.3.13)$$

Solving equation *(2.3.13)* with *(p+1)* estimated autocorrelation lags $R_{xx}(0)$, ..., $R_{xx}(p)$, and using the fact $R_{xx}(-m)=R_{xx}^*(m)$ will allow the determination of the *AR* parameters a_k and the noise variance σ_w^2.

One of the most efficient algorithms to solve these equations is known as *Levinson-Durbin* algorithm, which can solve it with P^2 operations *[13]* and *[57]*.

An equivalent representation of equation *(2.3.13)* in terms of the *PSD* as a function of frequency *f* is :

$$P_x(f) = \sum_{-\infty}^{\infty} R_{xx}(n)exp(-j2\pi fn\Delta t) \qquad (2.3.14)$$

where

$$R_{xx}(n) = \begin{cases} R_{xx}(n) & for\ |n| \le p \\ -\sum_{k=1}^{p} a_k R_{xx}(n-k) & for\ |n| > p \end{cases} \qquad (2.3.15)$$

From equation *(2.3.15)* above, it is easy to see that the *AR* modelling preserves the known lags and recursively extends the lags beyond the window of the known lags. Equation *(2.3.14)* is identical to *BT PSDE - Equ.(2.2.1)* - up to lag *p*, but continues with an infinite extrapolation of autocovariance function rather than windowing it to zero. It is for this reason, the *AR* modelling does not suffer from the side lobe leakage effect, and the extrapolation implied by equation *(2.3.15)* is responsible for the *high resolution* property of the *AR* spectral estimation *[33]*. See *Fig(2.1)* for the *PSD* estimate by *Yule-Walker* method.

The most popular approach for *AR* parameters estimation with *N* data samples was introduced by *Burg* in *1967, [6]*. *Burg* argued that the autocorrelation extrapolation should be selected to yield positive definite autocovariance function with maximum entropy. Thus the process with such an autocovariance sequence would be the " *most random* " one possible on knowledge of only the autocovariance lag values from *0* to *p*.

The maximum entropy relationship to *AR PSD* assuming a Gaussian random process is :

$$\int_{-1/2\Delta t}^{1/2\Delta t} ln\ P_x(f)df \qquad (2.3.16)$$

where $P_x(f)$, representing the *PSD* of the time series x_n, can be found by maximizing equation *(2.3.16)* subject to the constraint that the *(p+1)* known lags satisfy the *Wiener-Khinchine* theorem ;

$$\int_{-1/2\Delta t}^{1/2\Delta t} P_x(f)exp(-j2\pi fn\Delta t)df = R_{xx}(n) \qquad (2.3.17)$$

where $n = 0,1,.....,p$, and the solution is found, by the use of *Lagrange* multipliers *[33]*, to be equivalent to the *AR PSD -Equ.(2.3.9)* -as shown below :

$$P_x(f) = \frac{\sigma_p^2\ \Delta t}{\left| 1 + \sum_{k=1}^{p} a_{pk}\ exp(-j2\pi fk\Delta t) \right|^2} \qquad (2.3.18)$$

where $a_{pk},.....,a_{pp}$ and σ_p^2 are the P^{th} order prediction parameters and prediction error power, respectivly.

Now, let us consider a more practical situation where one has data rather than autocovariance lags. By operating directly on the data without estimating the autocovariance lags, it is possible to obtain better *AR* parameters estimate

and hence better *AR* spectral estimates.

Least squares prediction techniques are used in this case, either forward only linear predictions for the parameters estimate, or they employ the combination of the forward and backward linear prediction, as *Burg* algorithm works -*see below*-, so linear predictions and *AR* modelling of a random process are intimately related to each other.

Now, if one wishes to predict x_n on the basis of the previous p samples *[23]*, then :

$$\hat{x}_n = -\sum_{k=1}^{p} a_{pk}\, x_{n-k} \qquad (2.3.19)$$

and the forward prediction error is :

$$e_{pn} = x_n - \hat{x}_n = \sum_{k=0}^{p} a_{pk}\, x_{n-k} \qquad (2.3.20)$$

where $a_{p0}=1$, by definition, and the prediction error energy s simply :

$$E_p = \sum_n \left| e_{pn} \right|^2 = \sum_n \left| \sum_{k=0}^{p} a_{pk}\, x_{n-k} \right|^2 \qquad (2.3.21)$$

Equation *(2.3.21)* can be written in matrix form as follows :

$$E = XA \qquad (2.3.22)$$

The optimum value of the *AR* (prediction) parameters can be obtained simply by equating the derivatives of *Equ.(2.3.21)* to zero, the result will be :

$$\sum_{k=0}^{p} a_{pk} \left(\sum_{n} x_{n-k}\, x^{*}_{n-i} \right) = 0 \quad , \; i=1,2, \ldots, p \qquad (2.3.23)$$

and the minimum error energy is given by :

$$E_p = \sum_{k=0}^{p} a_{pk} \left(\sum_{n} x_{n-k}\, x^{*}_{n} \right) \qquad (2.3.24)$$

Equations *(2.3.23)*, and *(2.3.24)* can be combined in a single matrix equation form as follows :

$$(X_K^H X_K) A = (E_p \; 0 \; 0 \; \ldots\ldots 0)^T \qquad (2.3.25)$$

According to the summation limits for the error power E_p which appeared in equations *(2.3.23)* and *(2.3.24)*, equation *(2.3.25)* will be regarded - solved - as *covariance* equations, *Yule Walker* equations, *prewindowed linear* equations, or *postwindowed linear* equations *[33]*.

Now, if the process is stationary, the coefficients of the backward prediction error filter will be identical to those of the forward one.

Equation *(2.3.20)* represents the forward linear prediction error of a wide sense stationary process. The

backward linear prediction error of such process can be written as :

$$b_{pn} = \sum_{k=0}^{p} a^{*}_{pk}\, x_{n-p+k} \qquad (2.3.26)$$

where $p \le n \le N-1$

Burg, in his attempt to estimate the prediction (or *AR*) parameters, minimizes the sum of the forward and backward prediction error energies.

$$E_p = \sum_{n=p}^{N-1} \left| e_{pn} \right|^2 + \sum_{n=p}^{N-1} \left| b_{pn} \right|^2 \qquad (2.3.27)$$

To ensure a stable *AR* filter *(i.e poles within the unit circle)*, *Burg* constrains the *AR* parameters to satisfy the Levinson recursion, so :

$$a_{pk} = a_{p-1,k} + a_{pp}\, a^{*}_{p-1,p-k} \qquad (2.3.28)$$

Thus using this constraint - *Equ.(2.3.28)* -, one needs only to estimate a_{ii} for $i=1,2,....,p$, which can be obtained simply by setting the derivatives of E_p - *Equ. (2.3.27)* - w.r.t. a_{ii} to zero, then the result will be :

$$a_{ii} = \frac{-2\sum_{k=i}^{N-1} b^{*}_{i-1,k}\, e_{i-1,k}}{\sum_{k=i}^{N-1}\left(\left| b_{i-1,k-1} \right|^{2} + \left| e_{i-1,k} \right|^{2} \right)} \qquad (2.3.29)$$

It is obvious that $a_{ii} \leq 1$ for all i. Equations *(2.3.28)* and *(2.3.29)* together will generate a stable all-pole filter. See *Fig(2.4)* for the *PSDE* using *Burg* algorithm.

One of the difficulties associated with the *AR* modelling is that the order p is not known a priori, so if the computed order was too low, the obtained spectra will be highly smoothed, on the other hand, if the computed order was too high, it will introduce spurious frequencies in the estimate.

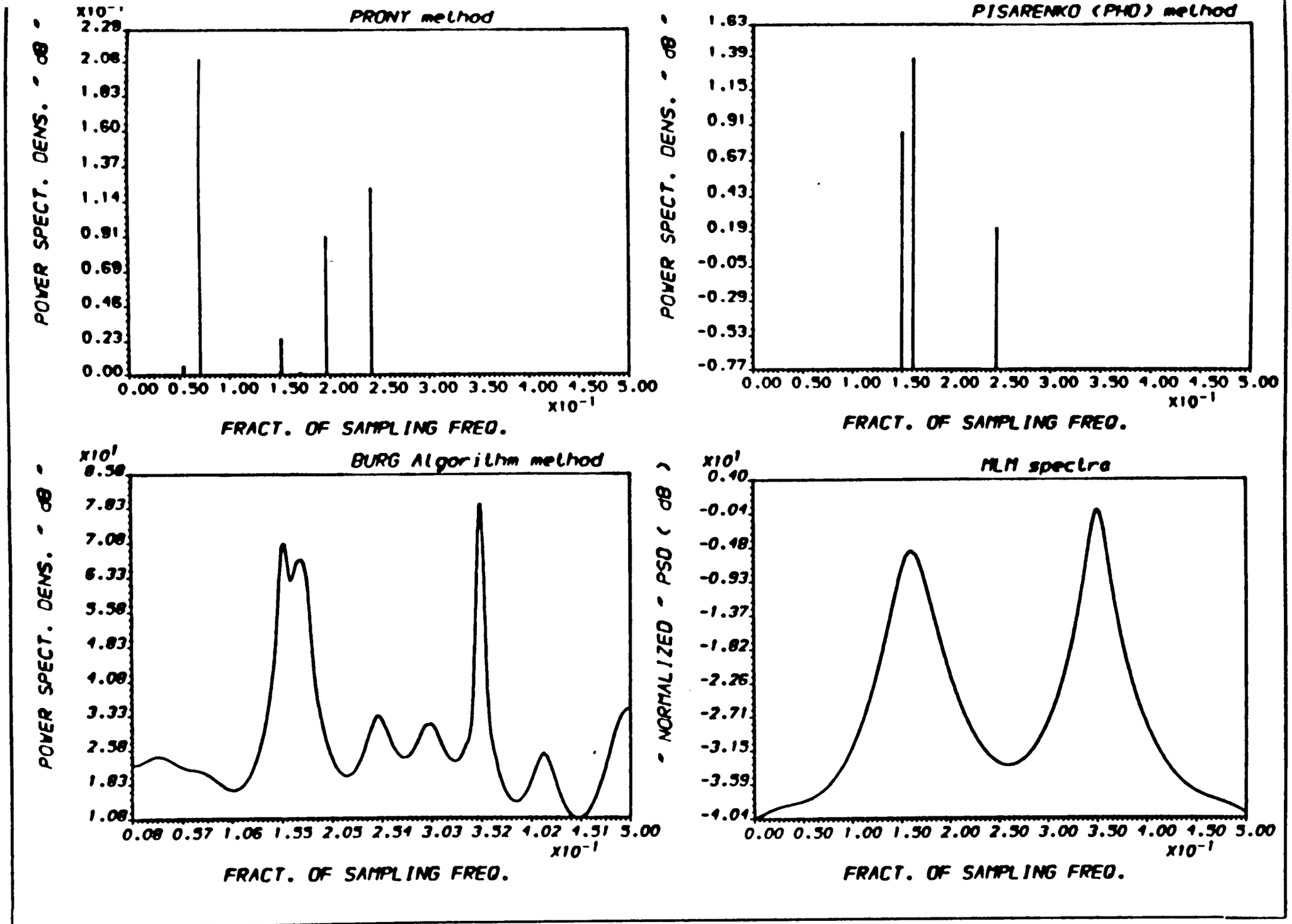

FIG.(2.4) POWER SPECTRAL DENSITY ESTIMATES
* For different PSDE methods *

AR modelling, and *Burg* algorithm in particular, give good spectral estimate with considerably higher frequency resolution when compared with conventional and other modelling estimates. On the other hands, it suffers from many problems, such as frequency biases and Spectral Line Splitting *(SLS) -SLS is the occurrence of two or more spectral peaks where only one peak must exist-*, see *Fig(2.5)*. The latter problem - *i.e (SLS)* - was widely studied by many researchers, for example *Fougere et al [15]*, who studied this phenomenon in detail, noted that the *SLS* was most likely to occur when :

1) *The signal-to-noise ratio is high.*
2) *The initial phase of the sinusoidal components is some odd multiple of* $\pi/4$.
3) *The data duration has an odd number of quarter cycles of the sinusoidal components.*
4) *The number of estimated AR parameters is a large percentage of the number of data samples.*

Fougere [16] said that the cause of the *SLS* in the *Burg* algorithm was due to the fact that the prediction error power is not truly minimized, and he presented a rather complicated minimization which will ensure convergence and get rid of the *SLS* as well.

Many Least-Squares algorithms have been suggested so far to correct the phenomenon of *SLS* in the *AR* estimation methodes, for example, *Ulrych-Clayton [54]* and *Nattal [41]* independently suggested a Least Square algorithm which minimizes the prediction error power E_p which can be effectively performed by equating the derivatives of E_p w.r.t. all the prediction parameters a_{pk} and not just a_{ii} (as in the case of *Burg* algorithm). A fast computational algorithm has been developed *[35]* to solve the normal

equations obtained.

Recently, *M.K.Ibrahim [24]* proposed a solution to the problem of *SLS* in *Burg* algorithm for the case of a single sinusoid. In his modification a new estimate of the first-order reflection coefficients was proposed, which was obtained by minimizing the forward and the backward prediction error energies of the second-order filter w.r.t. a_{21} and a_{22} and then using the *Levinson* recursion. He applied a generalization of this estimate to the weighted Burg algorithm, where an improvement in the speed of the Data-Adaptive Weighted Burg Technique *(DAWBT)* is achieved. He then suggested *[25]* a modification to the Optimum Tapered Burg *(OTB)* algorithm, which was developed by *Kaveh* and *Lippert [31]*, the new improved technique gave spectral estimates which exhibit no spontaneous line splitting *(SLS)* and are independent of the initial phase in the case of single sinusoid.

The effect of white noise on the *AR* spectra is to produce a smoothed spectrum *[32]*. This smoothing or loss of resolution has been shown to be due the fact that the estimated *AR* poles are drawn into the origin of the Z-plane due to the introduction of spectral zeros due to the noise. So the high resolution ability of the *AR* spectral estimation decreases as the *SNR* decreases, *[36]* and *[37]*, and the all poles model assumed is no longer valid in the presence of observation noise, and the solution for this is contained in the Auto Regressive Moving Average *(ARMA)* model, as follows

Assume y_n defines an *AR* process x_n corrupted by observation noise w_n, then

$$y_n = x_n + w_n$$

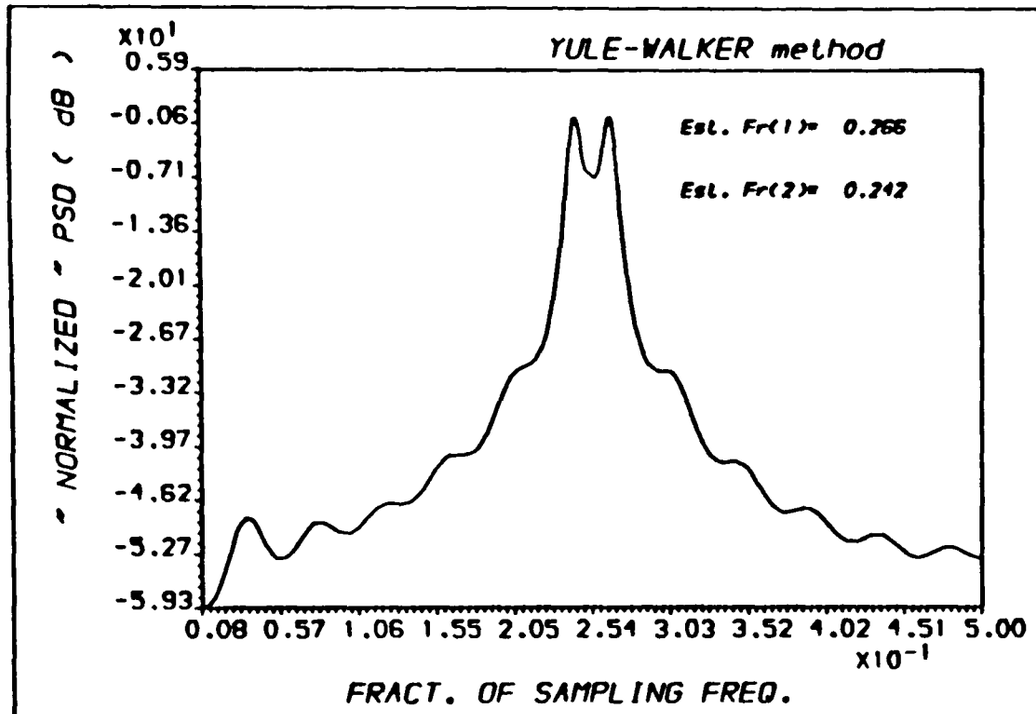

RP : Noisy sinusoid

NMAX : 25

SAMP.FR. : 1.000

AMPLITUDS : 1.00

FREQS. : 0.2500

Init.Phase : 0.87

SNRs (dB): 50.000

STAND.DEV. : 0.003162277660168 4

OUTPUT A.ALI -"PLOT2M"- Ex.(5/ 25) RUN :23-FEB-90 10:51:42

FIG.(2.5) POWER SPECTRAL DENSITY ESTIMATES

SLS in Auto Regressive Modelling

x_n and w_n are assumed to be uncorrelated, and w_n has zero mean and variance equals σ_w^2 .Then the power spectra of the overall process is :

$$P_y(z) = \frac{\sigma_c^2 \, \Delta t}{\left| A(z) \right|} + \sigma_w^2 \, \Delta t$$

where σ_c^2 is the convolutive *(input)* noise variance.

$$\text{or} \qquad P_y(z) = \frac{\left[\sigma_c^2 + \sigma_w^2 \left| A(z) \right|^2 \right] \Delta t}{\left| A(z) \right|^2} \qquad (2.3.30)$$

which indicates that the *PSD* of y_n is no longer characterized by the all pole model. Equation *(2.3.30)* has zeros as well as poles *(ARMA model)* and the estimation of P_y using purely *AR* technique is equivalent to an approximation to the more general *ARMA* technique, *[30].*

One last point is that the *AR* modelling is appropriate to Noise Driven Data Generation Systems *(NDDGS)* and is inappropriate to the Additive Noise Data Generation System *(ANDGS).* However the distinction between these two types is important. There are, for the purpose of distinction, two ways of incorporating noise into Data Generation Systems *(DGS),* these are as follows :

a) As INPUT -Convolutive Noise (CN).
b) As output -Additive (or Measurement) Noise (AN).

See *Fig(2.6)* for theblock diagrams of the two types.

2.3.2.2. ARMA spectra :

The process is said to be an *ARMA(p,q)* process if it is generated according to (or modelled by) the Linear Difference Equation *(LDE)* - *Equ.(2.3.1)* -, and so its power spectral density can be estimated using equation *(2.3.7)*. The poles a_K are assumed to be within the unit circle of the z-plane (to ensure a stable filter), whereas the zeros b_K may lie any where in the z-plane.

Our task in this section is to determine the values of the a_K and b_K parameters of this model in order to be able, then, to estimate the *PSD* of the process. Many techniques have been proposed to estimate the *ARMA* parameters. The problem in using these techniques is that, they involve many matrix computations and iterative optimization operations *[33]*. If a best least squares modelling is desired, it is then found that the generation of the optimal a_K, b_K parameters involves the least mean square solution of the highly non linear *Yule-Walker* equations which is computationally inefficient and normally not practical for real time processing. So, in order to provide a linear solution for the *ARMA* model's *AR* parameters, many researchers proposed the use of the Sub-Optimum Technique *(SOT)* which generally estimate the *AR* and *MA* parameters separately rather than jointly. One such techniques *[8]*, which was proposed by *J.A.Cadzow* in *1979*, is called the *Extended Yule-Walker*, which can be represented in matrix form as follows :

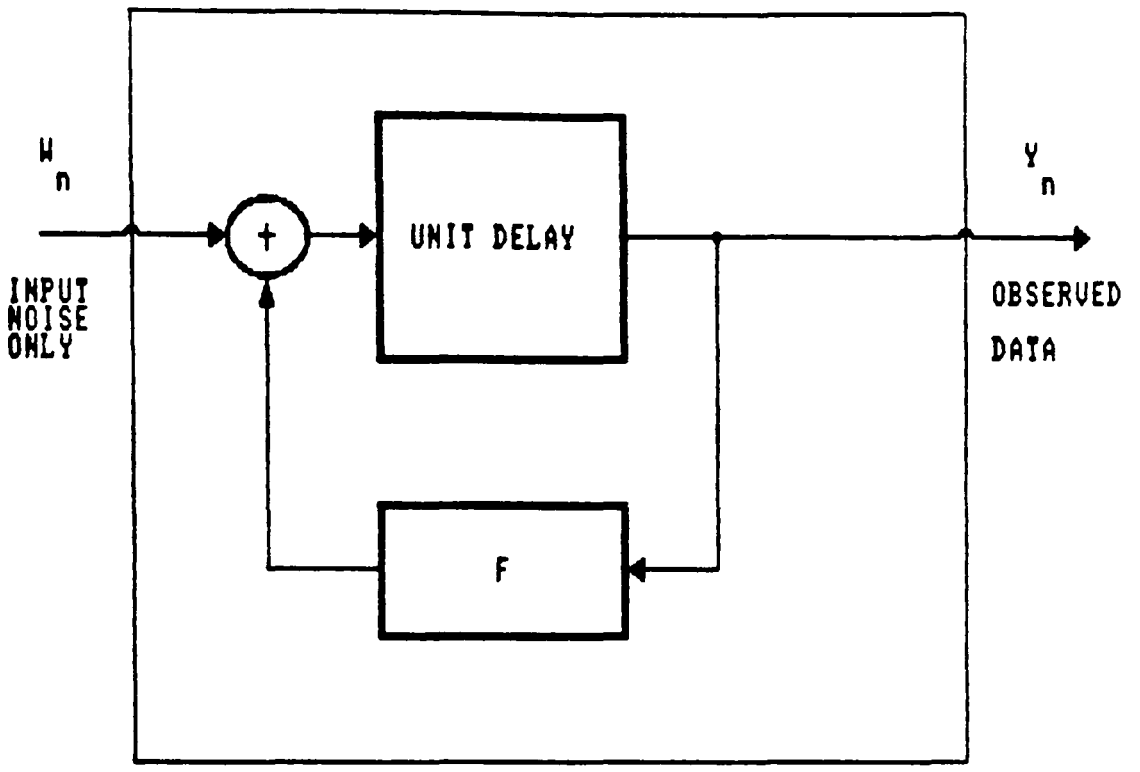

$$Y_{n+1} = FY_n + W_n$$

A. CONVOLUTIVE MODEL; INPUT NOISE ONLY

NOISE FREE SIGNAL (system Impulse Responce) CONVOLVED WITH THE NOISE.

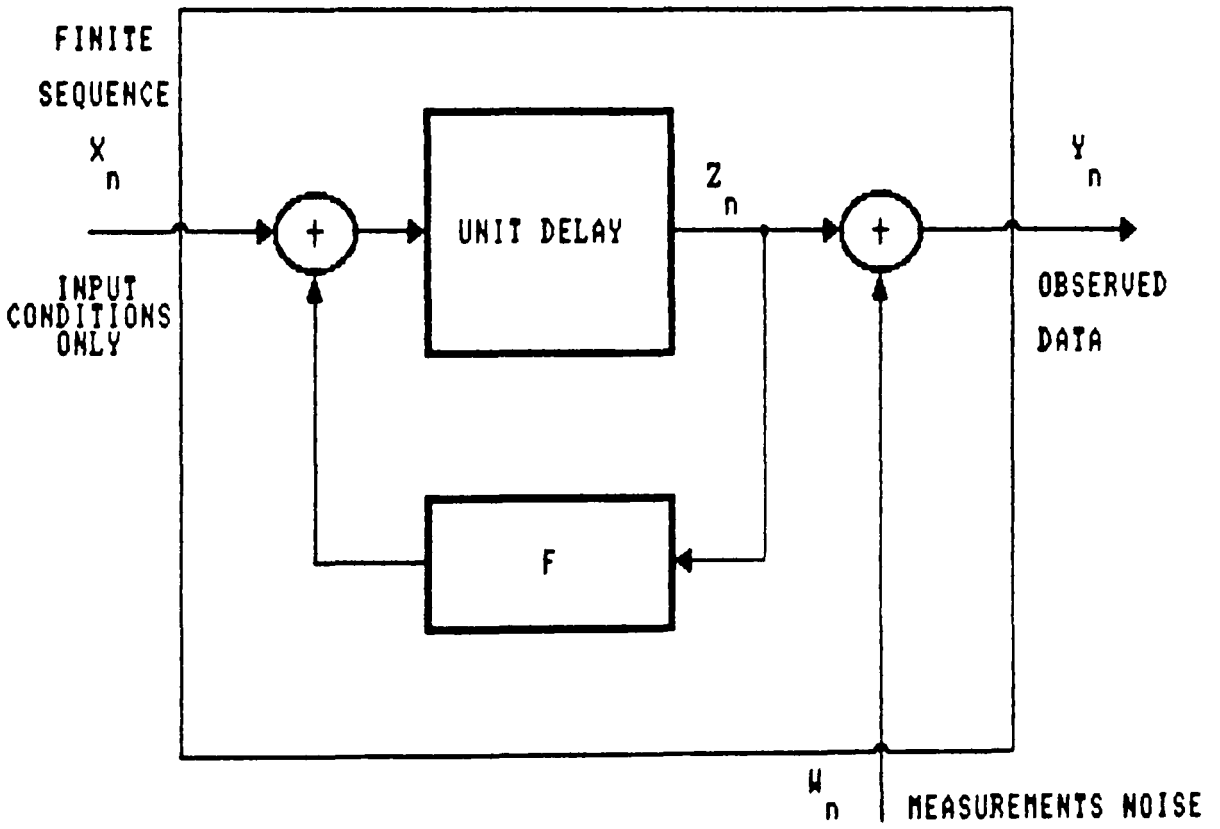

$$Y_n = Z_n + W_n$$

B. ADDITIVE MODEL; MEASUREMENTS NOISE ONLY.

NOISE FREE SIGNAL (Z_n) IS ADDED TO THE NOISE.

Fig.(2.6) THE TWO WAYS OF INCORPORATING NOISE INTO DATA GENERATING SYS.

$$\begin{bmatrix} R_{xx}(q) & R_{xx}(q-1) & \cdots & R_{xx}(q-p+1) \\ R_{xx}(q+1) & R_{xx}(q) & \cdots & R_{xx}(q-p+2) \\ \vdots & \vdots & & \\ R_{xx}(q+p-1) & R_{xx}(q+p-2) & \cdots & R_{xx}(q) \end{bmatrix} \begin{bmatrix} a_1 \\ a_2 \\ \vdots \\ a_p \end{bmatrix}$$

$$= \begin{bmatrix} R_{xx}(q+1) \\ R_{xx}(q+2) \\ \vdots \\ R_{xx}(q+p) \end{bmatrix} \qquad (2.3.31)$$

An algorithm requiring (p^2) operations has been developed by *Zohar [57]* to solve these equations. The *ARMA* model's *AR* parameters can then be found simply by solving the set of linear equations :

$$A(z) = 1 + \sum_{k=1}^{p} a_k \, z^{-k} \qquad (2.3.32)$$

This is equivalent to applying the *ARMA* process -time series x_n- to the P^{th}order non recursive filter with transfer function *A(z)* whose coefficients correspond to the *AR* parameters obtained upon solving equation *(2.3.31)*. This filtering procedure produces the so-called Residual time series as shown in *Fig(2.7)* below :

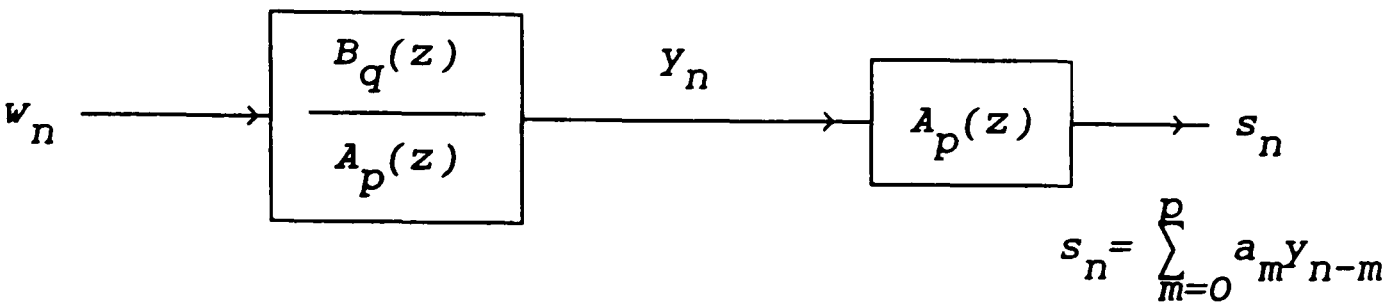

Fig.(2.7) Filtering the *ARMA* process with the all-zero filter $A(z)$.

Another technique, *[21]* was developed by *D.Group, D.J.Krouse* and *J.B.Moor,* which equates the impulse response of the *ARMA* filter, whose parameters are sought, to the *AR* filter impulse response with infinite number of parameters as follows :

$$\frac{B(z)}{A(z)} = \frac{1}{C(z)} \qquad (2.3.33)$$

where $$C(z) = 1 + \sum_{k=1}^{\infty} c_k \, z^{-k}$$

Thus c_k can be estimated using any of the previously mentioned techniques and then relating them to the *ARMA* parameters - *Equ.(2.3.33)* -.

As a third method, a least squares input output identification technique has been proposed to estimate the *ARMA* parameters, which involves the estimation of the unknown cross correlation between the input and the output. This unknown cross correlation will cause the normal equations to be again, nonlinear. In practice the excitation

noise process is estimated from the time series itself by a boot-strap approach, as with the lattice filter configuration *[17]* for example, and hence the cross correlation can be estimated then, which leads to the estimation of the *ARMA* parameters.

2.3.2.3. MA spectra :

As stated in section *(2.3.1.3)* the *MA* process is the one that can be obtained as the output of an all zero filter driven by a white noise process.

$$x_n = \sum_{k=0}^{q} b_k \, w_{n-k} \qquad (2.3.34)$$

where b_k, $k=0,1, \ldots, q$ are the *MA* model parameters (filter coefficients) and w_n is the driving white noise with $E[w_n]=0$, and $E[w_{n+k} \, w_n^*] = \sigma_w^2 \delta_k$.

The auto-correlation function of such a process is defined, *[33]*, by :

$$R_{xx}(k) = \begin{cases} \sigma_w^2 \sum_{i=0}^{q-k} b_i \, b_{i+k}^* , & \text{for } k = 0,1,\ldots,q \\ 0 , & \text{for } k > q \end{cases} \qquad (2.3.35)$$

and the *PSD* estimate can be defined, *[7]* and *[33]*, as :

$$P_{MA}(f) = \sum_{k=-q}^{q} R_{XX}(k)\ exp(-j2\pi fk\Delta t) \qquad (2.3.36)$$

Hence, if only an estimate to the *MA* spectra is required and if *(q+1)* lags of the autocorrelation function are available, then the use of equation *(2.3.36)* can achieve that. But if the *MA* model parameters are required, then we need to solve the nonlinear set of equations *-Equ.(2.3.35)-*, and so, we need to determine the model order.

Chow [10] suggested (when only the data samples are available) the use of the unbiased estimate - *Equ. (2.1.5)* - for the autocorrelation lags. He stated that the *MA* model order is that for which the autocorrelation lags approaches zero rapidly. So having obtained the model order, we can use equation *(2.3.11)* -repeated here- to compute the moving average model spectra.

$$P_{MA}(f) = \sigma_w^2 \Delta t \left| 1 + \sum_{k=1}^{q} b_k\ exp(-j2\pi fk\Delta t) \right|^2 \qquad (2.3.37)$$

2.3.2.4. PRONY'S method :

Though *Prony's* method is not a spectral estimation technique in the usual sense, a spectral interpretation can be provided for it. Originally it is a technique for modelling data of equally spaced samples by a linear combination of exponentials (P exponentials, each has arbitrary amplitude A_k, phase θ_k, frequency f_k and damping factor α_k).

Let $X^T = x_0, x_1, \ldots\ldots, x_{N-1}$ be, as before, the observation -or data samples- vector to which *Prony's* method tries to fit the model is given by :

$$\hat{x}_n = \sum_{k=1}^{p} b_k \, z_k^n \qquad for \quad 0 \leq n \leq N-1 \qquad (2.3.38)$$

where $b_k = A_k exp(j\theta_k)$

and $z_k = exp\ [\ (\alpha_k + j2\pi f_k)\ \Delta t\ ]$ (2.3.39)

Equation *(2.3.38)* represents a set of nonlinear equations in the unknown b_k parameters. In matrix form, it can be written as :

$$\hat{X} = \Phi B \qquad (2.3.40)$$

where $\hat{X} = [\ x_0\ x_1\ x_2\ \ldots\ x_{N-1}\ ]^T$

$$\Phi = \begin{bmatrix} 1 & 1 & \ldots\ldots\ldots & 1 \\ z_1 & z_2 & \ldots\ldots\ldots & z_p \\ \vdots & \vdots & & \vdots \\ z_1^{N-1} & z_2^{N-1} & \ldots\ldots\ldots & z_p^{N-1} \end{bmatrix}$$

and $B = [\ b_1\ b_2\ b_3\ \ldots\ b_p\ ]^T$

In order to find the exponential model parameters (A_k, θ_k, f_k and α_k), we need to minimize the squared error ε, defined as :

$$\varepsilon = \sum_{n=0}^{N-1} \left| x_n - \hat{x}_n \right|^2 \qquad (2.3.41)$$

which is a difficult nonlinear least squares minimization. There are a lot of methods to do this job, such as that suggested by *McDonough* and *Huggins [39]*. But *Prony's* method is simpler and provides satisfactory solution though it doesn't minimize equation *(2.3.41)*. It can be developed as shown below;

Let $\psi(z)$ be a polynomial defined as :

$$\psi(z) = \prod_{k=1}^{p} (z - z_k) = \sum_{i=0}^{p} a_i \, z^{p-i} \qquad (2.3.42)$$

Using equation *(2.3.38)*, the *(n-m)* sample estimates can be written as :

$$\hat{x}_{n-m} = \sum_{l=1}^{p} b_l \, z_l^{n-m} \qquad 0 \le (n-m) \le N-1 \qquad (2.3.43)$$

Multiplying both sides by a_m and summing over the past *(p+1)* products gives :

$$\sum_{m=0}^{p} a_m \, \hat{x}_{n-m} = \sum_{l=1}^{p} b_l \sum_{m=0}^{p} a_m \, z_l^{n-m} \qquad (2.3.44)$$

for $p \le n \le N-1$

Now, by substituting $z_1^{n-m} = z_1^{n-p} z_1^{p-m}$, equation *(2.3.44)* can be written as :

$$\sum_{m=0}^{p} a_m \hat{x}_{n-m} = \sum_{l=1}^{p} b_l z_l^{n-p} \sum_{m=0}^{p} a_m z_l^{p-m} \qquad (2.3.45)$$

$$= \left(\sum_{l=1}^{p} b_l z_l^{n-p} \right) \psi(z)\Big|_{z=z_l} = 0$$

$$\therefore \quad \sum_{m=0}^{p} a_m \hat{x}_{n-m} = 0$$

$$\text{or} \quad \hat{x}_n = - \sum_{m=1}^{p} a_m \hat{x}_{n-m} \qquad \text{for} \quad p \le n \le N-1 \qquad (2.3.46)$$

Define e_n as the estimation error, *i.e*

$$e_n = x_n - \hat{x}_n \qquad (2.3.47)$$

and substitute *Equ.(2.3.46)* in *Equ.(2.3.47)* we get :

$$x_n = - \sum_{m=1}^{p} a_m x_{n-m} + \sum_{m=0}^{p} a_m e_{n-m} \qquad (2.3.48)$$

As in *Pisarenko Harmonic Decomposision (PHD) -see section (2.4.1)-*, equation *(2.3.48)* represents a special *ARMA(p+1,p+1)* model with identical *MA* and *AR* parameters, but

unlike *PHD, the* a_i coefficients are not constrained to produce unit modulus roots.

To establish the extended *Prony* method, one needs to define the last summation term in equation *(2.3.48)* as ϵ, *i.e :*

$$\epsilon = \sum_{m=0}^{p} a_m e_{n-m} \qquad (2.3.49)$$

Substitute *Equ.(2.3.49)* in *Equ.(2.3.48)* and rewrite, we get :

$$x_n = -\sum_{m=1}^{p} a_m x_{n-m} + \epsilon \qquad (2.3.50)$$

Thus *Prony's* method sub-optimally minimizes $\Sigma_{n=p}^{N-1}|\epsilon_n|^2$ instead of the true optimum minimization of $\Sigma_{n=p}^{N-1}|e_n|^2$ which leads to a set of nonlinear equations that are difficult to solve.

Careful inspection of equation *(2.3.50)* leads to the fact that the parameters estimation is now reduced to an *AR* linear prediction parameters estimation which has been dealt with previously in this section .

Thus *Prony's* extended method can be summarized by the following *four steps :*

1) Determine the a_i *parameters by least squares estimate of equation (2.3.50).*

2) *Determine the* z_i *roots by rooting the polynomial equation (2.3.42).*

3) *Determine the* b_m *parameters by a least square minimization of* $\Sigma|x-\hat{x}|^2$. *A well known solution for this minimization is given by :*

4) *Compute the parameters of the exponential model as follows :*

a. *Amplitude* $A_i = | b_i |$

b. *Phase* $\theta_i = \tan^{-1}[Im(b_i)/Re(b_i)]$

c. *Frequency* $f_i = \tan^{-1}[Im(z_i)/Re(z_i)]/2\pi\Delta t$

d. *Damping Factor* $\alpha_i = \ln| z_i|^2/\Delta t$

and e. *The PSD* $\hat{P}(f) = | \hat{X}(f) |^2$

where

$$\hat{X}(f) = \sum_{m=1}^{p} A_m \exp(j\theta_m) \frac{2\alpha_m}{[\alpha_m^2 + (2\pi [f-f_m])^2]}$$

See *Fig(2.4)* for the *PSDE* using this method.

2.4. NON PARAMETRIC SPECTRAL ESTIMATION METHODS :

Unlike the Parametric Technique *(PT)*, no model parameters are implicitly computed in estimating the *PSD* using these approaches. This category includes *Pisarenko Harmonic Decomposition (PHD)* approach, *Maximum Likelihood Method (MLM)*, as well as the *Eigen Vector Decomposition (EVD)* approaches.

2.4.1. PISARENKO HARMONIC DECOMPOSITION method :

Pisarenko Harmonic Decomposition (PHD) method is used for estimating frequencies of sinusoids corrupted by additive white noise. The main key to this method is the determination of the smallest eigen vector of the data covariance matrix. The algorithm is developed as follows :

A deterministic process consisting of p real sinusoids of the form $sin(2\pi f_i \Delta t)$ can be represented as $2p^{th}$ order difference equation of real coefficients of the form :

$$x_n = -\sum_{m=1}^{2p} a_m x_{n-m} \qquad (2.4.1)$$

In this case, the a_m are coefficients of the symmetric polynomial $\psi(z)$

$$\psi(z) = z^{2p} + a_1 z^{2p-1} + \ldots\ldots\ldots + a_{2p} z + 1 \qquad (2.4.2)$$

Assuming unit modulus roots of the form $z_i = exp(j2\pi f_i \Delta t)$, where f_i are arbitrary frequencies between $-1/2\Delta t$ *and* $1/2\Delta t$, the polynomial equation can be written,*[33]*, as :

$$\psi(z) = \sum_{i=1}^{p} (z-z_i)(z-z_i^*) \qquad (2.4.3)$$

For sinusoids in additive white noise, the random process will be :

$$y_n = x_n + w_n = -\sum_{m=1}^{2p} a_m x_{n-m} + w_n \qquad (2.4.4)$$

where y_n is the noisy process, x_n -*as above*- is the deterministic process and w_n is the white Gaussian noise, uncorrelated with the sinusoids, hence;

$$E[\, w_n w_{n+k} \,] = \sigma_w^2 \delta_k$$

$$E[\, w_n \,] = 0$$

and $$E[\, x_n w_m \,] = 0$$

Now, substituting $x_{n-m} = y_{n-m} - w_{n-m}$ into equation *(2.4.4)* gives :

$$\sum_{m=0}^{2p} a_m y_{n-m} = \sum_{m=0}^{2p} a_m w_{n-m} \qquad (2.4.5)$$

which has the structure of a special *ARMA(p,p)* process in which the *MA* and *AR* parameters are identical.

In matrix form, equation *(2.4.5)* can be written as :

$$Y^T A = W^T A \qquad (2.4.6)$$

where $Y^T = [\, y_n \;\; y_{n-1} \;\; \cdots\cdots\cdots \;\; y_{n-2p} \,]$

$A^T = [\, 1 \;\; a_1 \;\; a_2 \;\; \cdots\cdots\cdots \;\; a_{2p} \,]$

$W^T = [\, w_n \;\; w_{n-1} \;\; \cdots\cdots\cdots \;\; w_{n-2p} \,]$

Multiplying both sides of equation *(2.4.6)* by Y, substituting $Y_n = X_n + W_n$ in the right hand side and taking the expectation gives :

$$E[\, YY^T] = E\Big[(\, X + W \,)\, W^T \Big] \qquad (2.4.7)$$

But

$$E[\, YY^T] = R_{yy} = \begin{bmatrix} R_{yy}(0) & \cdots\cdots & R_{yy}(-2p) \\ \vdots & & \vdots \\ R_{yy}(2p) & \cdots\cdots & R_{yy}(0) \end{bmatrix} \qquad (2.4.8)$$

and $$E[(\, X + W \,)\, W^T] = E[\, W\, W^T] = \sigma_w^2\, I \qquad (2.4.9)$$

where R_{yy} is the covariance matrix of the random process.
σ_w^2 is the noise variance.
and I is the identity matrix.

Using *Equ.(2.4.8) and (2.4.9),* equation *(2.4.7)* can be written as :

$$R_{yy}\, A = \sigma_w^2\, A \qquad (2.4.10)$$

Thus, if the autocorrelation function $R_{yy}(k)$ is known, then the *ARMA* parameters can be found as the solution of the eigen equation *-Equ.(2.4.10)-* in which σ_w^2 is the smallest eigen value and A is the corresponding eigen vector. Equation *(2.4.10)* forms the basis of the harmonic decomposition approach developed by *Pisarenko [46],* which gives the exact frequencies and powers of p real sinusoids in white noise.

Determination of the *ARMA* parameters vector *A* will provide the evaluation of the roots of the polynomial equation -*Equ.(2.4.2)*- which gives the exact frequencies.

The autocorrelation lags and the sinusoids power are related to each other as follows :

$$R_{yy}(0) = \sigma_w^2 + \sum_{i=1}^{p} p_i \qquad (2.4.11)$$

$$R_{yy}(k) = \sum_{i=1}^{p} p_i \cos(2\pi f_i k\Delta t) \qquad \text{for } k \neq 0$$

Or in matrix form :

$$R'_{yy} = FP \qquad (2.4.12)$$

where

$$R'_{yy} = \begin{bmatrix} R_{yy}(1) \\ \vdots \\ R_{yy}(p) \end{bmatrix} \quad , \quad P = \begin{bmatrix} p_1 \\ \vdots \\ p_p \end{bmatrix}$$

and

$$F = \begin{bmatrix} \cos(2\pi f_1 \Delta t) & \cdots\cdots\cdots & \cos(2\pi f_p \Delta t) \\ \vdots & & \vdots \\ \cos(2\pi f_1 p\Delta t) & \cdots\cdots\cdots & \cos(2\pi f_p p\Delta t) \end{bmatrix}$$

Thus, the sinusoids power can be computed using equation *(2.4.12)* and the noise power using equation *(2.4.11)*. See *Fig(2.4)* for the *PSDE* using *PHD* method.

2.4.2. MAXIMUM LIKELIHOOD SPECTRAL ESTIMATION method :

One of the most popular techniques for power spectral estimation which possesses high resolution capability and exhibts less variance, is the *Maximum Likelihood Method (MLM)*. It is originally developed by *Capon [9]*, in *1969*, for frequency wavenumber analysis. In *MLM*, one estimates the *PSD* by effectively measuring the power out of a set of narrow-band filters, or we can say it is a "*sliding*" band-pass filter which adjusts itself to the random process under consideration in such a way that the spectral estimate at one frequency is least affected by the spectral components of other frequencies. These filters are Finite Impulse Response *(FIR)* type with *k* weights *(taps)*.

Now, if $X^T = [x_1 \; x_2 \; ..... \; x_k]$ represents the observation vector, and $A^T = [a_1 \; a_2 \; ..... \; a_k]$ be the weights vector, then :

$$y = a_1x_1 + a_2x_2 + ... \; a_kx_k \qquad 1 \le k \le N \qquad (2.4.13)$$

represents the output of the aforementioned set of filters. In matrix form, equation *(2.4.13)* can be written as :

$$Y = A^TX \qquad (2.4.14)$$

The average power can be computed by taking the expectation of equation *(2.4.14), i.e*

$$P = E[\; Y \; Y^* \;] = A^HR_{XX}A \qquad (2.4.15)$$

where H denotnes the complex conjugate transpose and $R_{XX} = E[XX^*]$, as before, is the covariance matrix.

If, we now constrain the gain of the system to the signals at particular frequencies to be unity by defining a frequency vector C as follows :

$$A^T C = 1 \qquad (2.4.16)$$

where $C = col[\ 1 \quad e^{j\omega}\ e^{j2\omega} \ldots\ldots\ e^{j(k-1)\omega}\ ]$

Then using *Lagrange* method, we can minimize the average output power subject to this constraint by defining a cost function $H(\omega)$ as shown below

$$H(\omega) = P + \alpha(\ 1 - A^T C\ ) \qquad (2.4.17)$$

where α is an arbitrary constant. The minimization can be achieved by differentiating equation *(2.4.17) w.r.t.* the weights vector A, and equating the derivative to zero, *-see Appendix Two-*, we will have;

$$A_{opt} = \frac{R_{XX}^{-1}\ C^H}{C^H\ R_{XX}^{-1}\ C} \qquad (2.4.18)$$

where A_{opt} is the optimum weight.

The Maximum Likelihood Spectral Estimate *(MLSE)* $-P_{ML}(\omega)-$ as a function of frequency ω, is then given by :

$$P_{ML}(\omega) = \frac{1}{C^H\ R_{XX}^{-1}\ C} \qquad (2.4.19)$$

Thus, we can see from equation *(2.4.19)* that in order to compute the *MLSE*, one needs only to estimate the covariance matrix R_{XX} of the observation vector. See *Fig(2.4)* for the *PSDE* using *MLM*.

2.4.3. EIGEN VECTOR DECOMPOSITION TECHNIQUES :

The Eigen Vector Decomposition Techniques *(EVDT)*, which has been developed originally for use in Array Signal Processing *(ASP)*, has a wide range of applications in both the space and time domain. In this section an overview is presented of the most important algorithms where eigen vectors of correlation type matrices are used.

2.4.3.1. PRINCIPAL COMPONENTS method :

The first area where eigen vectors of correlation type matrices have been used is the Principal Components *(PC)* analysis.

Let $V_1, V_2, \ldots\ldots\ldots, V_M$ be the orthonormalized eigen vectors of the covariance matrix R_{XX} such that V_1 corresponds to the largest eigen value λ_1, V_2 the second eigen vector corresponds to the second largest eigen value λ_2, and so on, in other words ;

$$\lambda_1 \geq \lambda_2 \geq \lambda_3 \geq \ldots\ldots\ldots \geq \lambda_M \geq 0$$

Then, the eigen vectors of R_{XX} are defined by the property :

$$R_{XX} V_i = \lambda_i V_i \quad , \qquad i = 1,2,\ldots\ldots\ldots,M \qquad (2.4.20)$$

where R_{XX} is estimated from the data samples using equation *(2.1.6)* after subtracting the samples mean $\bar{X}$, where

$$\bar{X} = \frac{1}{N} \sum_{i=1}^{N} x_i \qquad (2.4.21)$$

The j^{th} scalar principal component of X is then defined *[29]*, as :

$$\eta_j = V_j \quad X \qquad (2.4.22)$$

where $X = col[x_1 x_2 \ldots\ldots\ldots x_N]$ is the data samples vector.

Now, the method of principal components is used to find the principal component η_j that has, on average, large variance. So if X represents p sinusoidal signals in white Gaussian noise, then *[27]* :

$$\left.\begin{aligned} R_{XX} &= \sigma_w^2 \, I + \sum_{i=1}^{p} \lambda_i V_i V_i^H \\ \text{or} \quad R_{XX} &= R_{WW} + R_{SS} \end{aligned}\right\} \qquad (2.4.23)$$

where R_{WW} is the noise covariance matrix.

R_{SS} is the signal covariance matrix.

The p largest eigen vectors corresponding to the second term in the above equation *-Equ.(2.4.23)-* are called the signal subspace and the $(M-p)$ eigen vectors corresponding to the $(M-p)$ smallest eigen values *-they normally have the same value which equals to* σ_w^2- constitute an orthogonal subspace called the noise subspace.

Now, suppose that in one way or another, we can separate the two covariance matrices mentioned above *(see Chapter 4)*, and if we use the signal covariance matrix R_{ss} instead of the whole covariance matrix R_{xx} in computing the *ML spectra*, we still have a resonable estimate.

i.e $$P_{PC} = \left[C^{H} R_{ss}^{-1} C \right]^{-1} \qquad (2.4.24)$$

where *C*, as defined in the previous section, is a frequency vector, *-see Fig.(2.8) for the Principal Components estimate-*.

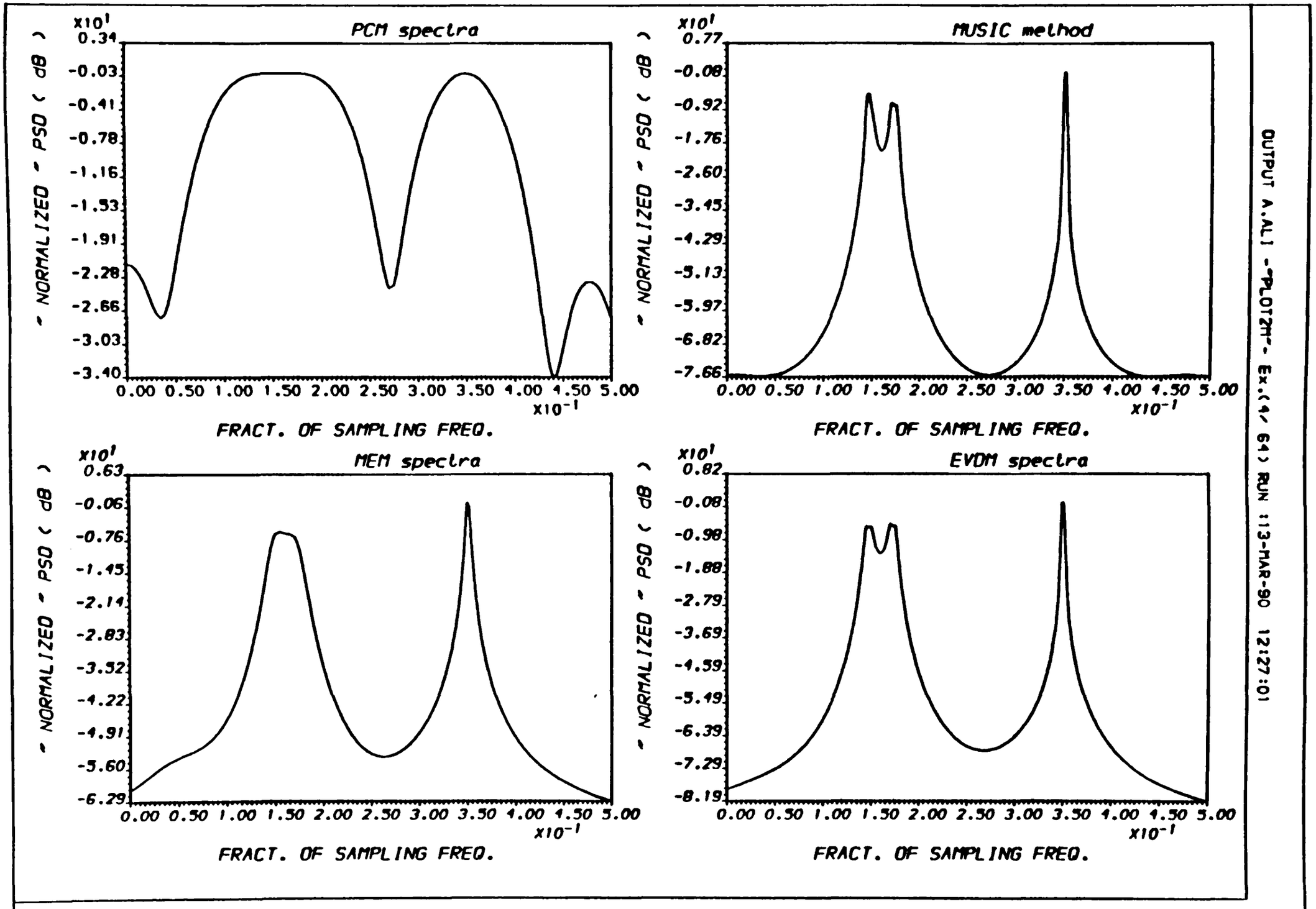

FIG.(2.8) POWER SPECTRAL DENSITY ESTIMATE
* For different PSDE methods *

2.4.3.2. MUSIC ALGORITHM method :

One of the recent eigen vector decomposition approaches which has superior resolution capabilities is the *MUltiple SIgnal Characterization (MUSIC)* algorithm developed by *Schmidt [51]* in *1979.*

Recall the *ML* spectral estimate - *Equ.(2.4.19)* - ;

$$P_{ML} = \frac{1}{C^H R_{XX}^{-1} C} \qquad (2.4.25)$$

Now, if we use a specially defined matrix B_{WEV} instead of the whole covariance matrix R_{XX} in the equation above, it can be rewritten as :

$$P_{MUSIC} = \frac{1}{C^H B_{WEV} C} \qquad (2.4.26)$$

where $B_{WEV} = \sum_{i=p+1}^{M} V_i V_i^H$ is the noise covariance matrix with the noise eigen values set to the same value *(taken here as unity)*, -see *Fig.(2.8)* for the *PSDE* using this method-.

2.4.3.3. EIGEN VECTOR method :

The *Eigen Vector (EV)* approach to power spectral density estimation developed by *D.H.Johnson* and *DeGraaf [27]* differs slightly from that of *Schmidt*. The only difference is that the noise covariance matrix is used without any constraint on its eigen values.

$$P_{EV} = \frac{1}{C^H R_{ww}^{-1} C} \qquad (2.4.27)$$

where $$R_{ww}^{-1} = \sum_{i=p+1}^{M} \frac{1}{\lambda_i} V_i V_i^H \qquad (2.4.28)$$

is the inverse of the noise covariance matrix computed from the *(M-p)* noise eigen vectors. *Fig.(2.8)* shows the *PSDE* using this algorithm.

2.5. MULTIDIMENSIONAL SPECTRAL ESTIMATION :

There are many situations where the signals are inherently multidimensional Such situations, which can be found in radar, sonar, radio astronomy, ..,etc, present many theoretical and practical difficulties that need to be tackled *[38]*. Most of the one-dimensional spectral approaches, such as the *DFT, MLM, Burg* algorithm, *AR,* and *Pisarenko* methods, are used in the m-dimensional spectra. A detailed study can be found in *ref.[38],* where the different approaches mentioned above are derived for the m-dimensional spectral estimation. A particular emphasis was given to *MEM* for its high resolution performance. Unlike the *1*-dimensional case where *MEM* and *AR* were equivalent, in the m-dimentional case the true *ME* estimate is distinctly different from the spectra derived by *AR* modeling. In fact the computation of the m-dimensional *ME* spectra appears to require the solution of a nonlinear equation problem.

A topic of current interest is that of Bispectrum and Trispectrum Estimation *[40]*. The general motivations behind the the use of bispectrum were the deviation from normality,

phase estimation, and detection and characterization of non linear mechanisms. that generate time series.

Chapter Three

PERFORMANCE TEST OF THE DIFFERENT PSDE APPROACHES

CHAPTER THREE

PERFORMANCE TEST
OF THE
DIFFERENT PSDE APPROACHES

3.1. INTRODUCTION :

In this chapter the different *PSDE* approaches, discussed in the previous chapter, are tested and compared for their performance capabilities and limitations. Three criteria are used to evaluate the performances of the above mentioned estimators, these are :

a) Detectability.
b) Resolution Capability.
c) Estimation Bias.

In the following a brief explanation will be given for each of these criteria.

3.1.1. DETECTABILITY :

This is defined as *the ability of the estimator to detect the signals, i.e* the degree to which the side lobes are small so that they are not confused with peaks corresponding to the signals. Thus, detection analysis assesses the conditions under which the number of signals present in the random process can be determined accurately.

3.1.2. RESOLUTION CAPABILITY :

Resolution is defined as *the ability of the estimator to resolve two closely separated signals.* However,

resolution becomes very difficult to be achieved as signals become more and more closely separated, since as we mentioned earlier in Chapter Two, in the real situations, only finite data samples are normally available.

If two signals are separated in frequency by a sufficient amount, their frequencies will be resolved, in which case the estimator exhibits two distinct maxima *(peaks)*. On the other hand, the estimator may fail to resolve the signals frequencies, in this case, the estimator displays a single maximum in some intermediate frequency.

3.1.3. ESTIMATION BIAS :

Finally, an estimator can both detect and resolve signals but yields inaccurate estimate of their frequencies. Thus Estimation bias can be defined as *the amount of deviation between the estimated frequency and the true one.*

3.2. TEST PROCEDURE :

A Fortran 77 subroutine was written for each of the different *PSDE* approaches mentioned in Chapter Two together with two main driving programs, whose flow charts are given in *Fig.(3.1)* to *Fig.(3.3)* and Fortran 77 listing in Attachment One, to allow the above mentioned tests to be done. The test data is generated according to the formula :

$$x_n = \sum_{i=1}^{p} A_i exp[j(n\omega_i+\phi_i)] + w_n \ , \quad i=0,1, \ldots, N-1 \quad (3.2.1)$$

where A_i is the amplitude and ϕ_i is the phase of the *ith* sinusoid, $\omega_i = 2\pi f_i$, and f_i is the normalised frequency, *(i.e the frequency of the ith sinusoid divided by the*

sampling frequency), w_n is a zero mean white Gaussian noise with variance equal to σ_w^2, and *N* is the number of data samples. The Signal/Noise Ratio *(SNR)* is computed from the formula :

$$SNR_i = 10log_{10}\left(\frac{A_i^2}{2\,\sigma_w^2}\right) \quad dB \qquad (3.2.2)$$

Then the resulting spectral estimate is normalized *w.r.t* its peak value and transformed in *dB*. Thus the quantity presented in the figures is the normalized *PSD* in dB. that is :

$$PSD(normal.) = 10\ log_{10}\left(\frac{PSD}{PSD_{max.}}\right) \quad dB \qquad (3.2.3)$$

3.3. DETECTABILITY TEST :

3.3.1. TEST EXAMPLE :

In performing the detection test on the different *PSD* approaches, we used, AS A TEST EXAMPLE, one sinusoidal signal of unit amplitude *A*, normalized frequency *f=0.25*, and phase ϕ*=o (Degrees)* contaminated by a white Gaussian noise. The *SNR* used was *10 dBs* and the noise variance σ_w^2 was calculated as follows :

$$\sigma_w^2 = \frac{A^2}{2 \times 10^{0.1 \times SNR}} \qquad (3.3.1)$$

and the data samples were generated according to *Equ.(3.2.1)*.

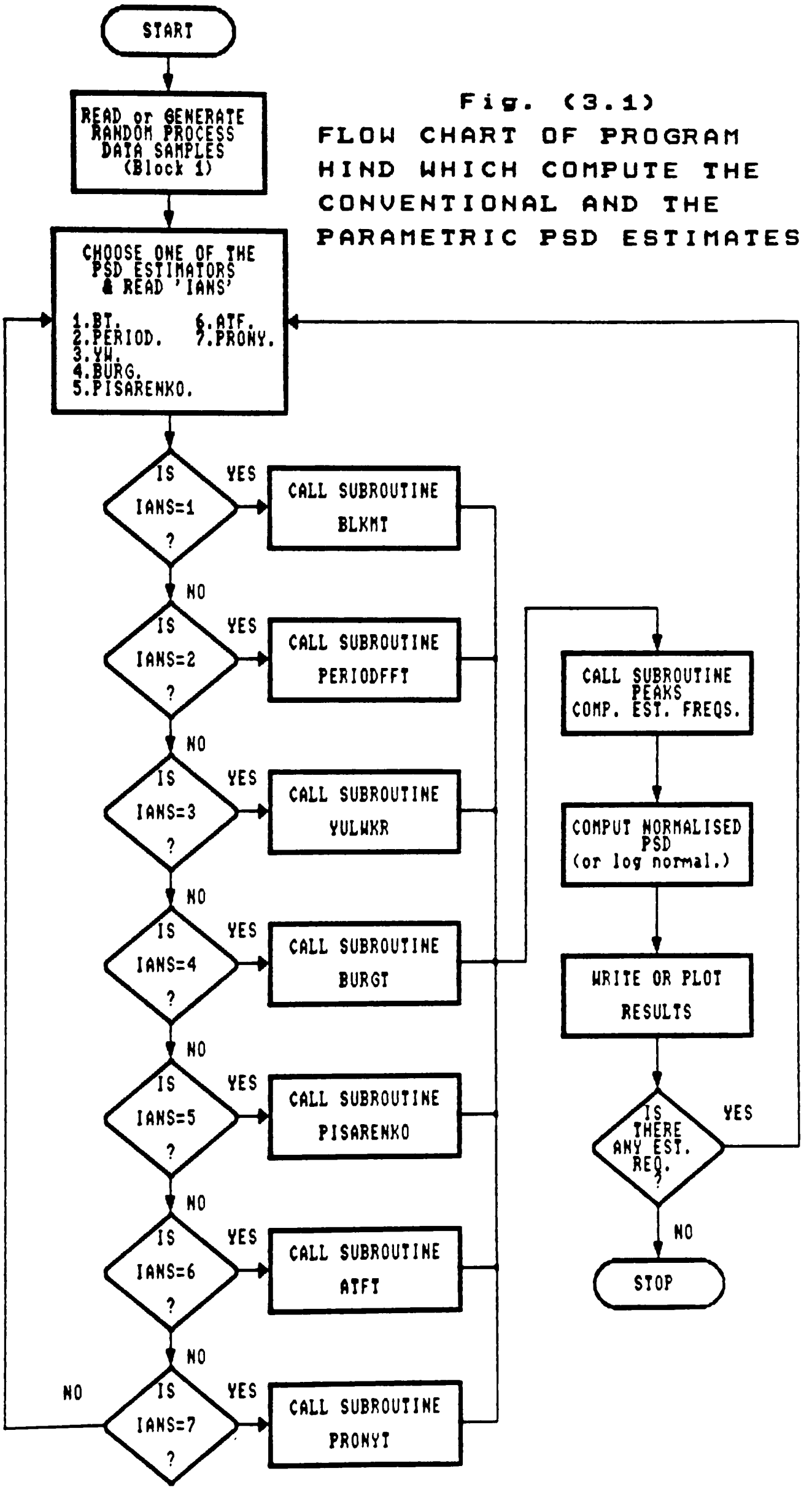

Fig. (3.1)
FLOW CHART OF PROGRAM HIND WHICH COMPUTE THE CONVENTIONAL AND THE PARAMETRIC PSD ESTIMATES

FIG. (3.2)

FLOW CHART FOR PROGRAM AHMED WHICH COMPUTES THE EIGENVALUE DECOMPOSITON TECHNIQUE ESTIMATES

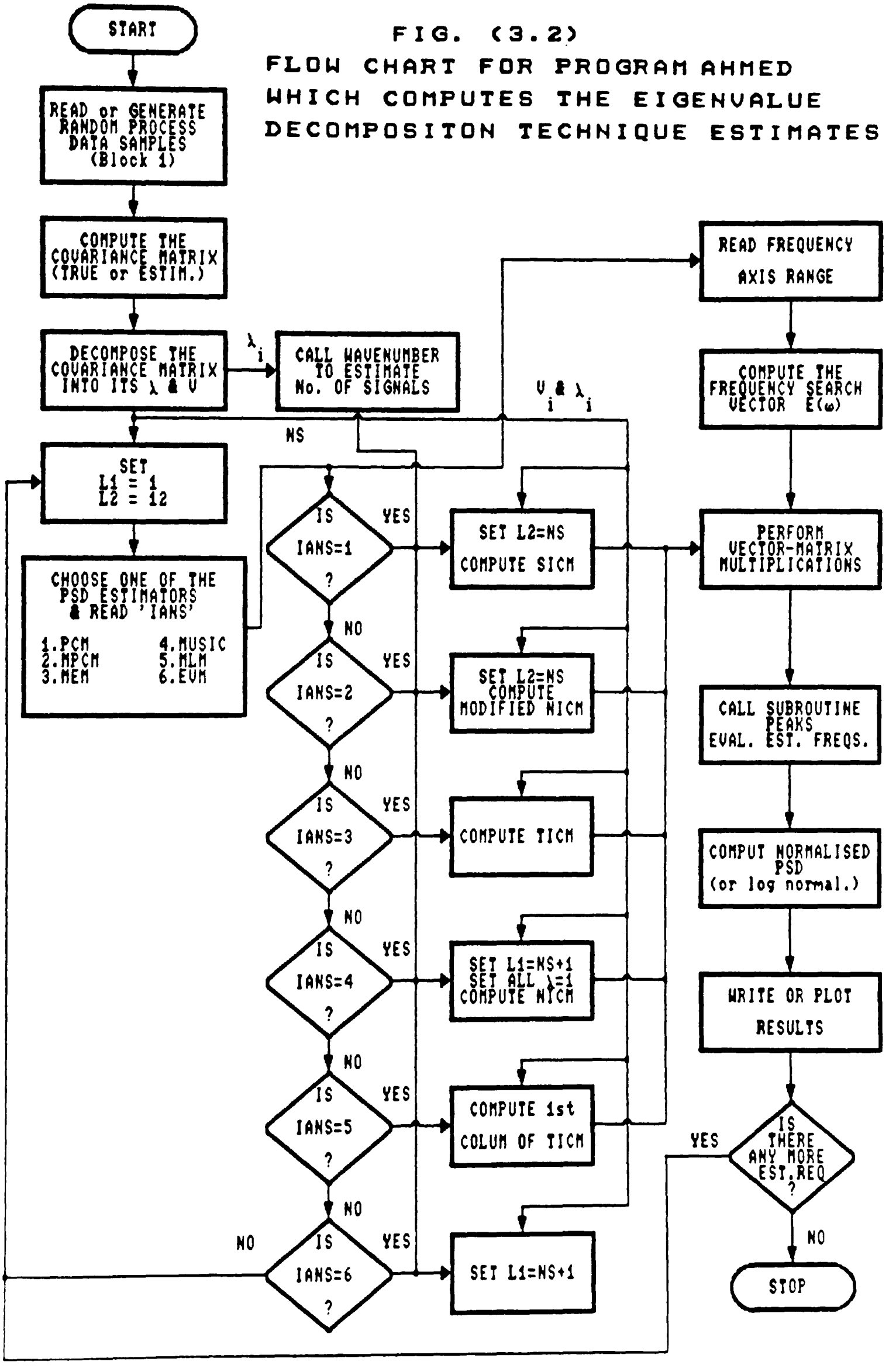

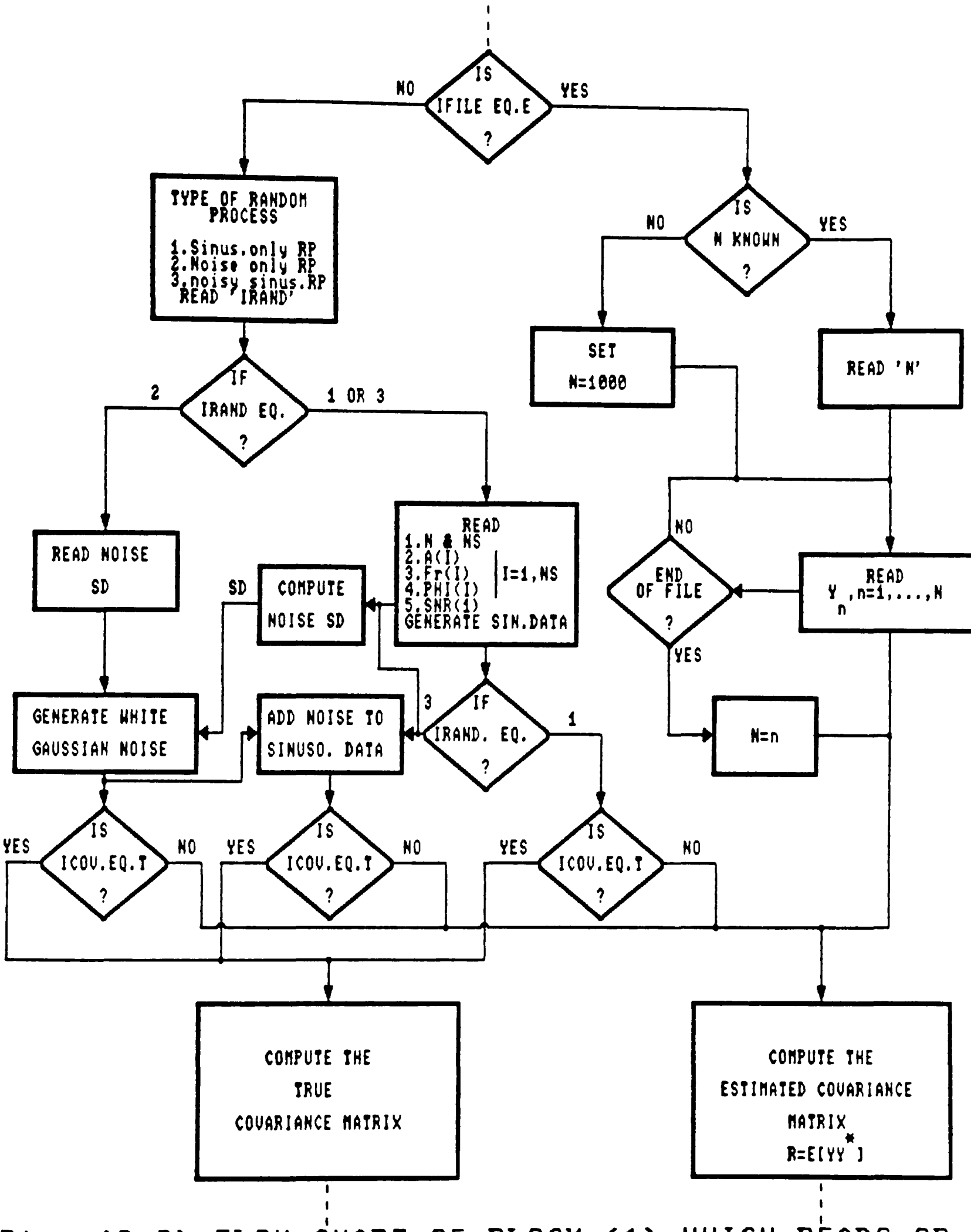

Fig. (3.3) FLOW CHART OF BLOCK (1) WHICH READS OR GENERATES DATA AND COMPUTES EITHER THE TRUE OR ESTIMATED COVARIANCE MARTIX FOR PROGRAMS HIND RAGAD AND AHMED

3.3.2. *ESTIMATORS DETECTION ABILITIES :*

The conventional *PSD* estimators have a common problem, that is they suffer from the ambiguities that arise due to the side lobe leakage, *-the side lobe of a strong signal can mask the main lobe of a nearby weak signal-.* Thus they cannot detect (assess) the signals that actually exist in the random process and are very sensitive to *SNR* variations, see *Fig.(3.4)* for the Periodogram and Blackman-Tukey *PSD estimates.*

Modeling approaches to *PSD* estimation have higher detection ability with better side lobe supression when compared with the conventional *PSD* estimators if the correct model is chosen to model the time series. *AR* modeling has the highest detectability among the modeling approaches, *-see Fig(3.4) for the estimate of Yule-Walker and Burg methods as examples of AR modeling-.*

Walker [33] was the first to consider the problem of estimating the *AR* parameters of an *AR* series corrupted by additive noise. He evaluated the asymptotic efficiency and variance of the parameter estimates, upon which the performance of the *AR* modeling depends. *Pagon [7]* proves that the correct model for an *AR* series plus noise is the *ARMA* model and through the use of nonlinear regression methods develops strongly consistent efficient estimates.

In Chapter Two it was mentioned that the *ARMA* process can be modeled by an *AR* model with infinite number of coefficients which is obvious from *Fig.(3.5) -another example of two sinusoids in white Gaussian noise is used-* which shows that the *Burg* algorithm estimator was incapable of detecting the two signals (resolving them as two separate peaks) when a small number *(4 and 8)* of coefficients were used and they were resolved when this number increased to

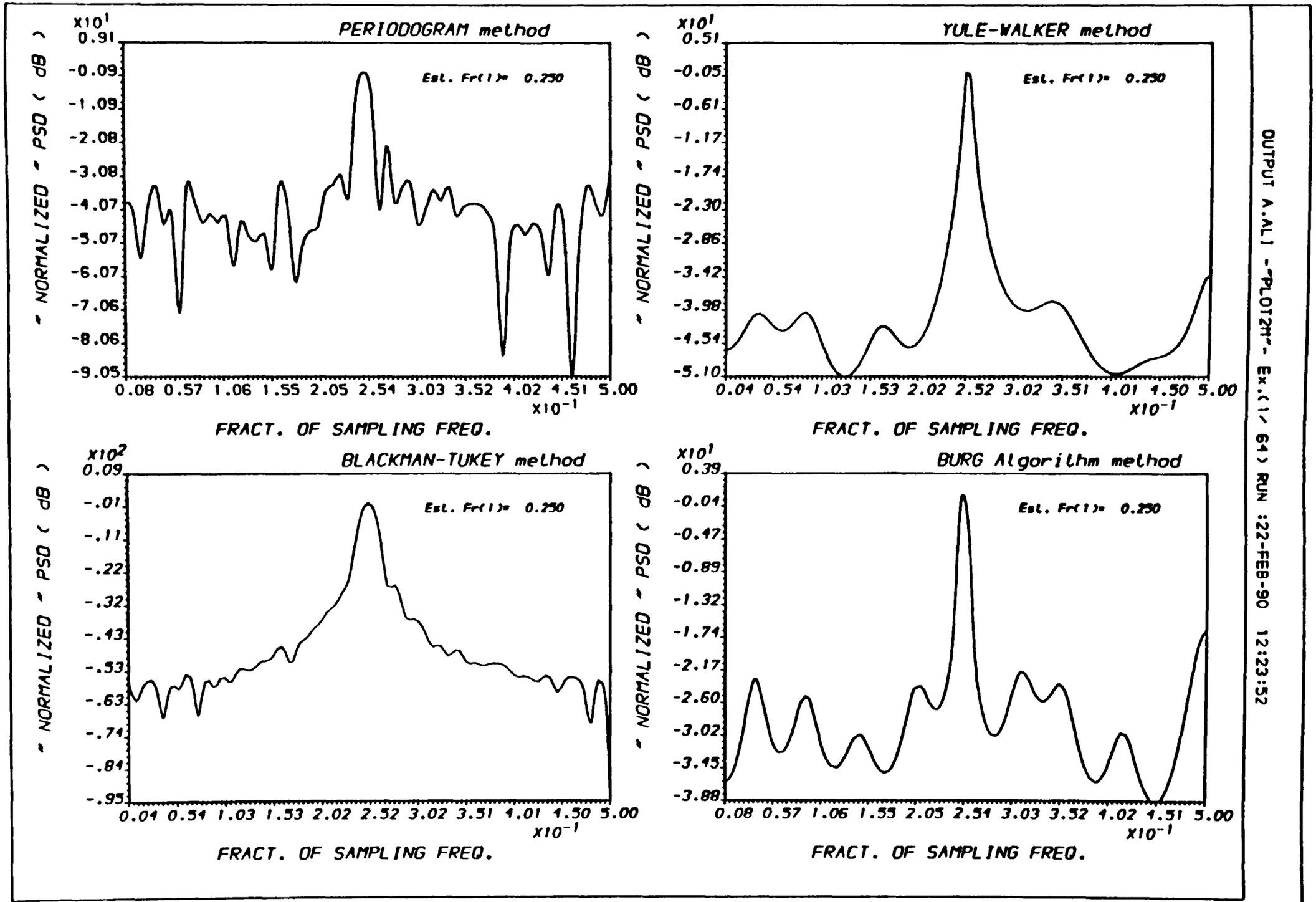

FIG.(3.4) POWER SPECTRAL DENSITY ESTIMATES
* For different PSDE methods *

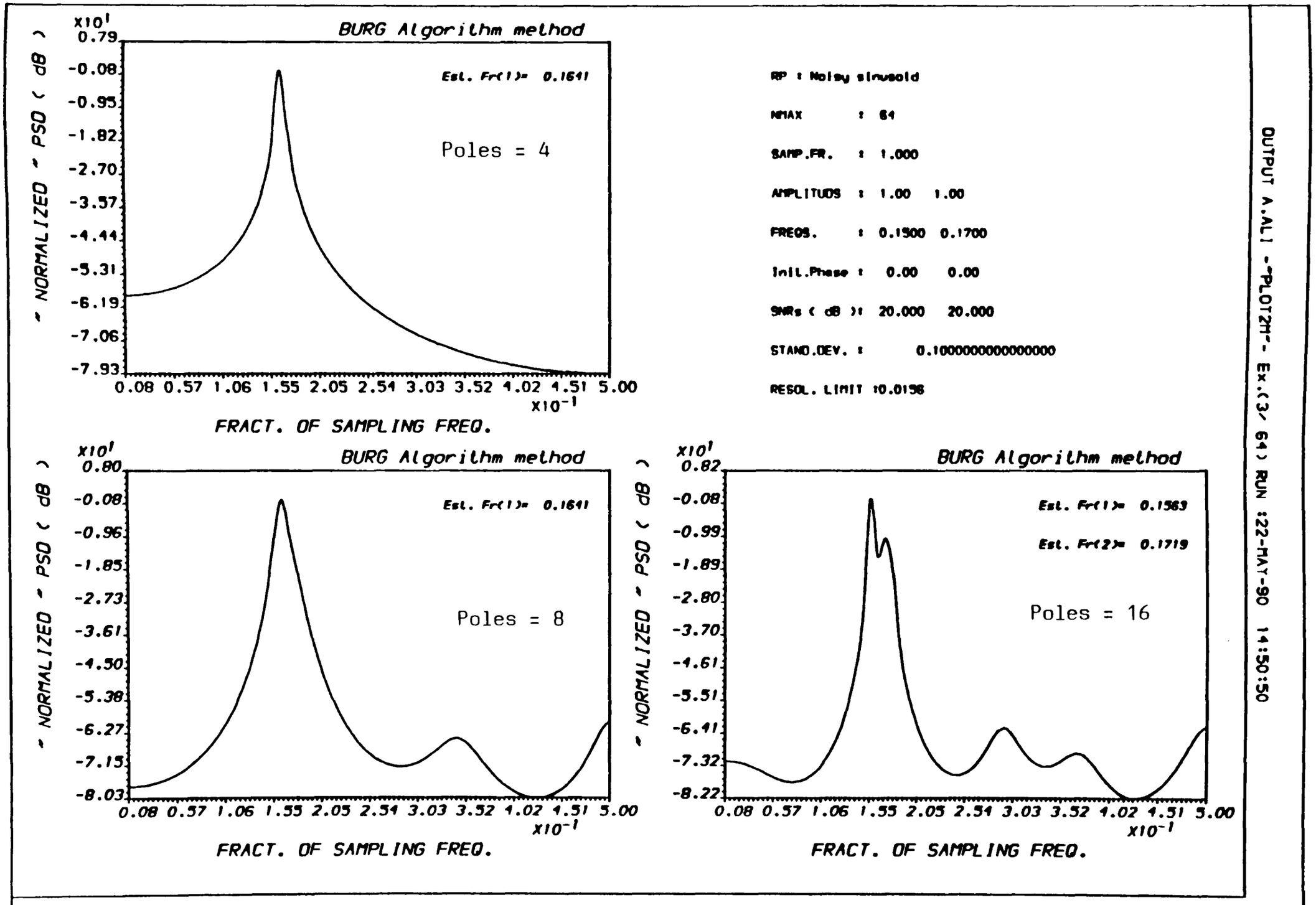

FIG.(3.5) POWER SPECTRAL DENSITY ESTIMATES
* For different PSDE methods *

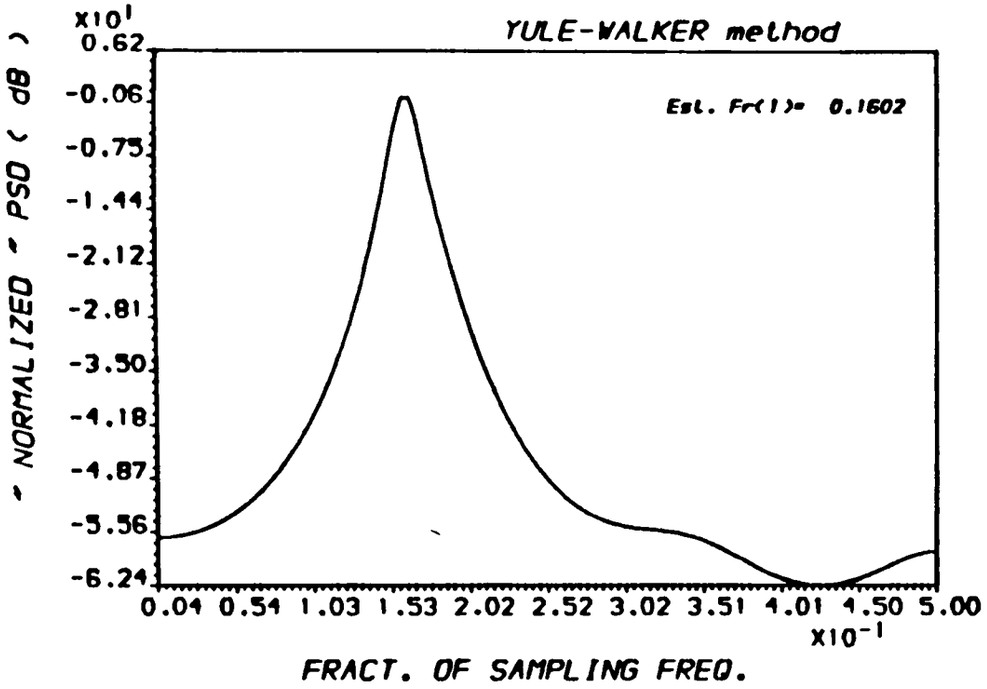

RP : Noisy sinusoid

NMAX : 64

SAMP.FR. : 1.000

AMPLITUDS : 1.00 1.00

FREQS. : 0.1500 0.1700

Init.Phase : 0.00 0.00

SNRs (dB): 30.000 30.000

STAND.DEV. : 0.031622776601683

RESOL. LIMIT :0.0156

No. of coeffs. = 6

OUTPUT A.ALL -PLOT2MT- Ex.(5/ 64) RUN :17-APR-90 12:19:34

FIG.(3.6) POWER SPECTRAL DENSITY ESTIMATES
* For different PSDE methods *

16. When a higher *SNR* value was used and due to the interpolation of the autocorrelation lags outside the observation window involved in the computation of *Burg* algorithm, it was capable of detecting these two signals at smaller number of coefficients whereas *Yule-Walker* algorithm could not resolve them, *see Fig.(3.6)*.

A major problem with *AR* modeling is that it exhibits Spectral Line Splitting *(SLS)*. This problem, as mentioned earlier in chapter *2*, was studied by many researchers who found that *SLS* is due to many factors such as the high *SNR*, the number of coefficients is a large percentage of data samples, etc. See *Fig.(3.7)*, for the estimate of the same signal, in which the *SLS* phenomenon is very clear.

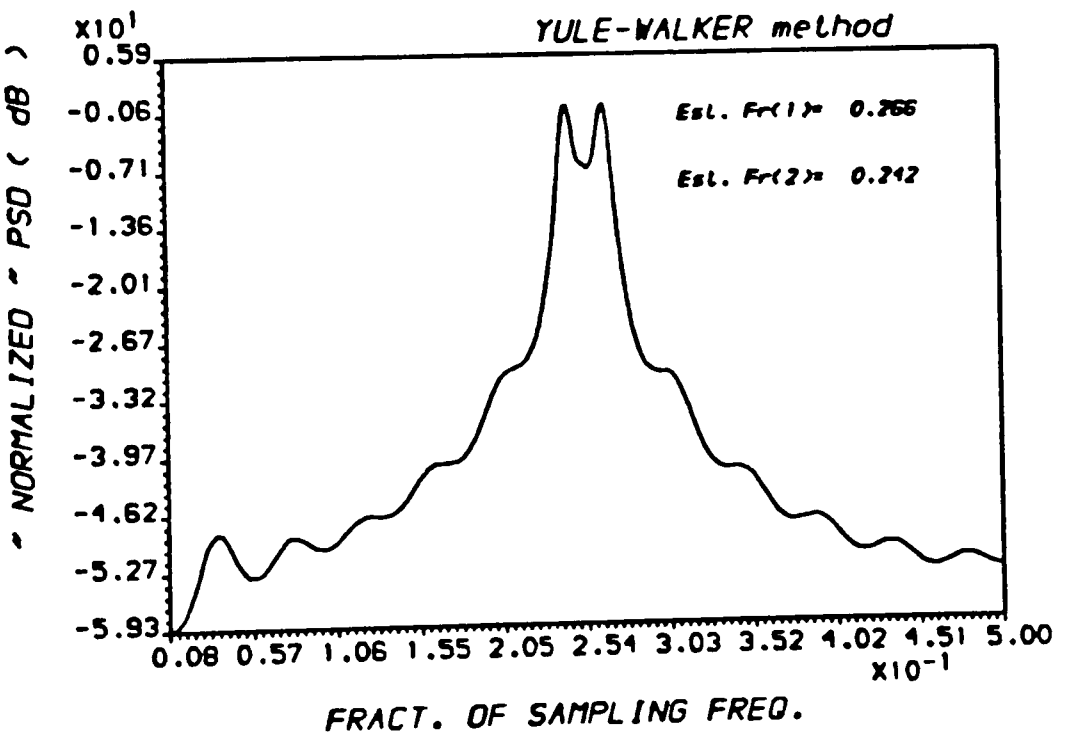

Fig.(3.7) Spontaneous Line Splitting in *AR* Power Spectral Density Estimation.

Non parametric spectral estimation methodes possess the best detection ability though some of them, such as *Pisarenko* and *MUSIC* algorithms, need a prior knowledge of the number of signals existing in the random process, whereas *MLM and MEM, -which can be regarded to have the best performances-,* do not need such information. The Principal Components Method possesses the worst detection ability due to the large side lobes associated, which nearly have the same signal power. See *Fig.(3.8)* and *Fig.(3.9)* for the estimates by these methods.

Finally Eigen Vector Decomposition Technique, and *MUSIC* algorithm in particular, can be regarded to have the best detectability among all the *PSDE* methods. *Fig.(3.9)* shows the spectra of these two methods in which the effect of setting the smallest eigen values to unity in *MUSIC* on whitening those portions of the spectra which are not at the signal frequency is obvious.

3.4. RESOLUTION TEST :

3.4.1. TEST EXAMPLE :

Three experimental tests were carried out to assess the resolution capabilities of the different algorithms. The random process used was composed of two equipower sinusoidal signals corrupted by white Gaussian noise. The data samples were generated according to equation *(3.2.1)*. The signals amplitudes were $A_1=A_2=1$, with the normalized frequencies sets were as follows *(a)* $f_1=0.15$ and $f_2=0.20$, *(b)* and *(c)* $f_1=0.15$, and $f_2=0.17$ being close to each other. The data length was *(64)* samples for tests *a* and *b*, and *(25)* samples for test *c*, whereas the initial phases were set to zero and the *SNR* used was *30 dBs* for all the three tests.

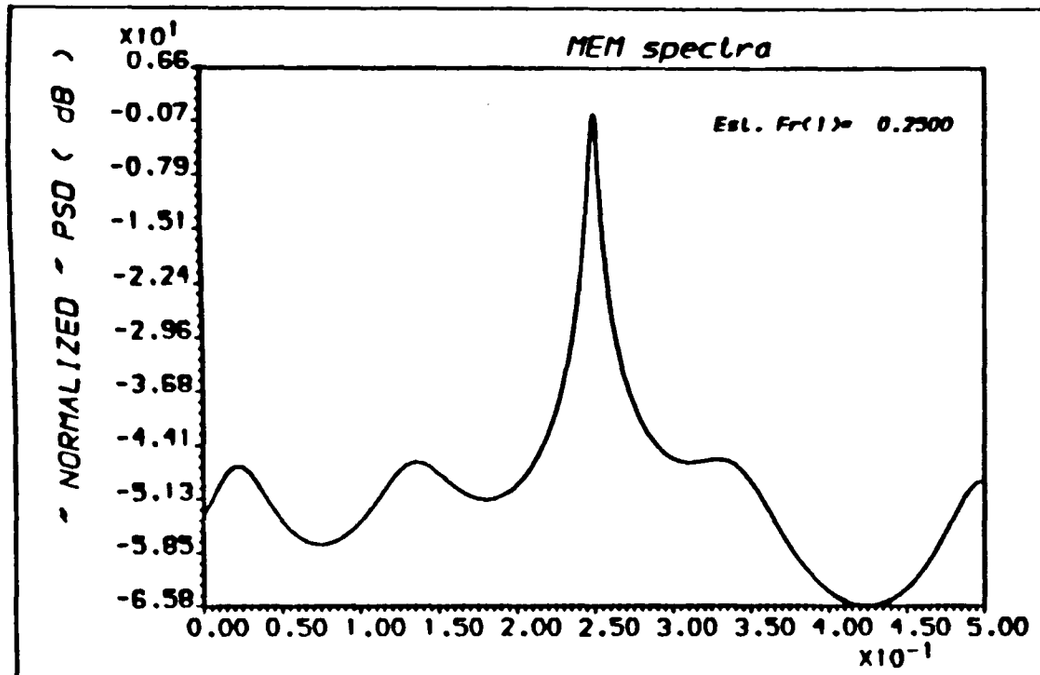

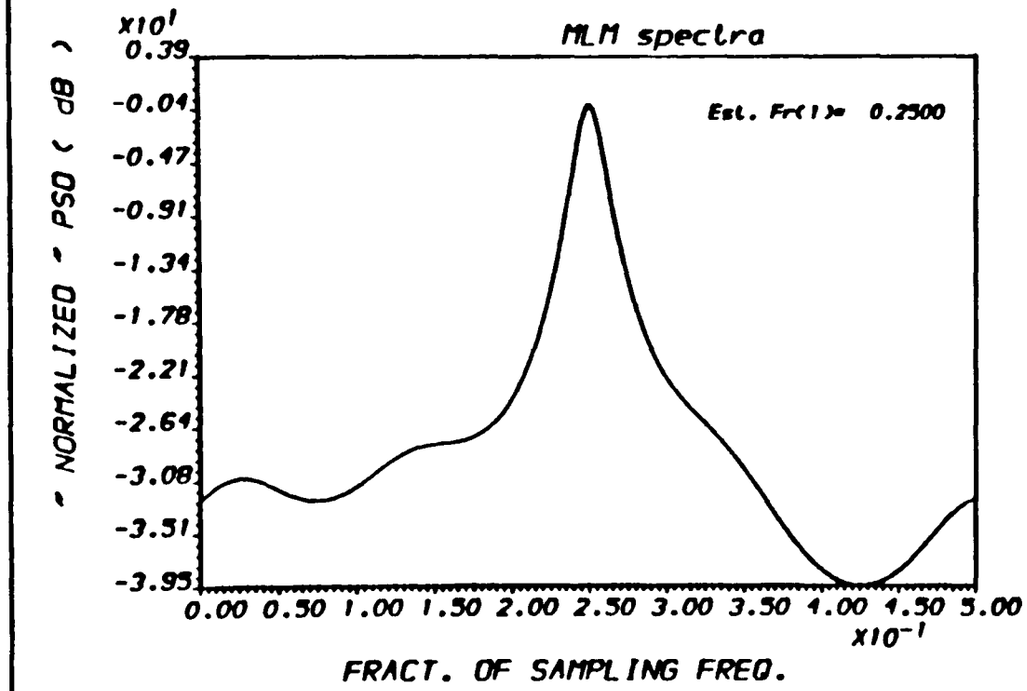

ARP : Noisy sinusoid

NMAX : 64

SAMP.FR. : 1.000

AMPLITUDS : 1.00

FREQS. : 0.2500

Init.Phase : 0.00

SNRs (dB): 10.000

STAND.DEV. : 0.31622776601683789

SIMULATED Coverience Matrix

OUTPUT A.ALI -"PLOT2MT- Ex.(1/ 64) RUN :14-MAR-90 12:14:36

FIG.(3.8) POWER SPECTRAL DENSITY ESTIMATE
* For different PSDE methods *

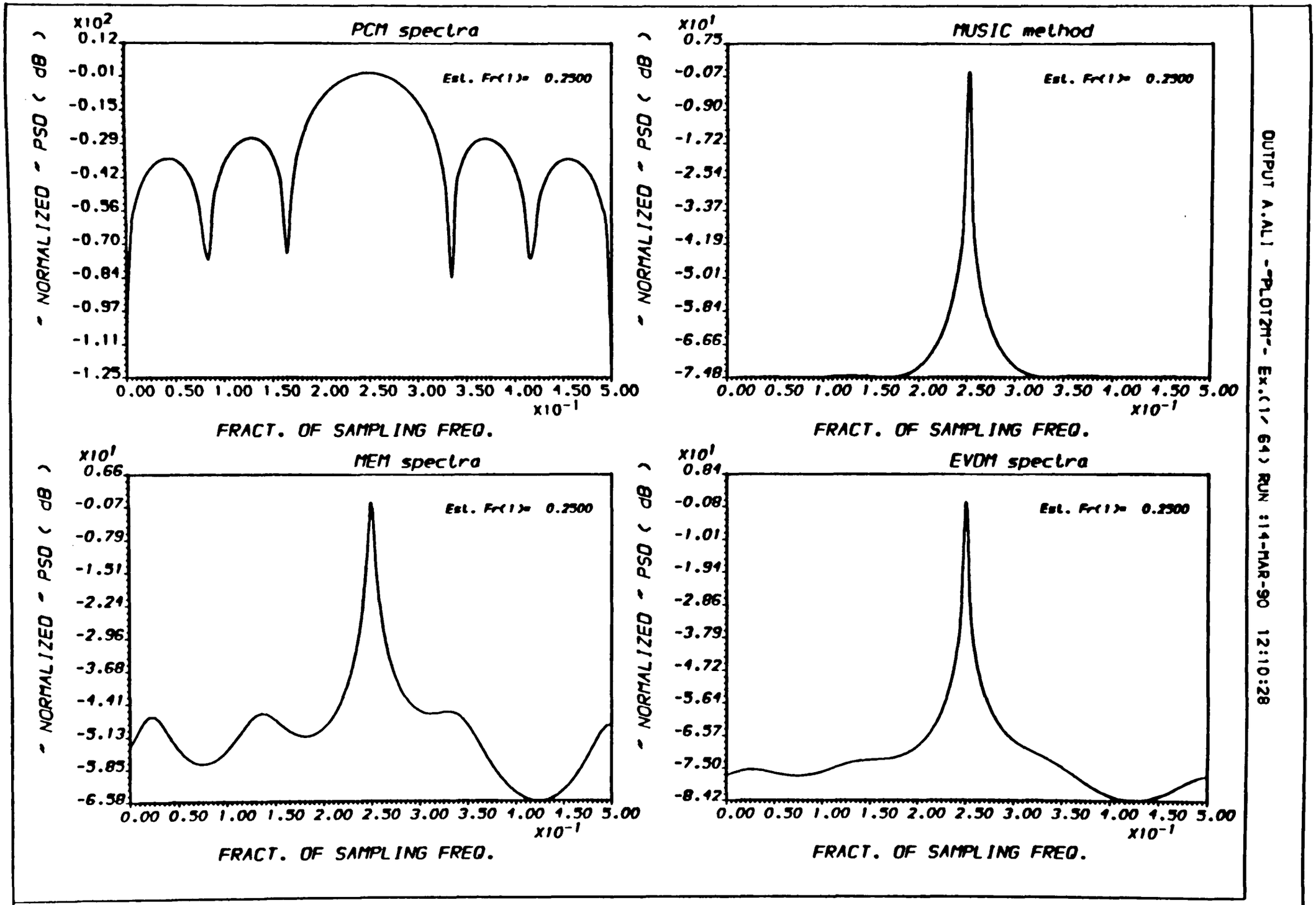

FIG.(3.9) POWER SPECTRAL DENSITY ESTIMATE
* For different PSDE methods *

3.4.2. *ESTIMATORS RESOLUTION CAPABILITIES :*

As the usual measure of resolution is the Fourier Resolution Limit *(FRL)* which equals *(1/NΔt)*, where *NΔt=T* is the data length, all the *PSDE* approaches were capable of resolving the two signals when the frequency separation *(0.05)* between the two signals was larger than the resolution limit *(0.01563)*, see *Fig(3.10) to Fig(3.12).* The two signal frequencies then separated by *($0.02f_s$), -test experiment b-*, which is still larger than the *FRL*, most of the estimators were capable of resolving the two signals and the only approaches which were incapable of the resolution, *-see Fig(3.13) to Fig(3.15)-*, were *MLM*, for which the *SNR* used was less than the threshold *SNR* value required to resolve these signals, and *PCM* which gave a broad peak instead due to the high minimum frequency separation it requires to resolve multiple signals, *-see Chapter 5 for more details-.*

T.Srinavsan, D.C.Swanson and F.W.Symons [52] presented a relationship between model order and data length for the *ARMA* time series model to resolve two closely separated sinusoids in white Gaussian noise. They stated that higher order *ARMA* models are required as the data becomes shorter due to the fact that the autocorrelation estimates become poor to achieve the required resolution.

The high resolution ability of the *AR* modeling is highly affected by the low levels of *SNR*, that is due to the smoothing caused by the noise, *-see Chapter 2-*. This effect can be clearly noticed in *Fig.(3.16)* which shows that the *Burg* and *Yule-Walker* algorithms were incapable of resolving the two signals when the *SNR* was as low as *5dB* and they resolved them, *-see Fig.(3.17)-*, when the *SNR* increased to as high as *10dB.*

In addition to what has been said in section *3.3.2,* about the conventional and modeling *PSDE* approaches, they share another major problem, that is the poor resolution obtainable from processing short data records which can be easily noticed by the incapability of these approaches to resolve the two signals when the frequency separation *(0.02)* between the two signals was less than the resolution limit *(0.04)* which leads us to the argument that these estimators are sensitive to short data records. *Fig(3.18)* to *Fig(3.20)* represent the results of the third test experiment performed using *25* data samples.

Although the Principal Components Method *(PCM)* is incapable of resolving the two signal freuencies separated by less than Fourier resolution limit *(FRL)* and gave a broad spectrum peak instead, the Eigen Vector Decomposition Technique *(EVDT)* lies at the top of the nonparametric approaches to *PSDE* in terms of its superior performance. It is least sensitive to finite averaging *(short data record)* and requires the least *SNR* to detect and resolve two closely separated signals, *-this matter will be studied further in Chapter 5-. Fig.(3.15)* shows the estimates of this group from which it is clear that *MUSIC [51]* approach has the same resolution capability as that of the *EV* Method *[27]* though their spectra have different appearances.

3.5. ESTIMATION BIAS TEST :

3.5.1. TEST EXAMPLES :

The test examples which had been used earlier in testing both the detection and resolution capabilities of the different *PSDE* approaches were used here for testing the Estimation Biases of the above estimators. In addition another test example performed for the purpose of this test,

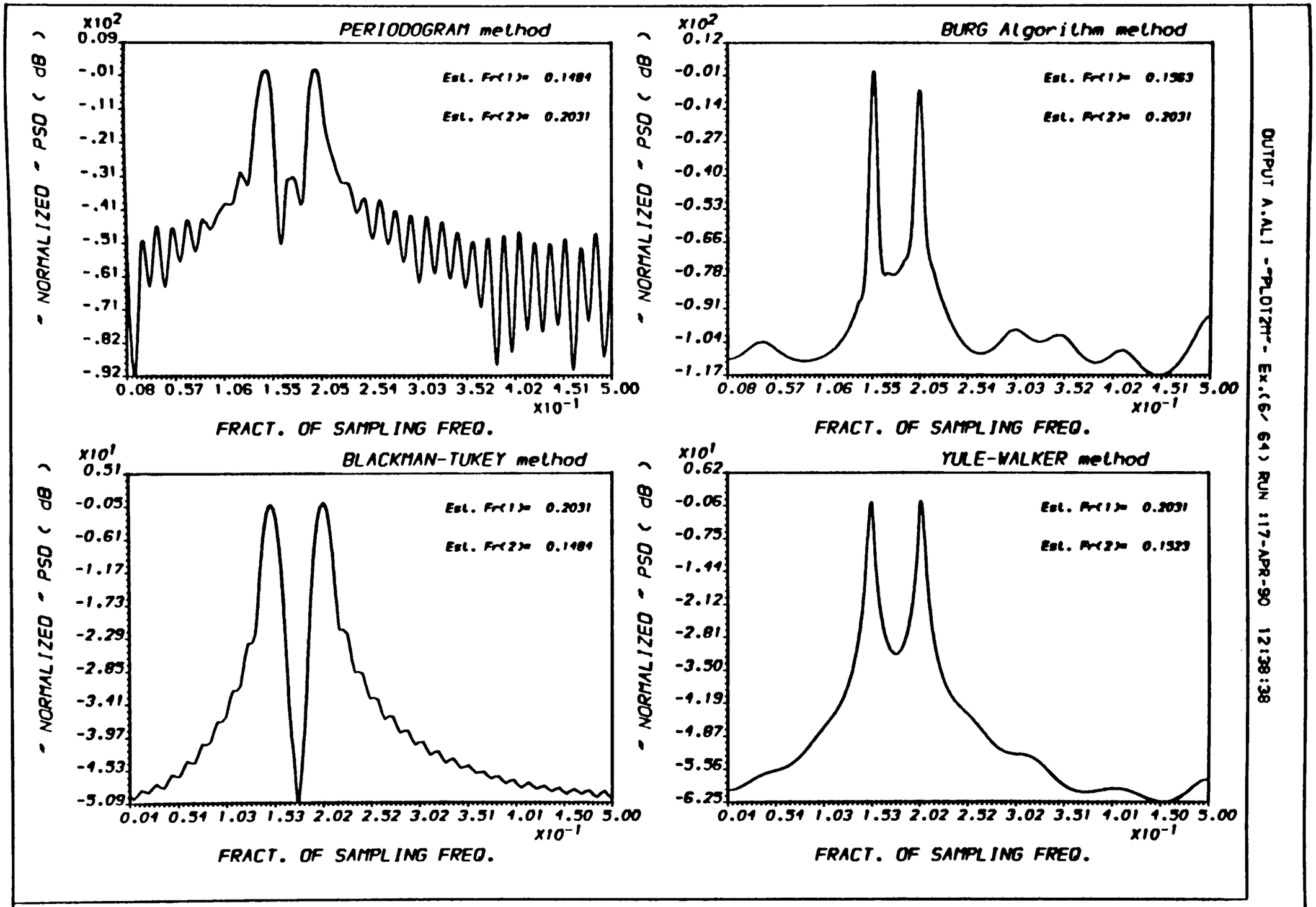

FIG.(3.10) POWER SPECTRAL DENSITY ESTIMATES
* For different PSDE methods *

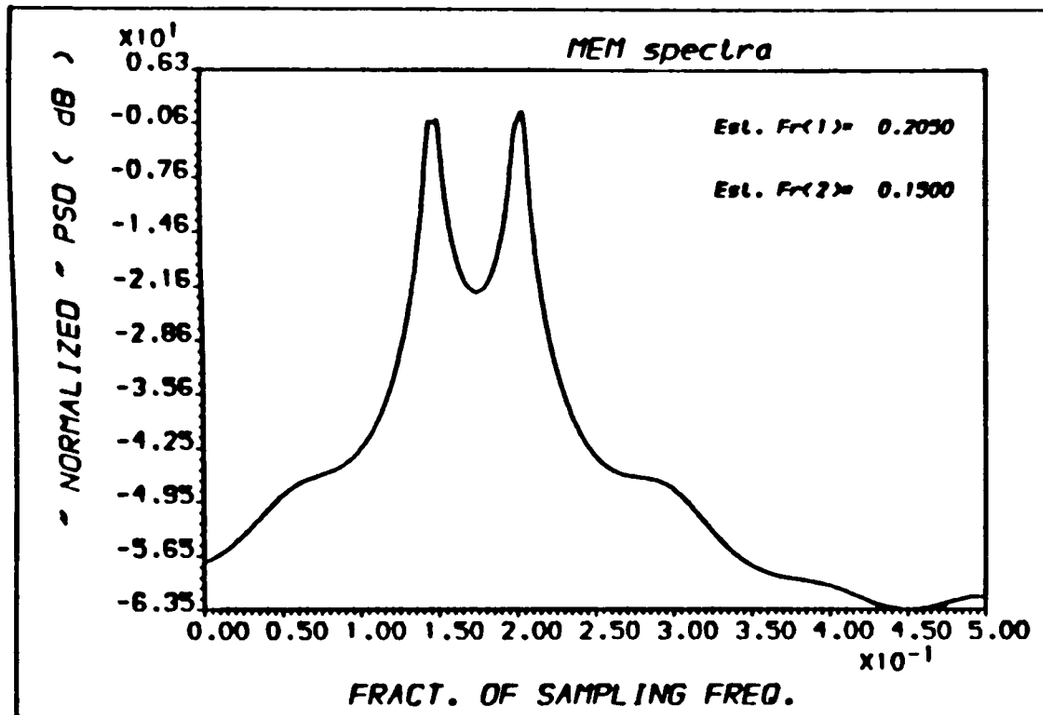

///// Noisy sinusoid

NMAX : 64

SAMP.FR. : 1.000

AMPLITUDS : 1.00 1.00

FREQS. : 0.1500 0.2000

Init.Phase : 0.00 0.00

SNRs (dB): 30.000 30.000

STAND.DEV. : 0.03162277660168838

RESOL.LIMIT :0.0156

SIMULATED Covariance Matrix

OUTPUT A.ALL -PLOT2MT- Ex.(6/ 64) RUN :17-APR-90 12:33:25

FIG.(3.11) POWER SPECTRAL DENSITY ESTIMATE
* For different PSDE methods *

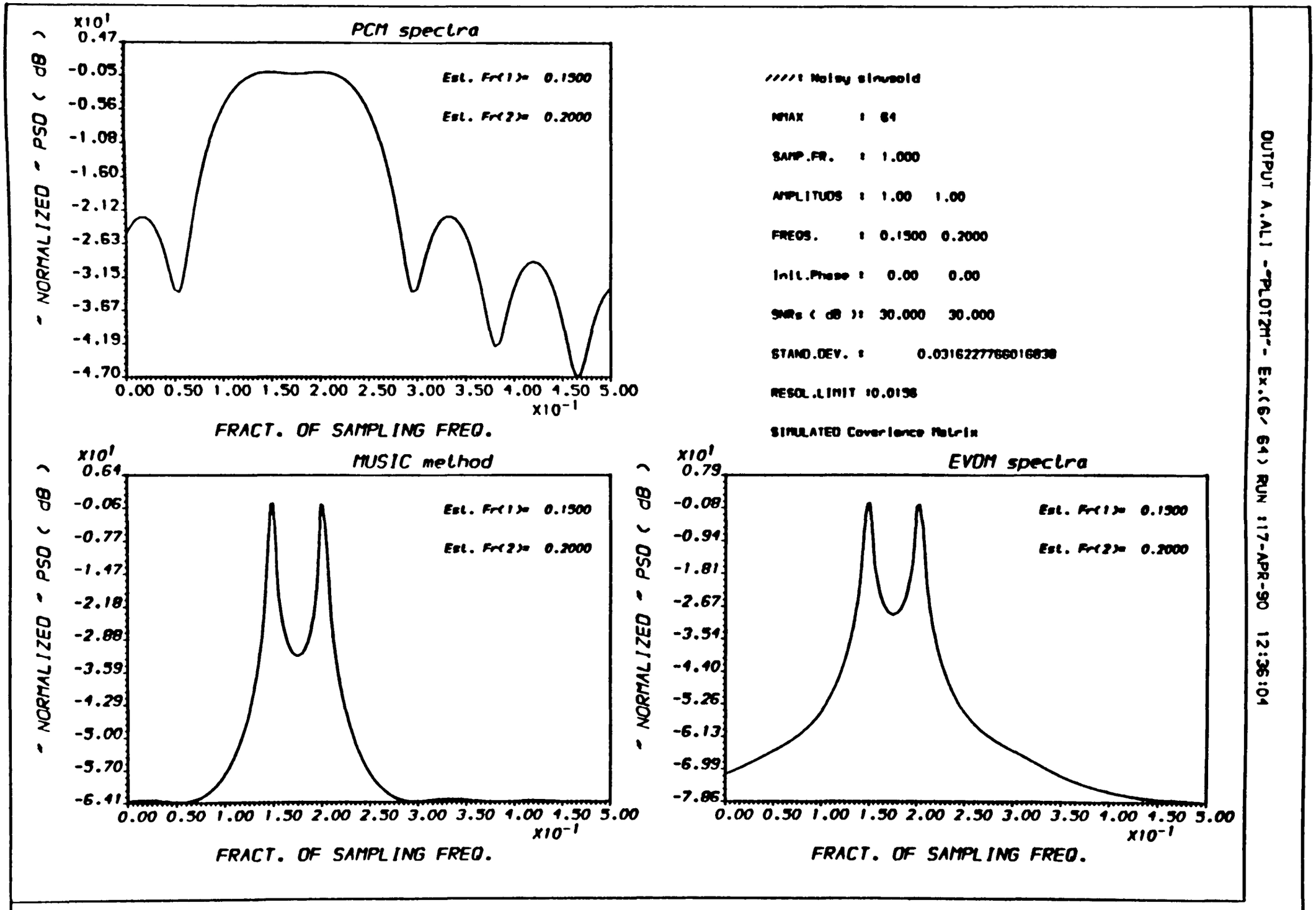

FIG.(3.12) POWER SPECTRAL DENSITY ESTIMATE
* For different PSDE methods *

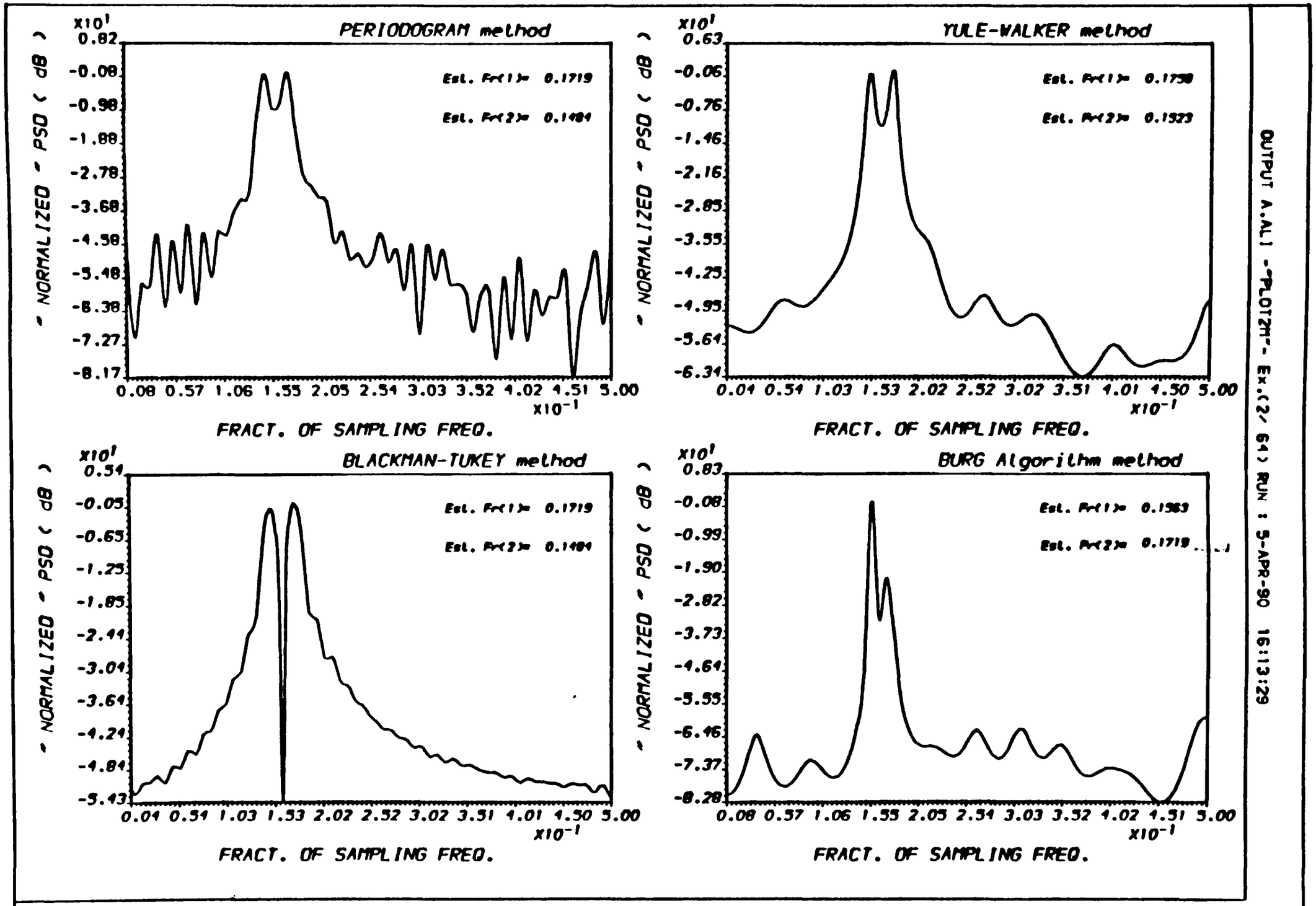

FIG.(3.13) POWER SPECTRAL DENSITY ESTIMATES
* For different PSDE methods *

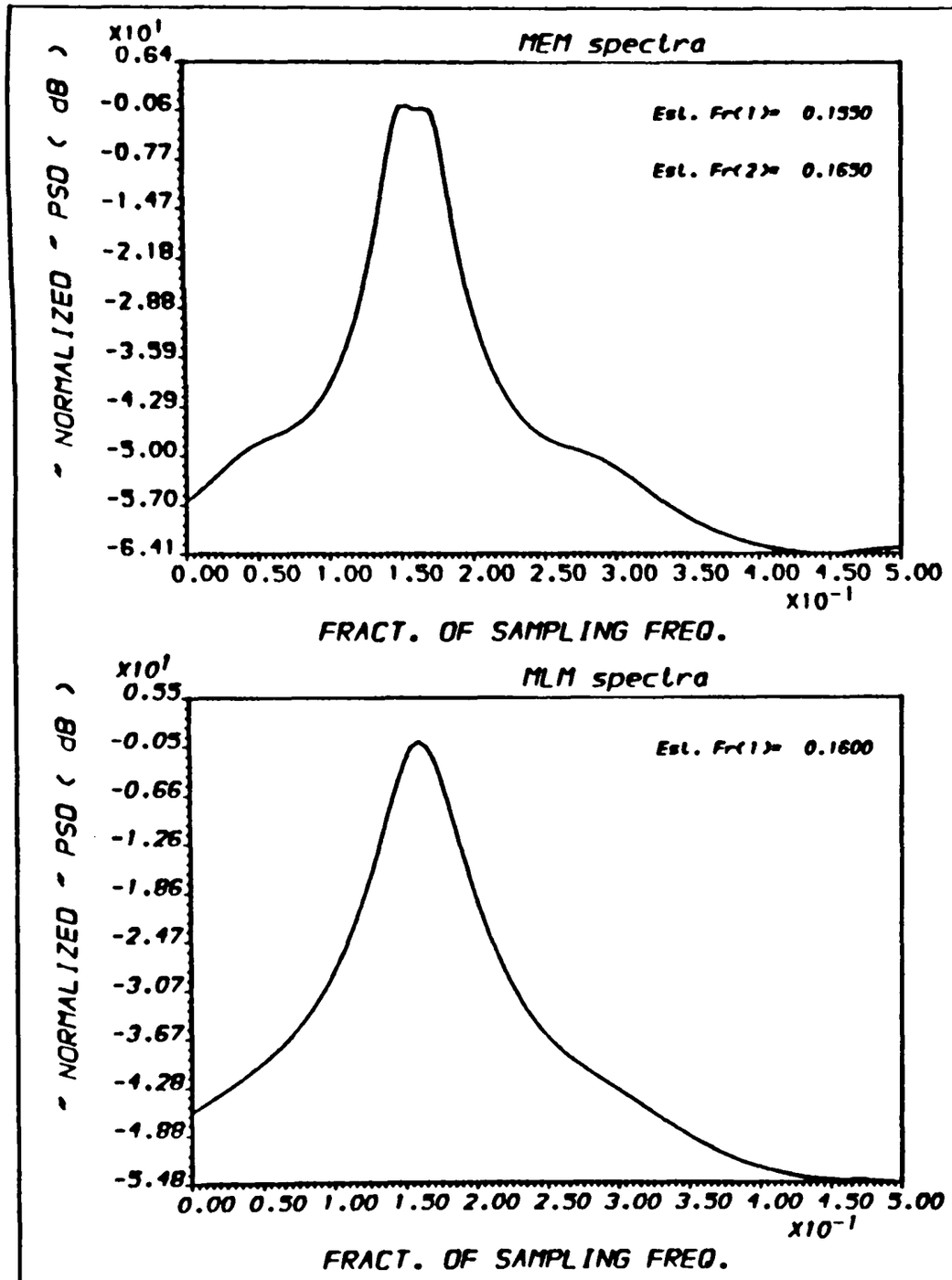


```
/////: Noisy sinusoid

 NMAX        :  64

 SAMP.FR.    :  1.000

 AMPLITUDS   :  1.00   1.00

 FREQS.      :  0.1500  0.1700

 Init.Phase  :   0.00    0.00

 SNRs ( dB ):  30.000   30.000

 STAND.DEV.  :       0.03162277660016838

 RESOL.LIMIT :0.0158

 SIMULATED Coverience Matrix
```

OUTPUT A.ALI -"PLOTZM"- Ex.(5,64) RUN :17-APR-90 11:44:21

FIG.(3.14) POWER SPECTRAL DENSITY ESTIMATE
* For different PSDE methods *

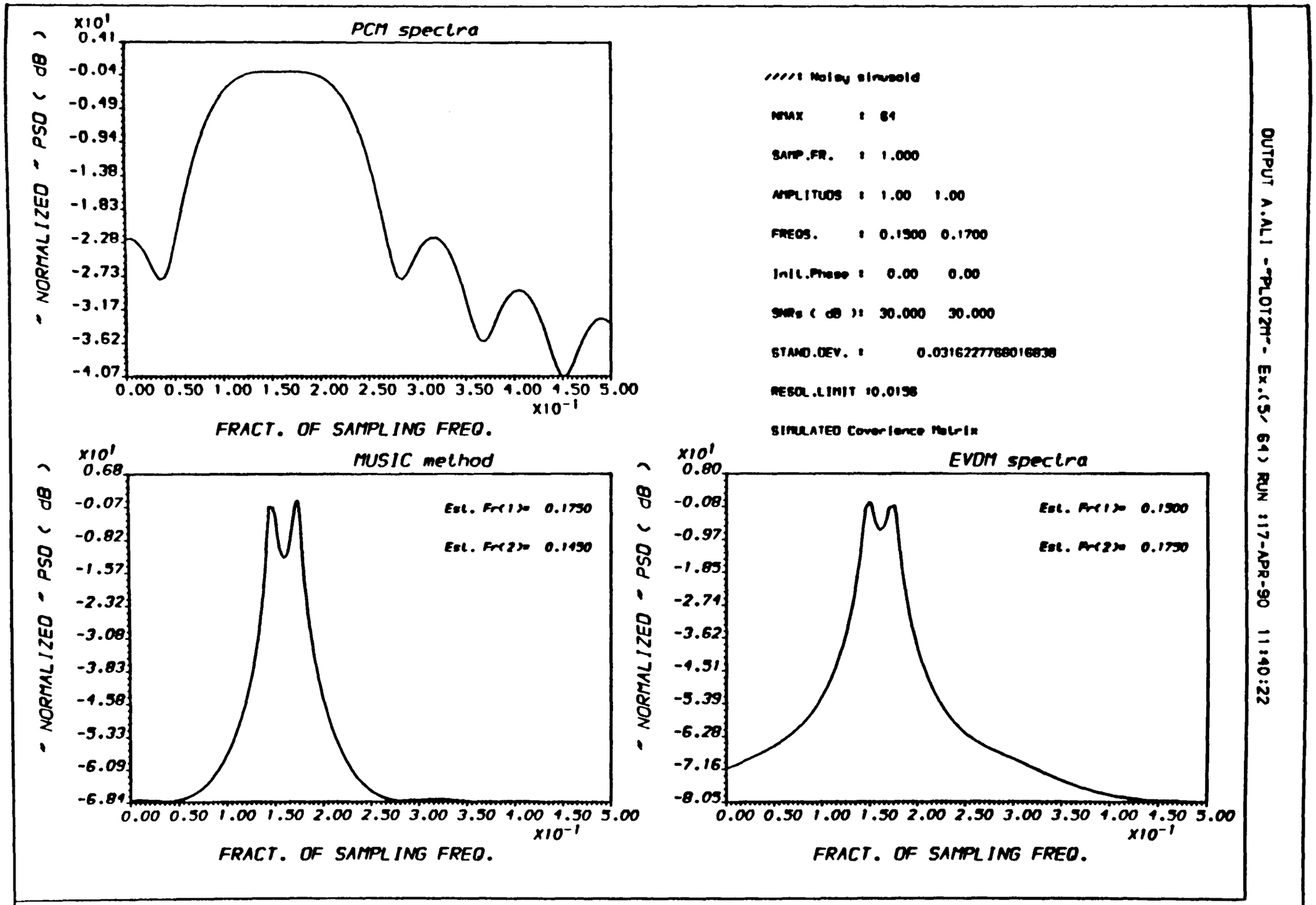

FIG.(3.15) POWER SPECTRAL DENSITY ESTIMATE
* For different PSDE methods *

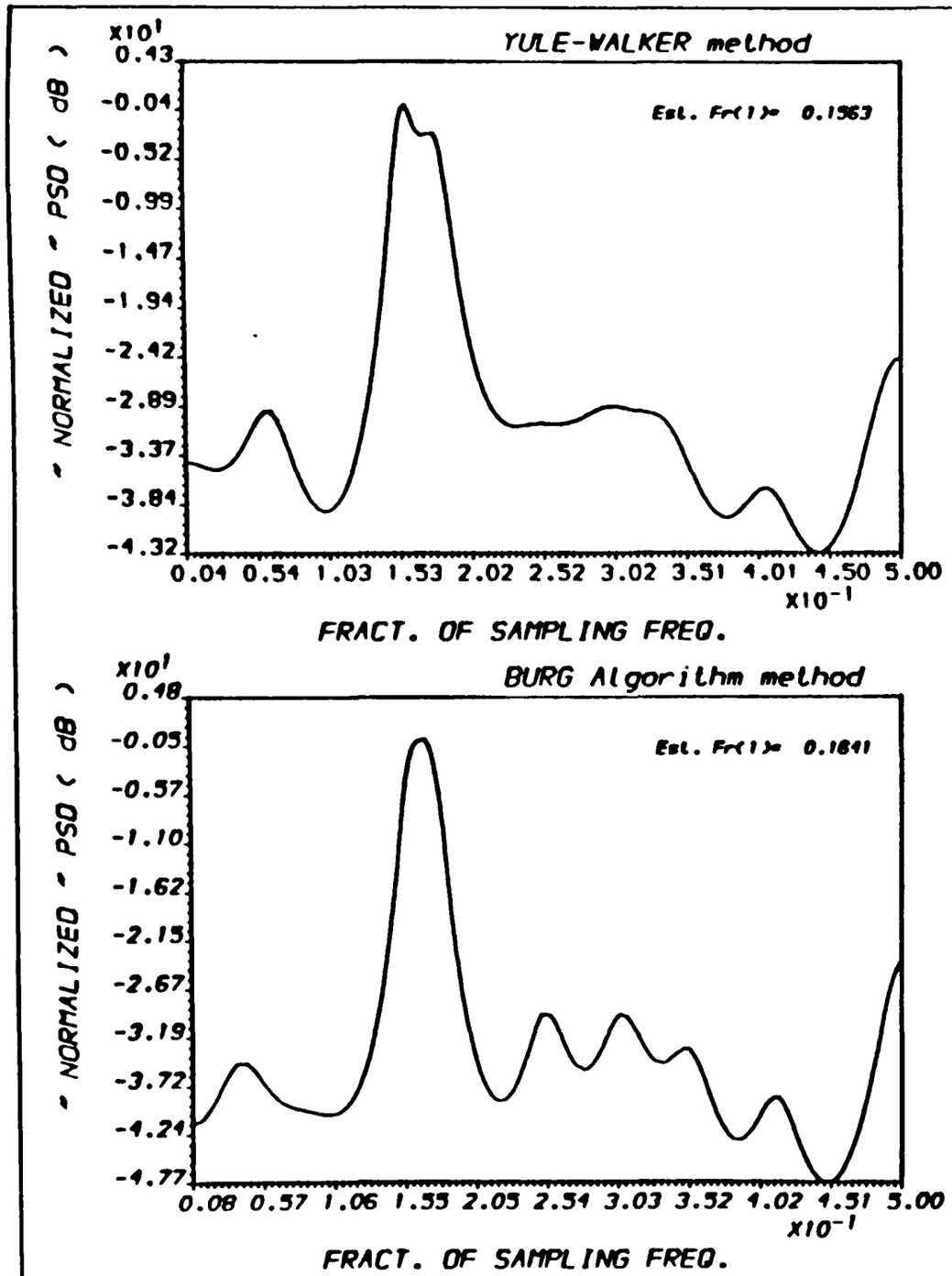

RP : Noisy sinusoid

NMAX : 64

SAMP.FR. : 1.000

AMPLITUDS : 1.00 1.00

FREQS. : 0.1500 0.1700

Init.Phase : 0.00 0.00

SNRs (dB): 5.000 5.000

STAND.DEV. : 0.5823413217808347

RESOL. LIMIT :0.0158

OUTPUT A.ALL -PLOT2MT- Ex.(3, 64) RUN :20-APR-90 14:47:00

FIG.(3.16) POWER SPECTRAL DENSITY ESTIMATES
* For different PSDE methods *

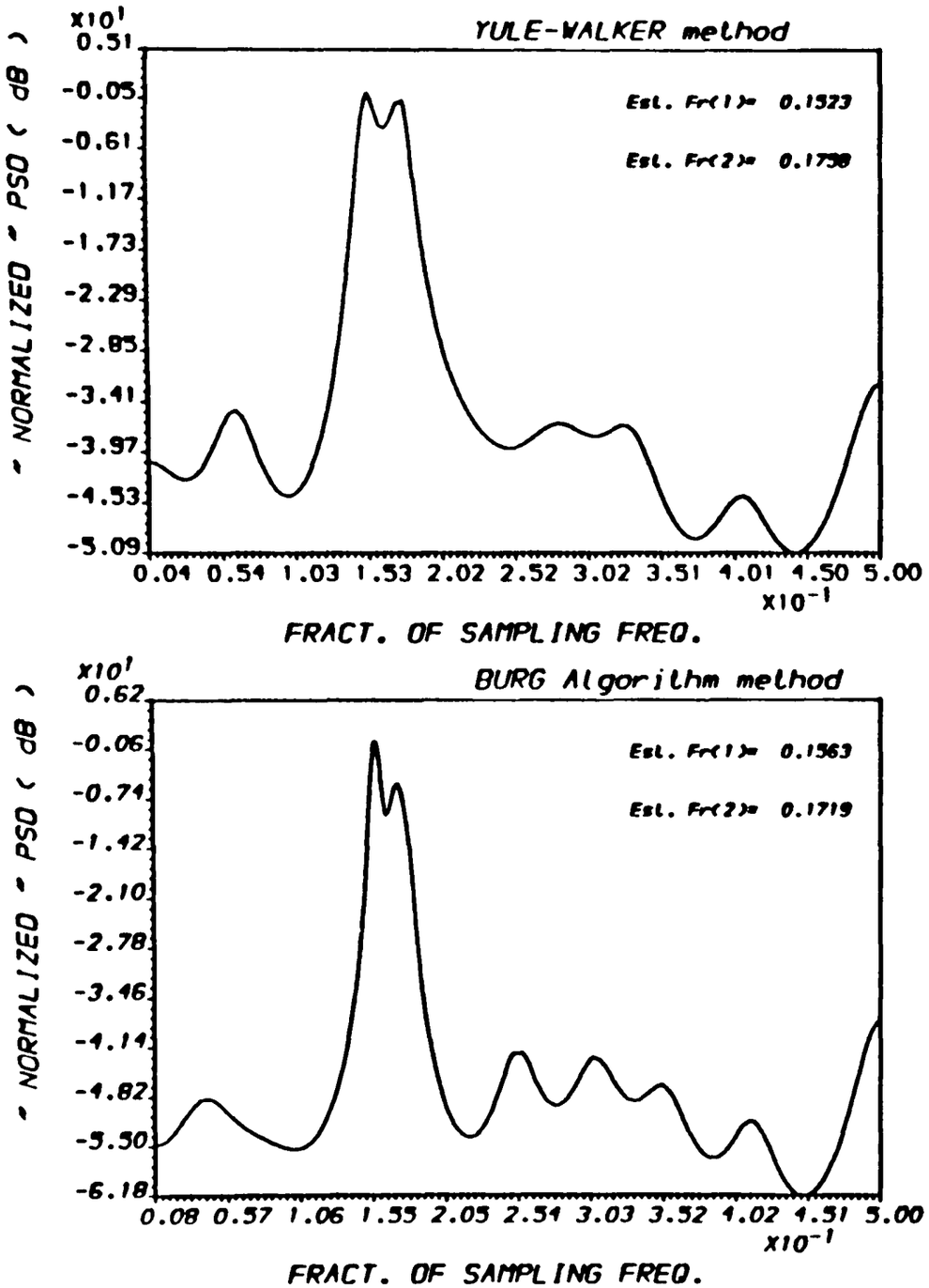

RP : Noisy sinusoid

NMAX : 64

SAMP.FR. : 1.000

AMPLITUDS : 1.00 1.00

FREQS. : 0.1500 0.1700

Init.Phase : 0.00 0.00

SNRs (dB): 10.000 10.000

STAND.DEV. : 0.31622776601683789

RESOL. LIMIT :0.0196

OUTPUT A.ALL -"PLOTZM"- Ex.(3/ 64) RUN :20-APR-90 14:44:22

FIG.(3.17) POWER SPECTRAL DENSITY ESTIMATES
* For different PSDE methods *

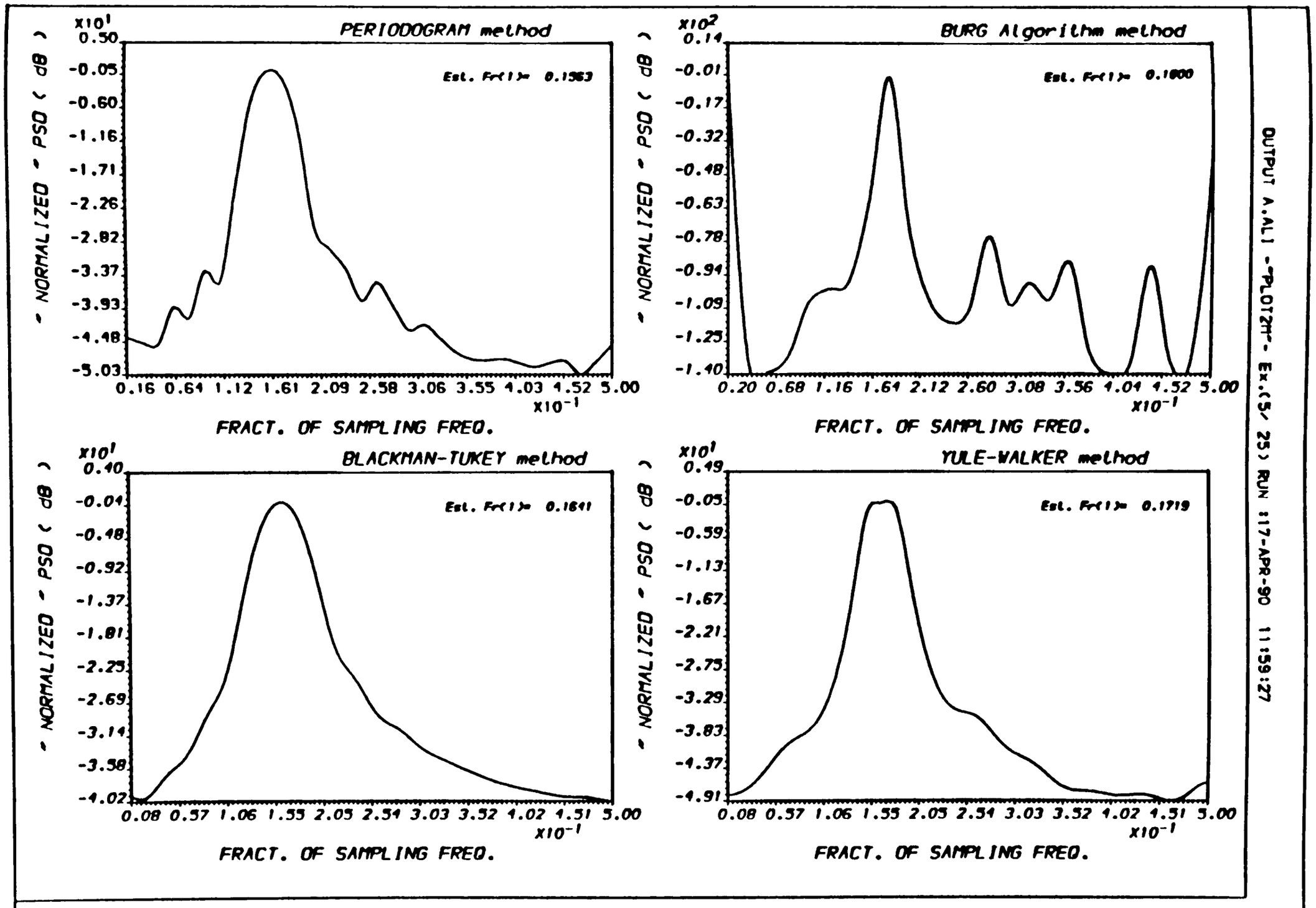

FIG.(3.18) POWER SPECTRAL DENSITY ESTIMATES
* For different PSDE methods *

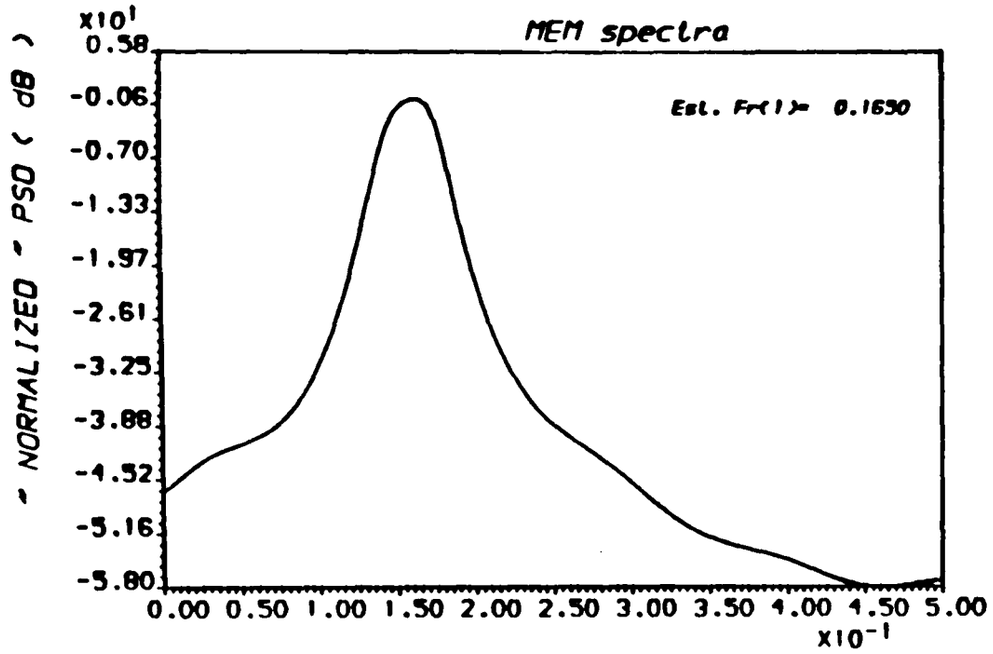


```
/////: Noisy sinusoid

NMAX        :  25

SAMP.FR.    :  1.000

AMPLITUDS   :  1.00   1.00

FREQS.      :  0.1500  0.1700

Init.Phase  :   0.00    0.00

SNRs ( dB ):  30.000   30.000

STAND.DEV.  :        0.031622776601683

REGOL.LIMIT :0.0400

SIMULATED Covariance Matrix
```

OUTPUT A.ALL -"PLOTZM"- Ex.(5/ 25) RUN :17-APR-90 11:53:51

FIG.(3.19) POWER SPECTRAL DENSITY ESTIMATE
* For different PSDE methods *

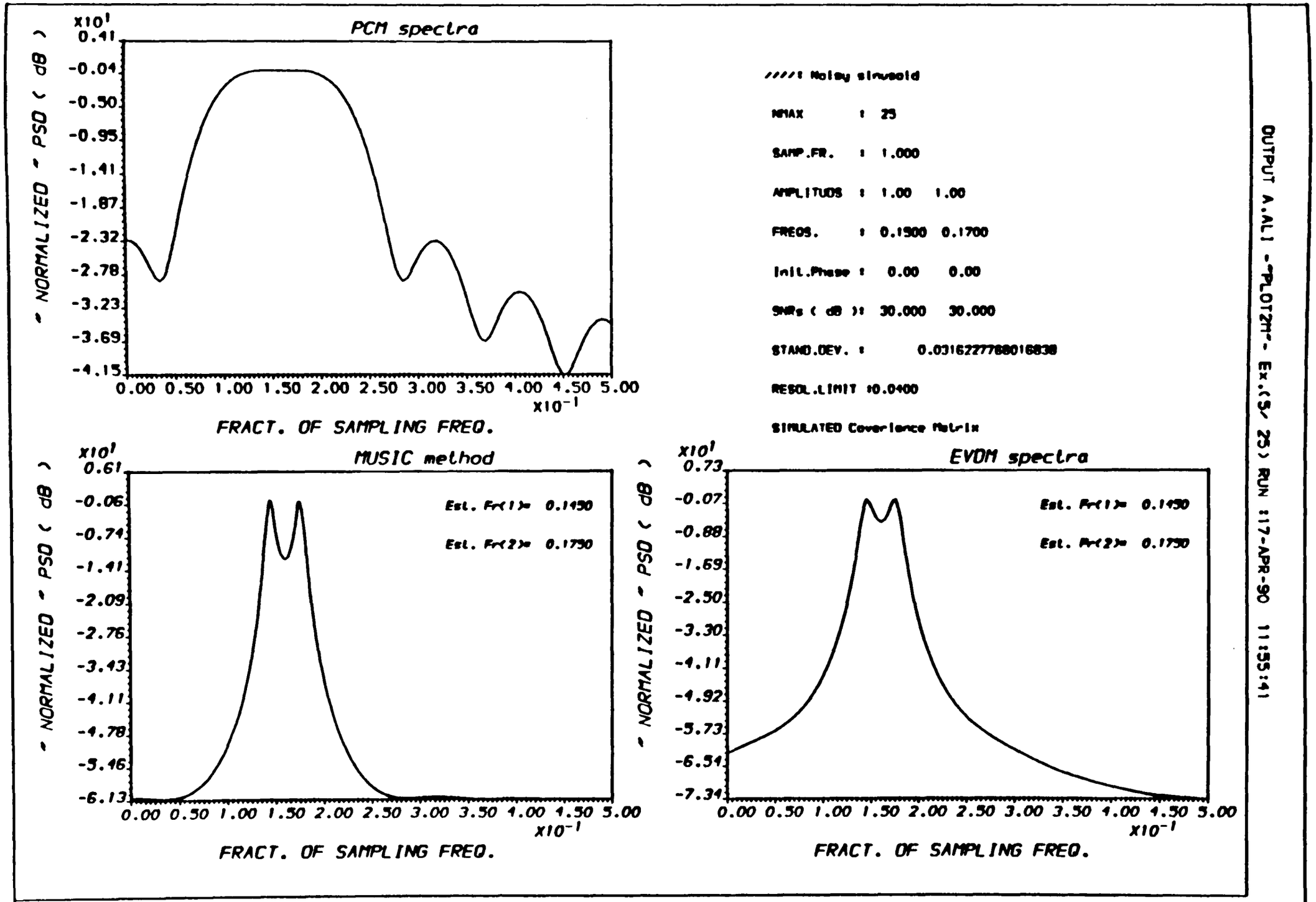

FIG.(3.20) POWER SPECTRAL DENSITY ESTIMATE
* For different PSDE methods *

in which the two equipower signals were assigned normalised frequencies of *(0.15) and (0.18)*.

3.5.2. ESTIMATORS PERFORMANCES :

It is of importance for the estimator which detects and resolves two closely separated signals to estimate their frequencies correctly. The incorrectness of estimation ,which is called Estimation bias, can be defined as *the amount by which the estimated frequencies deviate from the true ones* and which differs alot from one estimator to another. It is the purpose of this section to assess this amount of deviation.

All the *PSD* estimators, *-Fig.(3.4), Fig(3.8)* and *Fig.(3.9)-*, yield an unbiased estimates when there is only one signal present in the random process. On the other hand the estimates are generally biased when there are two signals or more in the random process. The amount of biases that the different estimators will have, depends normally upon how much the two signals frequencies are apart and upon their *SNR.* So, inspecting *Fig(3.10)* to *Fig(3.12)* and *Fig(3.21)* to *Fig(3.23)* shows that the conventional and the parametric approaches gave biased estimates for the two signals whatever large the frequency separation was which means that they are biased estimators, whereas the nonparametric approache gave less biase *(MEM)* or unbiased estimates *(MLM,PCM,MUSIC, and EVM)* when the two signals were sufficiently appart and gave biased estimates when the two signals were separated by less amount, *-see Fig(3.21)* to *Fig(3.23)-.*

As a result, we can say that *Eigen Vector Decomposition Technique* possesses the best performance among the different approaches to *PSDE* because, as we have just seen, it has the

best detection and resolution capabilities and exhibits less estimation biases.

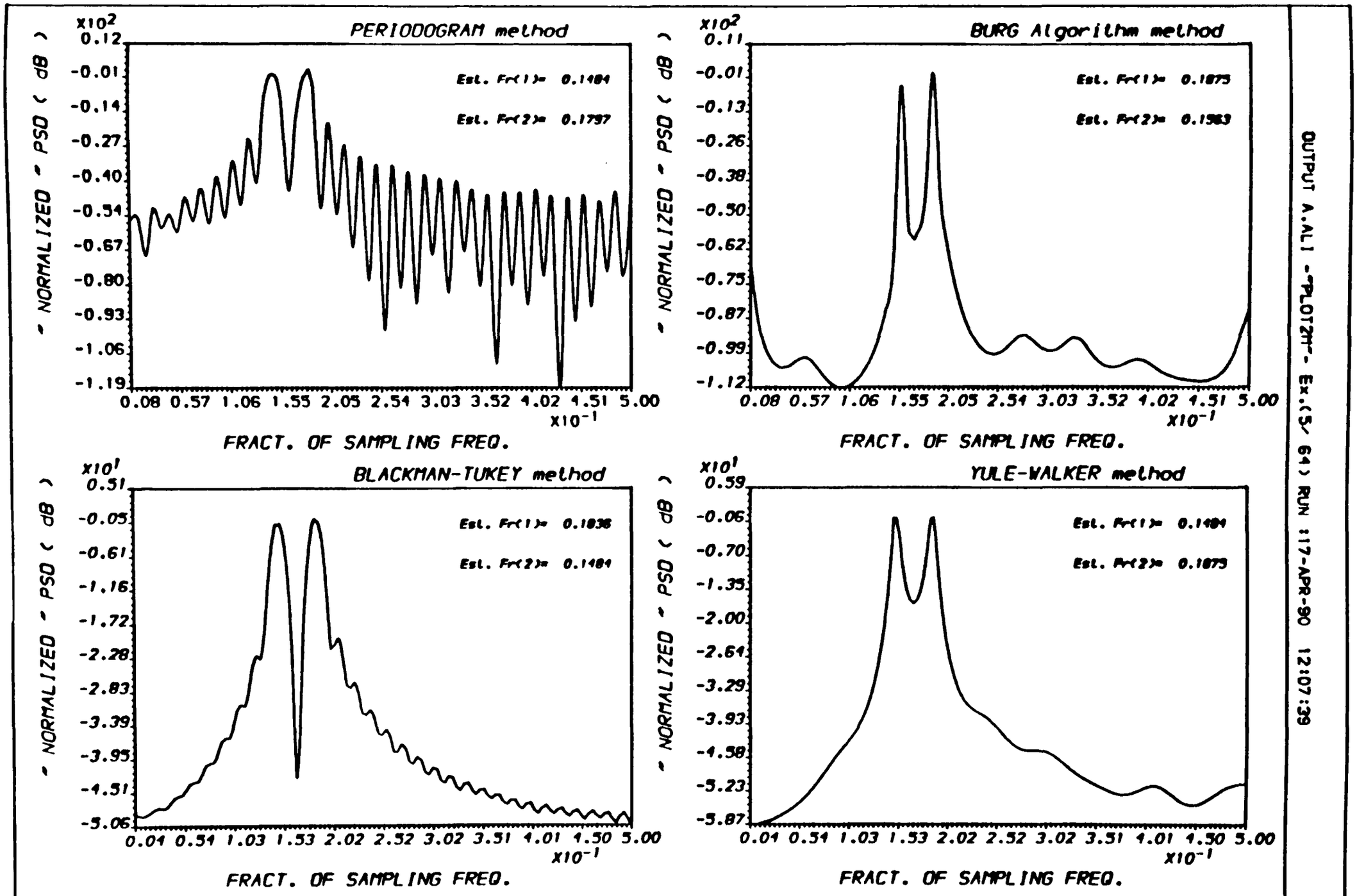

FIG.(3.21) POWER SPECTRAL DENSITY ESTIMATES
* For different PSDE methods *

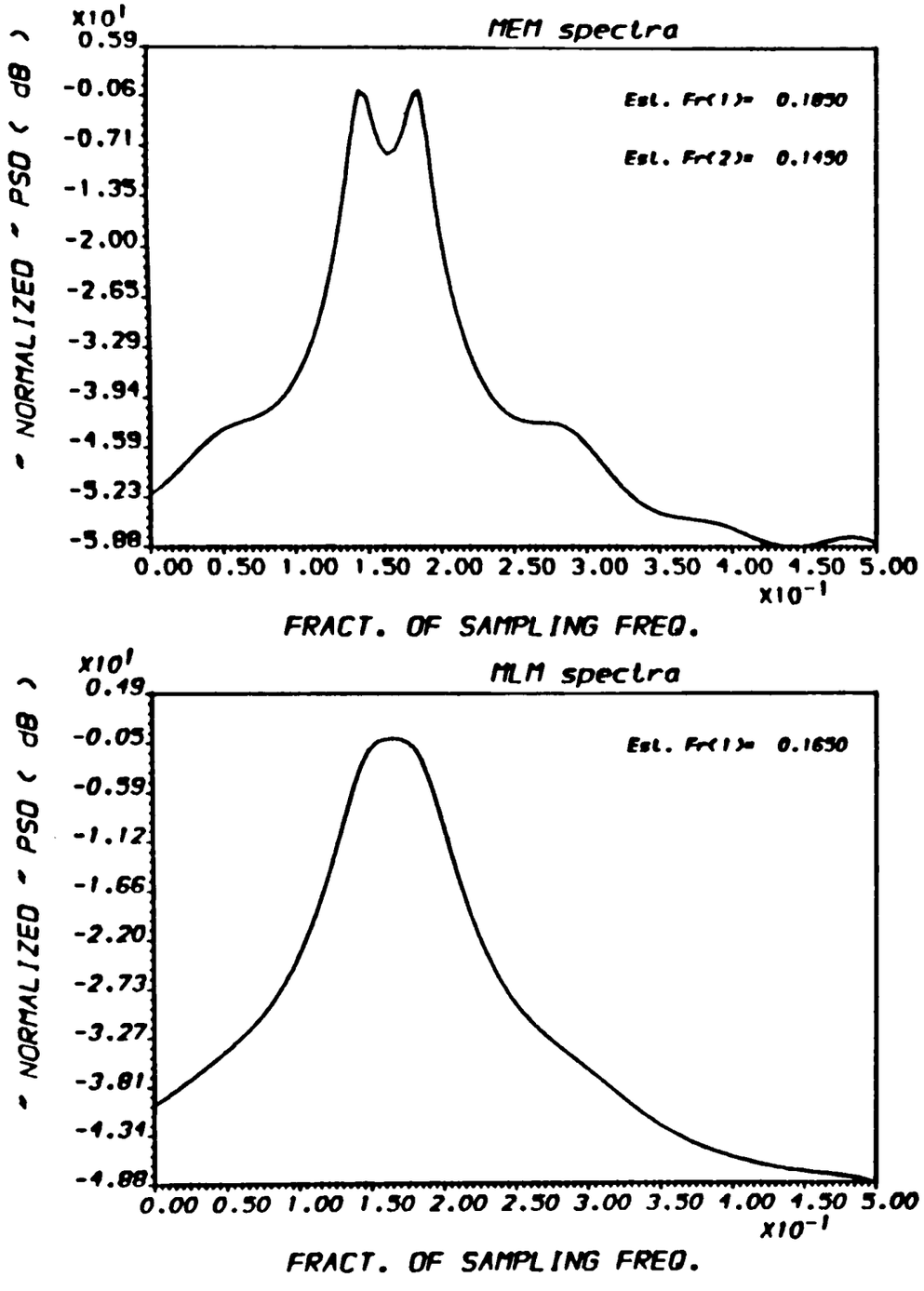


```
/////: Noisy sinusoid

NMAX        :  64

SAMP.FR.    :  1.000

AMPLITUDS   :  1.00   1.00

FREQS.      :  0.1500  0.1800

Init.Phase  :   0.00    0.00

SNRs ( dB ) :  30.000   30.000

STAND.DEV.  :        0.031622776601683838

RESOL.LIMIT :0.0158

SIMULATED Coveriance Matrix
```

OUTPUT A.ALL -"PLOT2MT- Ex.(5/ 64) RUN :17-APR-90 11:47:22

FIG.(3.22) POWER SPECTRAL DENSITY ESTIMATE
* For different PSDE methods *

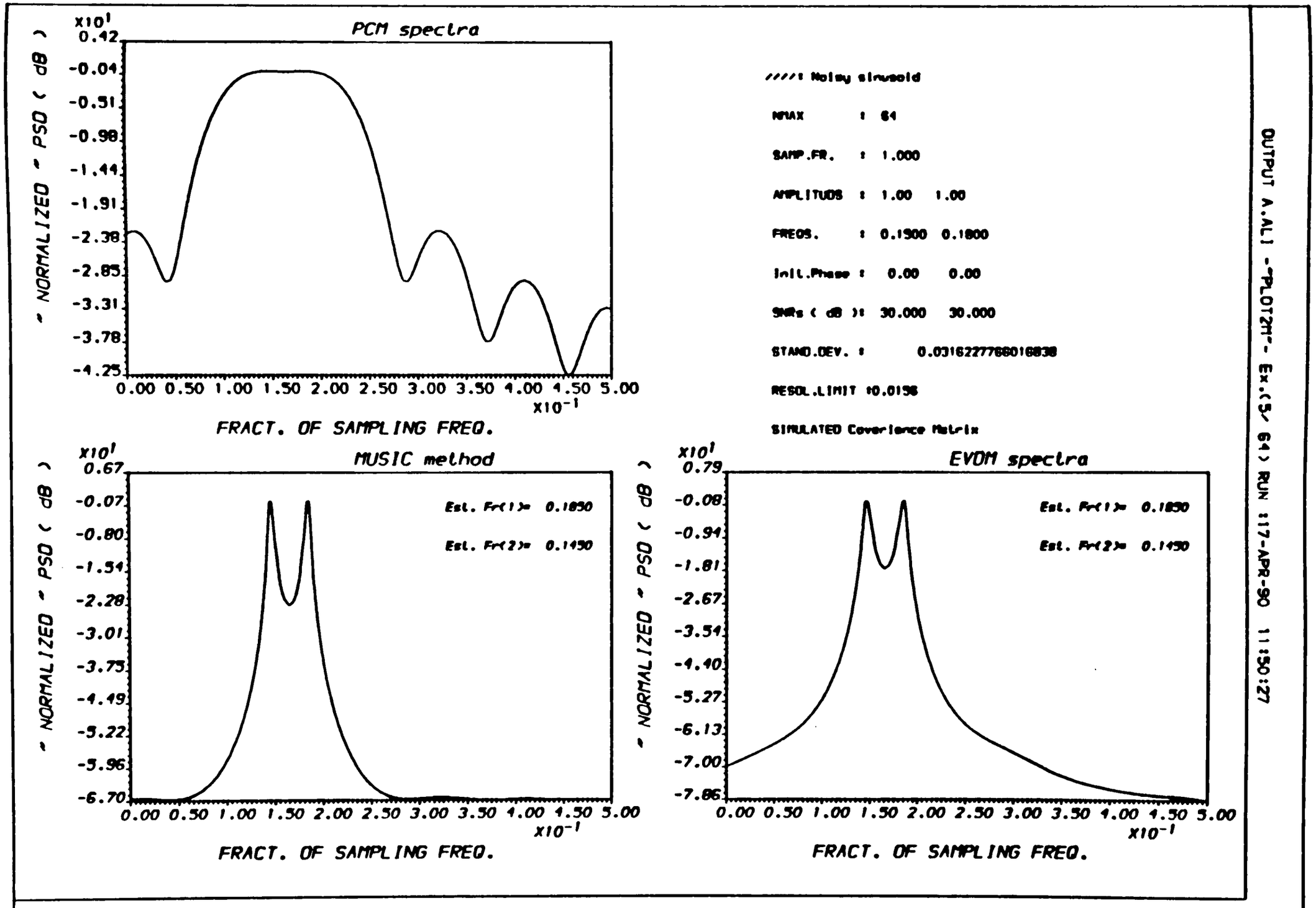

FIG.(3.23) POWER SPECTRAL DENSITY ESTIMATE
* For different PSDE methods *

Chapter Four

HIGH RESOLUTION PSD ESTIMATORS

CHAPTER FOUR

HIGH RESOLUTION PSD ESTIMATORS

4.1. INTRODUCTION :

Several techniques, such as *MLM* and *MEM,* which were developed originally for spectral estimation in the time domain have been employed in array signal processing, *-for the solution of Direction Of Arrival (DOA)* and *Source Location finding (SLF) problems-,* because of their high resolution capabilities. But the significantly degraded directional spectrum estimates they gave, due to the correlation between the emitting sources or the existence of coloured noise, created the neccessity for new methods possessing higher resolution and, or lower computational burden.

Eigen Vector Decomposition Technique *(EVDT)* for power spectral density estimation is the most promising approach. It is mainly used for the processing of signals received by spatially distributed arrays of sensors, which attracted considerable attention over the past twenty years.

The theory of the *MLM, MEM* and *EVDT* algorithms, which were mentioned briefly in the literature review chapter, are presented here in order to give the neccessary background for the development of the proposed new algorithm.

Finally, the partitioning of eigen vectors into two subspaces, the Signal Subspace *(SSP)* and the Noise Subspace *(NSS)* is presented in the last section, where a new criterion for separating the eigen values of these two subspaces is proposed and tested using both the true and the estimated covariance matrices.

4.2. THEORETICAL MODEL :

Let $X^T = [\, x_1 x_2 \ldots\ldots x_N \,]$ represents the data vector of a discrete, wide sense stationary random process, where

$$x_n = \sum_{i=1}^{p} A_i \, exp[j(n\omega_i + \phi_i)] + w_n \qquad (4.2.1)$$

$$= \sum_{i=1}^{p} s_{in} + w_n$$

The random process is assumed to consist of $p(\leq\infty)$ sinusoids contaminated by a white Gaussian noise. Each sinusoid has unknown amplitude A_i, normalised frequency ω_i $(0 \leq \omega_i \leq \pi)$ and phase ϕ_i which has a uniform probability distribution over $[0, 2\pi]$.

Now, let us suppose that we filtered this discrete time series through a filter, whose output gain, at a particular frequency (or frequencies), is constrained to unity.

$$i.e \quad A^H C = 1 \qquad (4.2.2)$$

where $A = col(a_0 \; a_1 \; \ldots\ldots \; a_{M-1})$ represents the filter coefficients *(weights)* vector, H denotes complex conjugate transpose and C is the constraint vector *(sometimes called the frequency search vector)*, the elrments of which at any frequency ω_n, $n=0,\ldots\ldots,N-1$, are given by :

$$c_i(\omega_n) = e^{ji\omega_n} \qquad i = 0,1,\ldots\ldots,M-1 \qquad (4.2.3)$$

The optimized filter coefficients subject to this constraint -*see section (2.4.2.)*-, will be :

$$A_{OPT} = \frac{R_{XX}^{-1}\, C^{H}}{C^{H}\, R_{XX}^{-1}\, C} \qquad (4.2.4)$$

and the Maximum Likelihood *(ML) PSD* estimate *[9]* and *[34]* is given by :

$$P_{ML} = \left[C^{H}\, R_{XX}^{-1}\, C \right]^{-1} \qquad (4.2.5)$$

where R_{XX}^{-1} is the Inverse Covariance Matrix *(ICM)*.

So the task at this stage is to compute the theoretical covariance matrix. Taking the expectation of equation *(4.2.1)* gives :

$$\left.\begin{aligned} R_{XX}(1,k) &= E\left[x_1 x_k^{*} \right] \qquad 1 = k = 1,2, \ldots\ldots ,M \\ &= E\left[\left(\sum_{i=1}^{p} s_{i1} + w_1 \right) \left(\sum_{i=1}^{p} s_{ik}^{*} + w_k^{*} \right) \right] \\ &= E\left[\left(\sum_{i=1}^{p} s_{i1} \right) \left(\sum_{i=1}^{p} s_{ik}^{*} \right) \right] + E\left[\sum_{i=1}^{p} s_{i1} w_k^{*} \right] \\ &+ E\left[w_1 \sum_{i=1}^{p} s_{ik}^{*} \right] + E\left[w_1 w_k^{*} \right] \end{aligned}\right\} (4.2.6)$$

Now, let us assume that the signals are independent, *i.e* uncorrelated between each other, and they are uncorrelated with the white Gaussian noise. Also, the noise is assumed to have zero mean and variance equals σ_w^2.Hence,

$$E\Big[\sum_{i=1}^{p} s_{il} w_k^*\Big] = E\Big[w_l \sum_{i=1}^{p} s_{ik}^*\Big] = 0 \qquad (4.2.7)$$

$$E\Big[w_l w_k^*\Big] = \begin{cases} 0 & \text{for } l \neq k \\ \sigma_w^2 & \text{for } l = k \end{cases} \qquad (4.2.8)$$

and $$E\Big[\Big(\sum_{i=1}^{p} s_{il}\Big)\Big(\sum_{i=1}^{p} s_{ik}^*\Big)\Big] =$$

$$= E\Big[\Big(\sum^{p} A_{il}\ exp[j(l\omega_i+\phi_i)]\Big)\Big(\sum^{p} A_{ik}^*\ exp[-j(k\omega_i-\phi_i)]\Big)\Big]$$

$$= E\Big[\sum_{i=1}^{p} A_{i1} A_{ik}^{*} \; exp[j(1-k)\omega_i] \Big]$$

$$= \begin{cases} \sum_{i=1}^{p} P_i & for \quad 1 = k \\ \sum_{i=1}^{p} P_i \; exp[j(1-k)\omega_i] & for \quad 1 \neq k \end{cases} \qquad (4.2.9)$$

where P_i is the power of signal i.

Using equations *(4.2.7) to (4.2.9)*, equation *(4.2.6)* can be reduced to :

$$R_{xx}(1,k) = \begin{cases} \sum_{i=1}^{p} P_i \; exp[j(1-k)\omega_i] & for \quad 1 \neq k \\ \sum_{i=1}^{p} P_i + \sigma_w^2 & for \quad 1 = k \end{cases} \qquad (4.2.10)$$

which means that the covariance matrix of the random process can be considered as the sum of the signal covariance matrix and the noise covariance matrix.

$$i.e \quad R_{xx} = R_{ss} + R_{ww} \qquad (4.2.11)$$

where R_{xx} is the Total random process Covariance Matrix *(TCM)*.

R_{ss} is the Signal Covariance Matrix *(SCM)*.

$$R_{ss}(1,k) = \begin{bmatrix} R_{ss}(1,1) & R_{ss}(1,2) & \cdots\cdots & R_{ss}(1,M) \\ R_{ss}(2,1) & R_{ss}(2,2) & \cdots\cdots & R_{ss}(2,M) \\ \vdots & \vdots & & \vdots \\ R_{ss}(M,1) & R_{ss}(M,2) & \cdots\cdots & R_{ss}(M,M) \end{bmatrix}$$

$R_{ss}(1,k)$ can be computed -*using Equ.(4.2.9)*- as follows :

$$R_{ss}(1,k) = \begin{cases} \sum_{i=1}^{p} P_i \exp[j(1-k)\omega_i] & \text{for } 1 \neq k \\ \sum_{i=1}^{p} P_i & \text{for } 1 = k \end{cases} \qquad (4.2.12)$$

$R_{ww} = \sigma_w^2 I$ is the Noise Covar. Matrix and I is the Identity matrix.

Substituting equation *(4.2.11)* in equation *(4.2.5)*, we get :

$$P_{ML} = \left[C^H [R_{ss} + R_{ww}]^{-1} C \right]^{-1}$$

orusing theory of matrices, equation*(4.2.5)*canbewritten as

$$P_{ML} = [C^H R_{ss}^{-1} C + C^H R_{ww} C]^{-1} \qquad (4.2.13)$$

which means that the *MLSE* of the total random process is in fact the sum of the *MLSE* of the signals only process and the *MLSE* of the noise only process, *-we will return to it later-*.

This power spectral density estimator *-Equ.(4.2.5) and so Equ.(4.2.13)-* is unable to resolve two closely separated sinusoids when the separation is less than the reciprocal of the observation time $T = N\Delta t$, *i.e less than Fourier Resolution Limit.*

4.3. MAXIMUM ENTROPY METHOD :

Maximum entropy method can be thought of as a discrete filter which adjusts itself to be least-disturbed by power at frequencies different from those to which it is tuned, *[26]*. This operation of the *ME* filter may be considered as minimizing the output power subject to the constraint

$$A^H Z = 1 \qquad (4.3.1)$$

where vector Z is the same vector C in equation *(4.2.2)*. Since there is a great flexibility in defining the constraint vector Z, *[20]* and *[27]*, it is useful to define it as :

$$Z^T = [\ 1,0,0,\ \ldots\ldots\ ,0\ ] \qquad (4.3.2)$$

which means that the constraint vector Z will force the weight vector A to have the first element equal to one.

Using this definition of the constraint vector *-Equ.(4.3.2)-*, the optimum weight, subject to the constraint specified in equation *(4.3.1)*, will be reduced to

$$A_{OPT} = \frac{R_{XX}^{-1} Z^*}{R_{XX}^{-1}(1,1)} \qquad (4.3.3)$$

where $R_{XX}^{-1}(1,1)$ is the first diagonal element in the inverse covariance matrix. The output power of this filter *[18]*, will be :

$$P_{ME} = \left| C^H A \right|^{-2} \qquad (4.3.4)$$

$$= \left| C^H \frac{R_{XX}^{-1} Z^*}{R_{XX}^{-1}(1,1)} \right|^{-2}$$

But $R_{XX}^{-1} Z^*$ equals the first column of R_{XX}^{-1}

$$\therefore \quad P_{ME} = \left[R_{XX}^{-1}(1,1) \right]^2 \left| \sum_{n=0}^{N-1} \sum_{i=1}^{M} c_i(\omega_n) R_{XX}^{-1}(i,1) \right|^{-2} \qquad (4.3.5)$$

where $c_i(\omega_n)$, $n=0, \ldots N-1$, as stated before, is the i^{th} element of the constraint vector C at frequency ω_n.

NOTE : It is also possible *[50]*, to define the constraint vector as $Z^T = (0,0,\ldots\ldots,1)$ which in turn means that we fix the end element weight to be unity. Then the output power will be given by :

$$P_{ME} = \left[R_{XX}^{-1}(M,M) \right]^2 \left| \sum_{n=0}^{N-1} \sum_{i=1}^{M} c_i(\omega_n) R_{XX}^{-1}(M-i+1,M) \right|^{-2} \qquad (4.3.6)$$

which gives the same spectral estimate as that obtained by equation *(4.3.5)*.

This method is sometimes called *"Power Inversion Constraint Method (PICM)"*, and is useful when the wanted signal is below the noise level.

4.4. EIGEN VECTOR DECOMPOSITION TECHNIQUES for PSDE :

There is a precise analogy between Direction Of Arrival *(DOA)* estimation in the space domain and the Frequency Estimation *(FE)* in the time domain, which allows almost all the array processing approaches, developed for bearing problems, to be used for frequency estimation problems.

This problem *-frequency estimation or retrieving-*, which is highly related to the *PSD* estimation, has been treated by many researchers so far. Among the most popular techniques is that developed by *Pisarenko* in *1969 -see chapter 2-*,which is based on the use of the smallest eigenvector of the observed process.

4.4.1. The SIGNAL SUBSPACE and the NOISE SUBSPACE :

The eigen values and eigen vectors of matrix R_{XX} are usually obtained by utilizing some standard methods of numerical analysis. However, eigen data can be obtained directly from the data samples by using the adaptive algorithms which can recursively update the eigen vector estimate using incoming new samples directly *[29]*. Using the theory of matrices *[23]*, the eigen vectors can be defined by the property :

$$R_{xx}V_i = \lambda_i V_i \qquad i = 1, \ldots\ldots, M \qquad (4.4.1)$$

where V_i, λ_i are the eigen vectors and the associated eigen values respectively.

Using this identity the covariance matrix can be represented by its eigen data -*see Appendix B*- as follows :

$$R_{xx} = \sum_{i=1}^{M} \lambda_i V_i V_i^H \qquad (4.4.2)$$

For the ideal case, where the covariance matrix is known and assuming, as before, that the signals are uncorrelated between each other and with the noise, equation *(4.4.2)* can be written as follows :

$$R_{xx} = \sum_{i=1}^{p} \lambda_i V_i V_i^H + \sigma_w^2 I \qquad (4.4.3)$$

But, as we know, in the actual situation the covariance matrix is normally estimated from the data samples, and the smallest eigen values will not have the same value (σ_w^2). So *Equ.(4.4.3)* will be as below :

$$R_{xx} = \sum_{i=1}^{p} \lambda_i V_i V_i^H + \sum_{i=p+1}^{M} \lambda_i V_i V_i^H \qquad (4.4.4)$$

where $\lambda_1 \geq \lambda_2 \geq \lambda_3 \geq \ldots\ldots \geq \lambda_M$, which means that we have p largest eigen values represent the p signals and $(M-p)$ smallest eigen values represent the noise signal.

Inspecting equation *(4.4.4)*, the first *RHS* term spanned by the *p* eigen vectors, corresponding to the *p* largest *(signal)* eigen values, is called the Signal Subspace *(SSP)*, whereas the second term spanned by the remaining *(M-p)* eigen vectors, corresponding to the *(M-P)* smallest *(noise)* eigen values, is called the Noise SubSpace *(NSP)*.

The separation of the signal subspace from the noise subspace *-which will be dealt with in section (4.5)-* is called Partitioning. The accuracy of the *EVDTs* depends mainly upon this partitioning, which is normaly difficult and not obvious.

4.4.2. EIGEN VECTOR method :

Let us assume that $C = BF$ can maximize the resolution of the estimator of equation *(4.2.5)*, where B is a matrix to be found, then

$$P_{ML} = \left[F^H B^H R_{XX}^{-1} BF \right]^{-1} \qquad (4.4.5)$$

Matrix B must have the property that those elements of the frequency vector F lying in its null space correspond only to the signal frequencies which actually exist in the random process.

Let $B = B_{WEV}$ be the matrix which consists of the sum of the outer products of the noise eigen vectors, then

$$B_{WEV} = \sum_{i=p+1}^{M} V_i V_i^H \qquad (4.4.6)$$

Now, due to the orthogonality relationship between the p largest eigen vectors *-signal subspace-*, and the $(M-p)$ smallest eigen vectors *-noise subspace-*, we have :

$$B_{WEV} V_i = 0 \qquad for \quad i = 1, \ldots\ldots, p$$

Or in other words, the p largest eigen vectors lie in the null space of the matrix B_{WEV}, and vector F represents any of these vectors, This is the only choice by which we can obtain perfect resolution of multiple signals from the *EVDT*, Thus :

$$B_{WEV}^{H} \; R_{XX}^{-1} \; B_{WEV} = \sum_{i=p+1}^{M} \frac{1}{\lambda_i} V_i V_i^{H} \qquad (4.4.7)$$

which represnts the noise inverse covariance matrix *(NICM)*. Equation *(4.4.5)* becomes :

$$P_{EV} = \left[F^{H} \left(\sum_{i=p+1}^{M} \frac{1}{\lambda_i} V_i V_i^{H} \right) F \right]^{-1} \qquad (4.4.8)$$

$$Or \qquad P_{EV} = \left[F^{H} \; R_{WW}^{-1} \; F \right]^{-1} \qquad (4.4.9)$$

which is the same as the second *RHS* term of equation *(4.2.13)*.

Equation *(4.4.9)* represents the Eigen Vector Method *(EVM)* proposed by *D.H.Johnson and S.R.DeGraaf [27]*, which allows the computation of the *ML* spectra, with higher resolution capability, by using only the Noise Covariance Matrix *(NCM)* instead of the Total Covariance Matrix *(TCM)* used in the

conventional *MLM ,-Equ.(4.2.13)-,* developed by *Capon [9].*

4.4.3. MUSIC method :

Now, if we assume that in equation *(4.4.8)* all the *(M-p)* smallest eigen values are set to the same value *(λ)*, then the *PSDE* will be as follows :

$$P_{MUSIC} = \left[K\left[F^{H}\left(\sum_{i=p+1}^{M} V_i V_i^{H} \right] F \right]^{-1} \right. \qquad (4.4.10)$$

Or

$$P_{MUSIC} = \left[K\left(F\ ^{H}B_{WEV}\ F \right) \right]^{-1} \qquad (4.4.11)$$

where $K = 1/\lambda$ is a constant, which is normally taken as *1.*

Equation *(4.4.11)* represents the MUltiple SIgnal Classifications *(MUSIC)* algorithim developed by *R.O.Schmidt [51],* which achieves the same degree of resolution as that obtained by the Eigen vector method mentioned above.

4.4.4. The NEW PROPOSED method :

Now, if we define matrix *B ,-the matrix to be found-,* in equation *(4.4.5)* as equal the noise covariance matrix R_{ww}, then;

$$B = R_{ww} = \sum_{i=p+1}^{M} \lambda_i V_i V_i^{H} \qquad (4.4.12)$$

and the matrix vector multiplication of equation *(4.4.7)* becomes as follows:

$$B^H R_{XX}^{-1} B = R_{WW}^H R_{XX}^{-1} R_{WW}$$

$$= \sum_{i=p+1}^{M} V_i V_i^H \quad = B_{WEV} \qquad (4.4.13)$$

Which means that this matrix vector multiplication represents a matrix consisting of the sum of the outer products of the Noise Eigen Vectors *(NEV)*.

Now, let us define another matrix B_{SEV}, which consists of the outer products of the largest eigen vectors ,-*the Signal Eigen Vectors (SEV)*-, as follows :

$$B_{SEV} = \sum_{i=1}^{p} V_i V_i^H \qquad (4.4.14)$$

The addition of the two matrices B_{WEV} *and* B_{SEV} of equations *(4.4.13) and (4.4.14)* respectively will constitute a new matrix B_{EV} as shown below :

$$B_{SEV} + B_{WEV} = \sum_{i=1}^{p} V_i V_i^H + \sum_{i=p+1}^{M} V_i V_i^H$$

$$= \sum_{i=1}^{M} V_i V_i^H \quad = \quad B_{EV} \qquad (4.4.15)$$

But a property of the eigen vectors of any matrix is that, the outer products of all its eigen vectors will constitute an Identity Matrix, so :

$$B_{EV} = B_{SEV} + B_{WEV} = I$$

Or $$B_{WEV} = I - B_{SEV}$$

$$= I - \sum_{i=1}^{p} V_i V_i^H \qquad (4.4.16)$$

Substituting equations *(4.4.13)* and *(4.4.16)* in equation *(4.4.5)* will constitute the *new estimate* as follows :

$$P_{mPC} = \left[F^H \left(I - \sum_{i=1}^{p} V_i V_i^H \right) F \right]^{-1}$$

$$= \left[F^H I F - F^H \left(\sum_{i=1}^{p} V_i V_i^H \right) F \right]^{-1} \qquad (4.4.17)$$

Or

$$\left.\begin{aligned} P_{mPC} &= \left[1 - F^H \left(\sum_{i=1}^{p} V_i V_i^H \right) F \right]^{-1} \\ &= \left[1 - F^H B_{SEV} F \right]^{-1} \end{aligned}\right\} \quad (4.4.18)$$

which has a very high resolution ability to the closely separated sinusoids in white Gaussian noise.

If we inspect carefully this new proposed estimator, *Equ.(4.4.18),* we can see that the only computations needed is to compute the outer products of the largest eigen values, *-the Principal Components (PC)-* of the *TCM* after decomposition, and then perform the frequency search by the vector products, *-see Fig.(4.1) for flow chart of how this method works-.* Further more, we can notice that these computations are exactly those specified by the first *RHS* term of the *MLSE -Equ.(4.2.13)* except that we have the signals eigen values set to unity.

The spectral estimate represented by the first *RHS* of equation *(4.2.13)* is called the *Principal Components Method (PCM)*, because it uses the principal eigen vectors. It has poor resolution and a lot of ambiguities due to the large side lobes included. However it gives the same spectral estimate obtainable from the conventional *Bartlett Estimate [34]*,which is given by :

$$P_{BT} = \frac{1}{N^2} C^H R_{XX} C \qquad (4.4.19)$$

4.5. PARTITIONING :

Several techniques, such as those presented in the previous sections, have been developed for the purpose of spectral estimation and for determining the bearings of acoustic sources, using either the smallest *(signal)* or largest *(noise)* eigen vectors of different correlation type matrices. In these methods, as we have already mentioned, the correlation matrix is first estimated from the available samples and then decomposed to its eigen values and their associated eigen vectors.

Now, if we suppose that we have a signal-only random process consisting of p sinusoids as follows :

$$x_n = \sum_{i=1}^{p} A_i exp[j(n\omega_i + \phi_n)] \qquad (4.5.1)$$

then its covariance matrix will have p non-zero eigen values, so it has a rank of p. But, if this random process is contaminated by white Gaussian noise, *see Equ.(4.2.1)*, then its covariance matrix will have $M>p$ non-zero eigen values as follows :

$$\lambda_1 \geq \lambda_2 \geq \lambda_3 \geq \ldots\ldots\ldots\ldots \geq \lambda_M \qquad (4.5.1)$$

and hence, the rank of this new covariance matrix is *M*.

As is mentioned in several places in this thesis, the white noise is assumed to be uncorrelated with the signals, so it does not have any components along the signal subspace, *-i.e the contribution due to noise on these projections must be zero-*. In this case, it is easy to distinguish between the signal eigen values and the noise eigen values, specially when the exact covariance matrix is known, *see Table (4.1),* or when the signal levels are above the noise level. But, with low *SNR*, this distinction will be difficult, so to partition the covariance matrix into signal and noise subspaces, we need some more accurate and reliable methods.

4.5.1. WAX and KAILATH method :

Many researchers have worked hard so far to develop such a method for determining the number of the signals in the random process under consideration. Among these methods was the approach based on the observation that *the number of signals can be determined from the multiplicity of the smallest eigenvalues of the covariance matrix of the random process -see table (4.1)-*. This approach was developed by *Wax* and *Kailath [55],* which is based on the application of Information Theoretic Criteria *(ITC)* for model identification introduced by *Akaike [2], Schwartz [49]* and *Rissanen [47].*

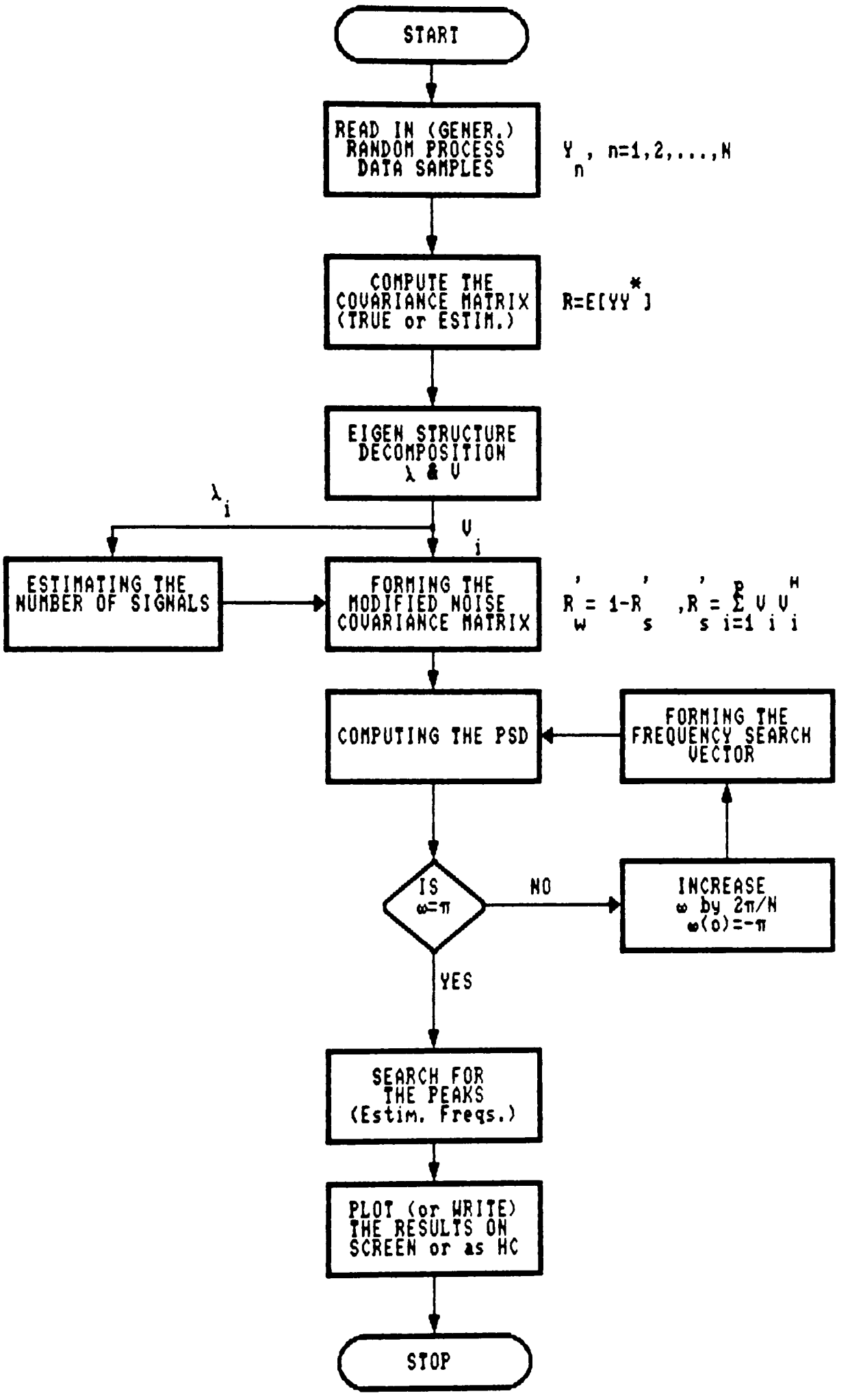

Fig.(4.1) FLOW CHART FOR THE PROPOSED ALGORITHM - Modified Principal Components Method (MPCM)

```
RP : Noisy sinusoid
NMAX        :  25
SAMP.FR.    :  1.000
AMPLITUDS   :  1.00   1.00
FREQS.      :  0.1500  0.1700
SNRs ( dB ):  20.000   20.000
STAND.DEV. :       0.1000000000000000
RESOL.LIMIT :0.0400
```

A. THE EIGEN VALUES OF THE TRUE COVARIANCE MATRIX ARE :

WR(1)=	0.9999999999999751D-02	WI(1)=	0.0000000000000000D+00
WR(2)=	0.9999999999999836D-02	WI(2)=	0.0000000000000000D+00
WR(3)=	0.9999999999999892D-02	WI(3)=	0.0000000000000000D+00
WR(4)=	0.9999999999999932D-02	WI(4)=	0.0000000000000000D+00
WR(5)=	0.9999999999999961D-02	WI(5)=	0.0000000000000000D+00
WR(6)=	0.9999999999999990D-02	WI(6)=	0.0000000000000000D+00
WR(7)=	0.1000000000000001D-01	WI(7)=	0.0000000000000000D+00
WR(8)=	0.1000000000000006D-01	WI(8)=	0.0000000000000000D+00
WR(9)=	0.1000000000000008D-01	WI(9)=	0.0000000000000000D+00
WR(10)=	0.1000000000000009D-01	WI(10)=	0.0000000000000000D+00
WR(11)=	0.1107922627001691D+01	WI(11)=	0.0000000000000000D+00
WR(12)=	0.2291207737299831D+02	WI(12)=	0.0000000000000000D+00

B. THE EIGEN VALUES OF THE ESTIMATED COVARIANCE MATRIX ARE :

WR(1)=	0.4155386787660106D-01	WI(1)=	0.0000000000000000D+00
WR(2)=	0.5998899499997195D-01	WI(2)=	0.0000000000000000D+00
WR(3)=	0.6940042877011540D-01	WI(3)=	0.0000000000000000D+00
WR(4)=	0.7684392129689654D-01	WI(4)=	0.0000000000000000D+00
WR(5)=	0.8317660889306407D-01	WI(5)=	0.0000000000000000D+00
WR(6)=	0.1094884547944087D+00	WI(6)=	0.0000000000000000D+00
WR(7)=	0.1422369873733004D+00	WI(7)=	0.0000000000000000D+00
WR(8)=	0.2192343936683020D+00	WI(8)=	0.0000000000000000D+00
WR(9)=	0.3602294074841305D+00	WI(9)=	0.0000000000000000D+00
WR(10)=	0.6535003547944589D+00	WI(10)=	0.0000000000000000D+00
WR(11)=	0.3072095441910018D+01	WI(11)=	0.0000000000000000D+00
WR(12)=	0.2049222948047228D+02	WI(12)=	0.0000000000000000D+00

Table (4.1) THE EIGEN VALUES OF THE TRUE AND THE ESTIMATED COVARIANCE MATRICES OF A RANDOM PROCESS CONSISTING OF TWO SINUSOIDAL SIGNALS OF EQUIPOWERS IN WHITE GAUSSIAN NOISE.

It was shown *[55]*, that the *Akaike* criterion *(AIC)* tends to overestimate the number of the signals in the large sample limit, so it gives inconsistent estimate, while the criterion introduced by *Schwartz* and *Rissanen (MDL)* yields consistent estimates.

We can represent these two criteria in a General Form Criterion *(GFC)* which is given by :

$$GFC(p) = -K_1 log[\ ML\ ] + K_2[\ NFAP\ ].K_3 \qquad (4.5.2)$$

where

$$ML = \left| \frac{\prod_{i=p+1}^{M} \lambda_i}{\left[\frac{1}{M-p} \sum_{i=p+1}^{M} \lambda_i \right]^{N-M}} \right|^{N} \qquad (4.5.3)$$

and the other parameters will differ according to the desired criterion as shown in Table *(4.2)* below. The Number of Free Adjustable Parameters *(NFAP)* will depend upon the model, and it is for our assumed model as indicated by the table.

Variable	*AIC*	*MDL*
K_1	*2*	*1*
K_2	*2*	*0.5*
K_3	*1*	*log N*
NFAP	*p(2M-p)+1*	*p(2M-p)+1*

Table (4.2) Table of values assigned to the *GFC* to act as *AIC* or *MDL* criterion

The number of the signals, *i.e the rank of the SCM,* is taken as the value of *p* for which the chosen criterion is minimized.

4.5.2. The NEW PROPOSED method :

A new simpler and computationally efficient method for determining the number of signals in the random process is proposed in this research. It utilizes the same General Form Criterion *(GFC)* presented by equation *(4.5.2)*, but with different values for its variables. This new method is summarized by the following steps :

1) Put the eigen values in a descending order.

2) Calculate the ML as follows :

$$ML = \left| \lambda_p - \lambda_{av.} \right| \qquad \text{where} \quad \lambda_{av.} = \frac{1}{M} \sum_{i=1}^{M} \lambda_i \qquad \Big\} (4.5.4)$$

3) Set the variables as follow :

$$K_1 = -1$$

$$K_2 = K_3 = 1$$

$$NFAP = p(1+1/M)$$

4) Calculate the value of p which minimises the value to the GFC. This value of p represents the number of sinusoidal signals present in the random process.

As an example, let us use the same random process that used in evaluating the eigen values of table *(4.1)* above. Table *(4.3)* shows the values of *GFC(p)* for *p=1,2,.....,M* from which we can see that this proposed criterion estimated the number of signals correctly by assigning the minimum value to *GFC(p)* at *p=2* for both the true and the estimated covariance matrix.

A. USING THE TRUE COVARIANCE MATRIX :

```
p=  1   GFC( 1)=          4.1231819229383292
p=  2   GFC( 2)=          2.063611762918455 1 *
p=  3   GFC( 3)=          3.943147418978524 3
p=  4   GFC( 4)=          5.026480672838997 9
p=  5   GFC( 5)=          6.109814165118050 6
p=  6   GFC( 6)=          7.193147657397103 5
p=  7   GFC( 7)=          8.276480672838997 9
p=  8   GFC( 8)=          9.359814165118050 6
p=  9   GFC( 9)=         10.443147180559945 2
p= 10   GFC(10)=         11.526481149676156 3
p= 11   GFC(11)=         12.609814165118050 9
p= 12   GFC(12)=         13.693148134234261 8
```

B. USING THE ESTIMATED COVARIANCE MATRIX :

```
p=  1   GFC( 1)=          3.994445841287888 1
p=  2   GFC( 2)=          2.122816469660467 9 *
p=  3   GFC( 3)=          3.629462066326714 9
p=  4   GFC( 4)=          4.895670595623363 2
p=  5   GFC( 5)=          6.056288803376410 1
p=  6   GFC( 6)=          7.179434666558573 1
p=  7   GFC( 7)=          8.279231755338935 4
p=  8   GFC( 8)=          9.375599708402489 8
p=  9   GFC( 9)=         10.462044630609510 3
p= 10   GFC(10)=         11.549024022217781 1
p= 11   GFC(11)=         12.636947309476569 0
p= 12   GFC(12)=         13.729212104400536 2
```

* Represents the minumum GFC value.

able (4.3) TABLE OF THE COMPUTED VALUES OF THE PROPOSED CRITERION USING THE TRUE AND THE ESTIMATED COVARIANCE MATRICES.

Chapter Five

CAPABILITY OF THE HIGH RESOLUTION PSDE APPROACHES TO ESTIMATE AND RESOLVE SIGNAL FREQUENCIES

A Comparison Study

CHAPTER FIVE

CAPABILITY OF THE HIGH RESOLUTION PSDE APPROACHES *TO* ESTIMATE AND RESOLVE SIGNAL FREQUENCIES

A comparison study

5.1. INTRODUCTION :

In chapter *3*, we mentioned that resolution is one of the main performance criteria *-such as computational complexity, detectability and estimation bias-* by which any *PSDE* method should be judged.

Resolution can be analyzed, however it is difficult, as for the asymptotic case of infinite averaging, which means that the "*true*" covariance matrix is assumed known, *[30]*. But as we mentioned earlier, the real world situation allows only a finite sequence of data samples, which in turn means a limited or finite amount of averaging is possible and hence the estimated covariance matrix is far from being good enough to give the correct *PSD* or the standard of resolution required.

In this chapter, the high resolution *PSDE* approaches *-MLM, MEM, EVM and the new proposed method (MPCM)-* presented in chapter four are studied further and a computer program was used to compare their resolution capabilities with respect to data length, *SNR,* frequency separation and relative phase variations for the cases of true and estimated covariance matrices. The effect of a third nearby strong signal on the resolution capabilies was investigated as well.

5.2. *PERFORMANCE OF THE ESTIMATORS :*

5.2.1. *USING TRUE COVARIANCE MATRIX :*

We have just mentioned that the infinite averaging assumes that the true covariance matrix is known, and it is of interest to study the behaviour of the above mentioned estimators using this covariance matrix rather than the estimated one. In this section, the performance of Maximum Likelihood *(ML)*, Maximum Entropy *(ME)*, Eigen Value Decomposition *(EVD)*, and the Modified Principal Components *(MPC)* methods to resolve two closely separated signals of equal powers is studied. Plots of the *PSDE* of these methods for the different situations are presented as well.

5.2.1.1. *THE EFFECT OF SNR VARIATIONS :*

A useful measure of the resolution capability of an estimator is the signal-to-noise ratio it requires to resolve two closely separated signals of equal powers contaminated by white Gaussian noise. The two signals used were of the normalized frequencies *0.15 and 0.17* being close to each other and the true covariance matrix was calculated according to *Equ.(4.2.10)*. The *SNR* was reduced gradually until each estimator was unable to resolve the two sinusoids.

*Fig(5.1)*shows the *PSD* estimates of the four estimators for the case of high *SNR* which indicates the ability of all of them to detect and resolve the two signals. When the *SNR* was reduced to the level where the two signals were just resolved by the *MLM*, the other estimators were able to resolve them *-see Fig(5.3)-*. This *SNR* value is called the *threshold SNR value of MLM*, which is higher than the threshold *SNR* values of the remaining three estimators which are computed in the same way and listed in Table *(5.1)* below. *MLM* gave biased estimate when the *SNR* reduced to

20dB and could not resolve the two signals when the *SNR* reached lower values as shown in *Fig(5.5)*. The plots for the *PSDE* of the other three estimators at the threshold *SNR* value of *MEM* are presented by *Fig(5.6)*.

The new proposed method has the same threshold *SNR* value as that for *EVM* proposed by *Johnson and DeGraaf [27]*, which seems to be common for all the *EVDT* methods. *Fig(5.1)* to *Fig(5.9)* show the effect of *SNR* variations on the different *PSD* estimators.

No.	*Estimator*	*Threshold SNR values (dB)*		
		True Covariance Matrix	*Estimated Covariance Matrix*	
			fr.set 1 0.15/.17	*fr.set 2 0.15/0.18*
1.	*MLM*	*21*	*>90*	*>90*
2.	*MEM*	*9*	*>90*	*3*
3.	*EVM*	*-90*	*5*	*0*
4.	*MPCM*	*-90*	*5*	*0*

Table(5.1) Threshold *SNR* values for the four approaches to *PSDE* using the true and estimat. covar. matrices.

5.2.1.2. THE EFFECT OF FREQUENCY SEPARATION VARIATIONS :

The true covariance matrix was generated in the same way as explained in the previous section with the two signals being apart by $(0.03f_s)$ in which case all the four estimators were capable of resolving the two signal frequencies, *-see Fig(5.10)-*. Then the second signal frequency was moved towards the first one causing the frequency separation to be less and less until situations

were reached where each assigned estimator was just able to resolve the two frequencies. This value of the frequency separation represents the minimum separation between the two signal frequencies below which the assigned estimator will be incapable of resolving them, *-see Fig(5.11) to Fig(5.13).*

Fig(5.14) shows that the *Johnson and DeGraaf* approch is capable of resolving the two sinusoids at closer separation *($0.0020f_s$)*. Since the resolution itself is a function of *SNR* it is obvious that these frequency separation limits are function of *SNR, -i.e when a lower SNR value was used, the frequency separation at which the assigned estimator was capable of resolving the two signals was bigger than that when SNR was high-*. Frequency separation of *($0.0020f_s$)* was the minimum separation with which *EVM* can resolve the two signals and when the frequency separation was reduced further *($0.001f_s$, and $0.000001f_s$)*, this method was incapable of resolving the two signals and it gave a single peak at *$0.15f_s$* only, *see Fig(5.15)*. So we can say that the point at which the peaks merge into one is a practical limit beyond which two components can not be easily separated from one another using this technique and that can be predicted from *Table(5.2)* which shows that the covariance matrix of this random process have only one very high eigen value.

5.2.1.3. THE EFFECT OF RELATIVE PHASE VARIATIONS :

Inspecting equation *(4.2.10)*, repeated below for simplicity, according to which the true covariance matrix is generated indicates that the initial phases of the sinusoids and hence the relative phase between them have no effect on the detection and resolution capabilities of these estimators because the two signals are assumed uncorrelated and hence the term representing them is no longer present, *-see Fig(5.16) and Fig(5.17) for the case of 0.0 and*

30.0degrees relative phases-, which gives no sign of any change in the estimators performances.

$$R_{xx}(l,k) = \begin{cases} \sum_{i=1}^{p} p_i exp[j(l-k)\omega_i] & for\ l \neq k \\ \sum_{i=1}^{p} p_i + \sigma_w^2 & for\ l = k \end{cases} \qquad (5.2.1)$$

A.) THE EIGEN VALUES OF THE TRUE COVARIANC MATRIX ARE :

WR(1)=	0.9999999999996570D-03	WI(1)=	0.0000000000000000D+00
WR(2)=	0.9999999999998341D-03	WI(2)=	0.0000000000000000D+00
WR(3)=	0.9999999999998663D-03	WI(3)=	0.0000000000000000D+00
WR(4)=	0.9999999999998967D-03	WI(4)=	0.0000000000000000D+00
WR(5)=	0.9999999999999697D-03	WI(5)=	0.0000000000000000D+00
WR(6)=	0.9999999999999925D-03	WI(6)=	0.0000000000000000D+00
WR(7)=	0.1000000000000006D-02	WI(7)=	0.0000000000000000D+00
WR(8)=	0.1000000000000017D-02	WI(8)=	0.0000000000000000D+00
WR(9)=	0.1000000000000132D-02	WI(9)=	0.0000000000000000D+00
WR(10)=	0.1000000000000140D-02	WI(10)=	0.0000000000000000D+00
WR(11)=	0.1000002822706993D-02	WI(11)=	0.0000000000000000D+00
WR(12)=	0.2400099999717729D+02	WI(12)=	0.0000000000000000D+00

B.) THE EIGEN VALUES OF THE ESTIMATED COVARIANCE MATRIX ARE :

WR(1)=	0.7544815993126509D-01	WI(1)=	0.0000000000000000D+00
WR(2)=	0.8704628326345209D-01	WI(2)=	0.0000000000000000D+00
WR(3)=	0.9845090575696383D-01	WI(3)=	0.0000000000000000D+00
WR(4)=	0.1126730328844634D+00	WI(4)=	0.0000000000000000D+00
WR(5)=	0.1293576975643023D+00	WI(5)=	0.0000000000000000D+00
WR(6)=	0.1603117780238424D+00	WI(6)=	0.0000000000000000D+00
WR(7)=	0.2237356705688339D+00	WI(7)=	0.0000000000000000D+00
WR(8)=	0.3248858047320566D+00	WI(8)=	0.0000000000000000D+00
WR(9)=	0.5456626704944536D+00	WI(9)=	0.0000000000000000D+00
WR(10)=	0.1113450229867880D+01	WI(10)=	0.0000000000000000D+00
WR(11)=	0.4665766093867134D+01	WI(11)=	0.0000000000000000D+00
WR(12)=	0.4041543279583682D+02	WI(12)=	0.0000000000000000D+00

TABLE No.(5.2) EIGEN VALUES OF THE TRUE AND THE ESTIMATED COVARIANCE MATRICES OF A RANDOM PROCESS COMPOSED OF TWO VERY CLOSELY SEPARATED SIGNALS IN WHITE GAUSSIAN NOISE

5.2.2. USING THE ESTIMATED COVARIANCE MATRIX :

When the covariance matrix is estimated from a finite number of observations, then it will be an approximation to the true one *[3]*. The effect of this approximation manifests itself as a perturbation on the noise subspace, which is mainly used in the *EVDT* methods, and consequently on their ability of frequency resolution.

Though the Eigen Vector Decomposition Techniques *(EVDT)* become the more interesting work in high resolution, their resolution capability,or precisely their ability to estimate the exact locations of signal frequencies, is highly affected by using the estimated covariance matrix, *i.e the peaks locations might be biased.* In this section the effects of the changes in the parameters mentioned earlier in the introduction to this chapter on the performance of *MLM, MEM, EVM,* and *MPCM* using the estimated covariance matrix are investigated.

5.2.2.1. THE EFFECT OF DATA LENGTH VARIATIONS :

The data length has different effects on the *PSDE* approaches, and it is one of the main features that specify the estimator to have a good performance or not. The detection and resolution capabilities of all the *PSD* estimators improved as the data length increases until the ideal case where the infinfte averaging is reached in which case the true covariance matrix becomes known. On the other hand, as the data length shortened the detection and resolution abilities of these estimators become worse and worse. In this section the effect of data length variations on the performance of *MLM, MEM, EVM,* and *MPCM* was investigated and we discovered that *MLM* was the most affected by the data length variations and that *MPCM* was the least affected estimator.

We started with *(401)* data samples which is quite a large number and with it all the estimators were able of detecting and resolving the two signals of normalized frequencies $0.15f_s$ *and* $0.18f_s$, but when the second signal frequency was moved to $0.17f_s$ *MLM* was unable to resolve the two signals and showed a single peak at the intermediate frequency $0.16f_s$ although the frequency separation was still larger than Fourier resolution Limit *(FRL), -see Fig(5.18) and Fig(5.19),-*. Then a data length of *(201)* samples was used and all the estimators, except *MLM*, were able to detect and resolve the two signal frequencies.

The data length was reduced further and further until it reahed a value *(41)* samples where all the three estimators,*-MEM, EVM, and MPCM-* resolved the two signals but with a great bias this time. *MEM* possessed the least bias which indicates that it was the best among the three in locating the frequencies when the data length was large enough. But when the data length *(N)* was assigned a value of *(25)* samples and less *MEM* was unable of detecting and resolving the two signals and gave a single peak at the mid frequency $(0.16f_s)$, *-see Fig(5.21) to Fig(5.24).*

Now, as *N* reduced more and more, the only technique that capable of detecting and resolving the two signals was the eigen vector decomposition technique *(EVDT)* represented by *EVM* and the new proposed method *(MPCM),Fig(5.25),* and the latter was the best because it gave more distinction between the two peaks, *-i.e it gave sharper peaks than EVM-*. The most interesting observation here is that this approach was capable of detecting and resolving the two signals when the data length was very short, *4* or even *2* data samples only, on a condition that the number of signals is known a priori, *-see Fig(5.26)-*.

5.2.2.2. THE EFFECT OF SNR VARIATIONS :

In section *(5.2.1.1)* we studied the effect of the *SNR* changes when we have the true covariance matrix. Now, in this section we will study the effect of *SNR* changes also, but using finite number of data samples *(or the estimated covariance matrix)*.

Fig(5.27) shows that *MLM* was unable to detect and resolve the two closely separated signals whatever *SNR* value been used, while the other three estimators detected and resolved the two signals with the same degree of accuracy. The *SNR* then reduced further and further until it reached a value of *3.0dB* which represents the *SNR* threshold value of *MEM*, and when it was reduced to *2.0dB*, *MEM* was not able to resolve the two signal frequencies, *-see Fig(5.28) to Fig(5.32)-*. These experimental tests were performed with the two signals at normalized frequencies of $0.15f_s$ and $0.18f_s$, then repeated with the two signals at the more closely spaced frequencies of $0.15f_s$ and $0.17f_s$ from which we noticed that *MEM* was unable to resolve the two signals whatever *SNR* value used as shown in *Fig(5.33)*. In order to check the threshold *SNR* value for the *EVDT*, the *SNR* was reduced more and more until it reahed a minimum value of *5.0dB* for this set of signal frequencies, below which no estimator could resolve the two signals, *-see Fig(5.34) to Fig(5.36)-*. The threshold *SNR* values were as given in *Table(5.1)*.

There are four points discovered from the two sets of experimental tests performed, the first was that when the *SNR* was high, the estimation biases for all the four estimators were high and as we reduced *SNR* the accuracy of resolution improved until we reached the threshold values where no resolution below them can be achieved. The second point was that the resolution of *MPCM* was the best. The third point was that the threshold *SNR* values for any

estimator is a function of the frequency separation between the two signals *(i.e how much they are close to each other)* which confirm what we said in chapter three about the *SNR* needed to resolve the two signals. The forth and last point was that the threshold *SNR* value for any estimator to resolve two closely separated signals using true covariance matrix is lower than that of the same estimator to resolve the same set of signals using the estimated covariance matrix,*-see Table(5.1)-*.

5.2.2.3. THE EFFECT OF FREQUENCY SEPARATION VARIATIONS :

As a reality, any estimator will be capable of detecting and resolving the two signals when their frequencies are sufficently apart and there will be a frequency separation limit for any estimator to be able to resolve these two signals beyond which no resolution can be achieved.

Fig(5.37) shows the four estimates of the four algorithms under study which indicates that all of them were capable of resolving the two signals *-though the estimates were biased-* when there was a separation between their frequencies of $(0.05f_s)$, which is more than the fourier resolution limit *(FRL)*. But when this separation reduced to $(0.03f_s)$ we noticed that *MLM* was unable to detect and resolve these two signals and it gave instead a single peak at $f=0.165f_s$, *-see Fig(5.38)-*, so this frequency separation represents the dead limit below which *MLM* is incapable of resolving the two signals. The dead limit value of frequency separation for *MEM*, which is indicated by *Fig(5.39)*, was found to be equal $(0.02f_s)$.

The methods of *EVDT* were capable of resolving the two signals with no limits to the frequency separation and this

feature was discovered when *EVM* and *MPCM* detected and resolved the two signals having approximately the same normalized frequencies $0.15f_s$ *and* $0.150001f_s$ *(i.e. frequency separation of* $0.000001f_s$*),* and gave two peaks at the wrong frequencies *-see Fig(5.42)-*, while these estimators gave one peak located at $(0.15f_s)$ when the true covariance matrix was used, *-see section (5.2.1.2)-*. This phenomenon can be predicted by checking the eigen values of the two matrices, *-see Table (5.2)-*, which shows that the estimated covariance matrix possesses two high eigen values representing the two peaks, where as the true covariance matrix possesses only one very high eigen value which in turn represents the only peaks that the estimates gave.

Finally, we performed two sets of experiments, one set with *SNR=40dB* and the second set with *SNR=10dB* from which we can see that the resolution of the *EVDT* methods improved at the lower *SNR* value which confirms what we have said in section *(5.2.2.2)*.

5.2.2.4. THE EFFECT OF THE RELATIVE PHASE VARIATIONS :

The power spectral density estimates of all the four estimators under consideration are presented in *Fig(5.43)* for the case of *0 degrees* relative phase. Again, *MLM* can not resolve the two signals, but when the relative phase between the two signals became *30 degreees* the resolution of all the estimators including *MLM* improved, with *MLM* possessing the least estimate bias. The estimation accuracy improved further when the relative phase was assigned a value of *90 degrees*, that is because the two signals were orthogonal and had no components towards each other, *i.e they are completely uncorrelated*. The resolution became worse and worse as the relative phase increased further and further until it reached the value of *180*

degrees at which the estimates were exactly those when the relative phase was equal to *0 degrees*, and that obviously because the two signals were in phase, *see Fig(5.43) to Fig(5.49).*

5.3. THE EFFECT OF A THIRD NEARBY STRONG SIGNAL :

The effect of the presence of a third strong signal on the resolution of the two closely separated sinusoids was investigated for both the true and the estimated covariance matrix cases.

5.3.1. TRUE COVARIANCE MATRIX CASE :

It was seen that this third signal has no effect on the detection and resolution capabilities of the Eigen Vector Eigen Value Decomposition Technique *(EVDT)* as far as it is located *(in frequency)* far enough, *-more than the minimum frequency separation limit mentioned in section (5.2.1.2)-. Fig(5.50)* to *Fig(5.53)* shows the effect of this third signal on the *PSDE* of the above mentioned estimators as it approaches the other frequencies.

The *PSD* estimates of *MLM* is presented in these figures as well, from which it is clear that the resolution capability of this method is highly affected by the presence of such a strong nearby signal. When this third signal was at $0.2f_s$, *-Fig(5.51)-, MLM* was capable of resolving the two closely separated signals which were at the normalized frequencies $0.15f_s$ and $0.17f_s$ respectively, but when it became nearer and nearer no resolution achieved because it entered the minimum frequency separation limit with which this method can not resolve the two signals, *-see Fig(5.52) and Fig(5.53)-.*

5.3.2. *ESTIMATED COVARIANCE MATRIX CASE :*

Earlier we mentioned the effect of the estimated covariance matrix upon the detection and resolution capabilities of the different approaches to *PSDE* under study due to the variations in the data legth, *SNR*, frequency separation and relative phase. In this subsection we will show how these capabilities are affected when a third strong signal is present nearby taking the actual case of short data length from which we estimated our covariance matrix.

Fig(5.54) shows that the power spectral density estimates of the four estimators for the case of no such third signal from which we can detect the inability of the *MLM* to resolve the two signals because they were separated by less than Fourier resolution Limit *(FRL)*. *Fig(5.55)* to *Fig(5.57)* show the effect of the third signal as it became closer and closer from which we can say that the detection and resolution capabilities of these estimators are highly affected and the only estimator that was capable of resolving the signals was the *MEM*.

5.4. *RESOLUTION OF TWO CLOSELY SEPARATED SIGNALS OF UNEQUAL POWERS :*

We were concerned so far with the detection and resolution of two closely separated signals of equal powers. It is of interest that we test the abilities of the different algorithms to detect and resolve the same signals when they have unequal powers, which seemed to be highly affected by the ratio of the signals powers. How much these abilities were affected was depending upon the type of the covariance matrix used, the signals *SNR* levels and the individual estimators as well.

5.4.1. TRUE COVARIANCE MATRIX CASE :

Fig(5.58) to *Fig(5.61)* show the power spectral density estimates of the four estimators for the cases that the ratio (A_2/A_1) was equal *(0.5, 0.25, 0.1,* and *0.05)* respectively, from which we can see that the detection and resolution capablities of *EVM* and *MPCM* estimators were completely unaffected by this ratio. The reason why they did not affected was that they possess a very low *(-90dB or even less)* threshold *SNR* values. *MLM* was the most affected estimator and *MEM* was the less affected and that can be predicted easily by carefully checking their threshold *SNR* values listed in *Table(5.1)* above.

Comparing *Fig(5.62)* with *Fig(5.58)* we can see that *MLM* and *MEM* were unable to resolve the two signals, *-Fig(5.61)-*, though the ratio of their amplitudes was *(0.5)* which was the same as that used in obtaining the estimates of *Fig(5.57)*, but because the weak signal *SNR* was *(7.5dB)*, *-less than the threshold SNR values-*, and the strong signal *SNR* was *(10dB)* which is just above the threshold *SNR* values of these two estimators. So, not only the ratio of the two signals which affect the resolution capabilities of *MLM* and *MEM*, but the signals *SNR* levels as well.

5.4.2. ESTIMATED COVARIANCE MATRIX CASE :

The case was completely different when the estimated covariance matrix was used, the two signals were unresolved by *MLM* and *MEM* estimators for the case of $(A_2/A_1=0.5)$ and that is obvious because the *SNR* levels of the high power signal, $(p_1=40dB)$, was less than the threshold *SNR* values of these two estimators listed in *Table(5.1)* above.

EVM and *MPCM* capabilities of resolving the two signals were highly affected by the use of the estimated covariance

matrix which can be easily seen by comparing *Fig(5.63)* and *Fig(5.58)*. *Fig(5.64)* and *Fig(5.65)* present the power spectral density estimates of these two methods only, for the remaining values assigned to the ratio p_2/p_1. It is clear from *Fig(5.65)* that these two methods gave the same levels of resolution for the two signals under test whatever values were assigned to the amplitudes ratio when it is less than *(0.1)* and this indicates that *Eigen Vector Decomposition Technique (EVDT)* is the less affected approach. The reason for this is that we still have two highly distinct eigen values, *see Table(5.3)*, upon which the degree of resolution of this technique is mainly dependent.

A.) THE EIGEN VALUES OF THE TRUE COVARIANCE MATRIX ARE :

WR(1)=	0.9999999999999233D-03	WI(1)=	0.0000000000000000D+00
WR(2)=	0.9999999999999576D-03	WI(2)=	0.0000000000000000D+00
WR(3)=	0.9999999999999671D-03	WI(3)=	0.0000000000000000D+00
WR(4)=	0.9999999999999806D-03	WI(4)=	0.0000000000000000D+00
WR(5)=	0.9999999999999880D-03	WI(5)=	0.0000000000000000D+00
WR(6)=	0.1000000000000006D-02	WI(6)=	0.0000000000000000D+00
WR(7)=	0.1000000000000033D-02	WI(7)=	0.0000000000000000D+00
WR(8)=	0.1000000000000048D-02	WI(8)=	0.0000000000000000D+00
WR(9)=	0.1000000000000060D-02	WI(9)=	0.0000000000000000D+00
WR(10)=	0.1000000000000075D-02	WI(10)=	0.0000000000000000D+00
WR(11)=	0.2178209400977524D-01	WI(11)=	0.0000000000000000D+00
WR(12)=	0.1210021790330802D+02	WI(12)=	0.0000000000000000D+00

B.) THE EIGEN VALUES OF THE ESTIMATED COVARIANCE MATRIX ARE :

WR(1)=	0.1806311947238607D-01	WI(1)=	0.0000000000000000D+00
WR(2)=	0.2242805280916115D-01	WI(2)=	0.0000000000000000D+00
WR(3)=	0.2820321009721945D-01	WI(3)=	0.0000000000000000D+00
WR(4)=	0.3087537397493176D-01	WI(4)=	0.0000000000000000D+00
WR(5)=	0.3367876167066347D-01	WI(5)=	0.0000000000000000D+00
WR(6)=	0.4152060915178024D-01	WI(6)=	0.0000000000000000D+00
WR(7)=	0.5960216536600802D-01	WI(7)=	0.0000000000000000D+00
WR(8)=	0.8667678201911521D-01	WI(8)=	0.0000000000000000D+00
WR(9)=	0.1414019318795685D+00	WI(9)=	0.0000000000000000D+00
WR(10)=	0.2820312842278482D+00	WI(10)=	0.0000000000000000D+00
WR(11)=	0.1193411068032746D+01	WI(11)=	0.0000000000000000D+00
WR(12)=	0.1027558900309252D+02	WI(12)=	0.0000000000000000D+00

TABLE No.(5.3) THE EIGEN VALUES OF THE TRUE AND THE ESTIMATED COVARIANCE MATRICES OF A RANDOM PROCESS CONTAINING TWO SIGNALS OF UNEQUAL POWERS (RELATIVE AMPLITUDES A2/A1=0.1) IN A WHITE GAUSSIAN NOISE

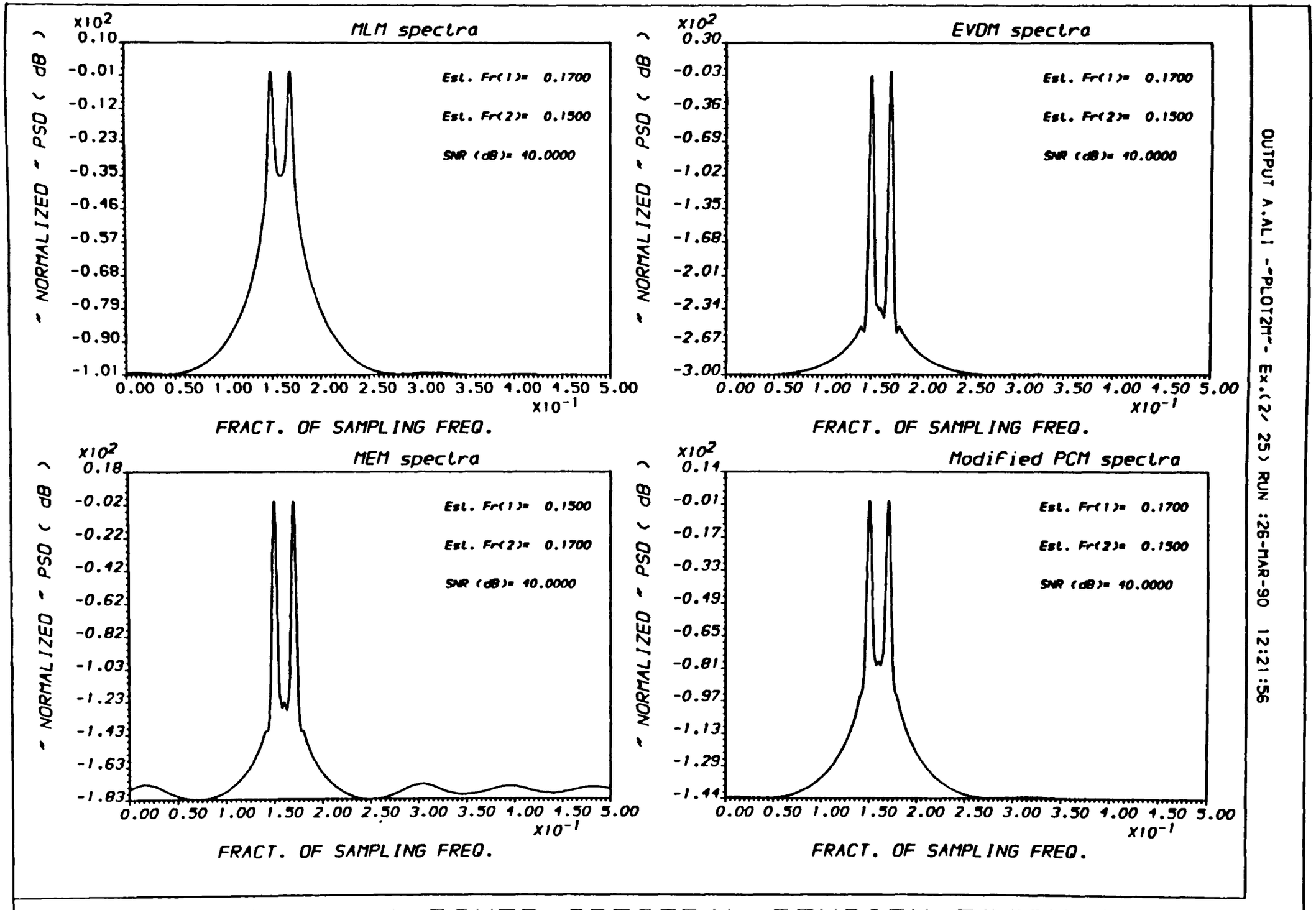

FIG.(5.1) POWER SPECTRAL DENSITY ESTIMATE
* For different PSDE methods *

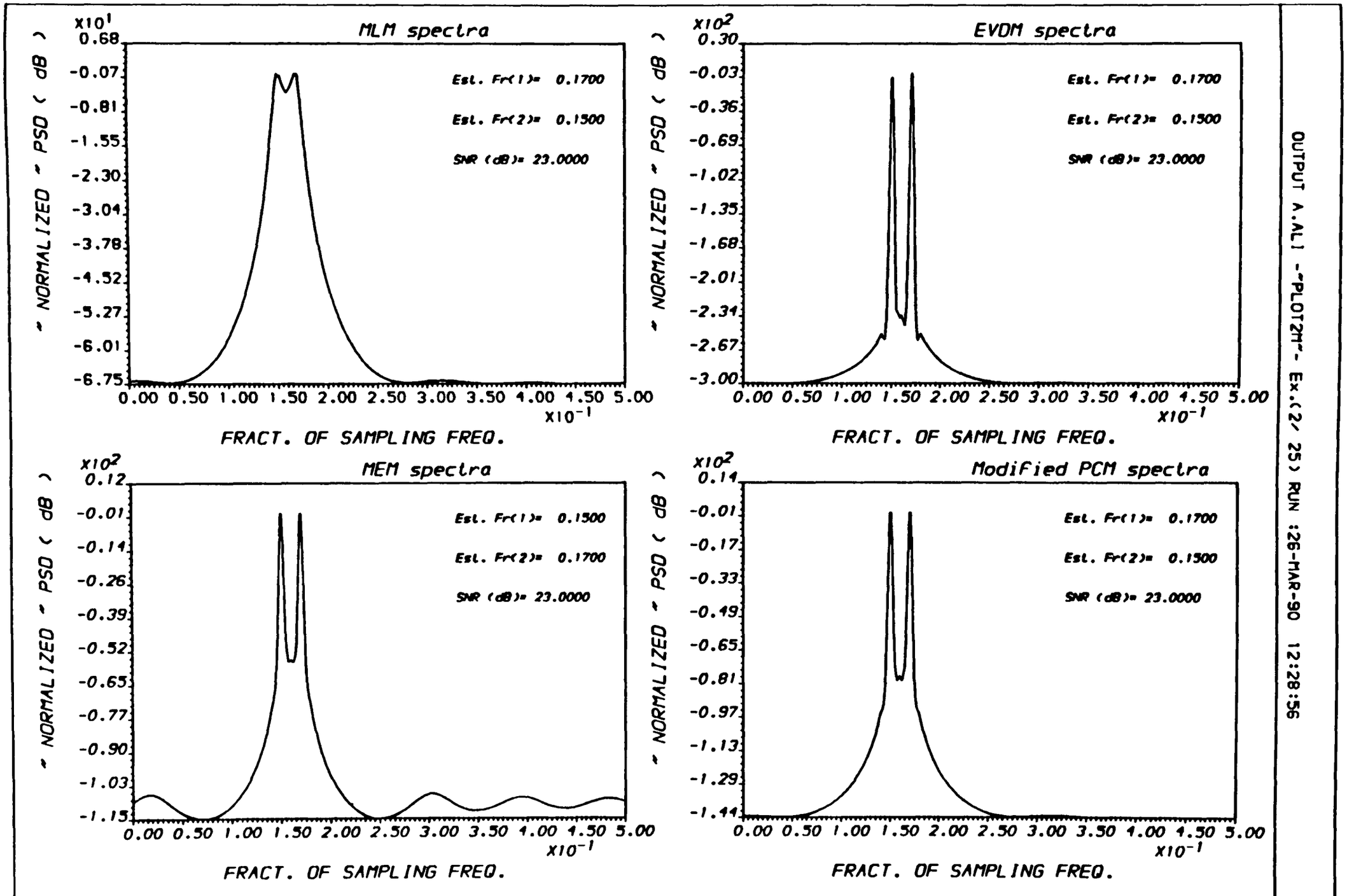

FIG.(5.2) POWER SPECTRAL DENSITY ESTIMATE
* For different PSDE methods *

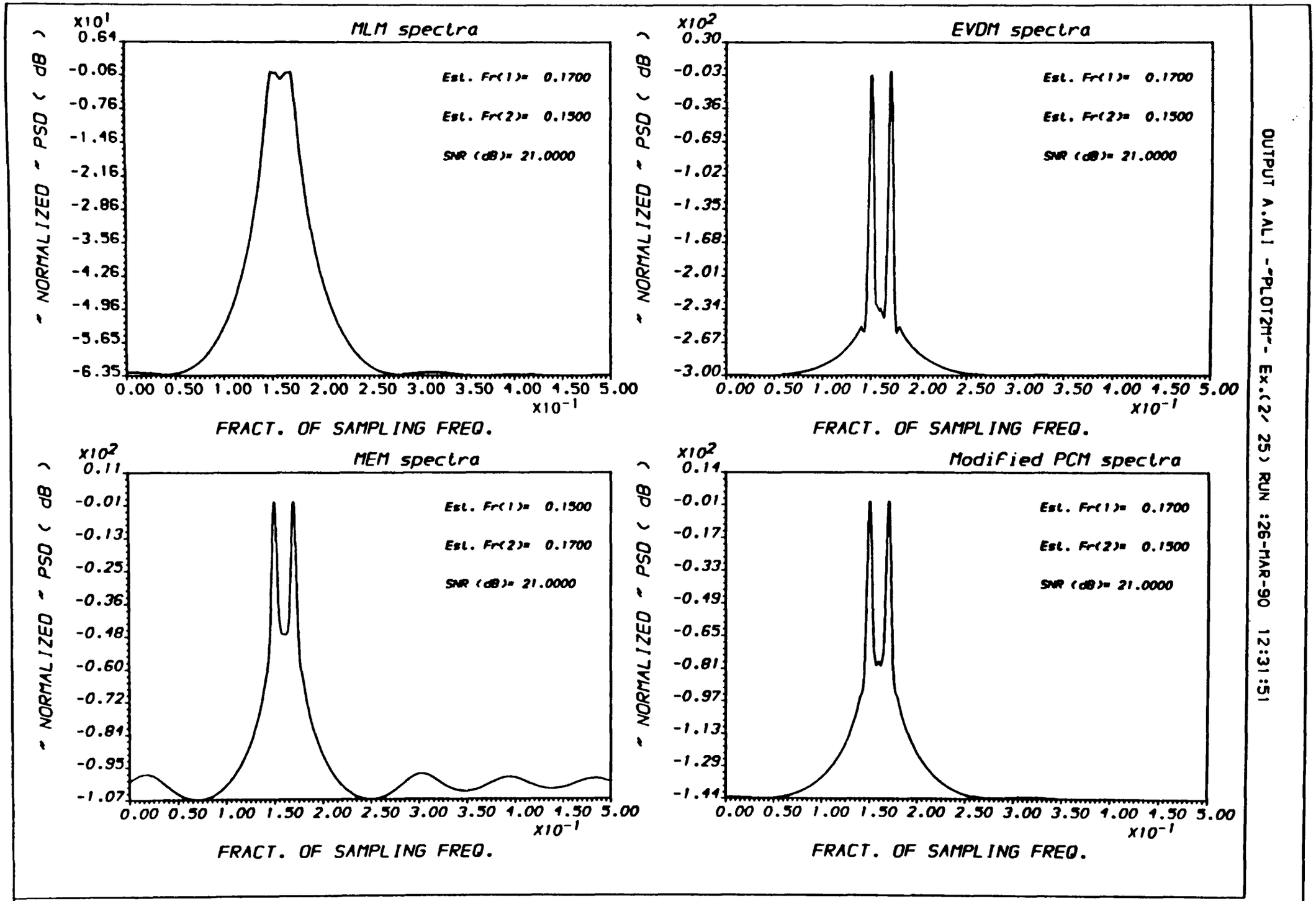

FIG.(5.3) POWER SPECTRAL DENSITY ESTIMATE
* For different PSDE methods *

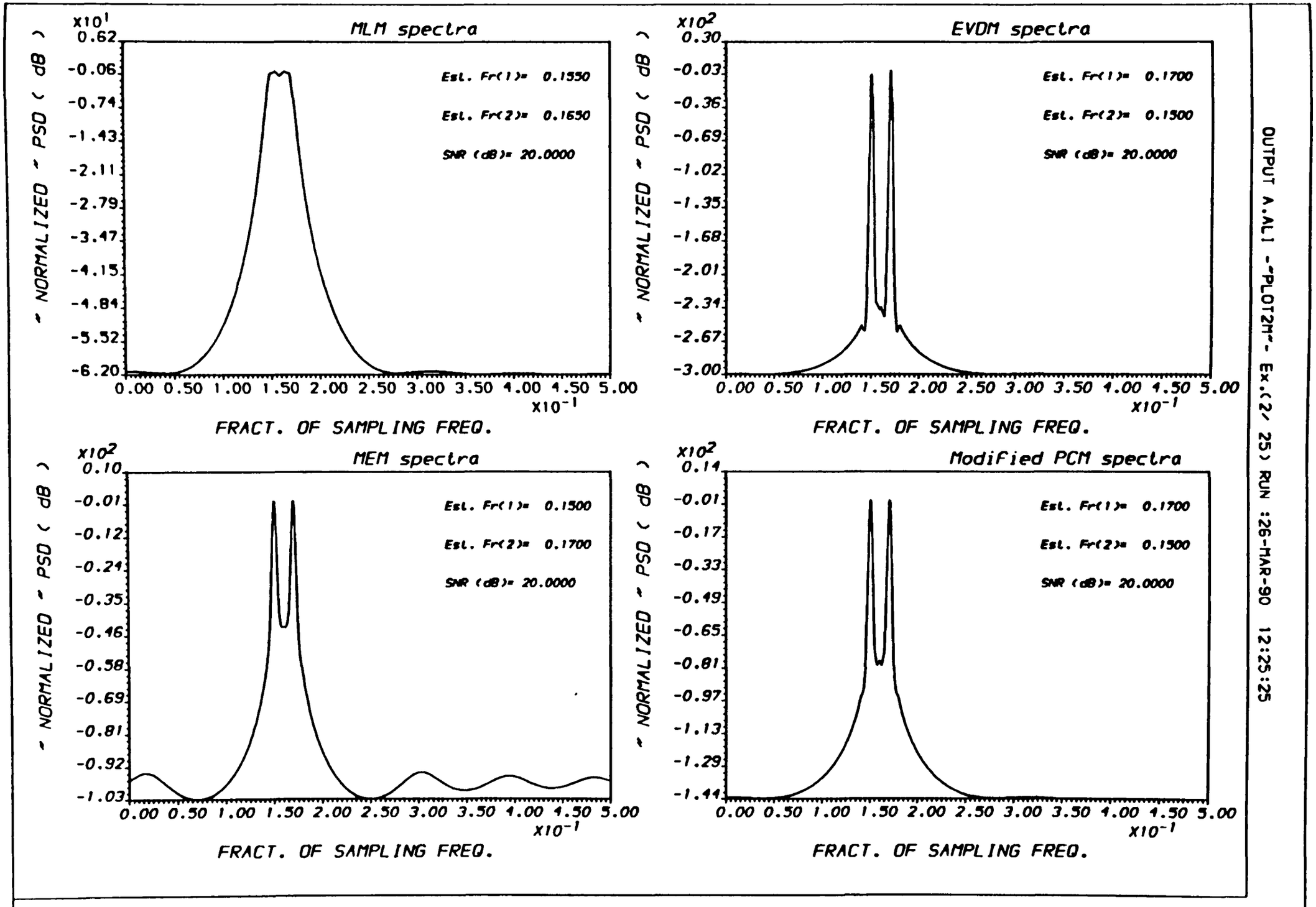

FIG.(5.4) POWER SPECTRAL DENSITY ESTIMATE
* For different PSDE methods *

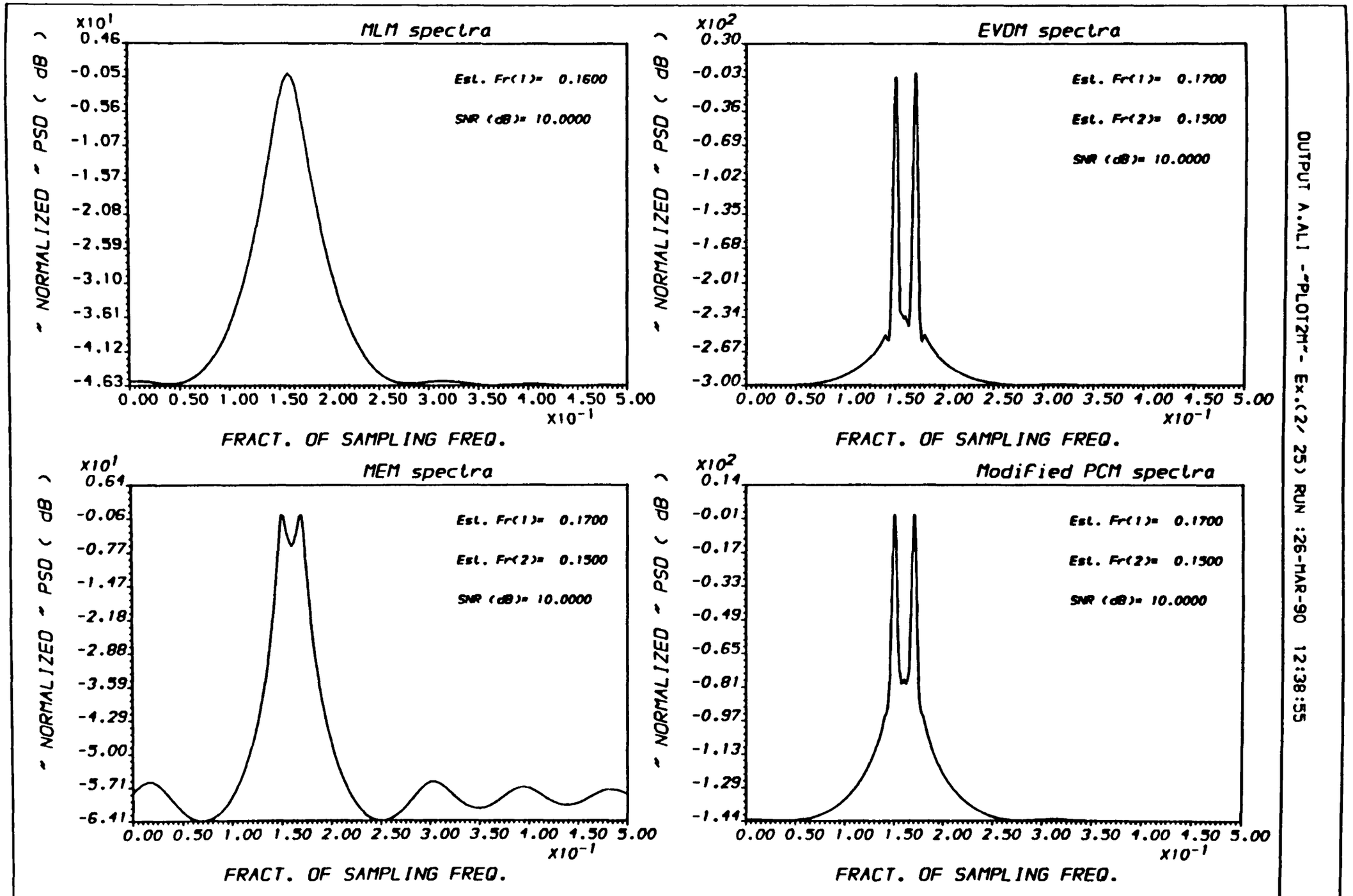

FIG.(5.5) POWER SPECTRAL DENSITY ESTIMATE
* For different PSDE methods *

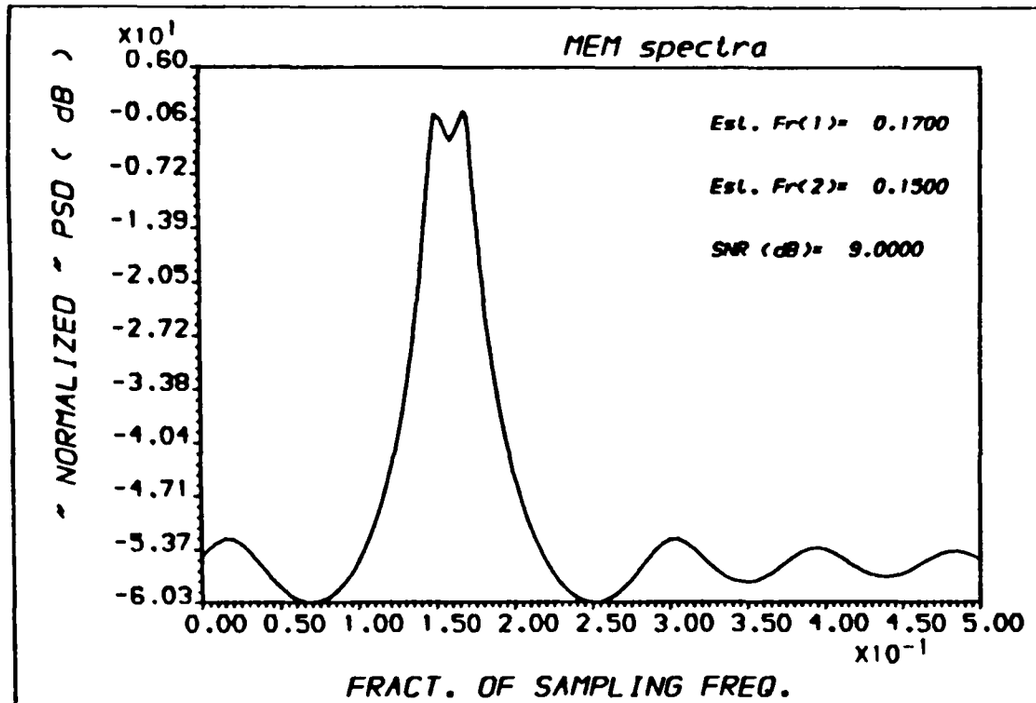

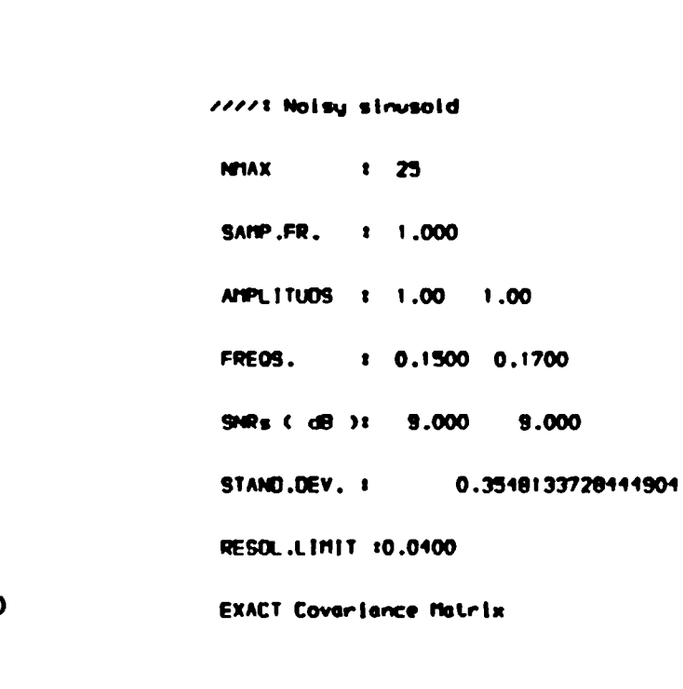

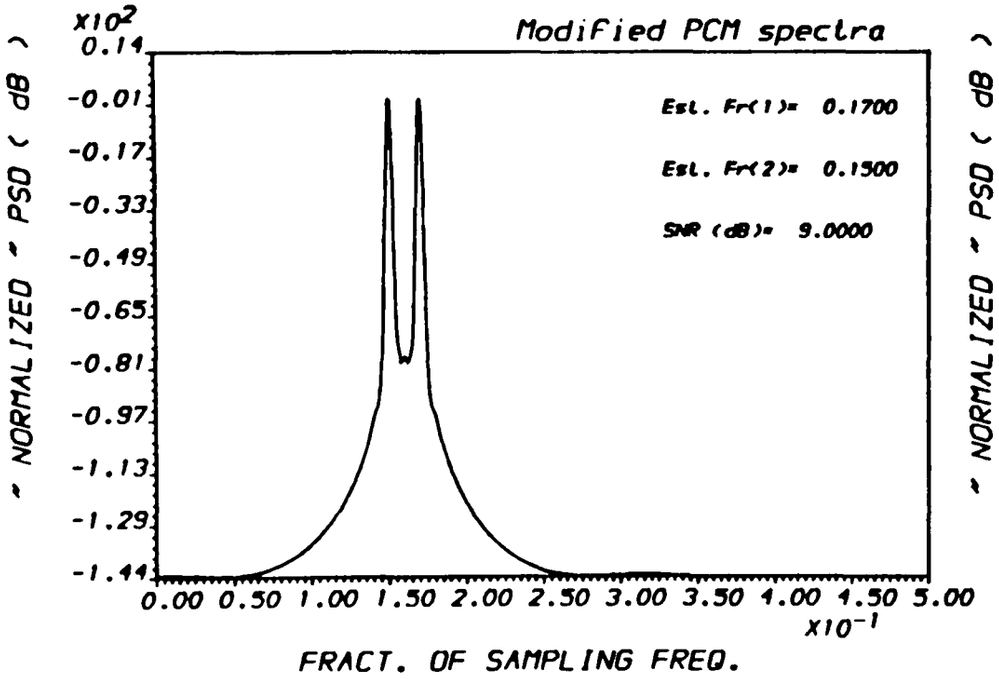

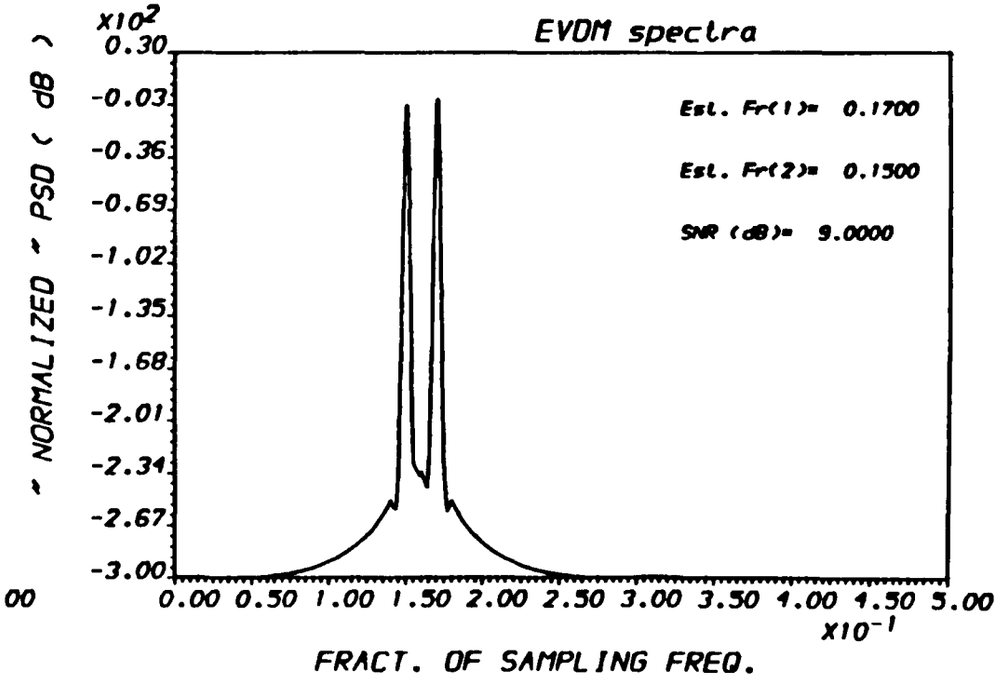

FIG.(5.6) POWER SPECTRAL DENSITY ESTIMATE
* For different PSDE methods *

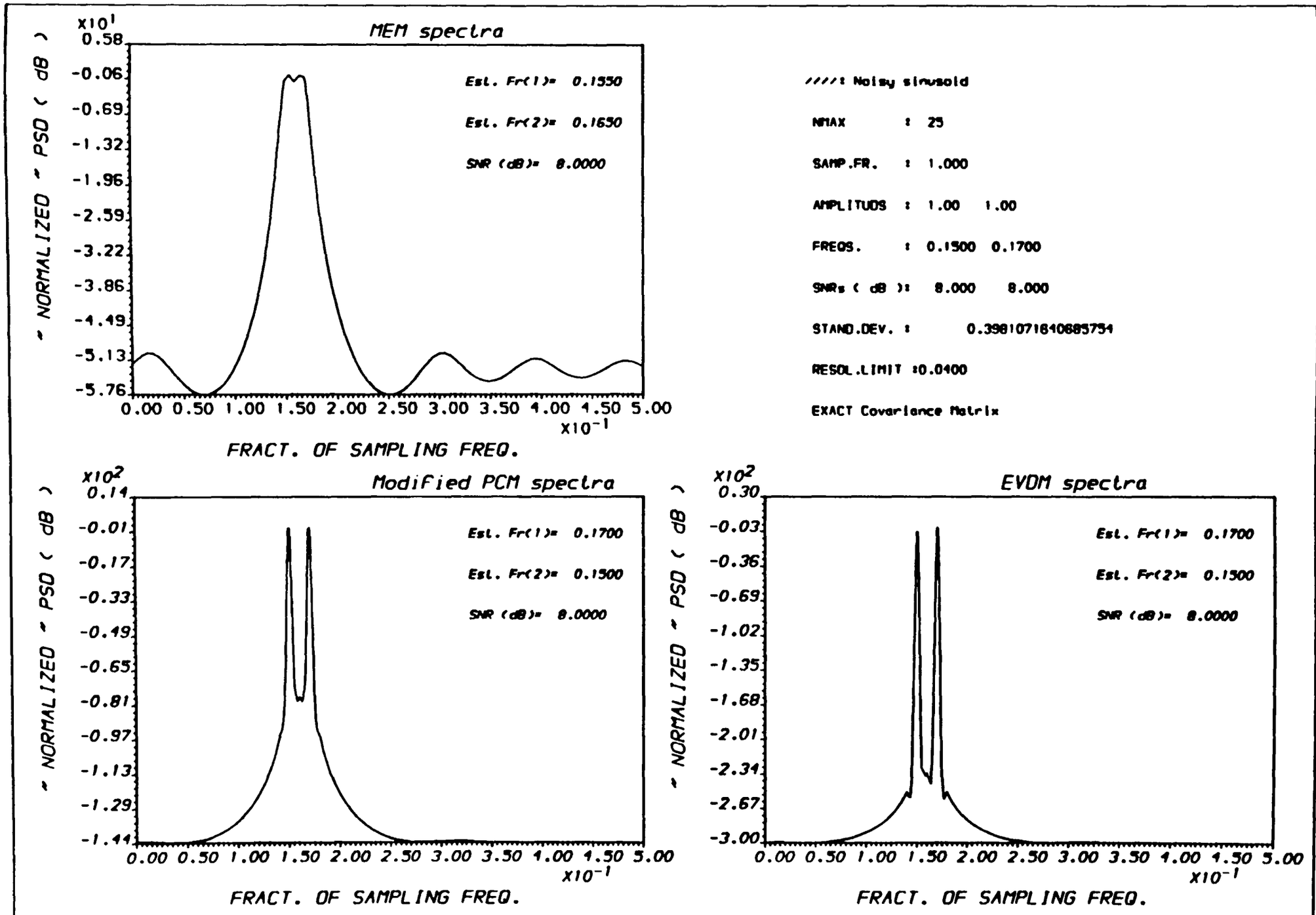

FIG.(5.7) POWER SPECTRAL DENSITY ESTIMATE
* For different PSDE methods *

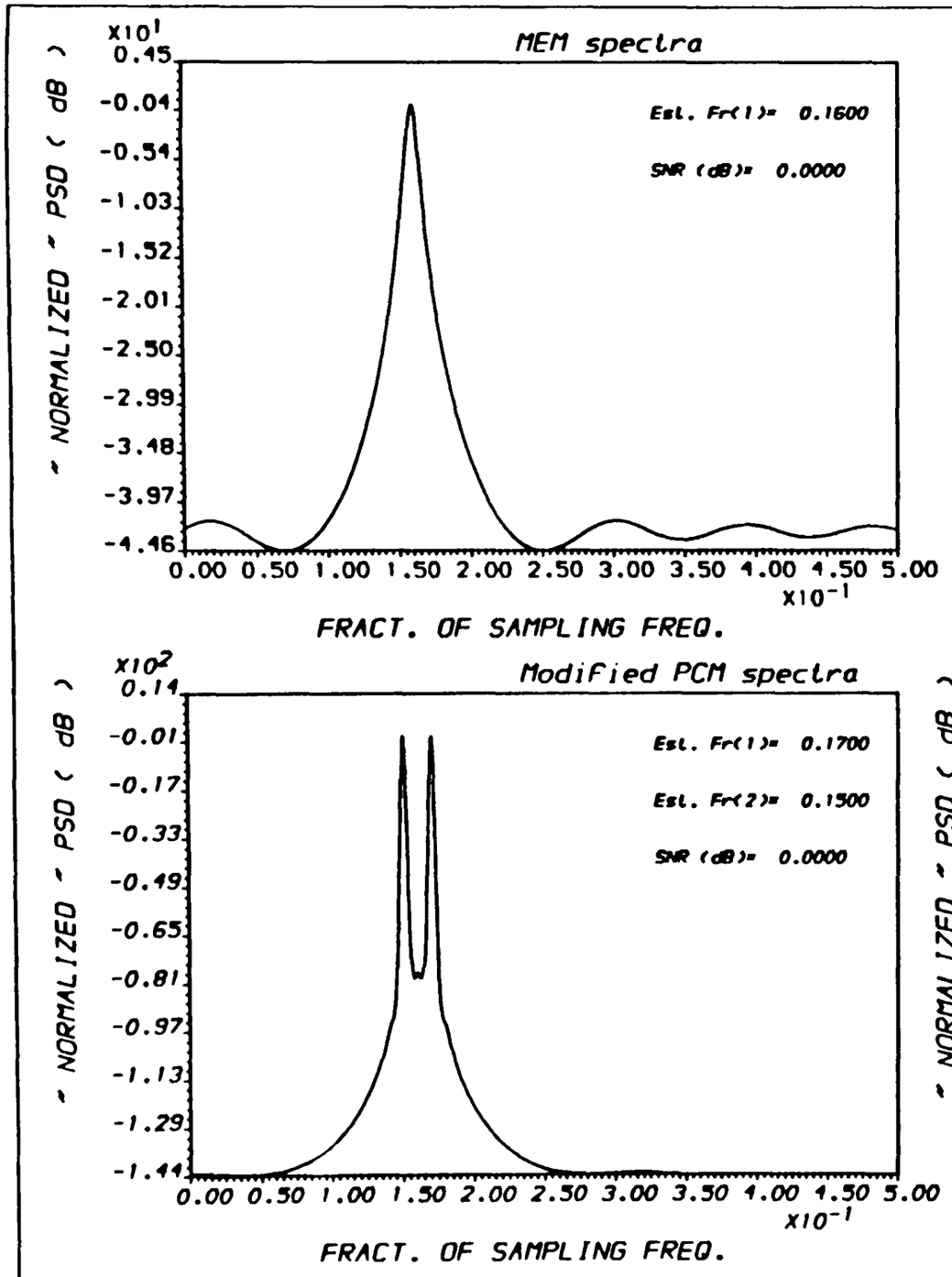

FIG.(5.8) POWER SPECTRAL DENSITY ESTIMATE
* For different PSDE methods *

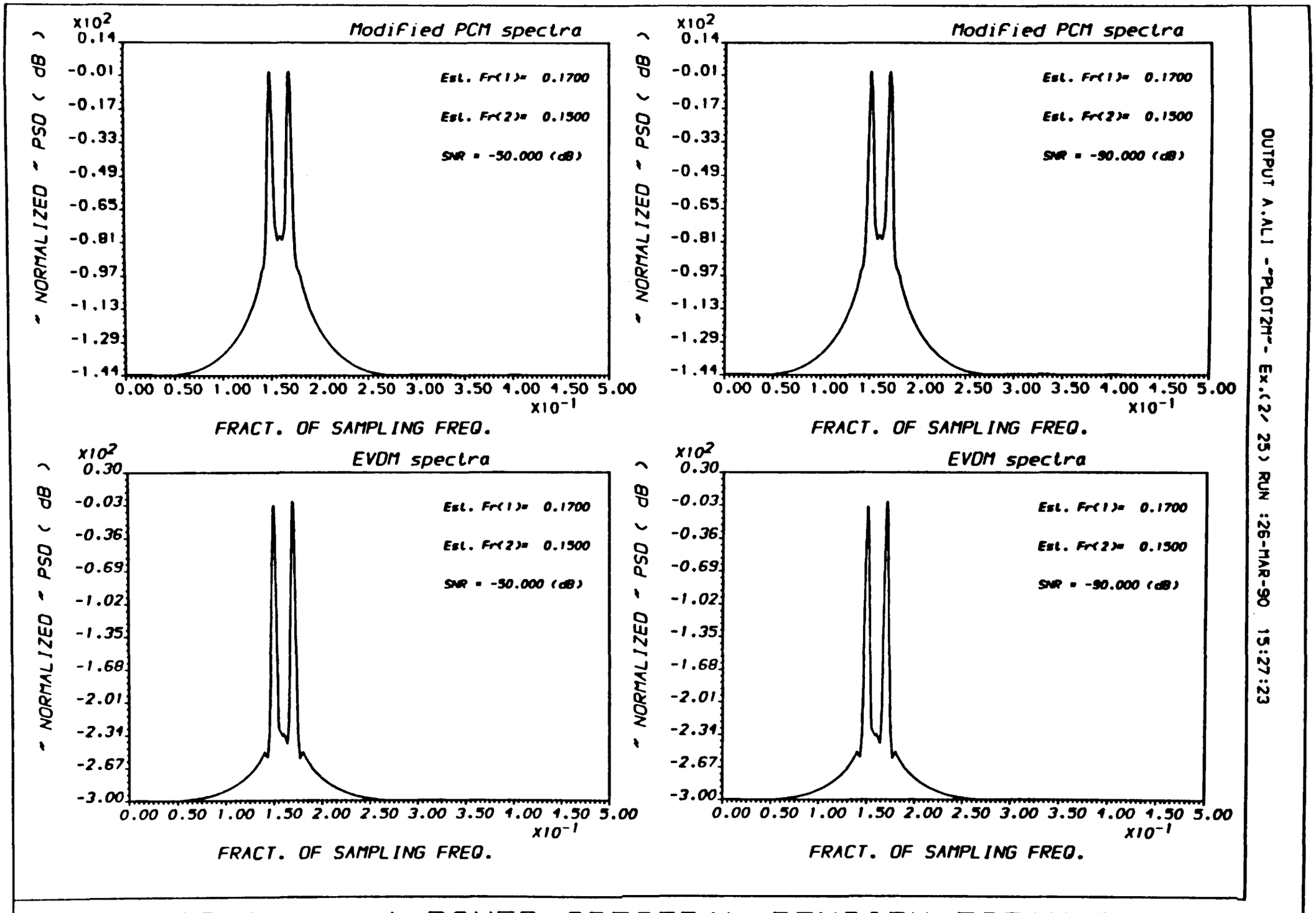

FIG.(5.9) POWER SPECTRAL DENSITY ESTIMATE
* For different PSDE methods *

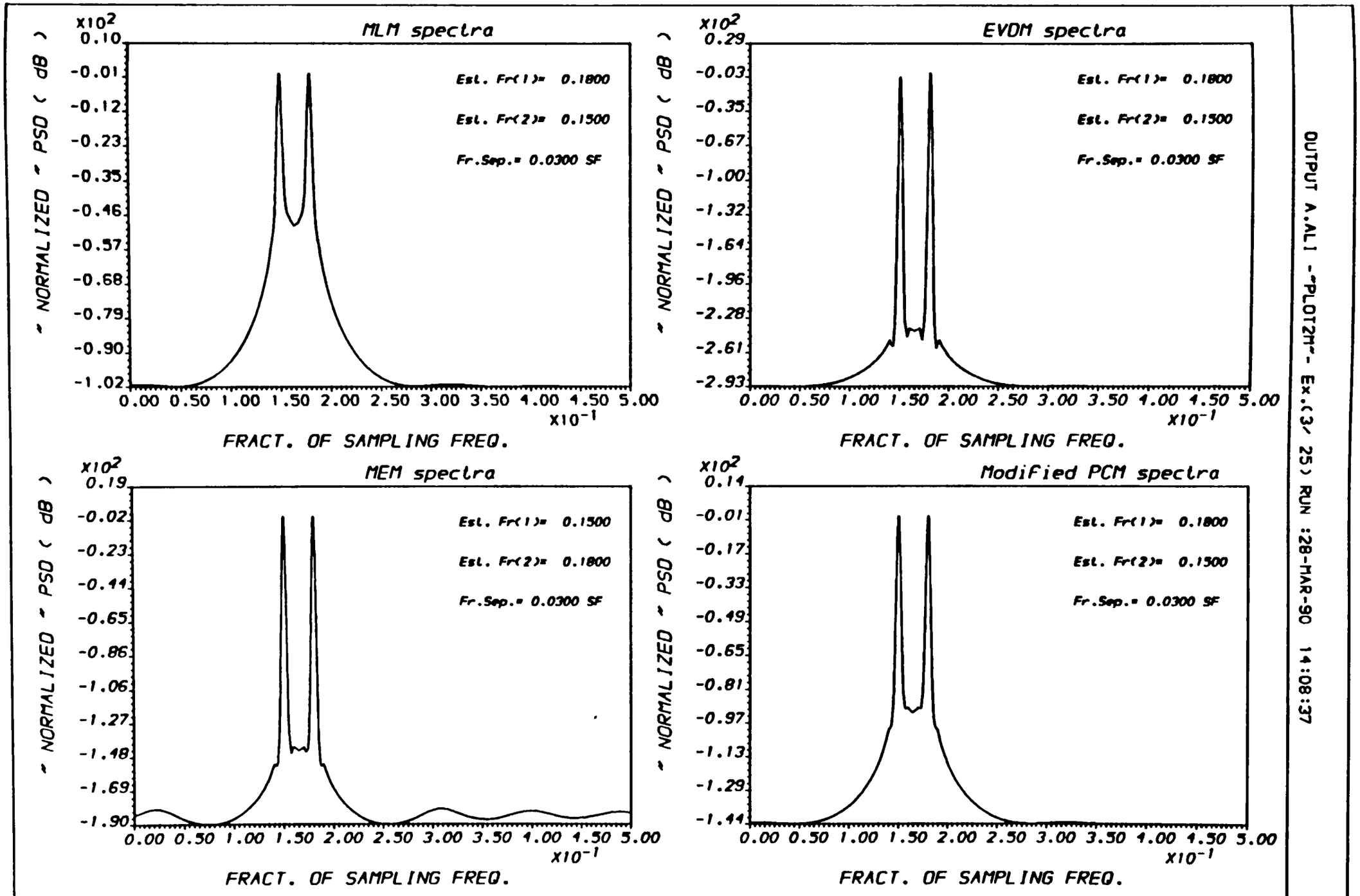

FIG.(5.10) POWER SPECTRAL DENSITY ESTIMATE
* For different PSDE methods *

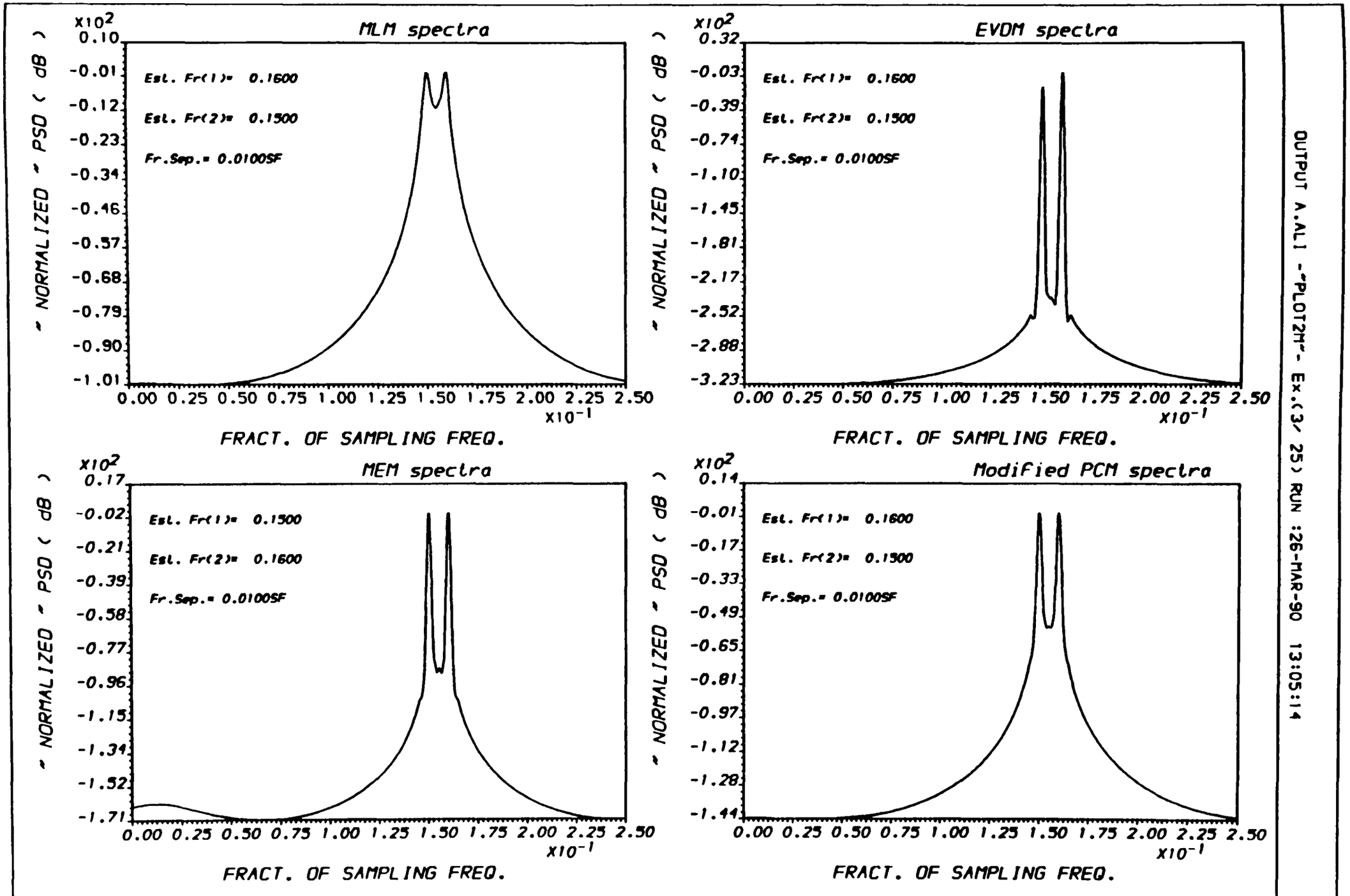

FIG.(5.11) POWER SPECTRAL DENSITY ESTIMATE
* For different PSDE methods *

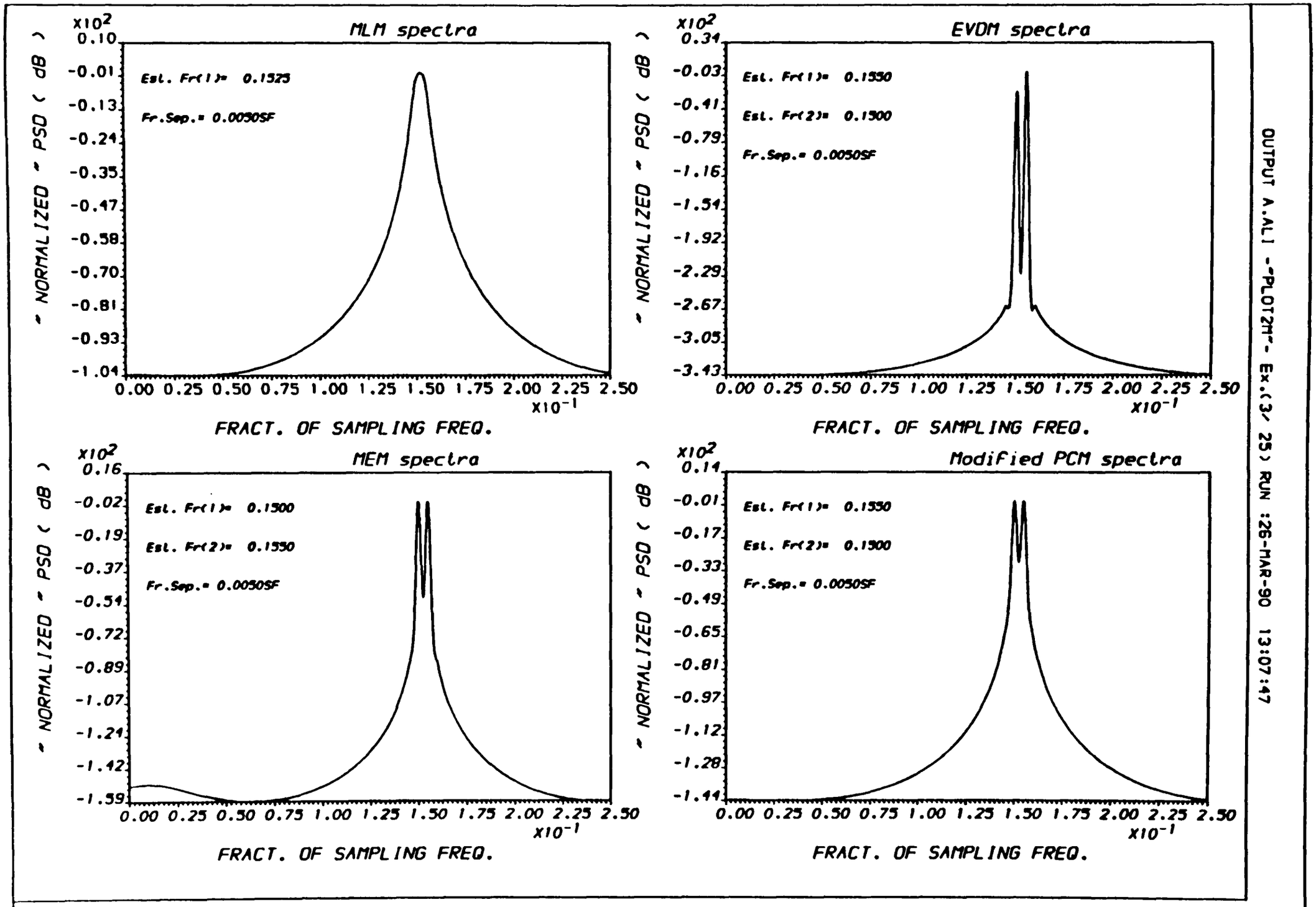

FIG.(5.12) POWER SPECTRAL DENSITY ESTIMATE
* For different PSDE methods *

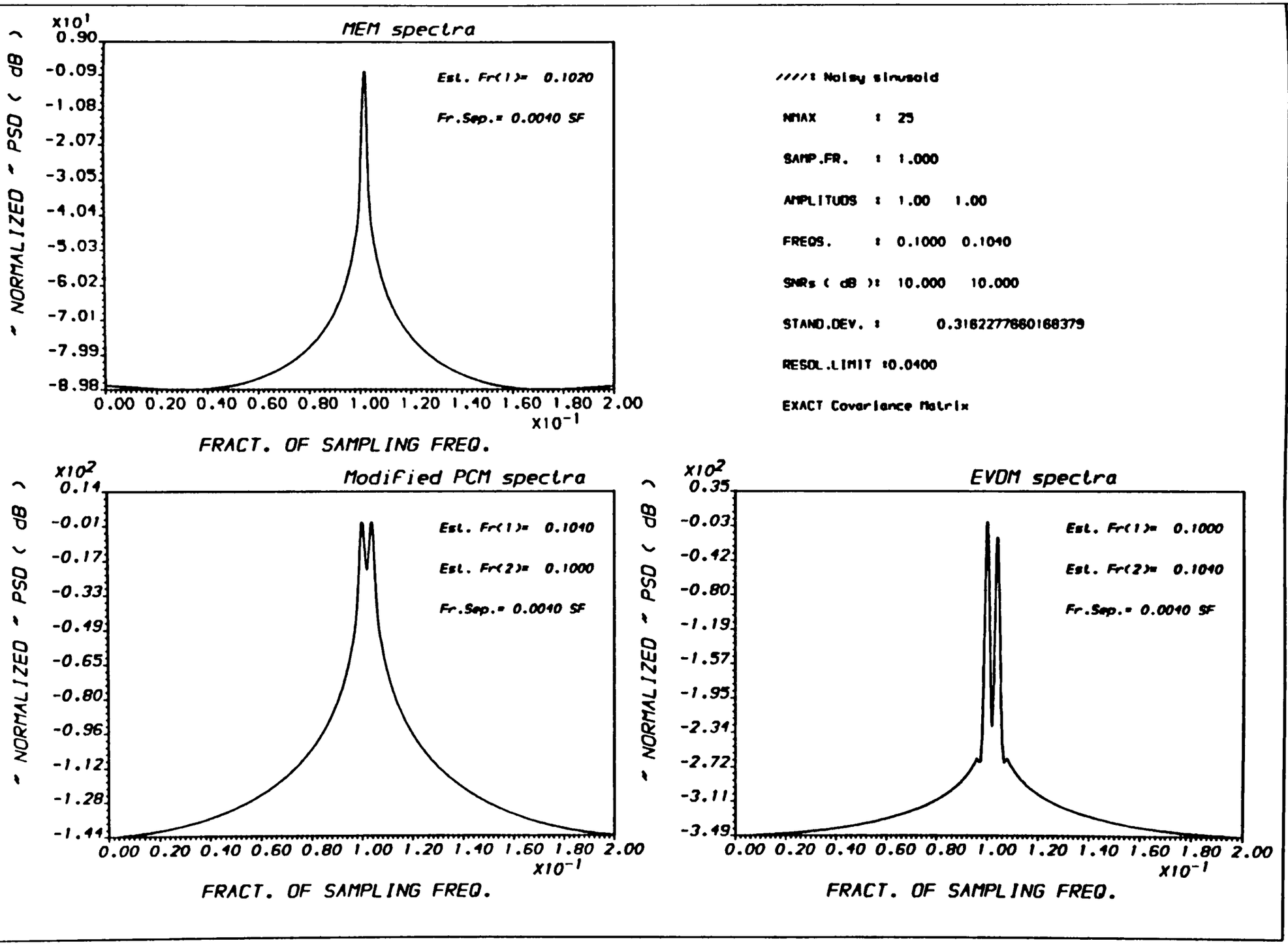

FIG.(5.13) POWER SPECTRAL DENSITY ESTIMATE
* For different PSDE methods *

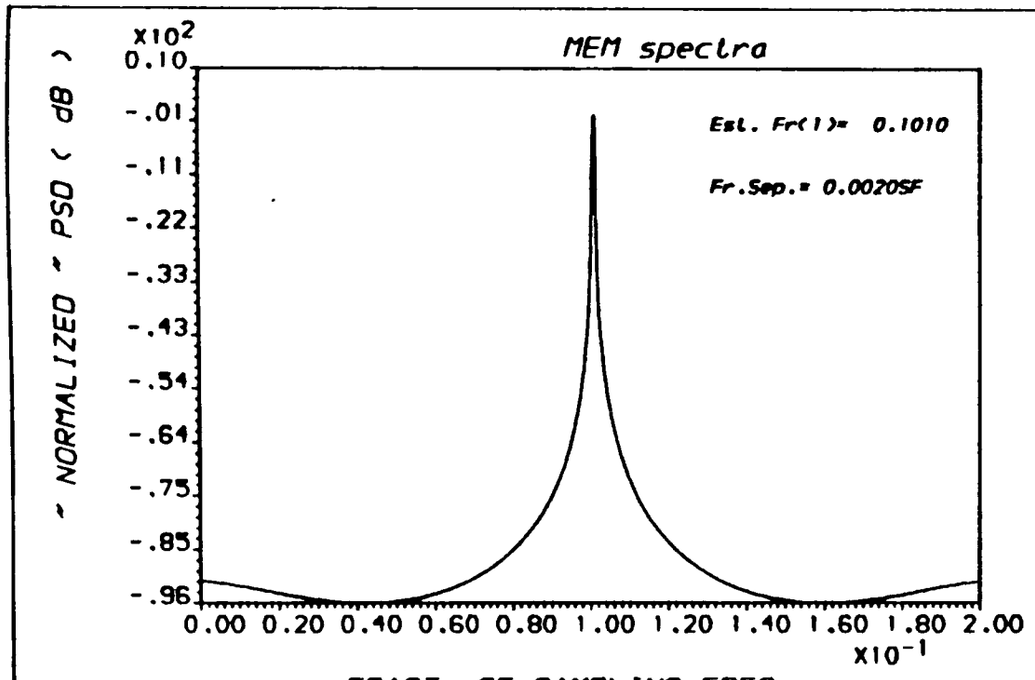

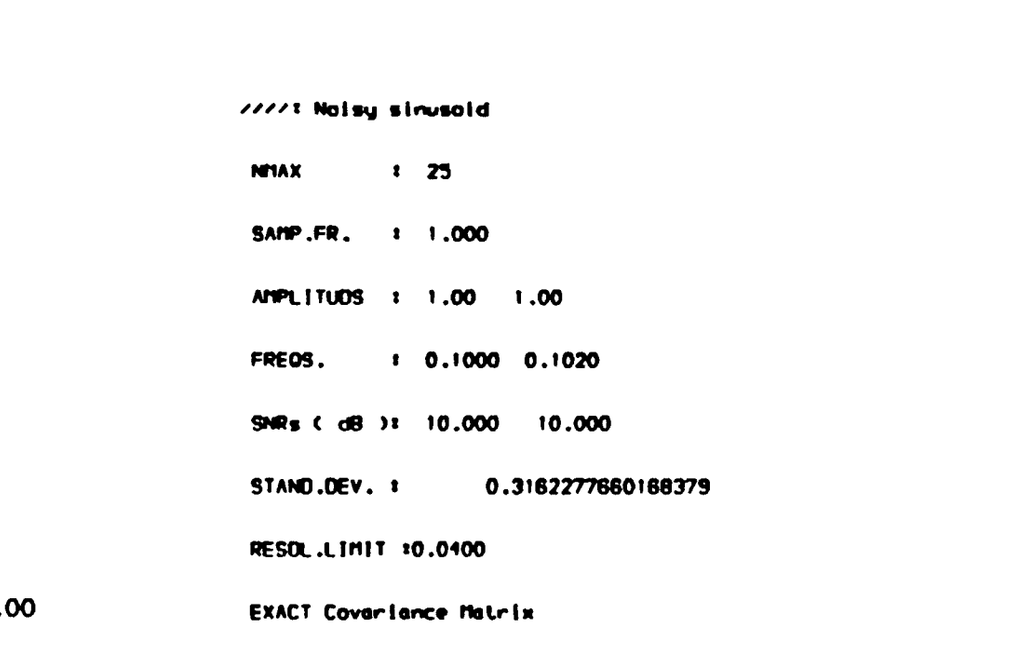

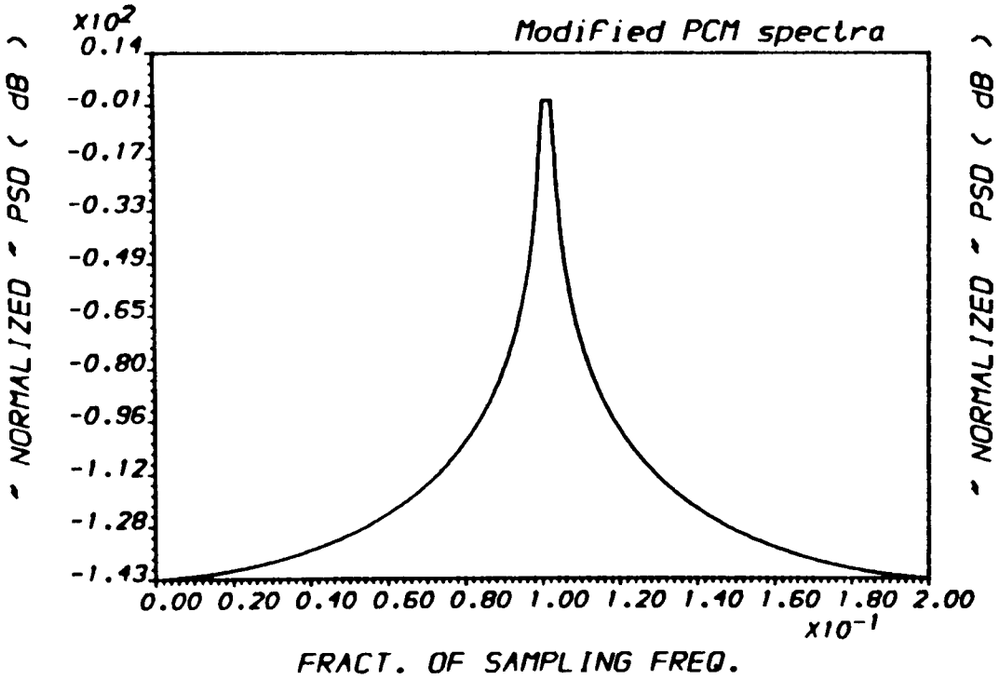


```
/////: Noisy sinusoid

NMAX        :  25

SAMP.FR.    :  1.000

AMPLITUDS   :  1.00   1.00

FREQS.      :  0.1000  0.1020

SNRs ( dB ):  10.000   10.000

STAND.DEV.  :       0.3162277660168379

RESOL.LIMIT :0.0400

EXACT Covariance Matrix
```

OUTPUT A.ALI -"PLOT2M"- Ex.(3/ 25) RUN :26-MAR-90 13:31:19

FIG.(5.14) POWER SPECTRAL DENSITY ESTIMATE
* For different PSDE methods *

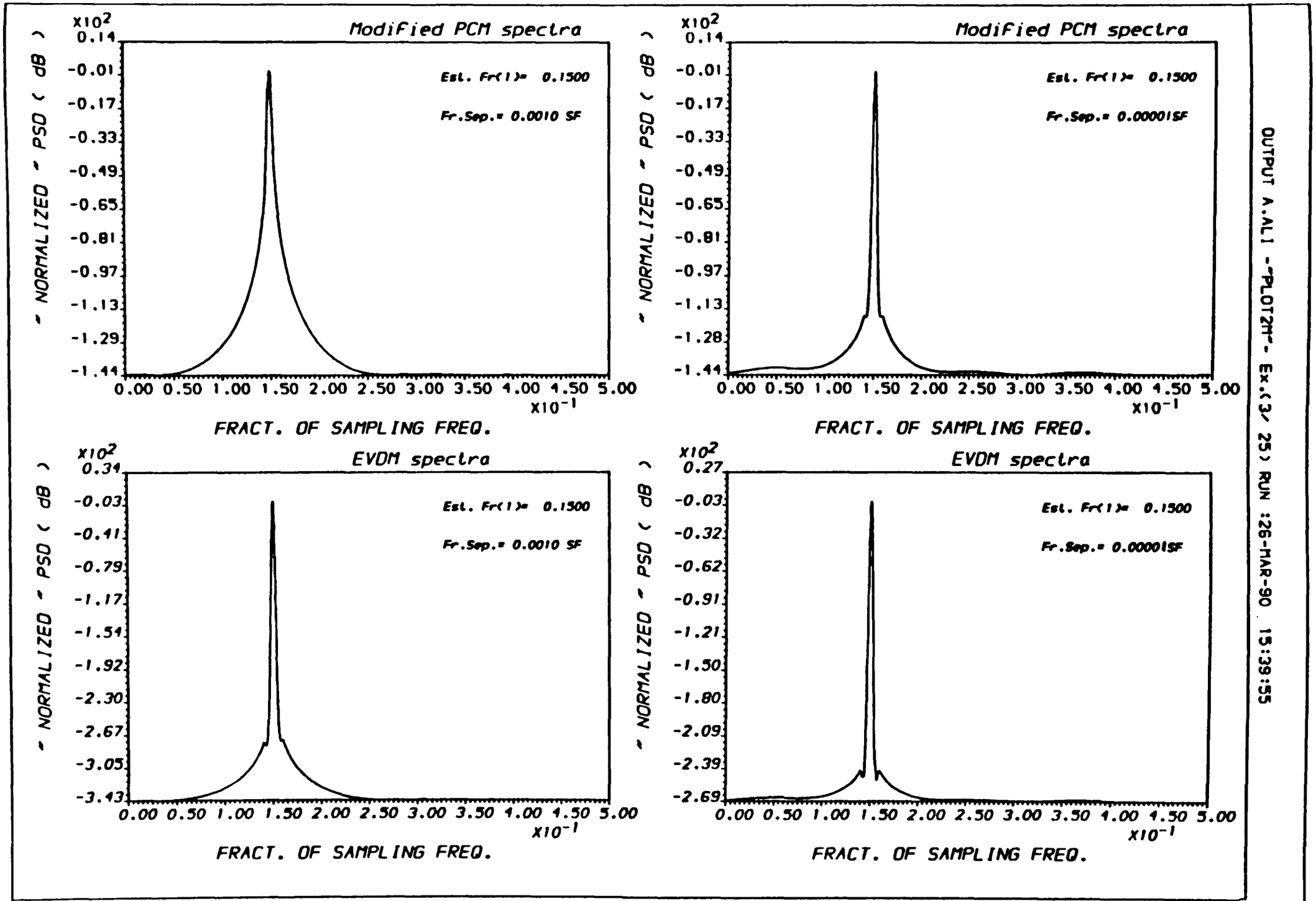

FIG.(5.15) POWER SPECTRAL DENSITY ESTIMATE
* For different PSDE methods *

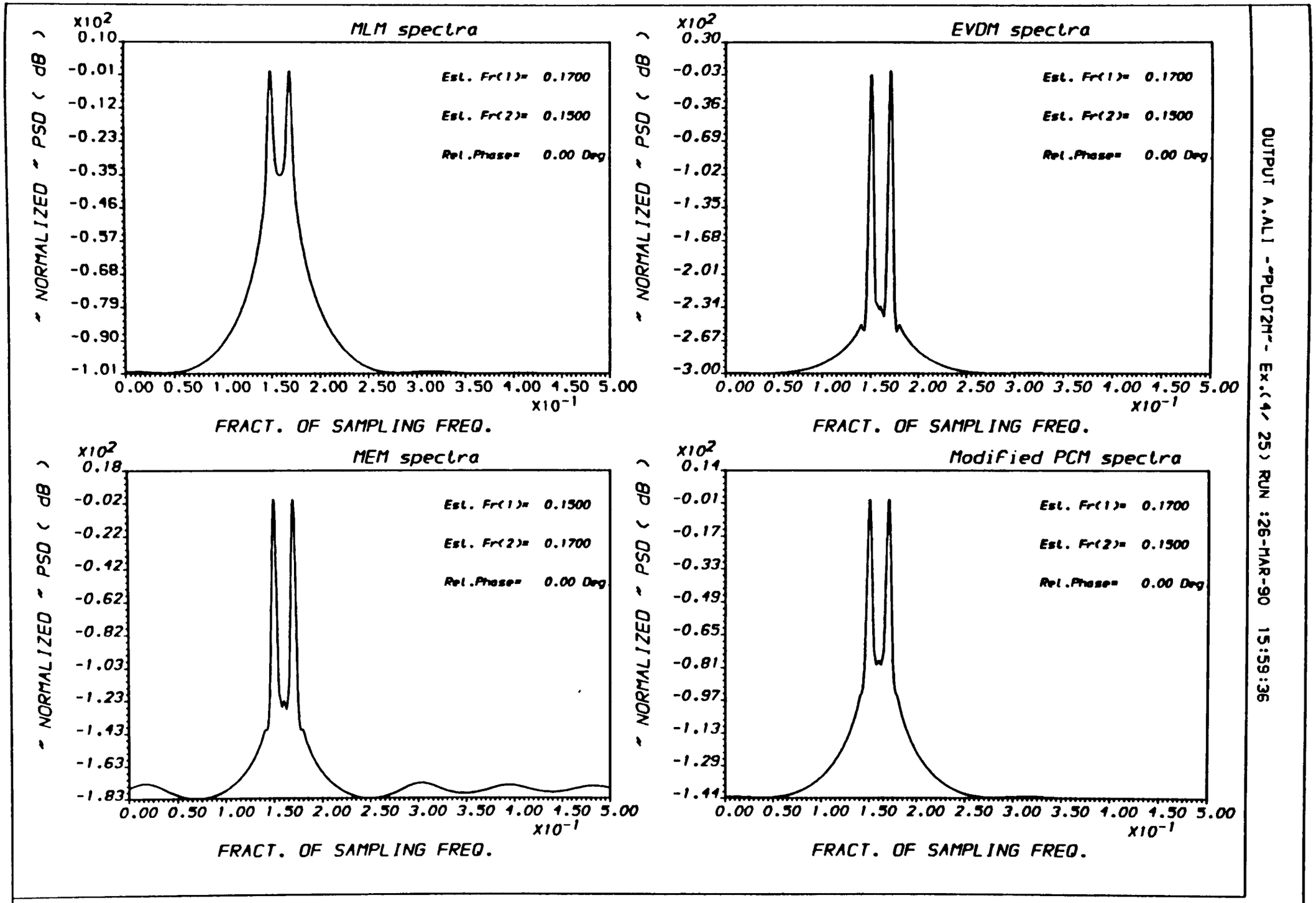

FIG.(5.16) POWER SPECTRAL DENSITY ESTIMATE
* For different PSDE methods *

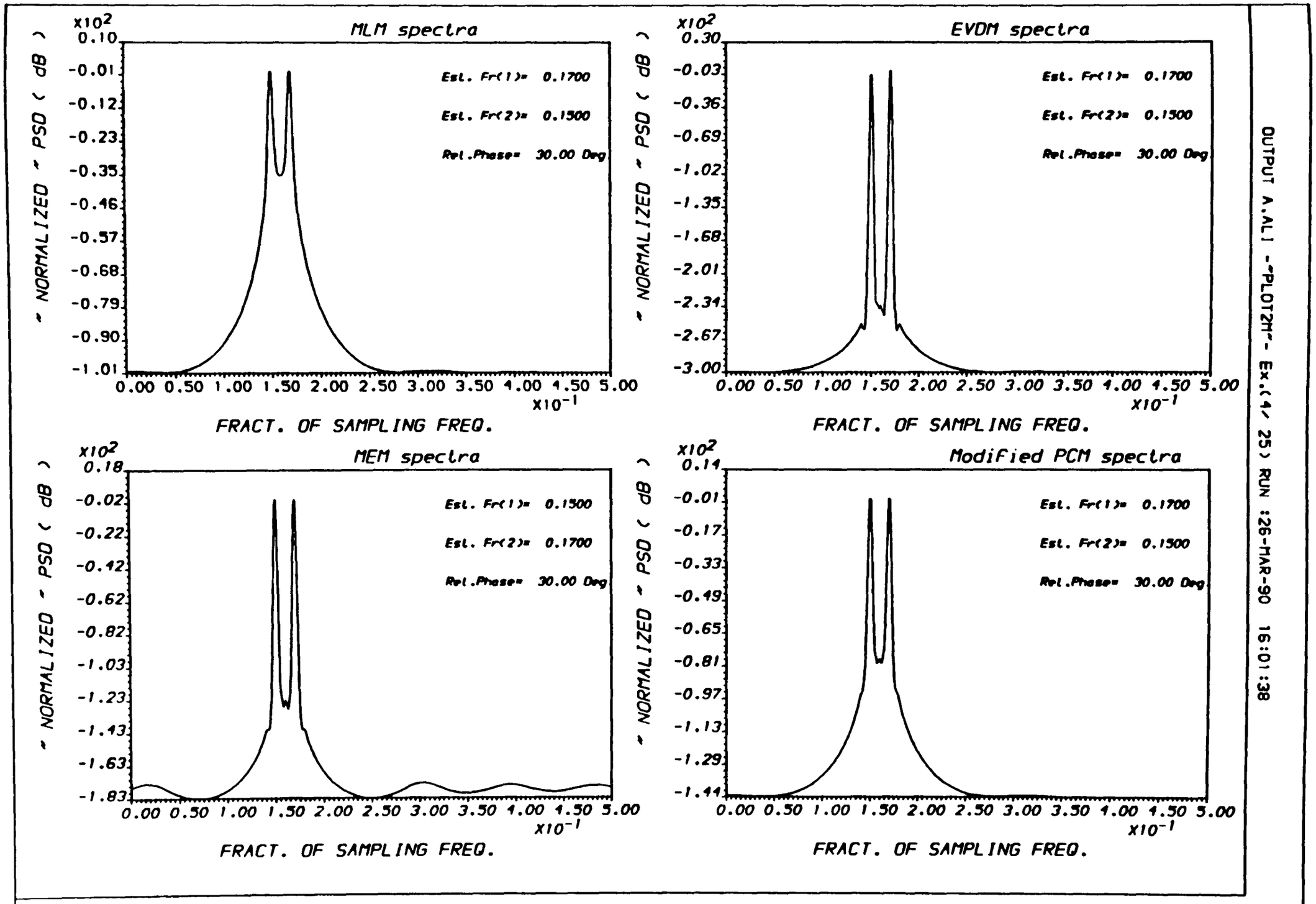

FIG.(5.17) POWER SPECTRAL DENSITY ESTIMATE
* For different PSDE methods *

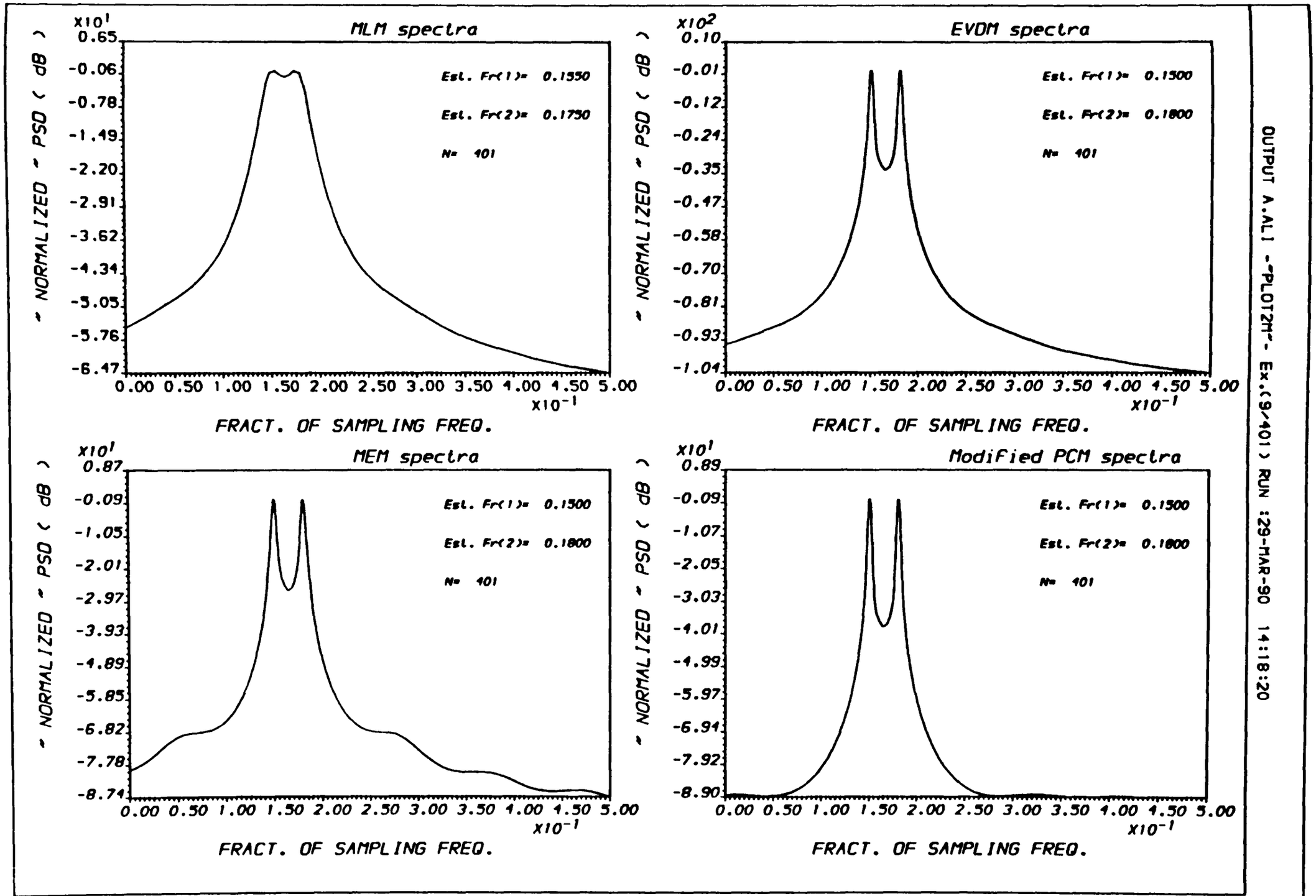

FIG.(5.18) POWER SPECTRAL DENSITY ESTIMATE
* For different PSDE methods *

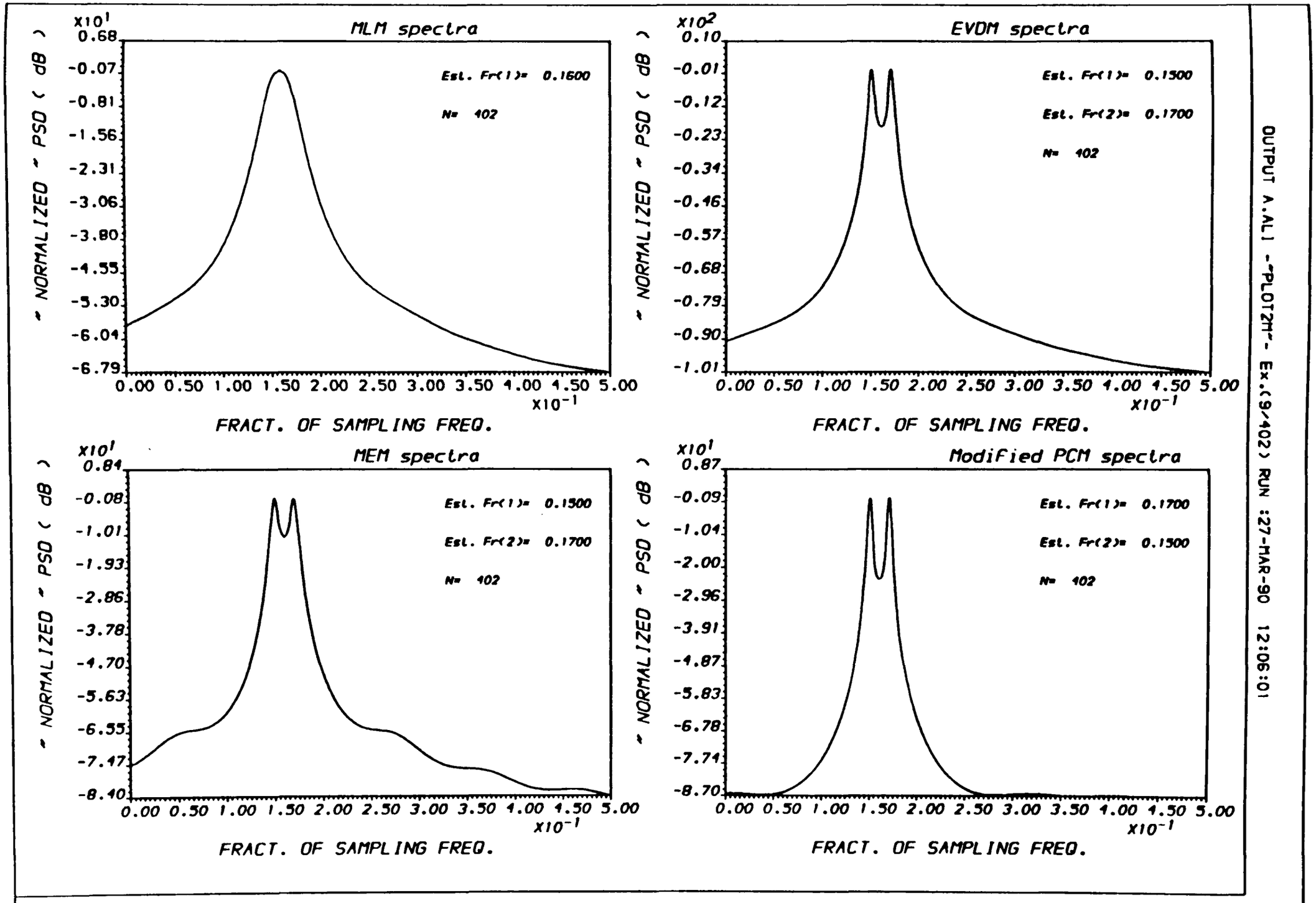

FIG.(5.19) POWER SPECTRAL DENSITY ESTIMATE
* For different PSDE methods *

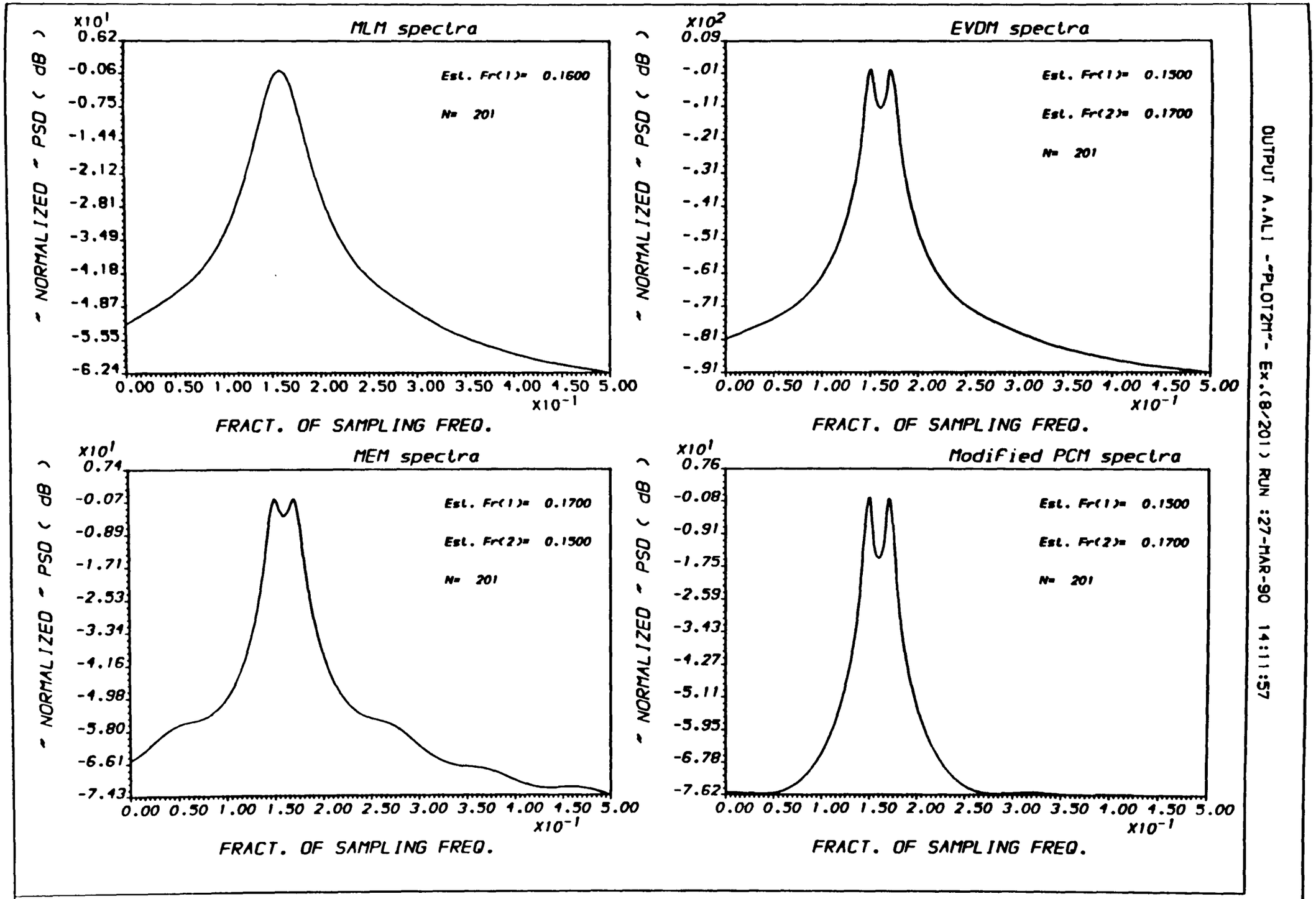

FIG.(5.20) POWER SPECTRAL DENSITY ESTIMATE
* For different PSDE methods *

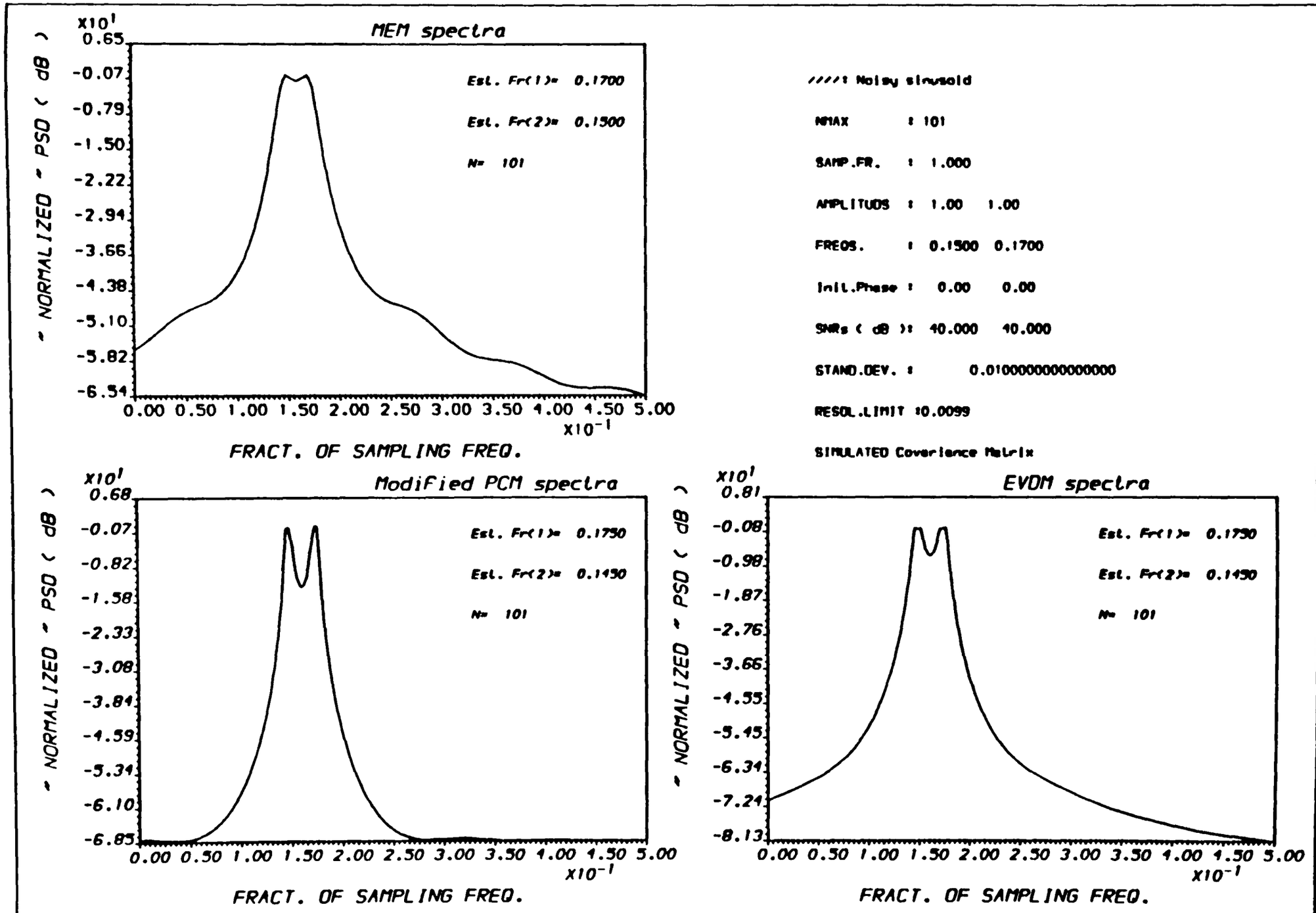

FIG.(5.21) POWER SPECTRAL DENSITY ESTIMATE
* For different PSDE methods *

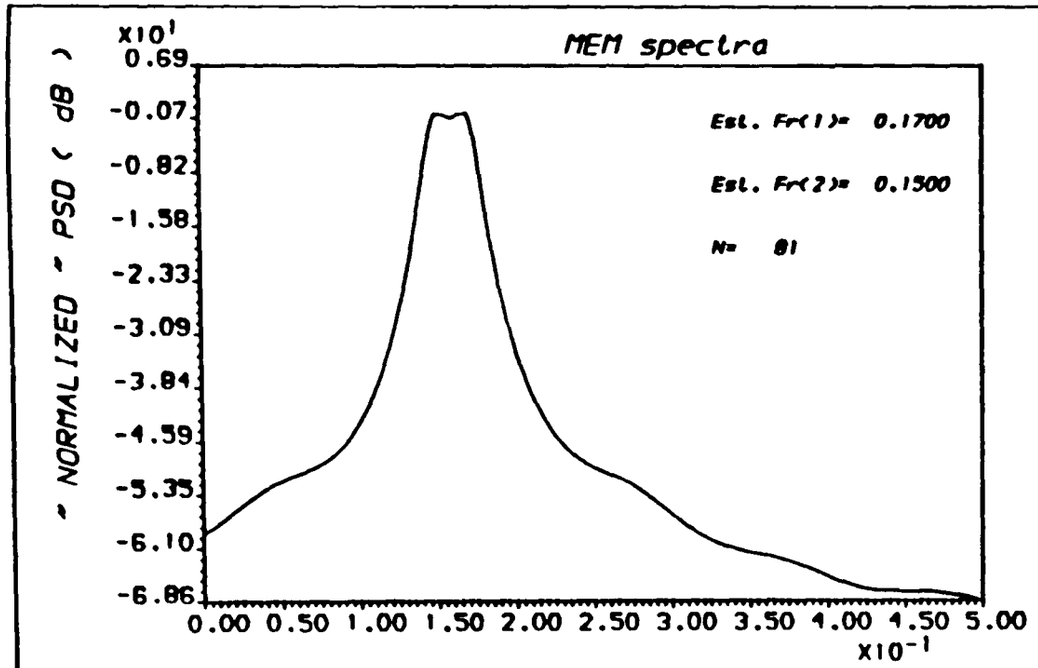

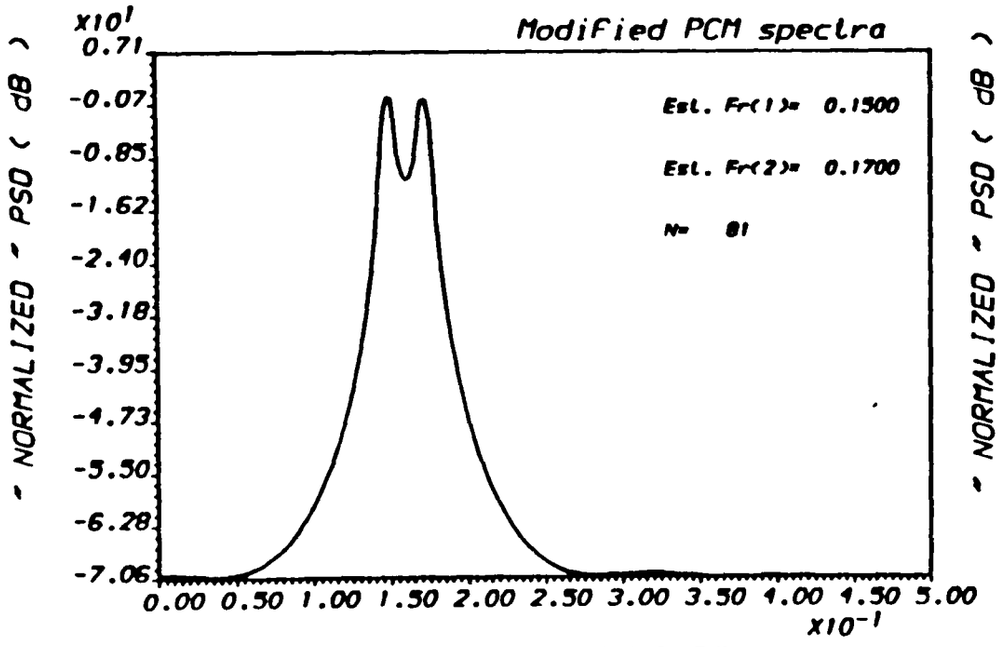


```
/////: Noisy sinusoid

 NMAX        :  81

 SAMP.FR.    :  1.000

 AMPLITUDS   :  1.00   1.00

 FREQS.      :  0.1500  0.1700

 Init.Phase  :   0.00    0.00

 SNRs ( dB ):  40.000   40.000

 STAND.DEV.  :        0.0100000000000000

 RESOL.LIMIT :0.0123

 SIMULATED Coverience Matrix
```

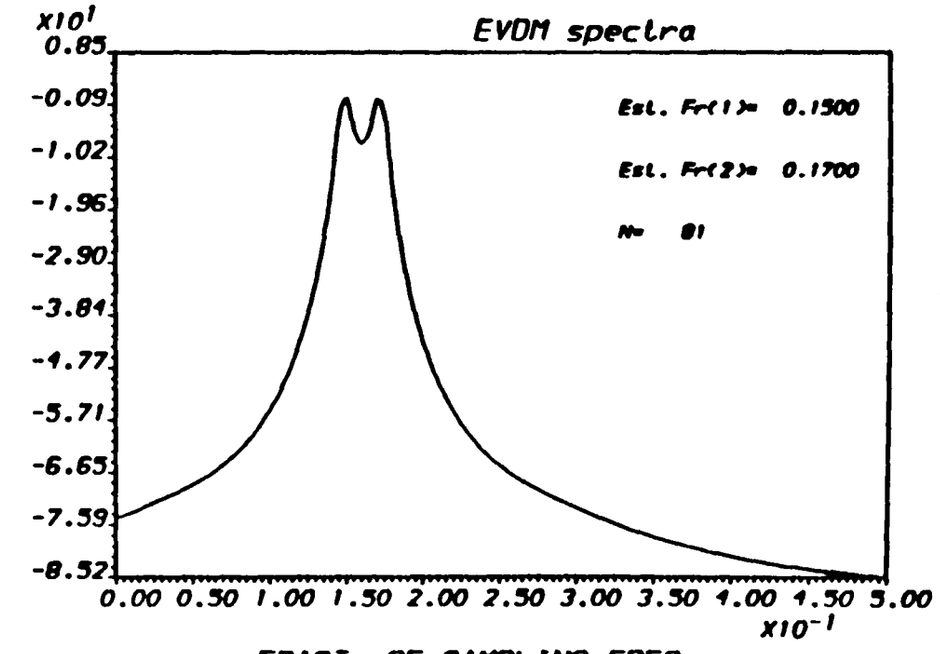

OUTPUT A.ALI -"PLOT2M"- Ex.(8/ 81) RUN :27-MAR-90 14:16:06

FIG.(5.22) POWER SPECTRAL DENSITY ESTIMATE
* For different PSDE methods *

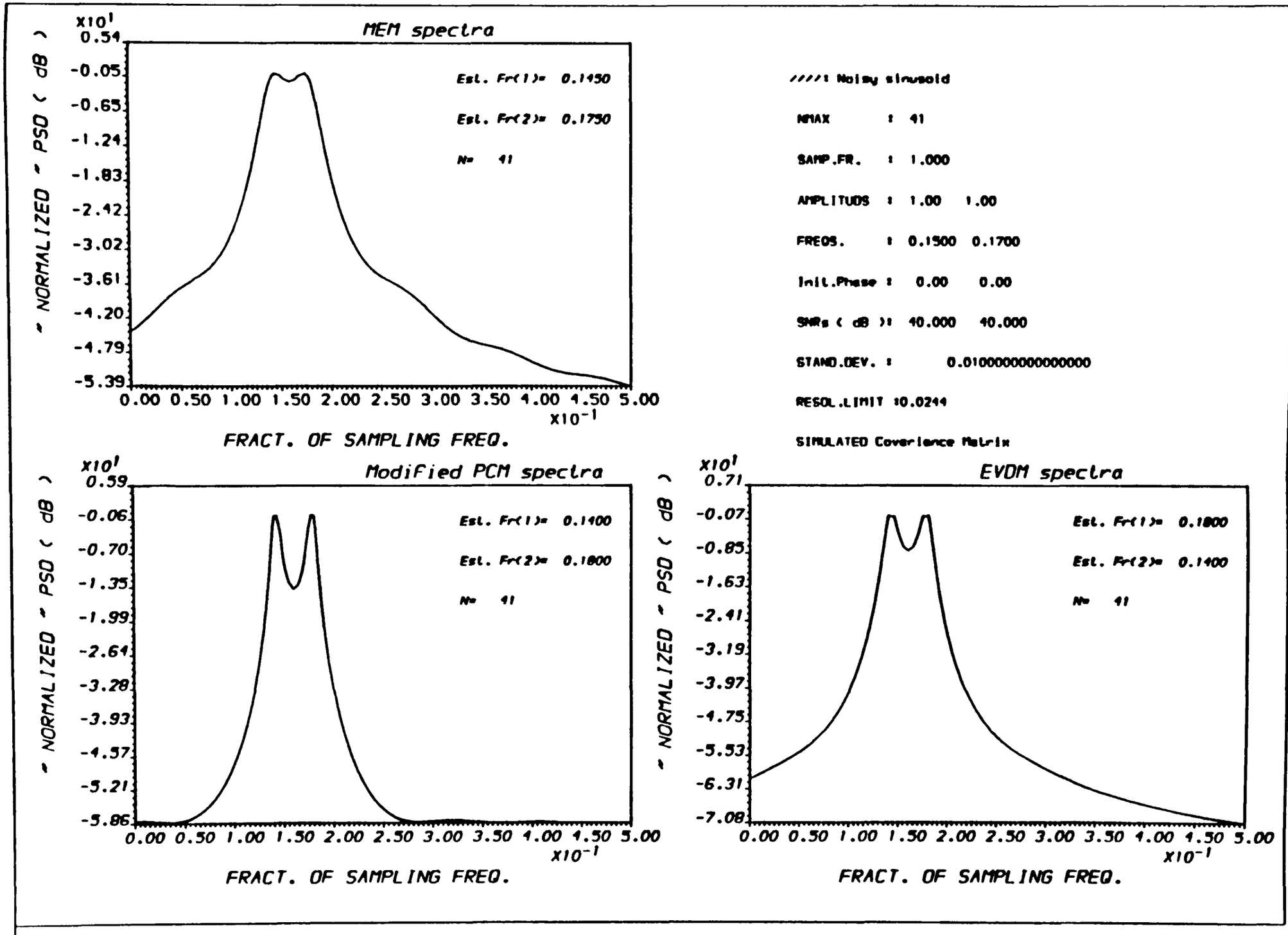

FIG.(5.23) POWER SPECTRAL DENSITY ESTIMATE
* For different PSDE methods *

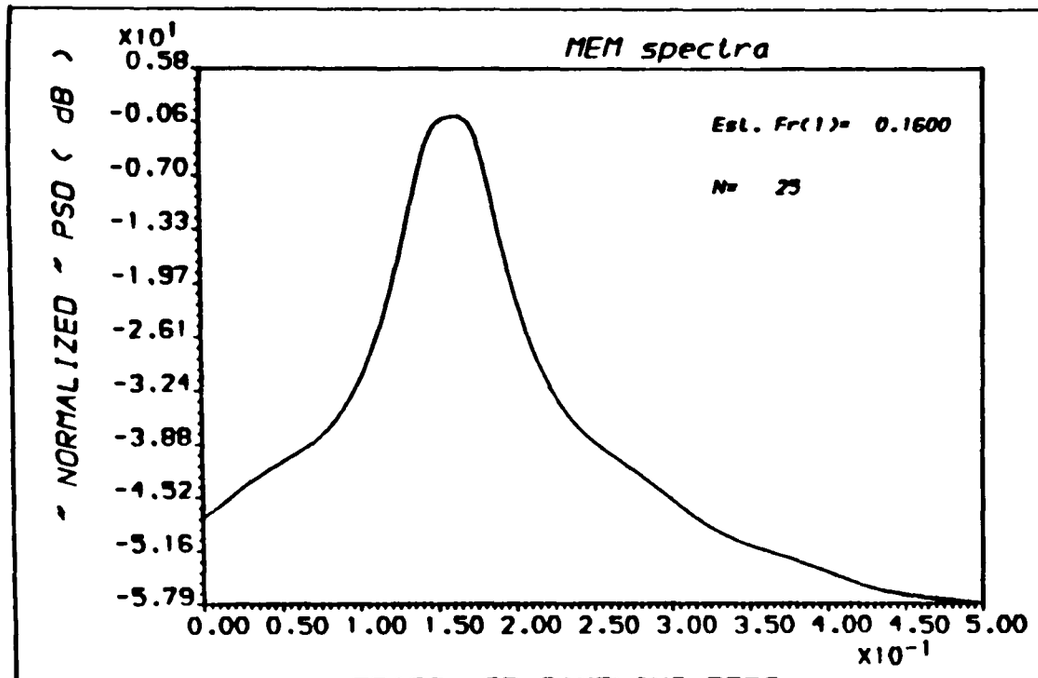

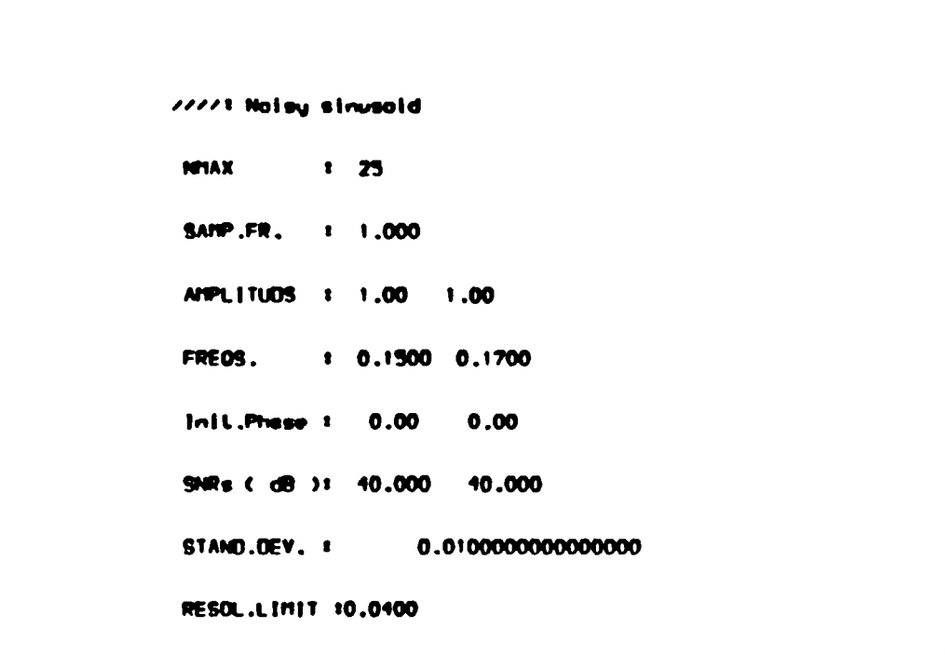

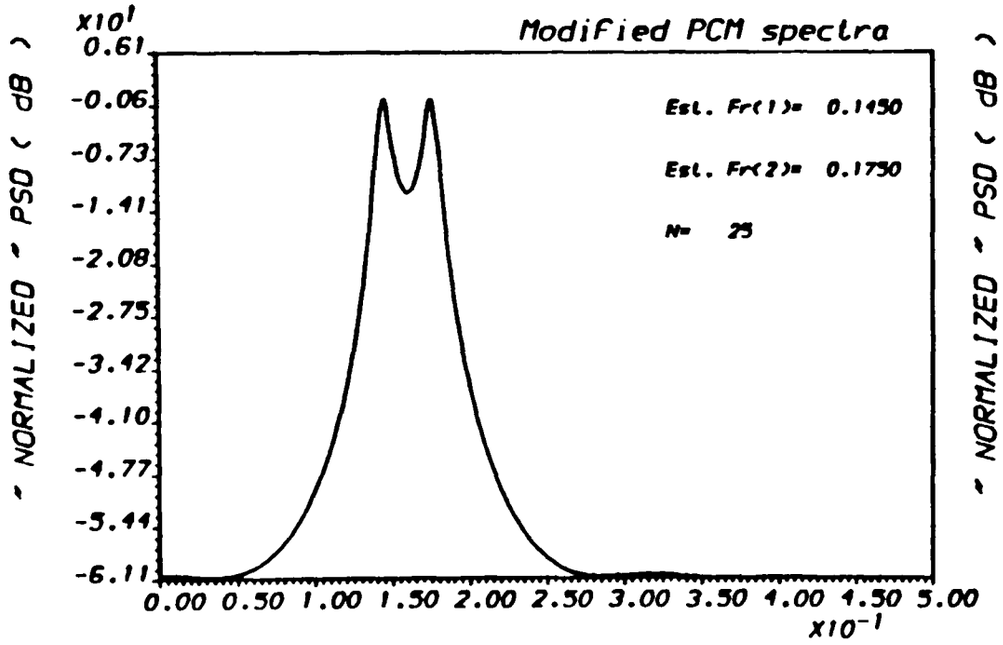

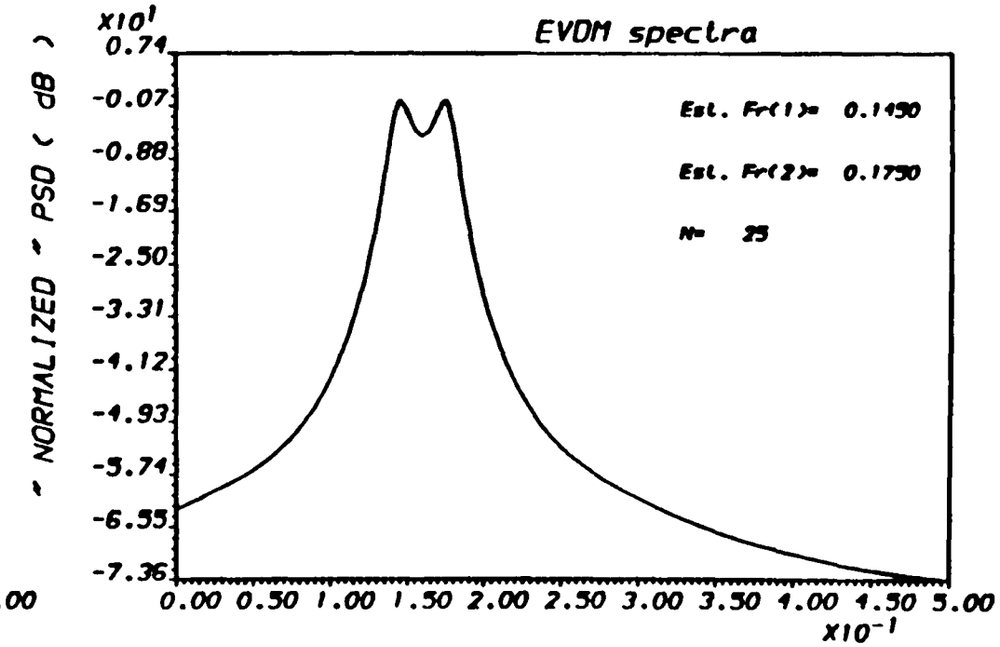

OUTPUT A.ALL -PLOTZM- Ex.(8/ 25) RUN :27-MAR-90 14:23:11

FIG.(5.24) POWER SPECTRAL DENSITY ESTIMATE
* For different PSDE methods *

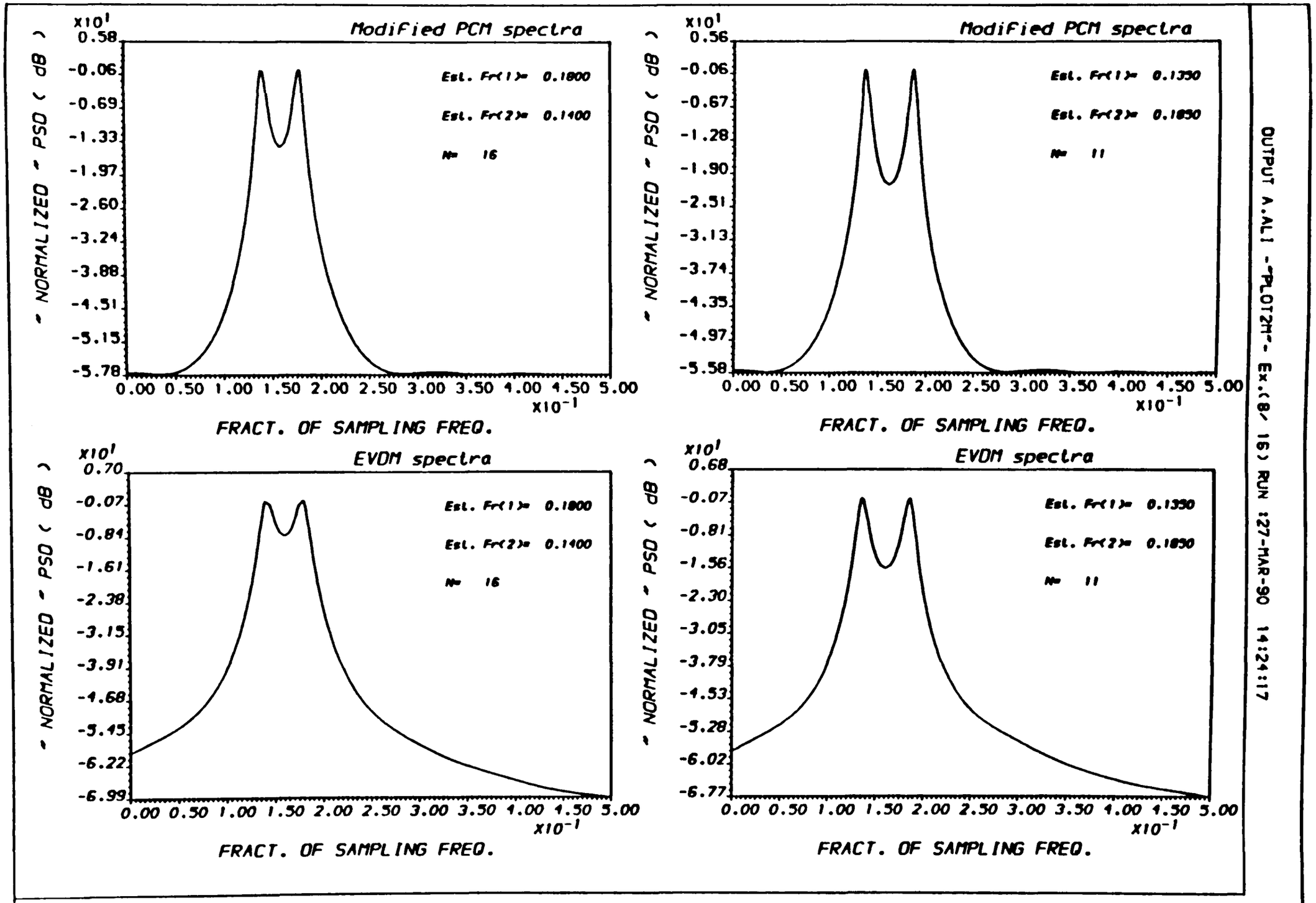

FIG.(5.25) POWER SPECTRAL DENSITY ESTIMATE
* For different PSDE methods *

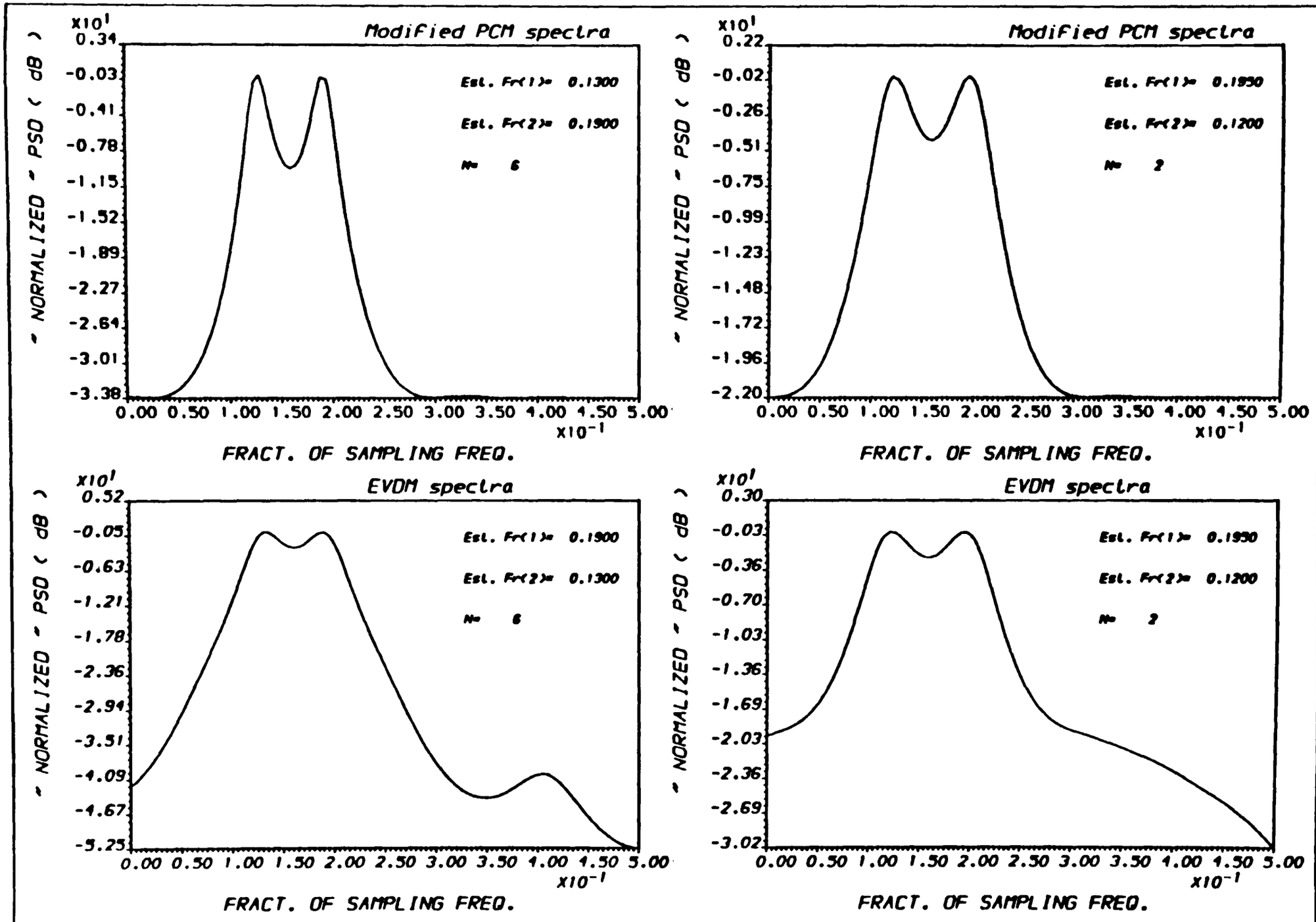

FIG.(5.26) POWER SPECTRAL DENSITY ESTIMATE
* For different PSDE methods *

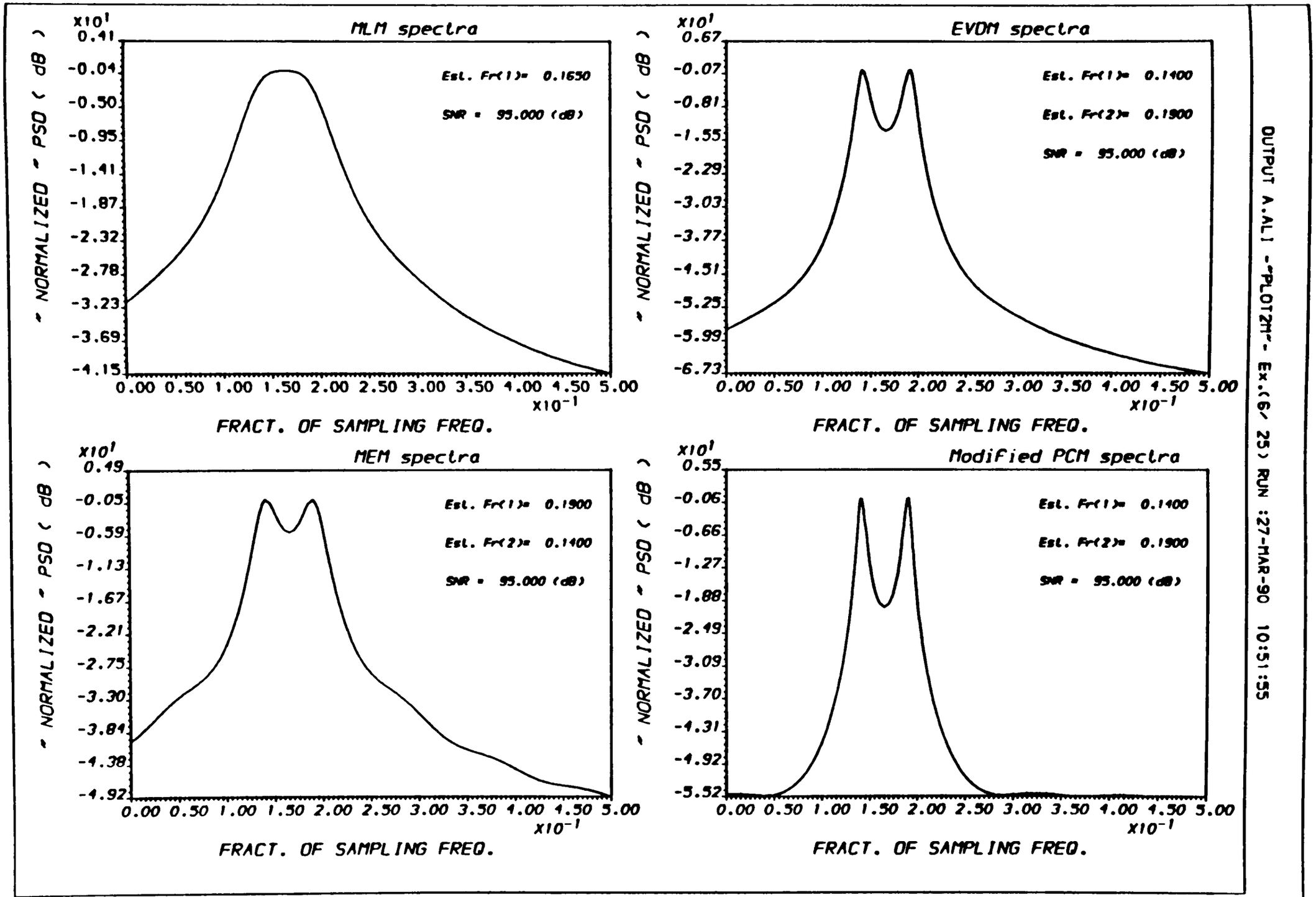

FIG.(5.27) POWER SPECTRAL DENSITY ESTIMATE
* For different PSDE methods *

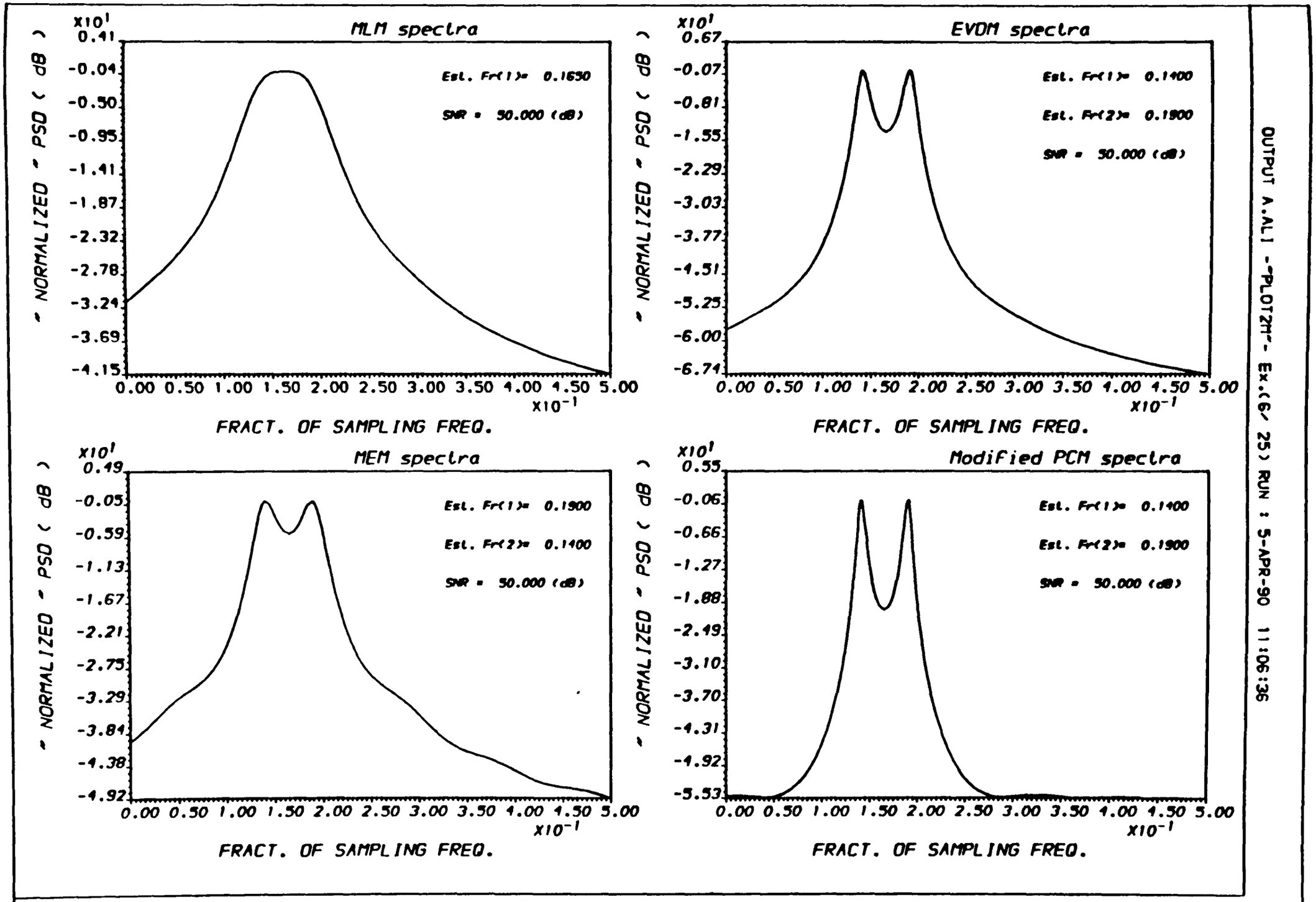

FIG.(5.28) POWER SPECTRAL DENSITY ESTIMATE
* For different PSDE methods *

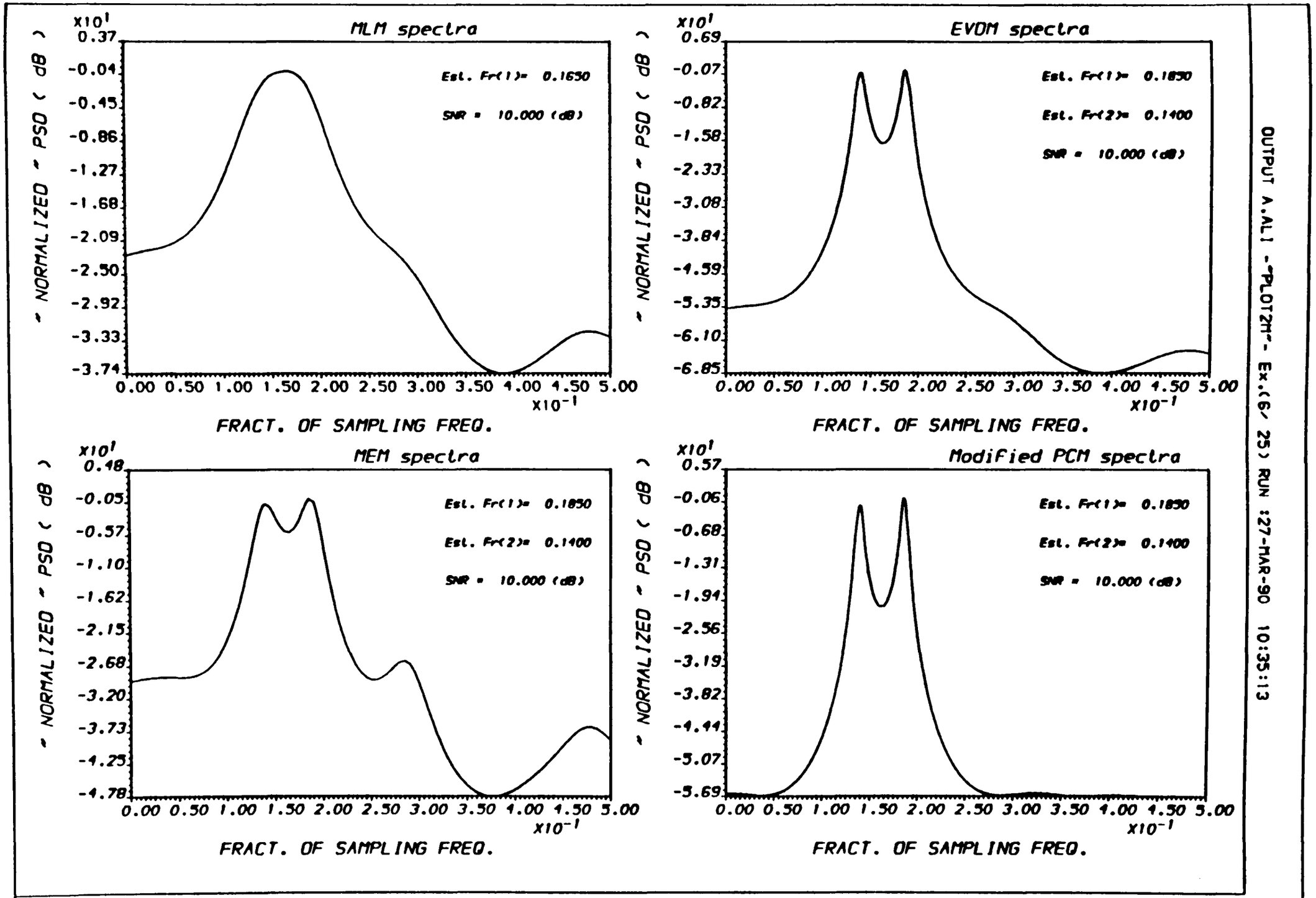

FIG.(5.29) POWER SPECTRAL DENSITY ESTIMATE
* For different PSDE methods *

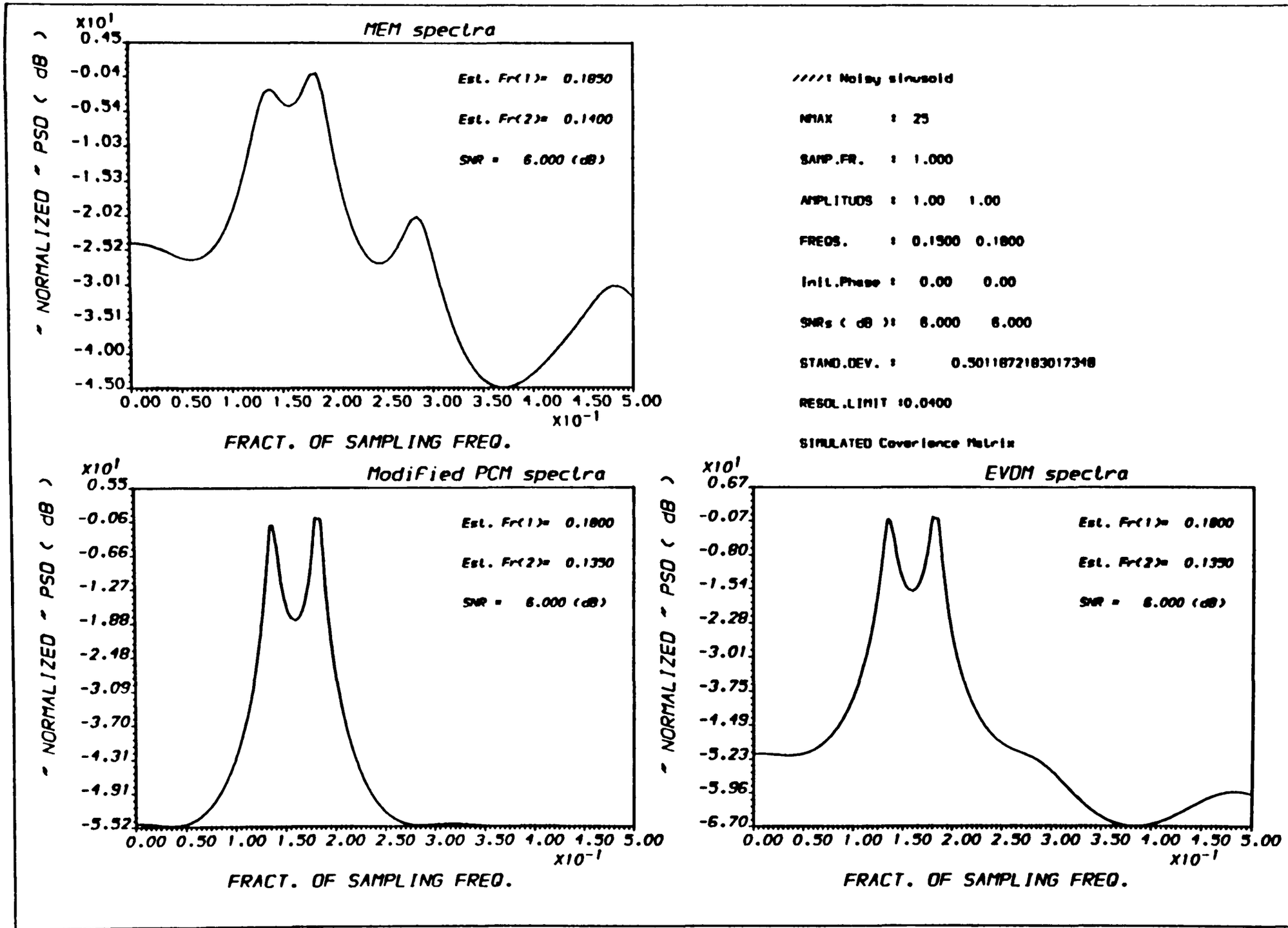

FIG.(5.30) POWER SPECTRAL DENSITY ESTIMATE
* For different PSDE methods *

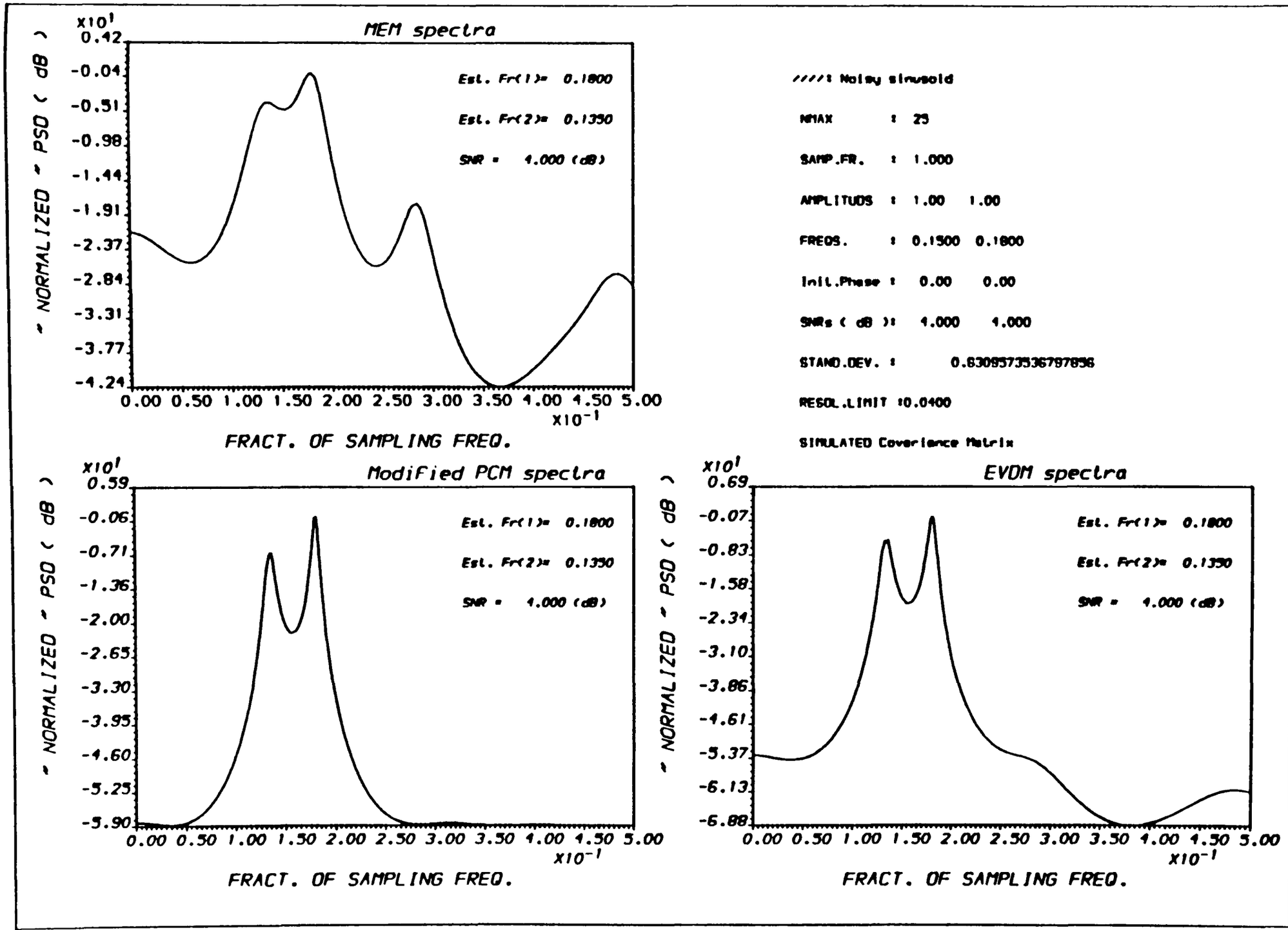

FIG.(5.31) POWER SPECTRAL DENSITY ESTIMATE
* For different PSDE methods *

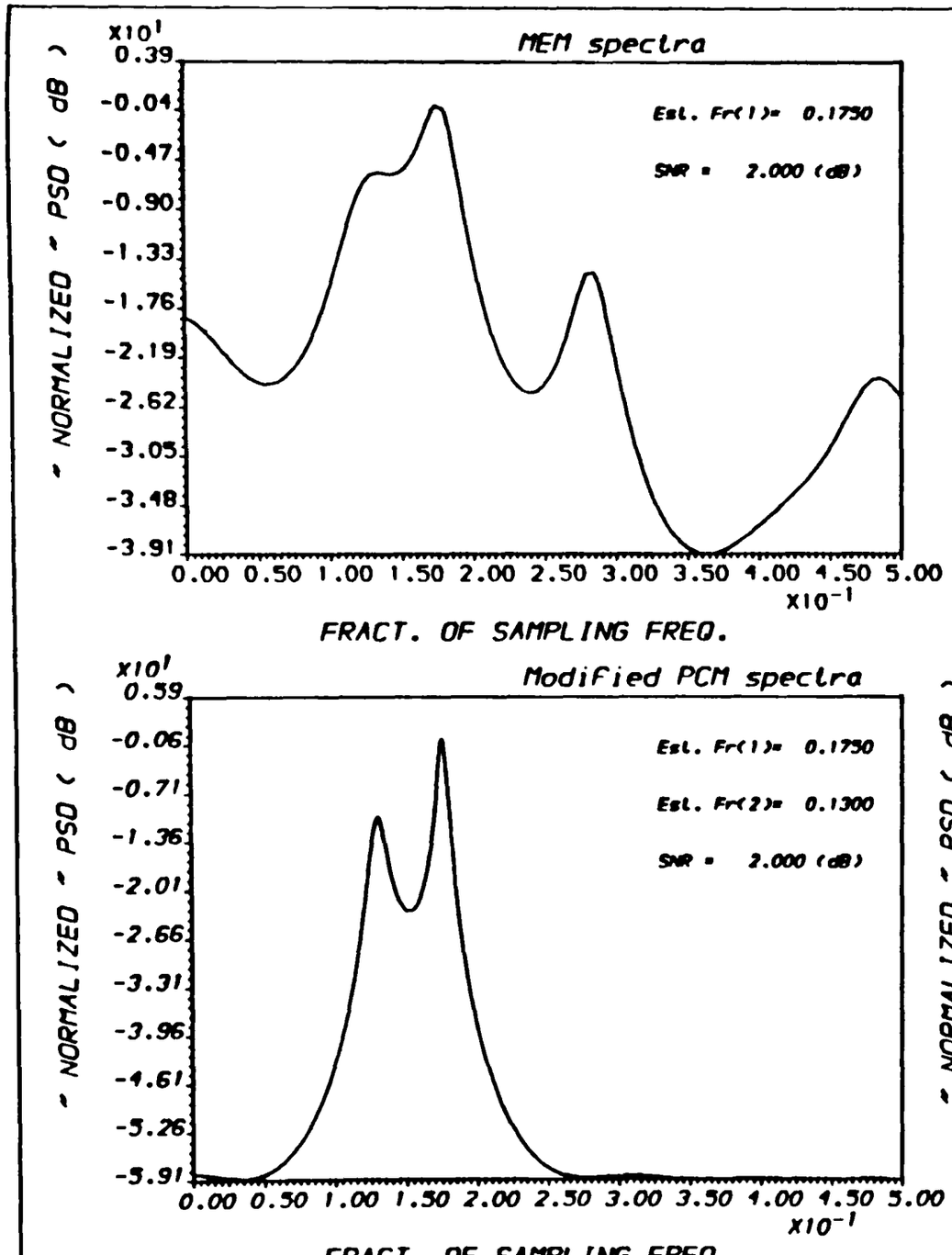

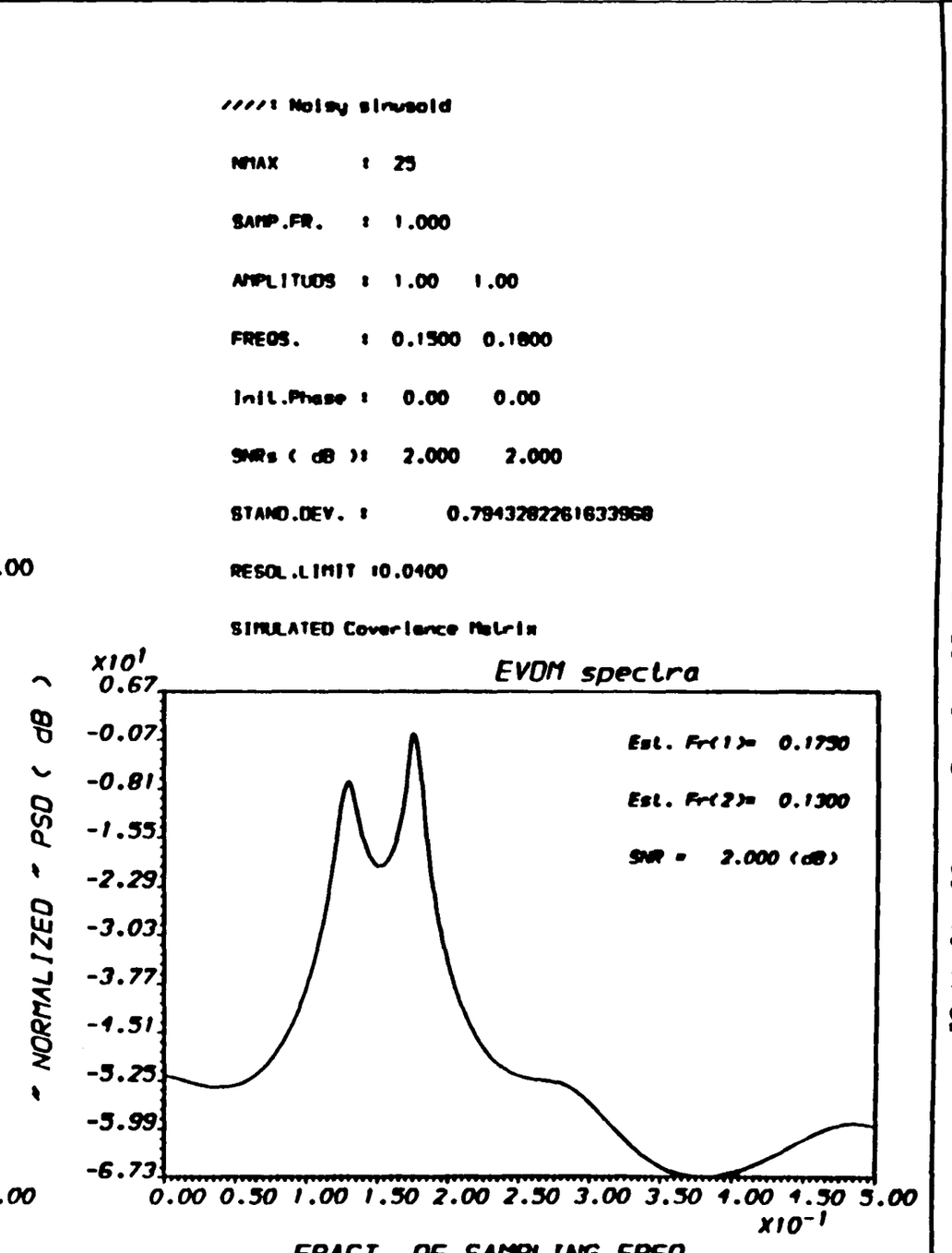

FIG.(5.32) POWER SPECTRAL DENSITY ESTIMATE
* For different PSDE methods *

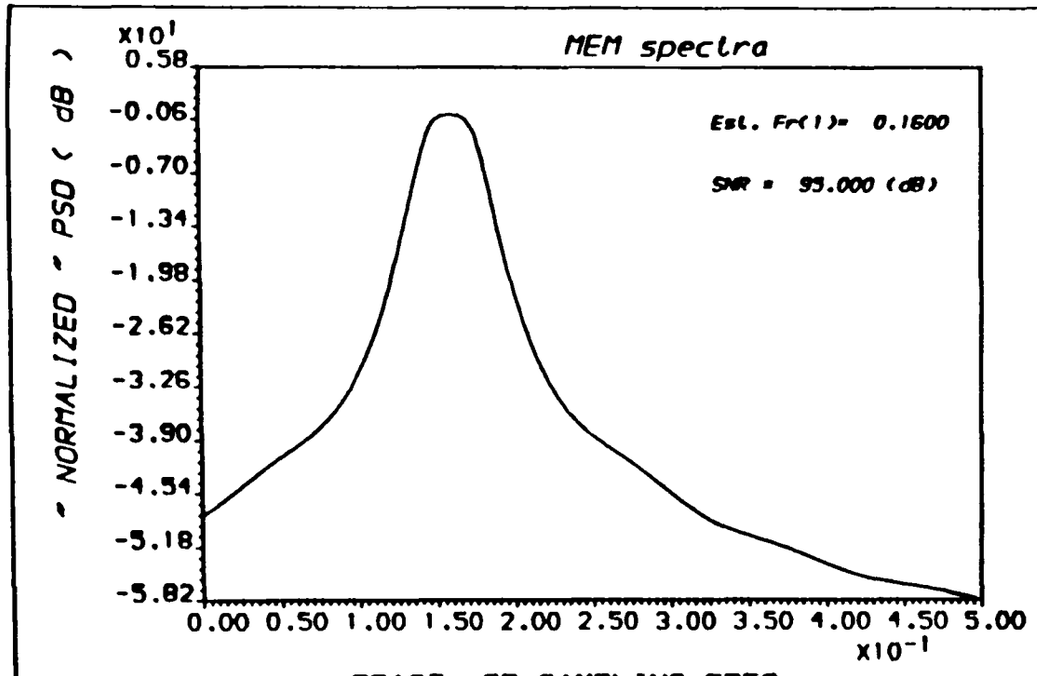


```
/////: Noisy sinusoid

 NMAX        :  25

 SAMP.FR.    :  1.000

 AMPLITUDS   :  1.00    1.00

 FREQS.      :  0.1500  0.1700

 Init.Phase  :   0.00     0.00

 SNRs ( dB ) :  95.000   95.000

 STAND.DEV.  :        0.00001778279417986

 RESOL.LIMIT :0.0400

 SIMULATED Coverlance Matrix
```


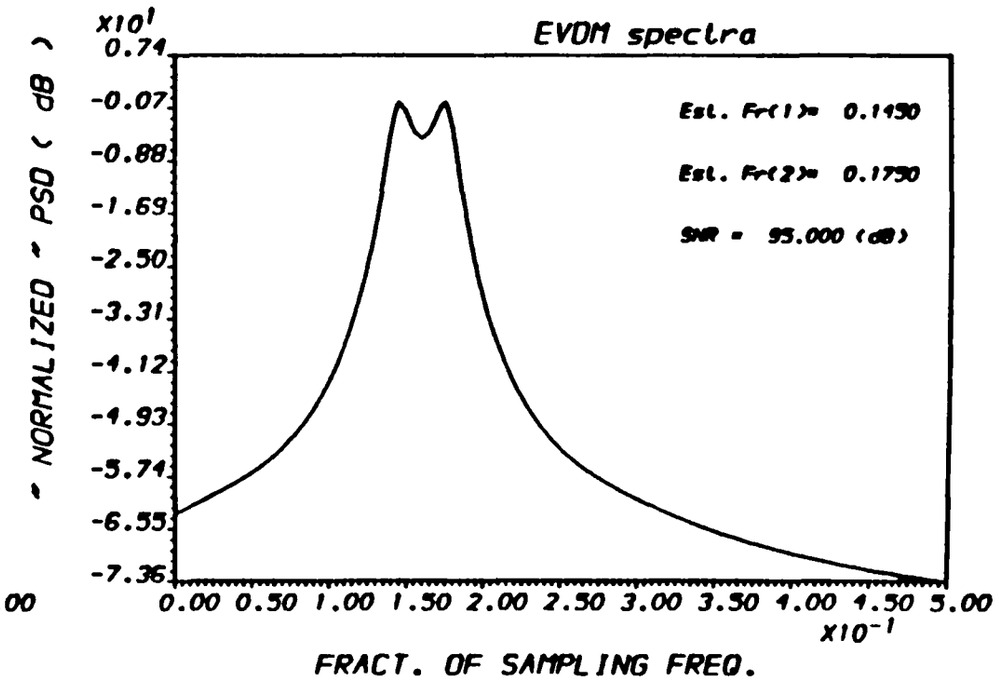

OUTPUT A.ALI -"PLOT2M"- Ex.(6/ 25) RUN :27-MAR-90 10:55:08

FIG.(5.33) POWER SPECTRAL DENSITY ESTIMATE
* For different PSDE methods *

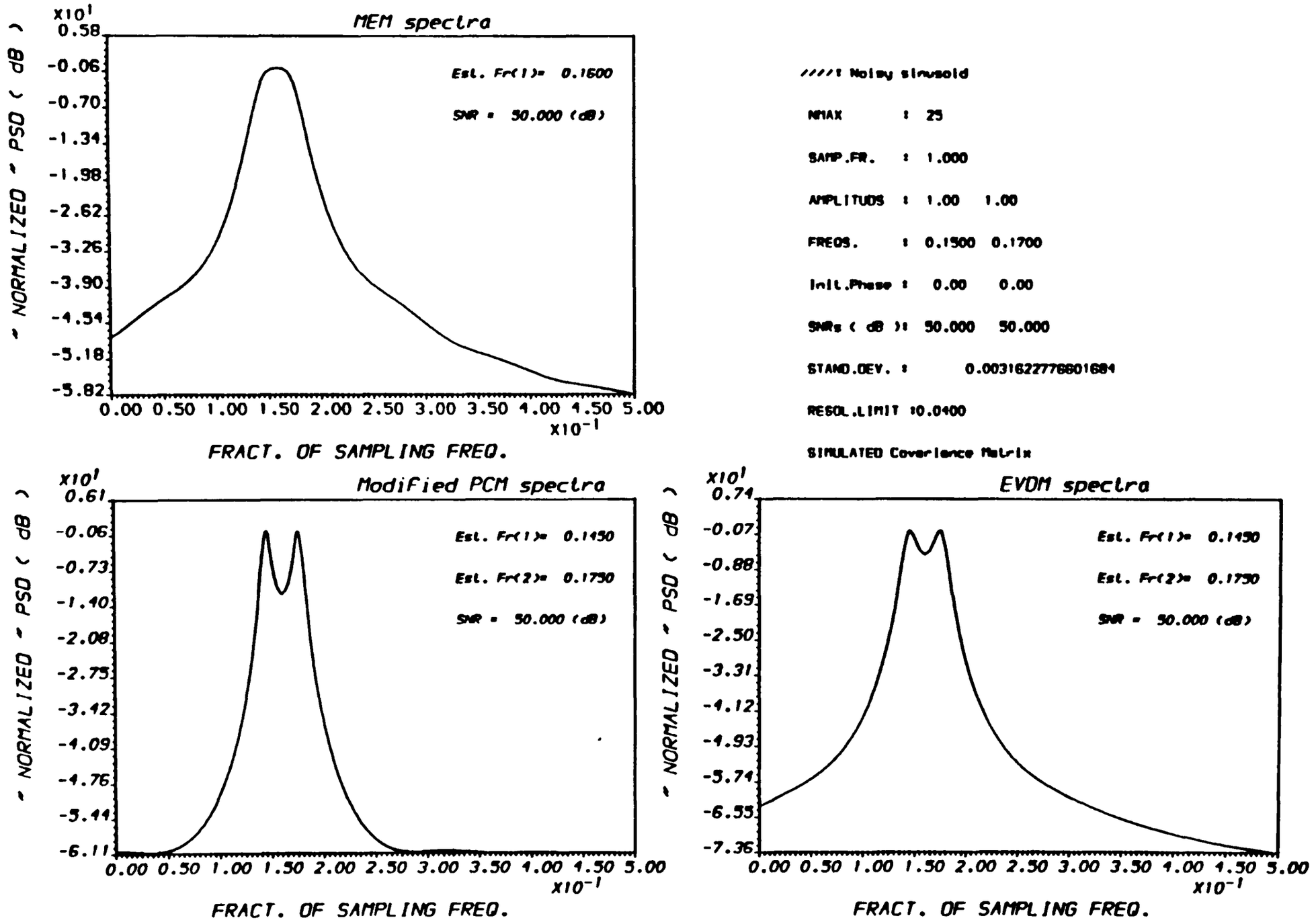

FIG.(5.34) POWER SPECTRAL DENSITY ESTIMATE
* For different PSDE methods *

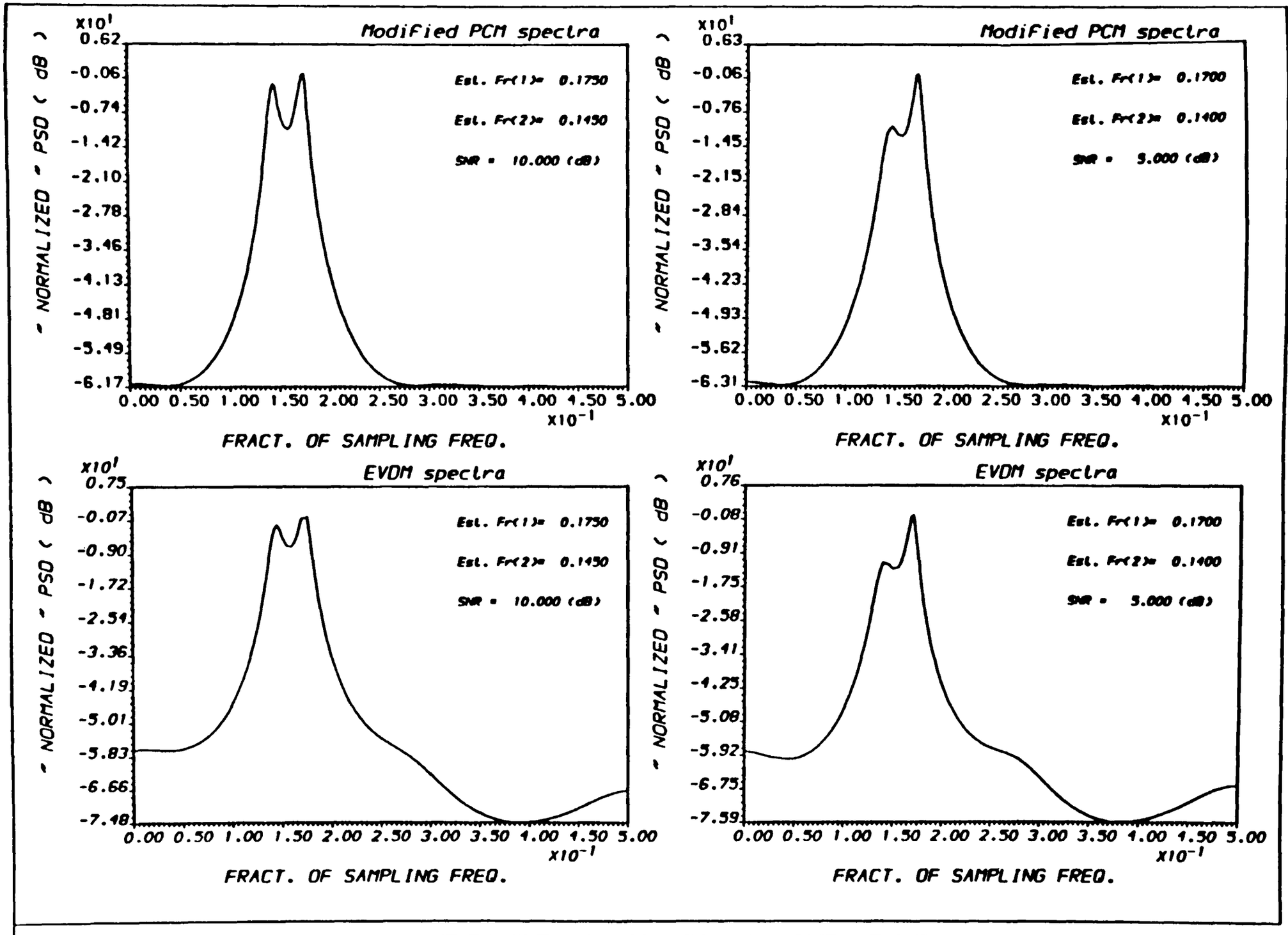

FIG.(5.35) POWER SPECTRAL DENSITY ESTIMATE
* For different PSDE methods *

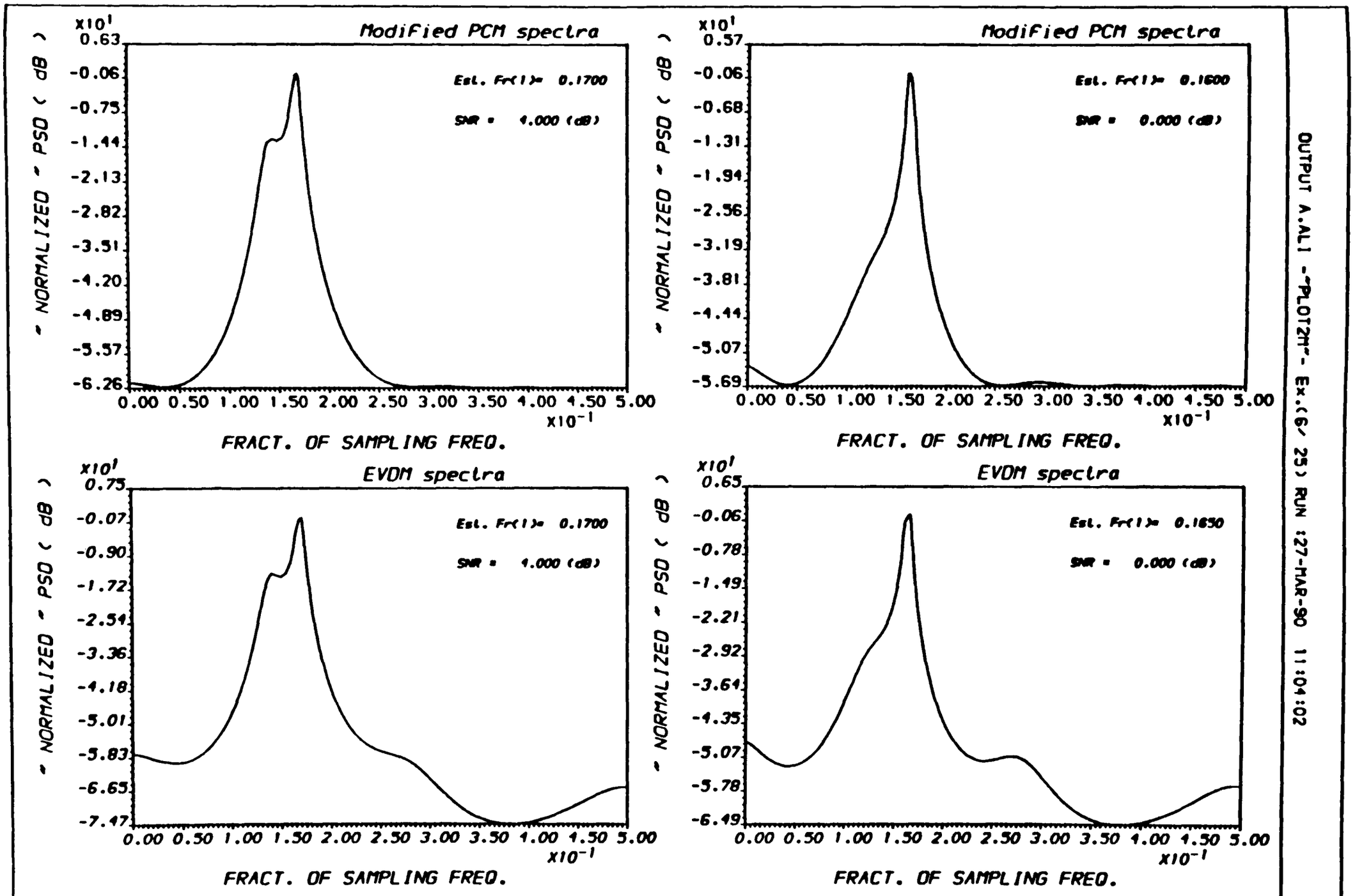

FIG.(5.36) POWER SPECTRAL DENSITY ESTIMATE
* For different PSDE methods *

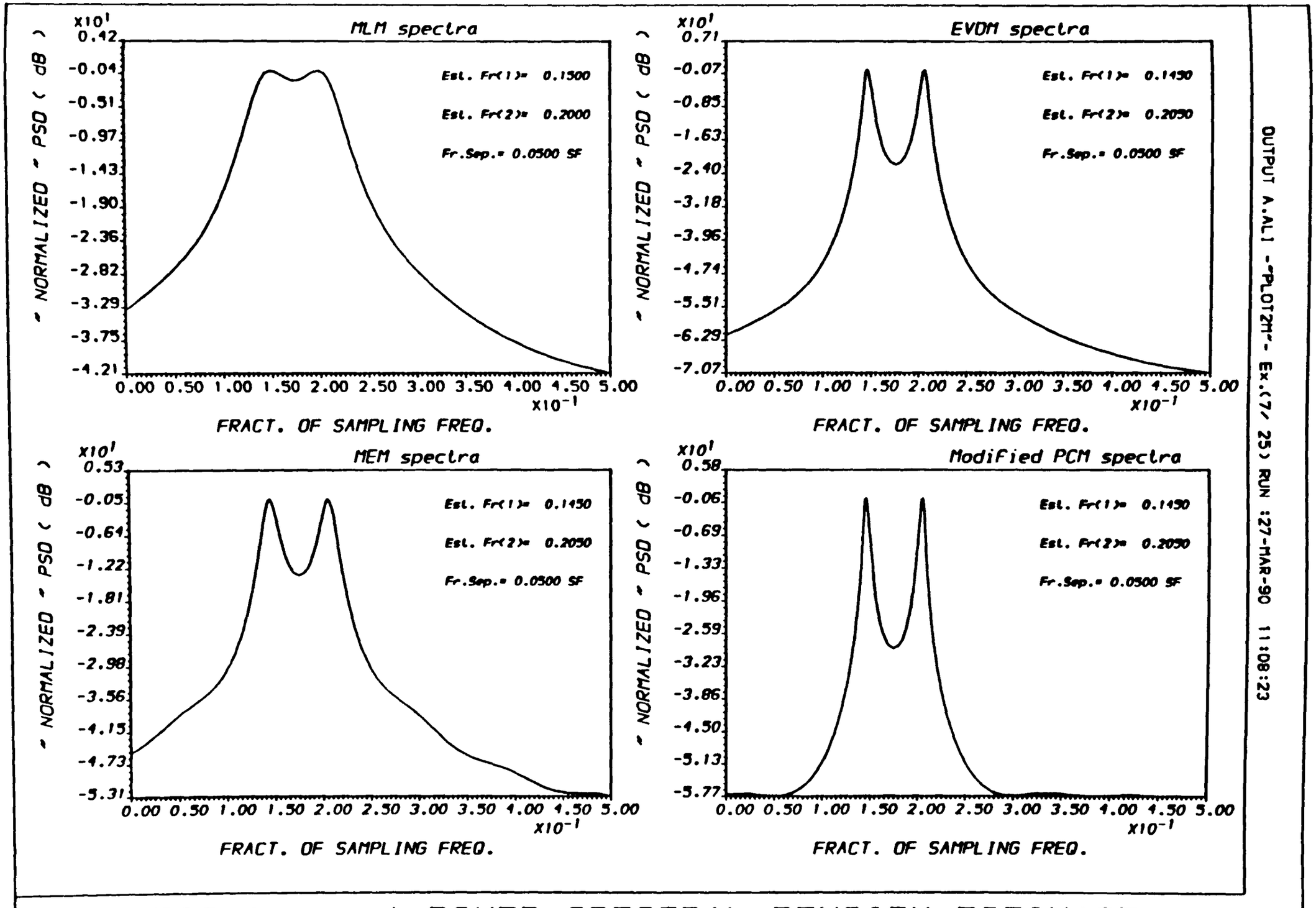

FIG.(5.37) POWER SPECTRAL DENSITY ESTIMATE
* For different PSDE methods *

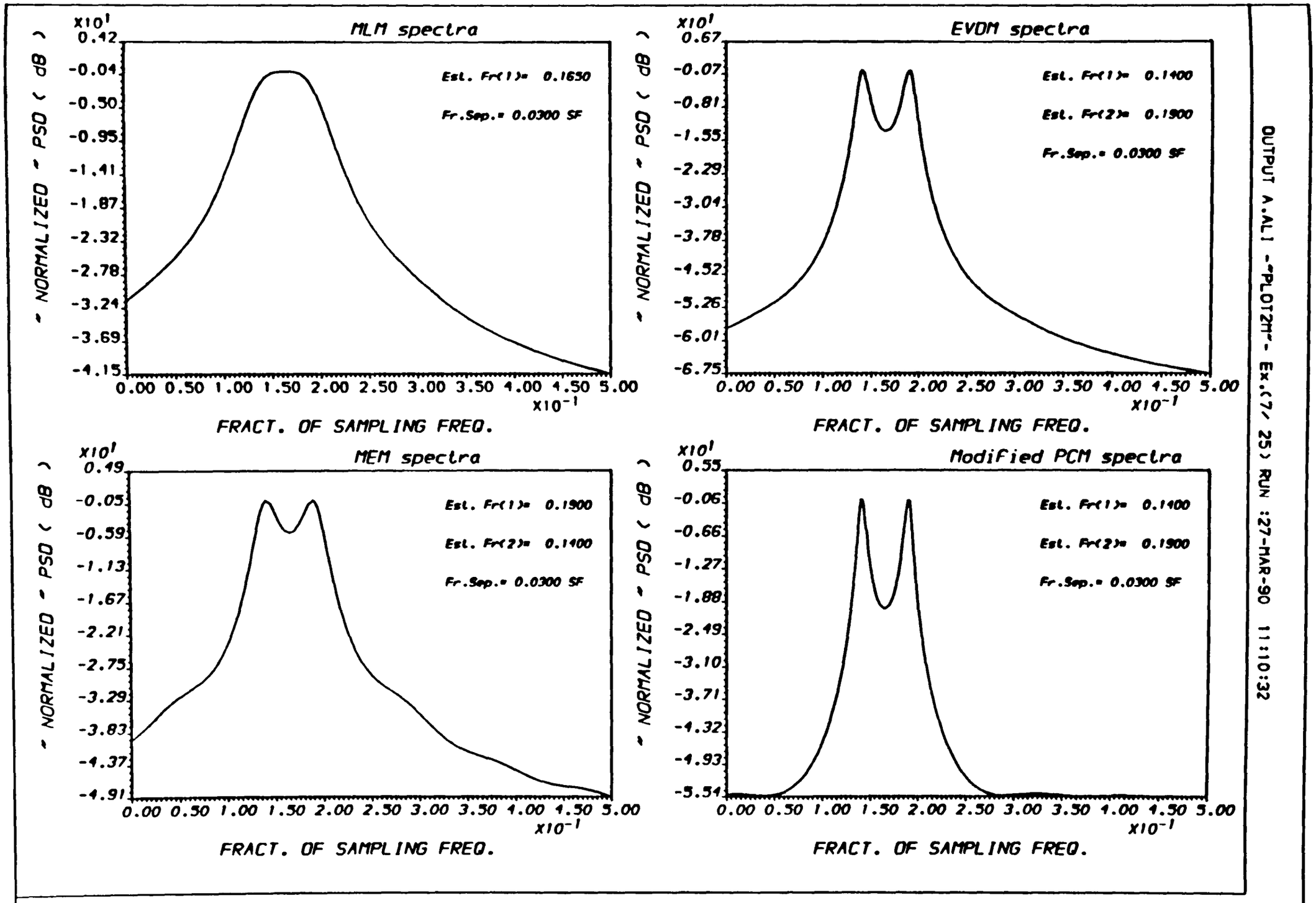

FIG.(5.38) POWER SPECTRAL DENSITY ESTIMATE
* For different PSDE methods *

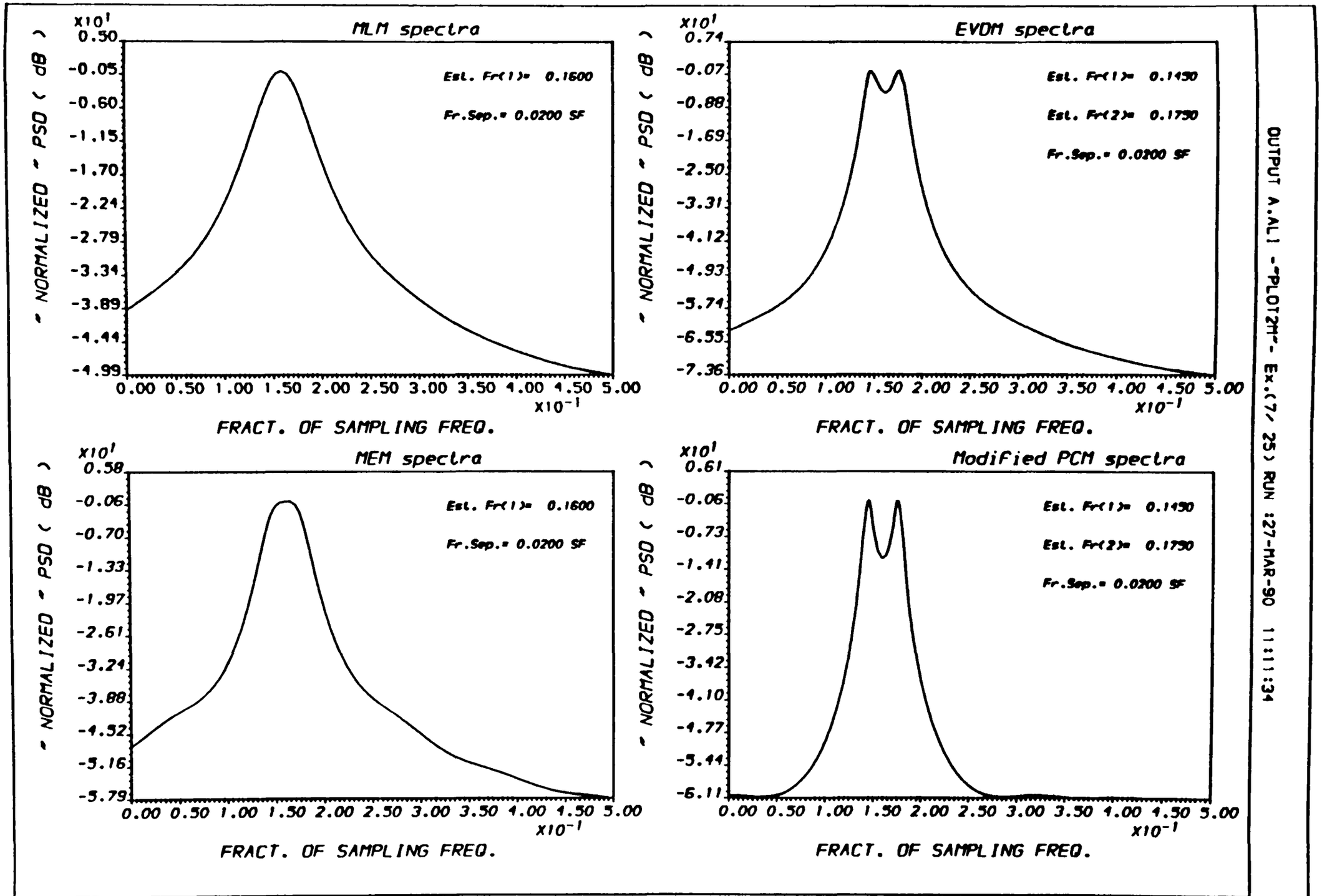

FIG.(5.39) POWER SPECTRAL DENSITY ESTIMATE
* For different PSDE methods *

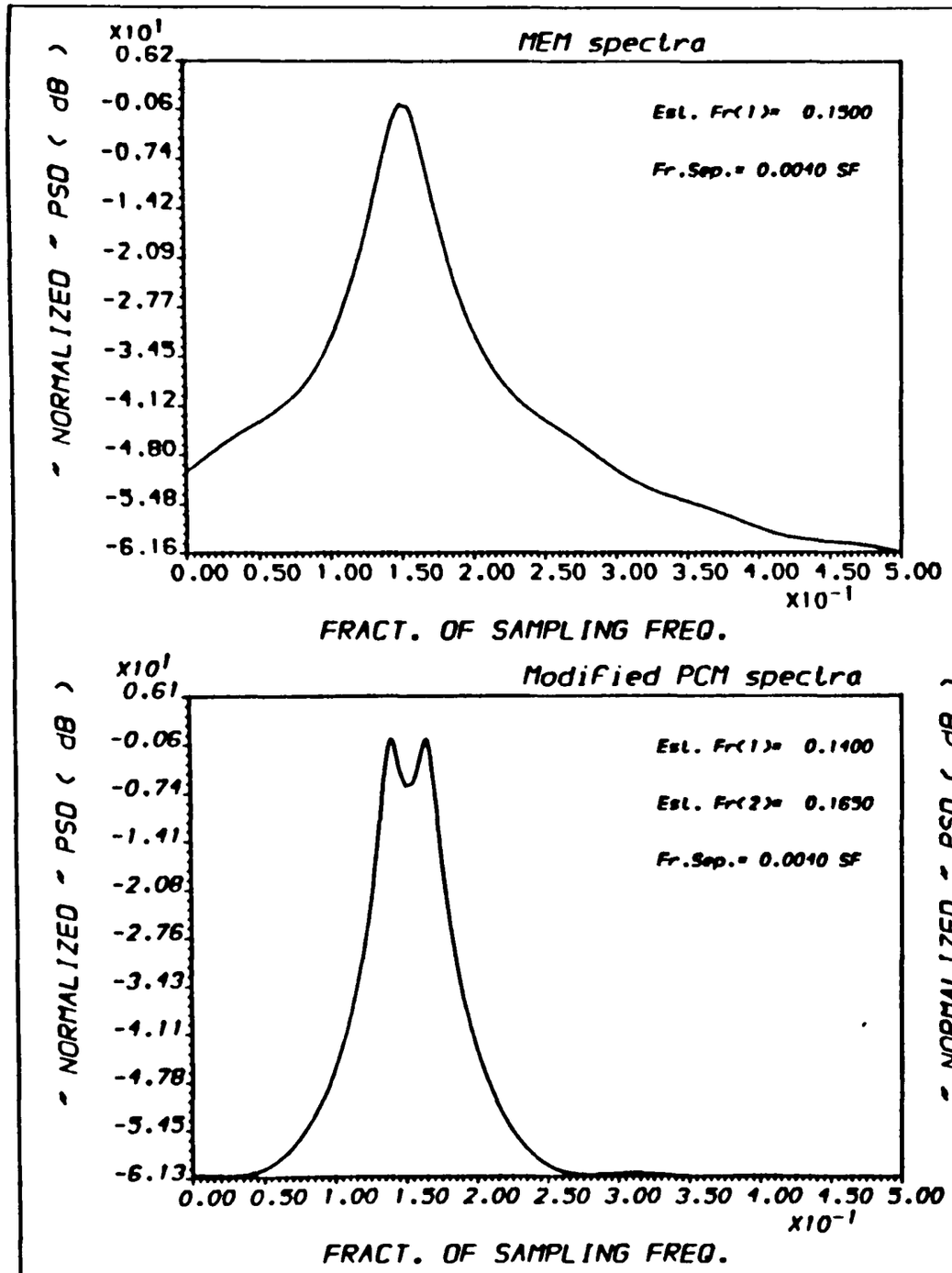

FIG.(5.40) POWER SPECTRAL DENSITY ESTIMATE
* For different PSDE methods *

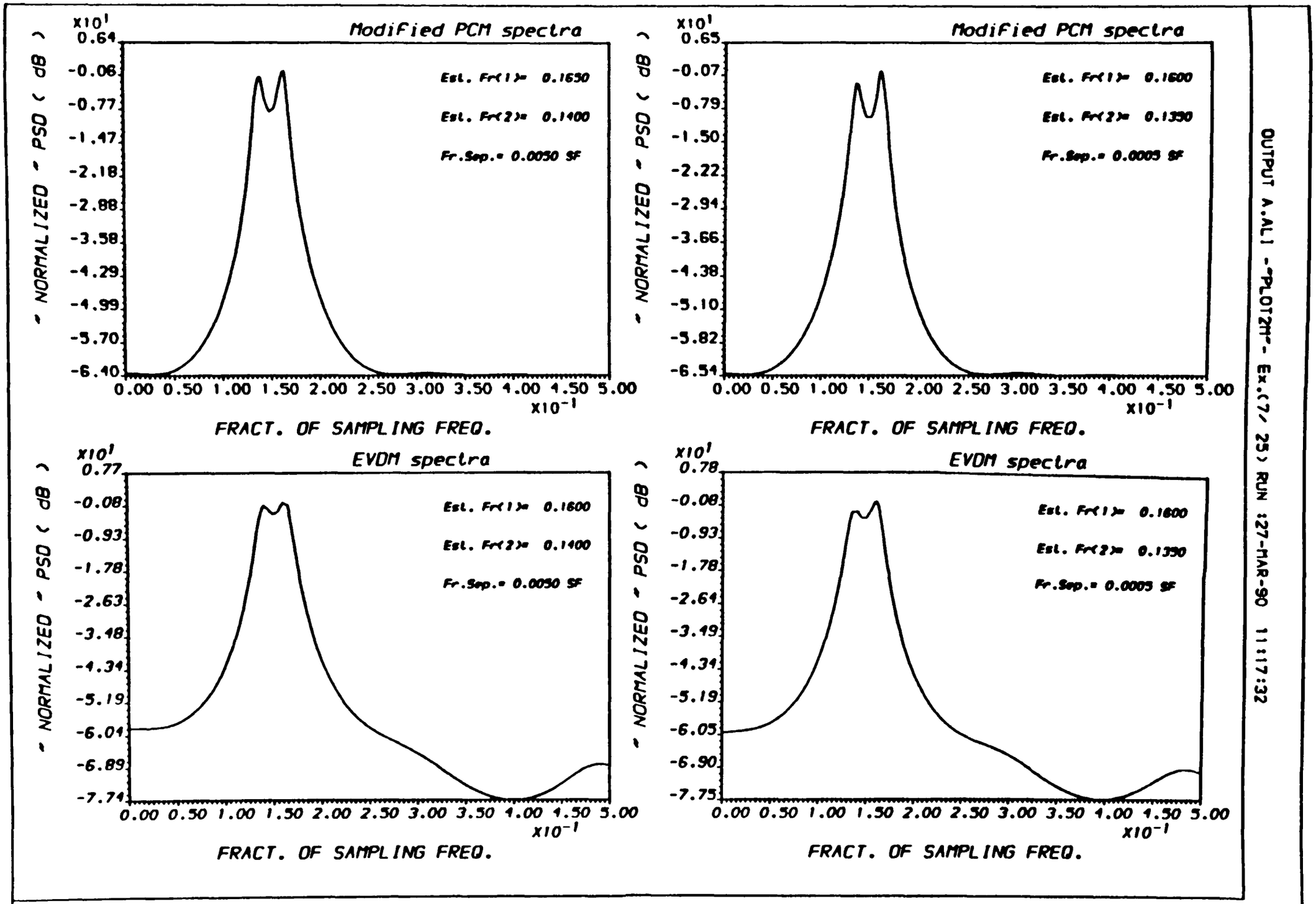

FIG.(5.41) POWER SPECTRAL DENSITY ESTIMATE
* For different PSDE methods *

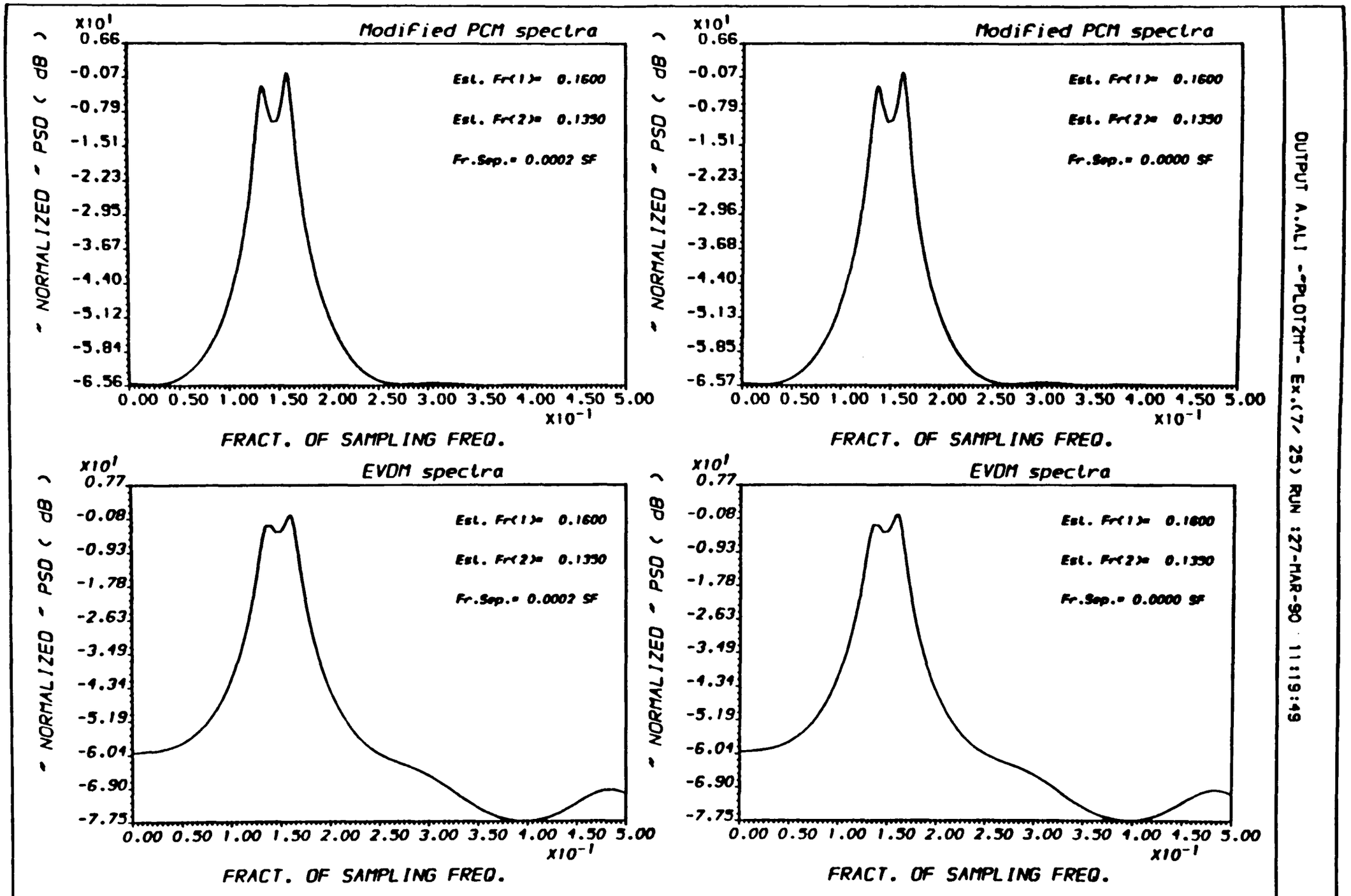

FIG.(5.42) POWER SPECTRAL DENSITY ESTIMATE
* For different PSDE methods *

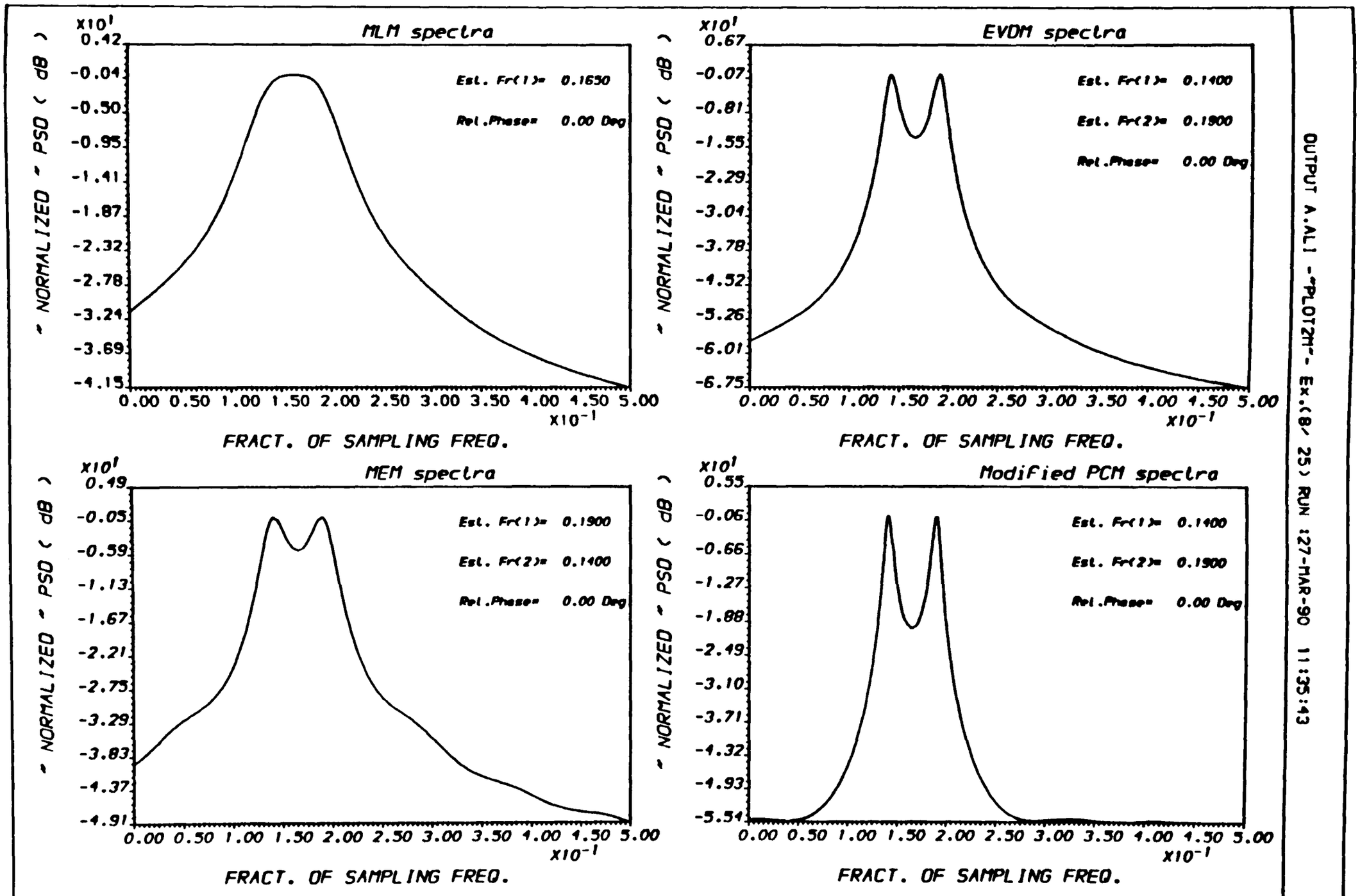

FIG.(5.43) POWER SPECTRAL DENSITY ESTIMATE
* For different PSDE methods *

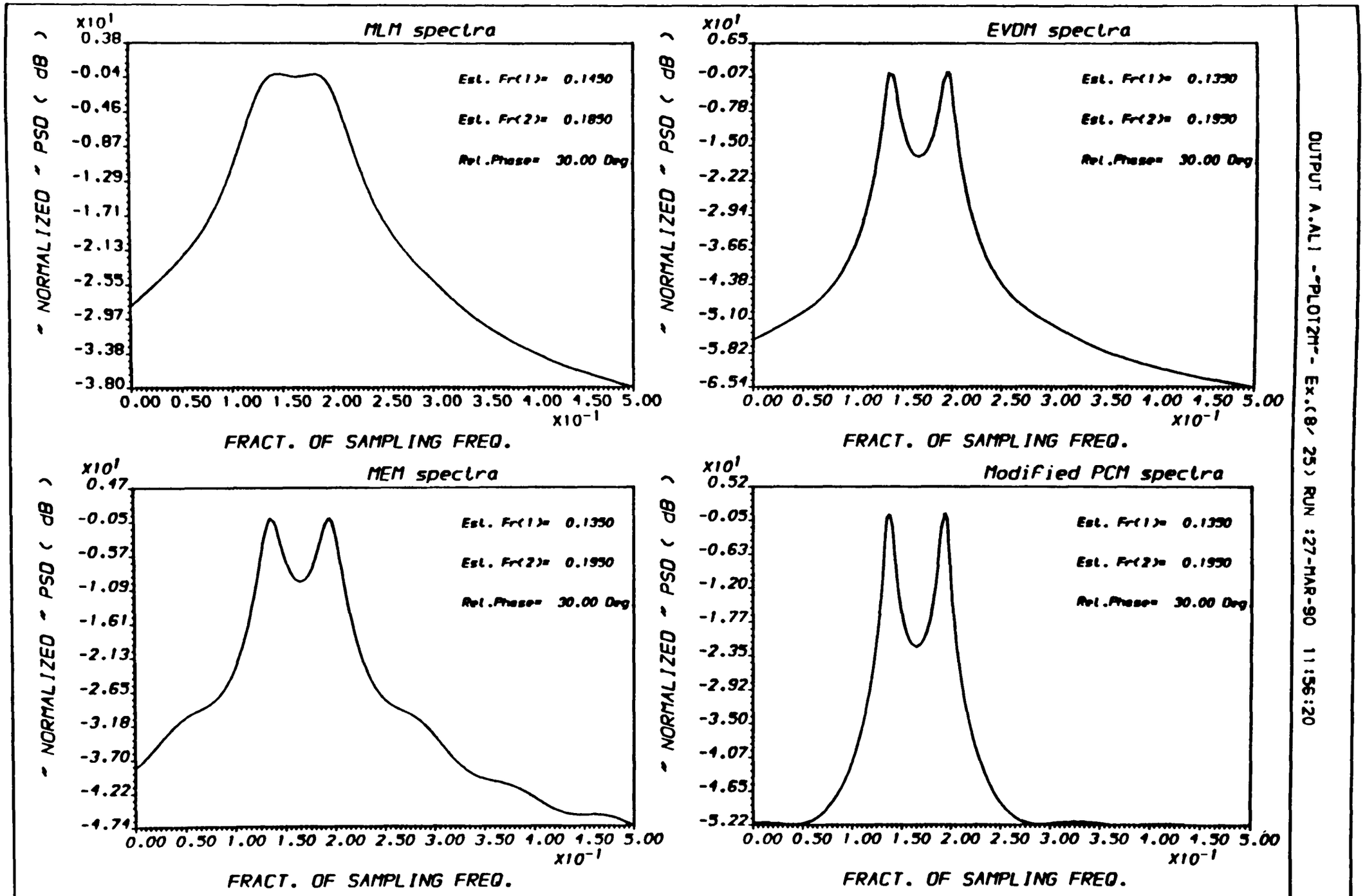

FIG.(5.44) POWER SPECTRAL DENSITY ESTIMATE
* For different PSDE methods *

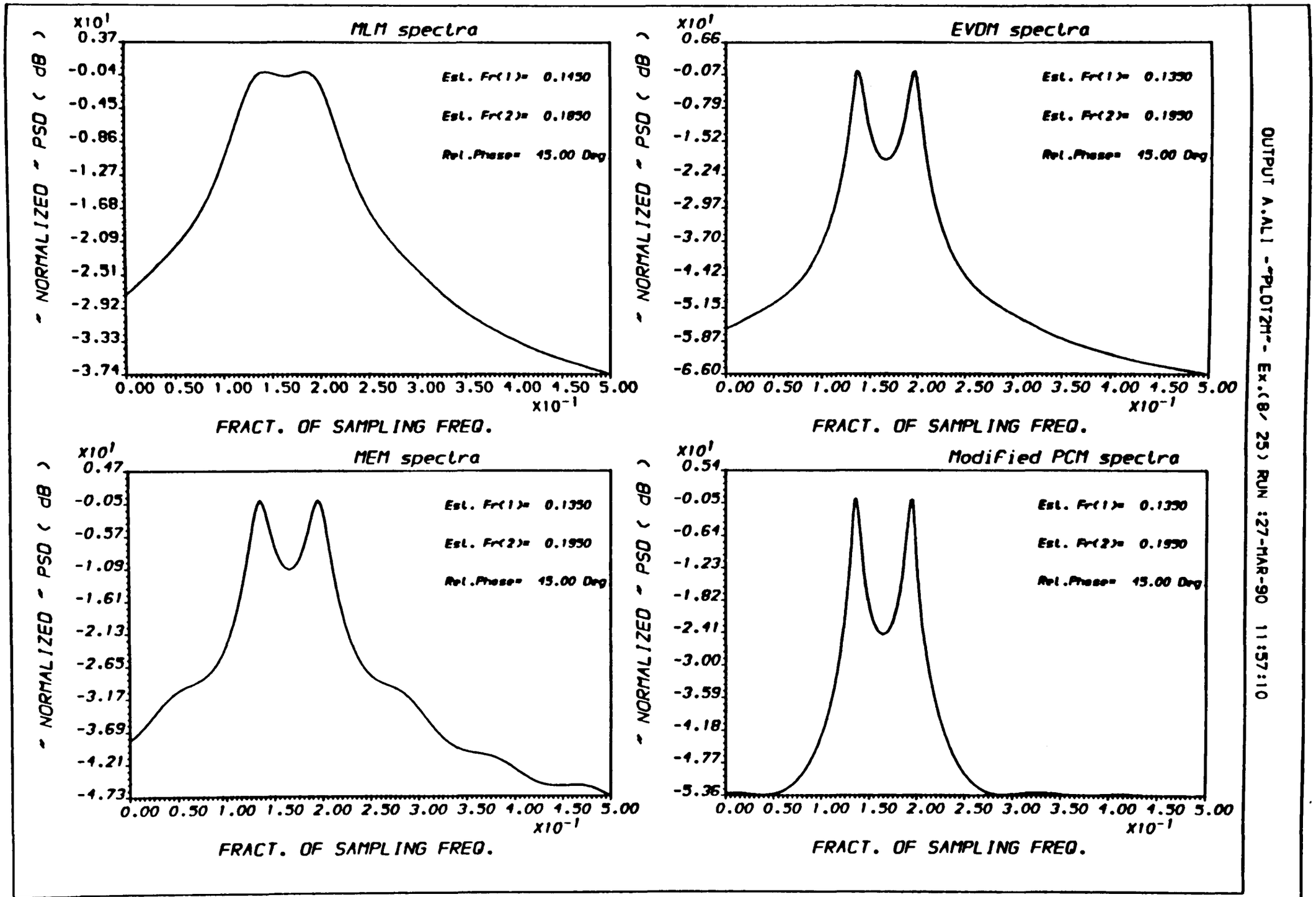

FIG.(5.45) POWER SPECTRAL DENSITY ESTIMATE
* For different PSDE methods *

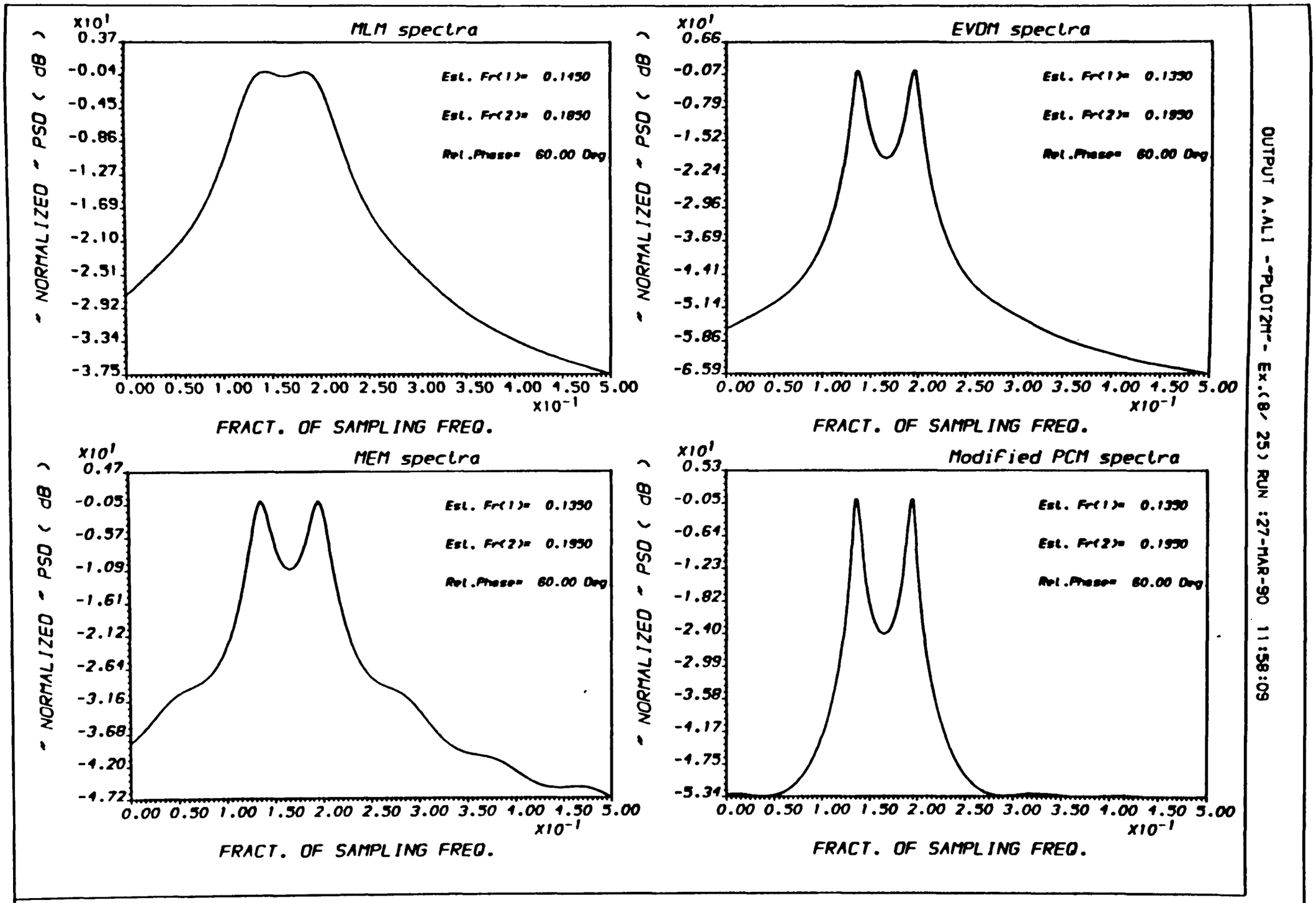

FIG.(5.46) POWER SPECTRAL DENSITY ESTIMATE
* For different PSDE methods *

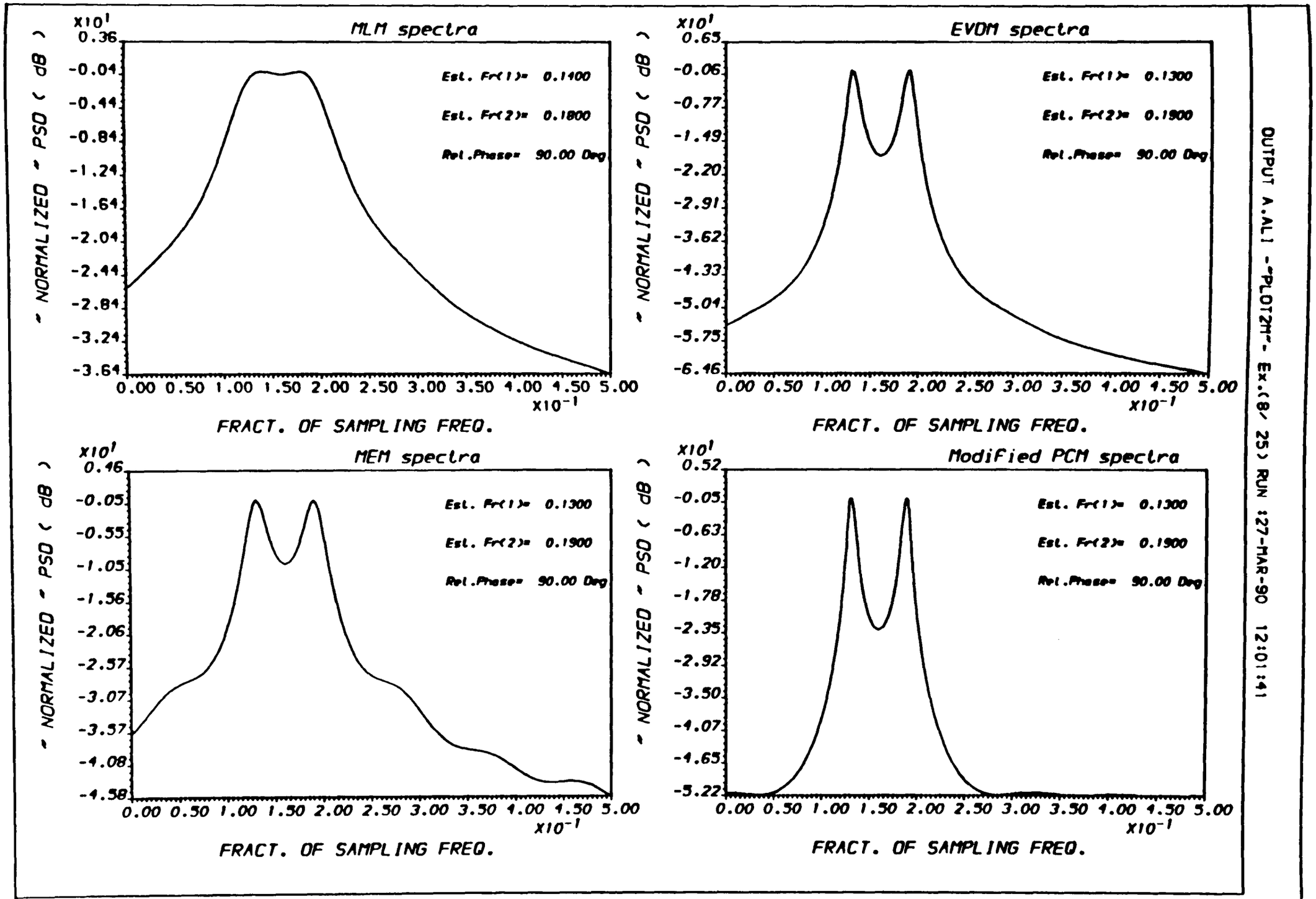

FIG.(5.47) POWER SPECTRAL DENSITY ESTIMATE
* For different PSDE methods *

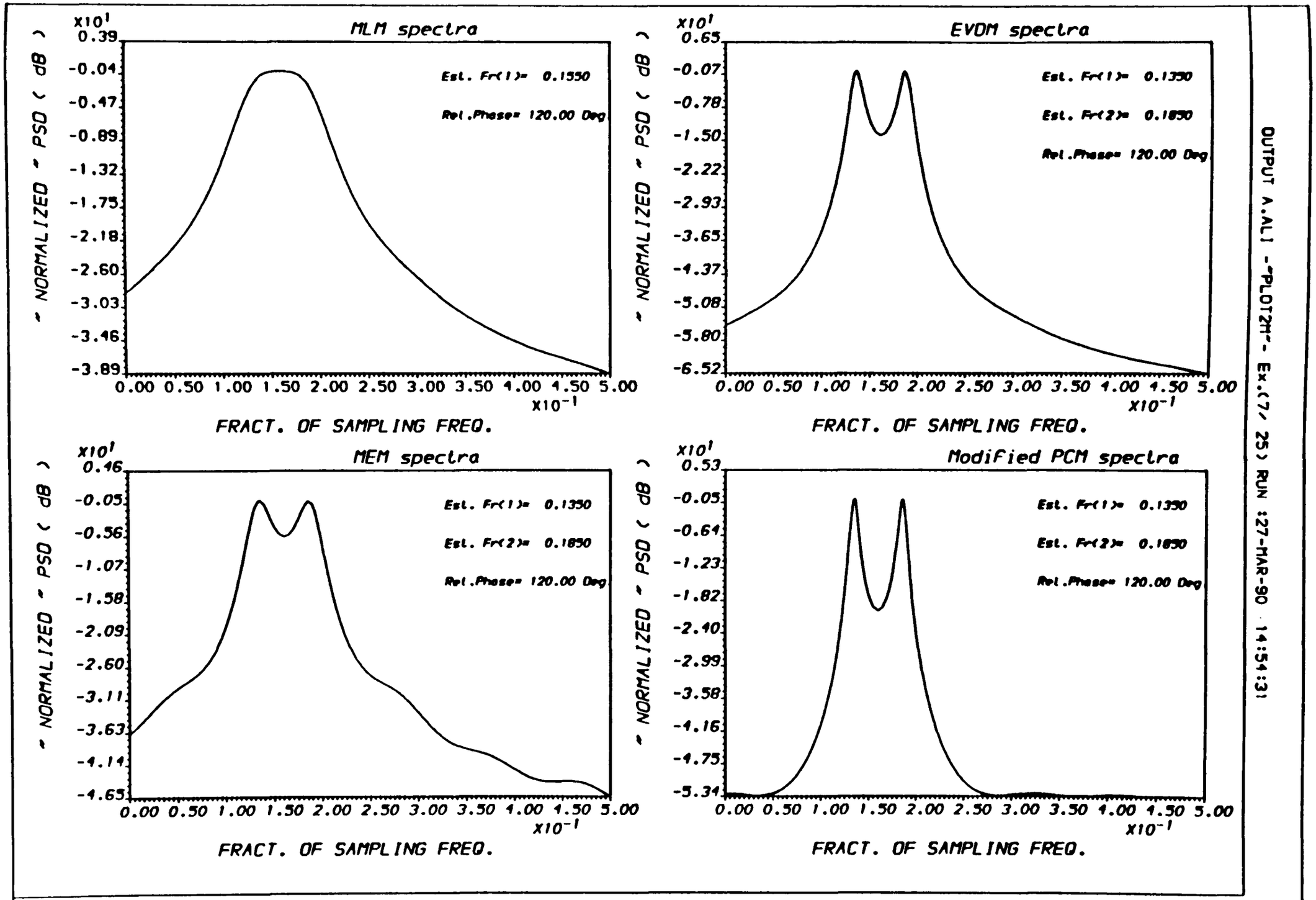

FIG.(5.48) POWER SPECTRAL DENSITY ESTIMATE
* For different PSDE methods *

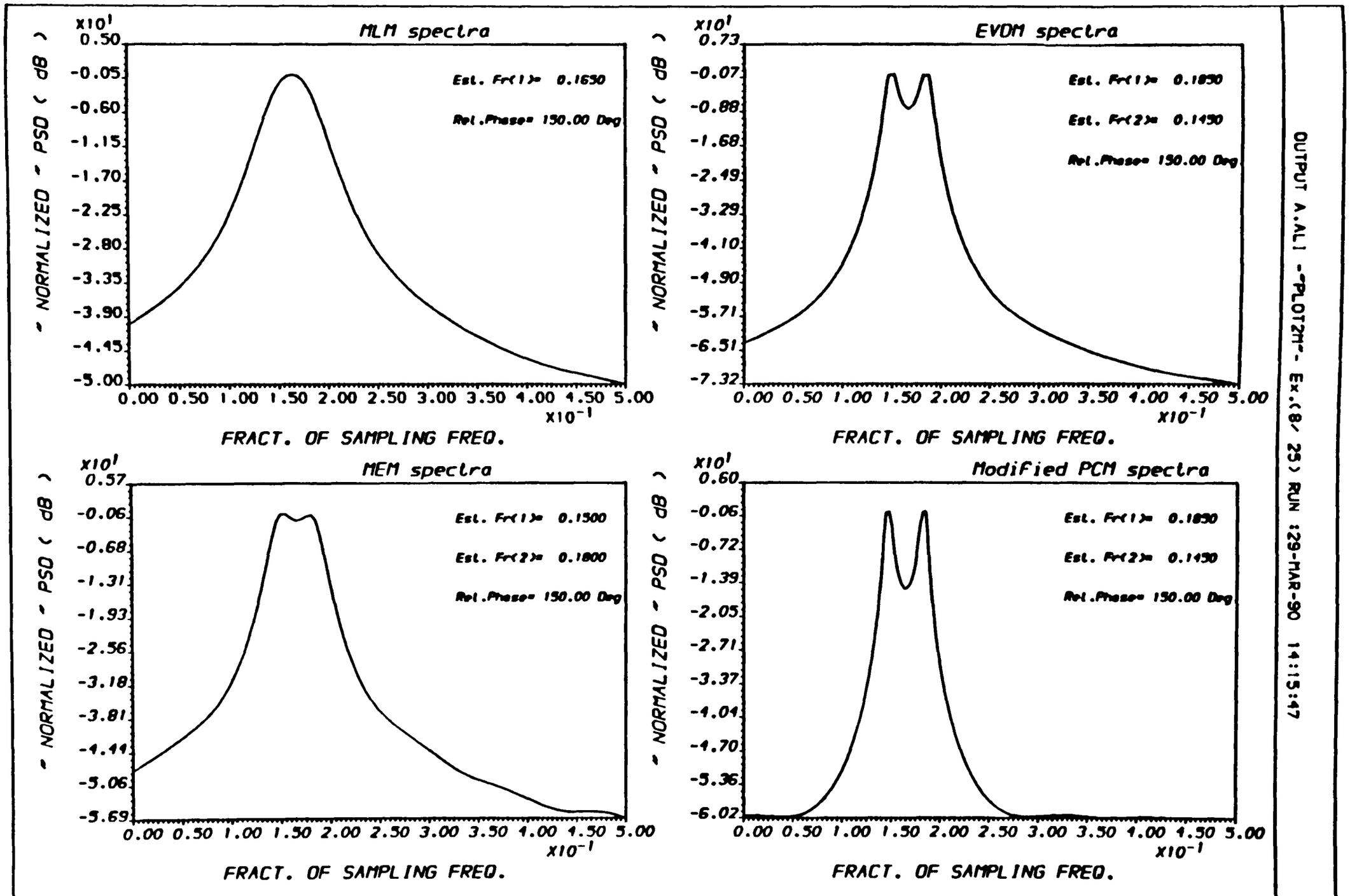

FIG.(5.49) POWER SPECTRAL DENSITY ESTIMATE
* For different PSDE methods *

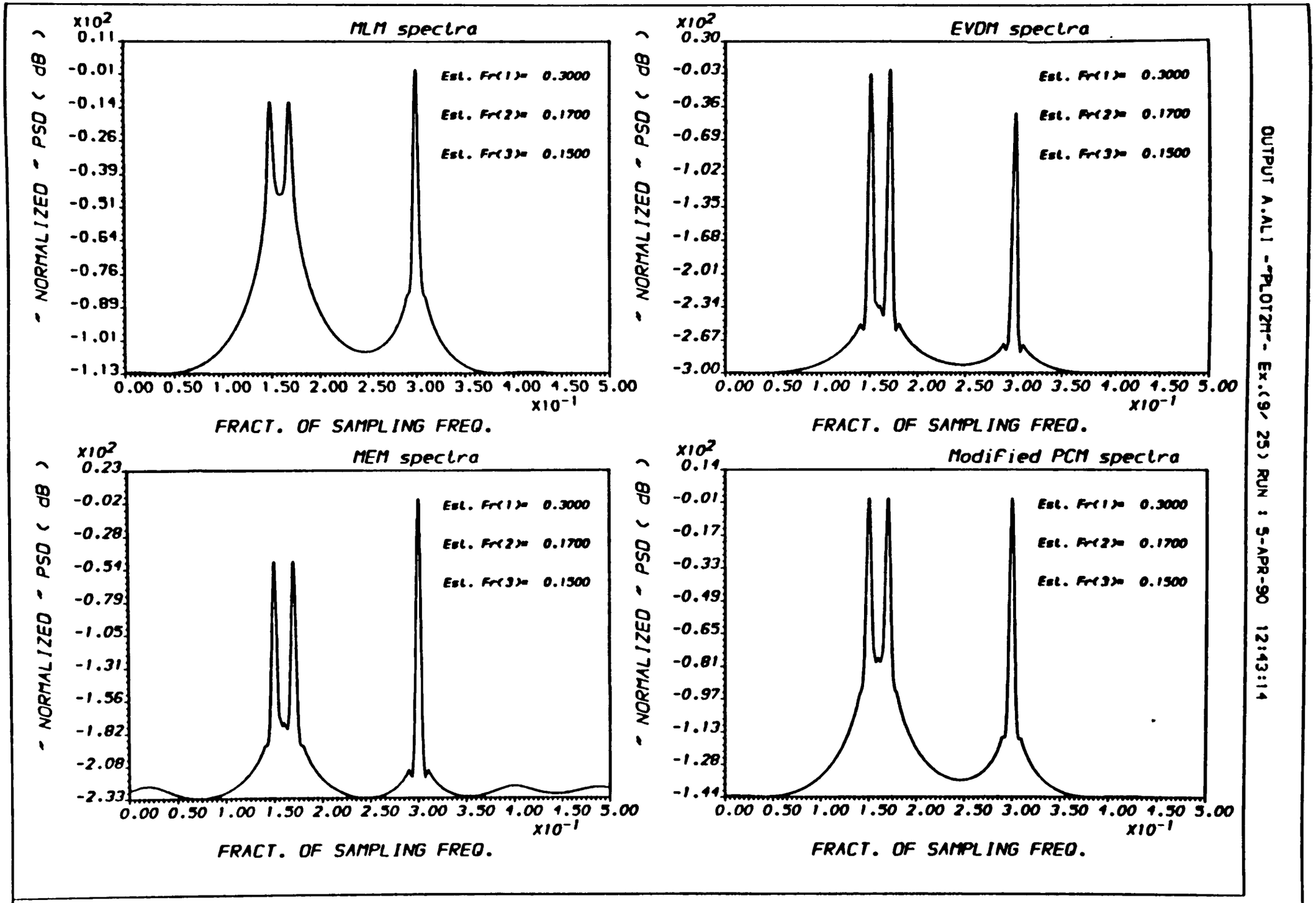

FIG.(5.50) POWER SPECTRAL DENSITY ESTIMATE
* For different PSDE methods *

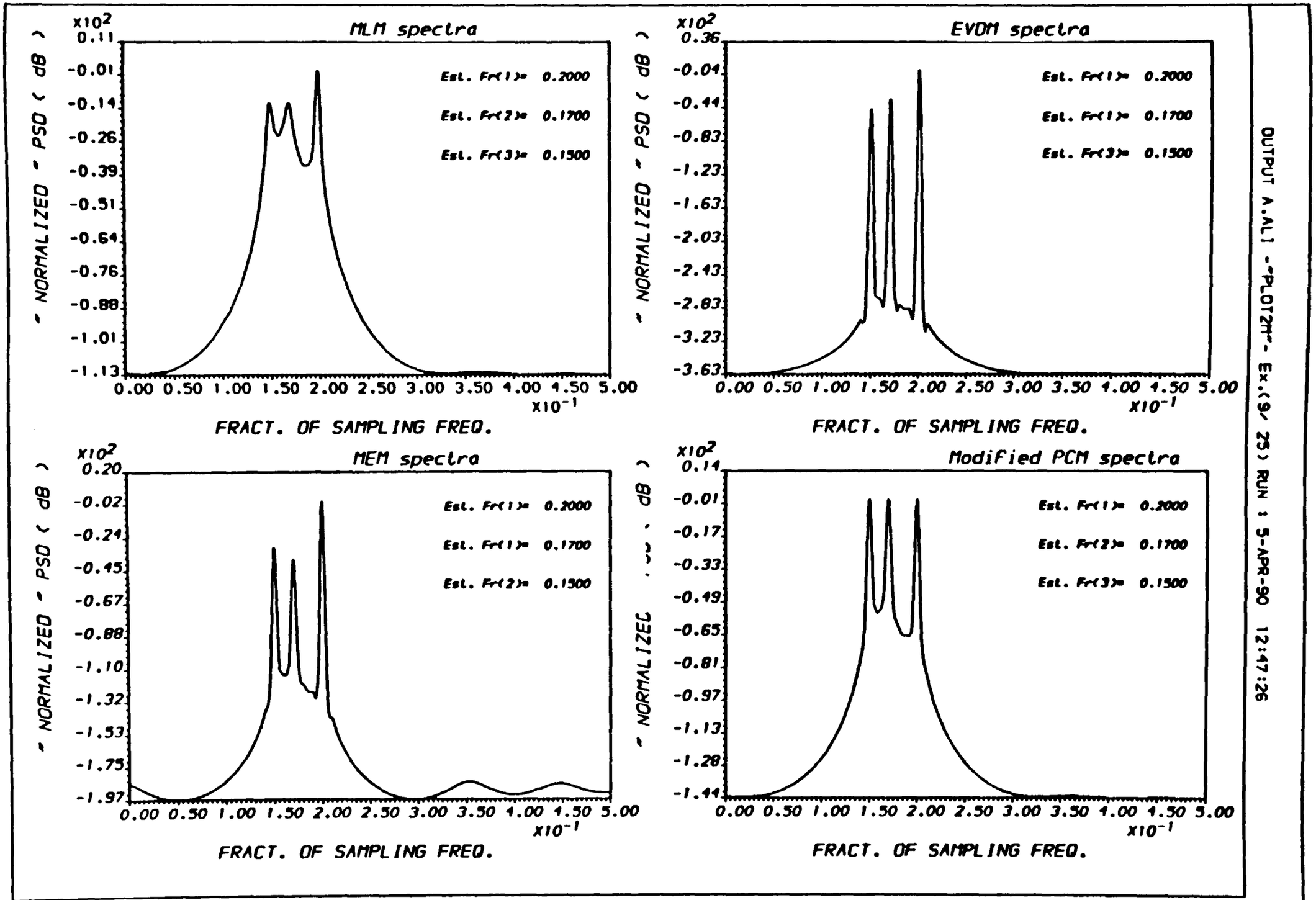

FIG.(5.51) POWER SPECTRAL DENSITY ESTIMATE
* For different PSDE methods *

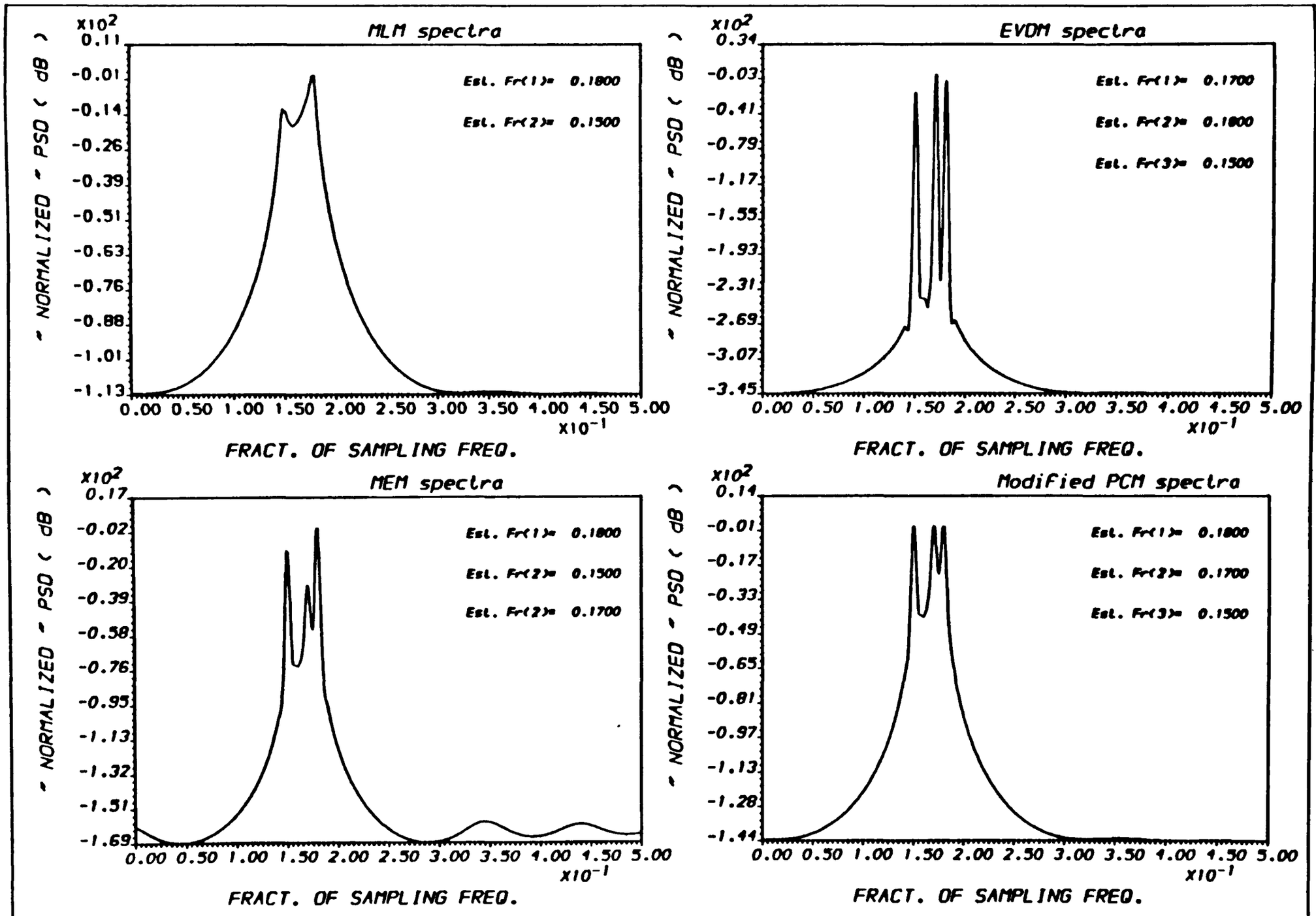

FIG.(5.52) POWER SPECTRAL DENSITY ESTIMATE
* For different PSDE methods *

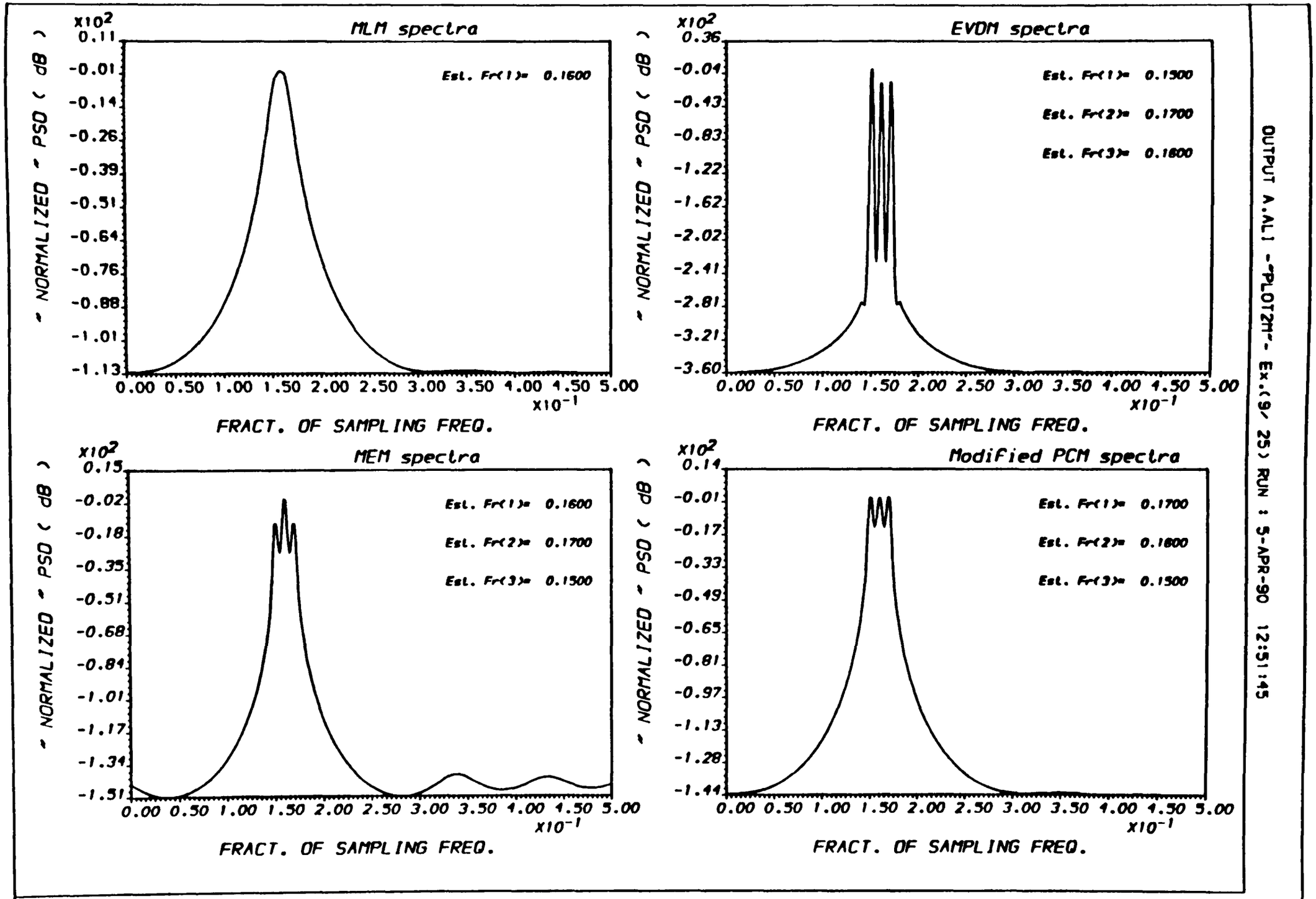

FIG.(5.53) POWER SPECTRAL DENSITY ESTIMATE
* For different PSDE methods *

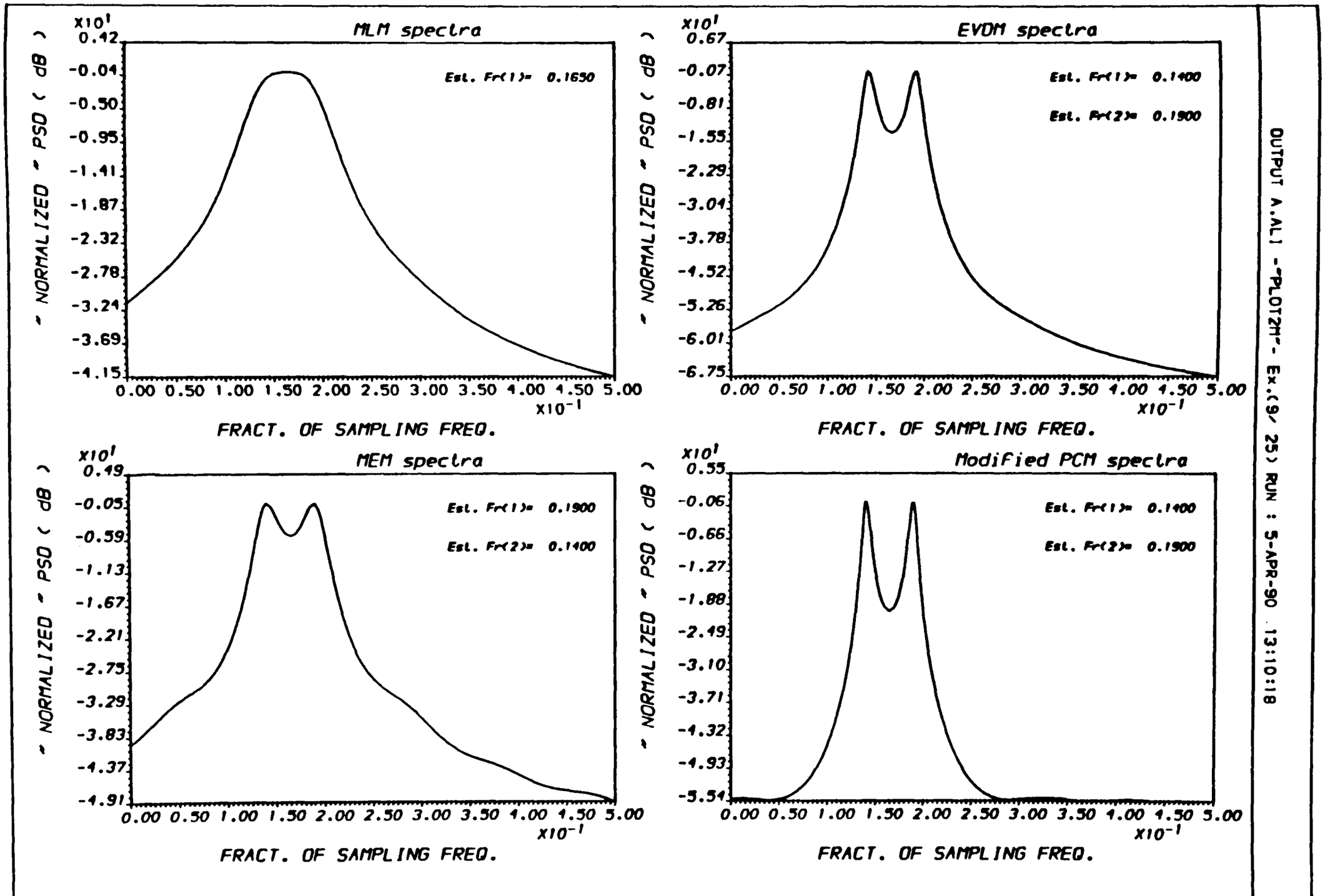

FIG.(5.54) POWER SPECTRAL DENSITY ESTIMATE
* For different PSDE methods *

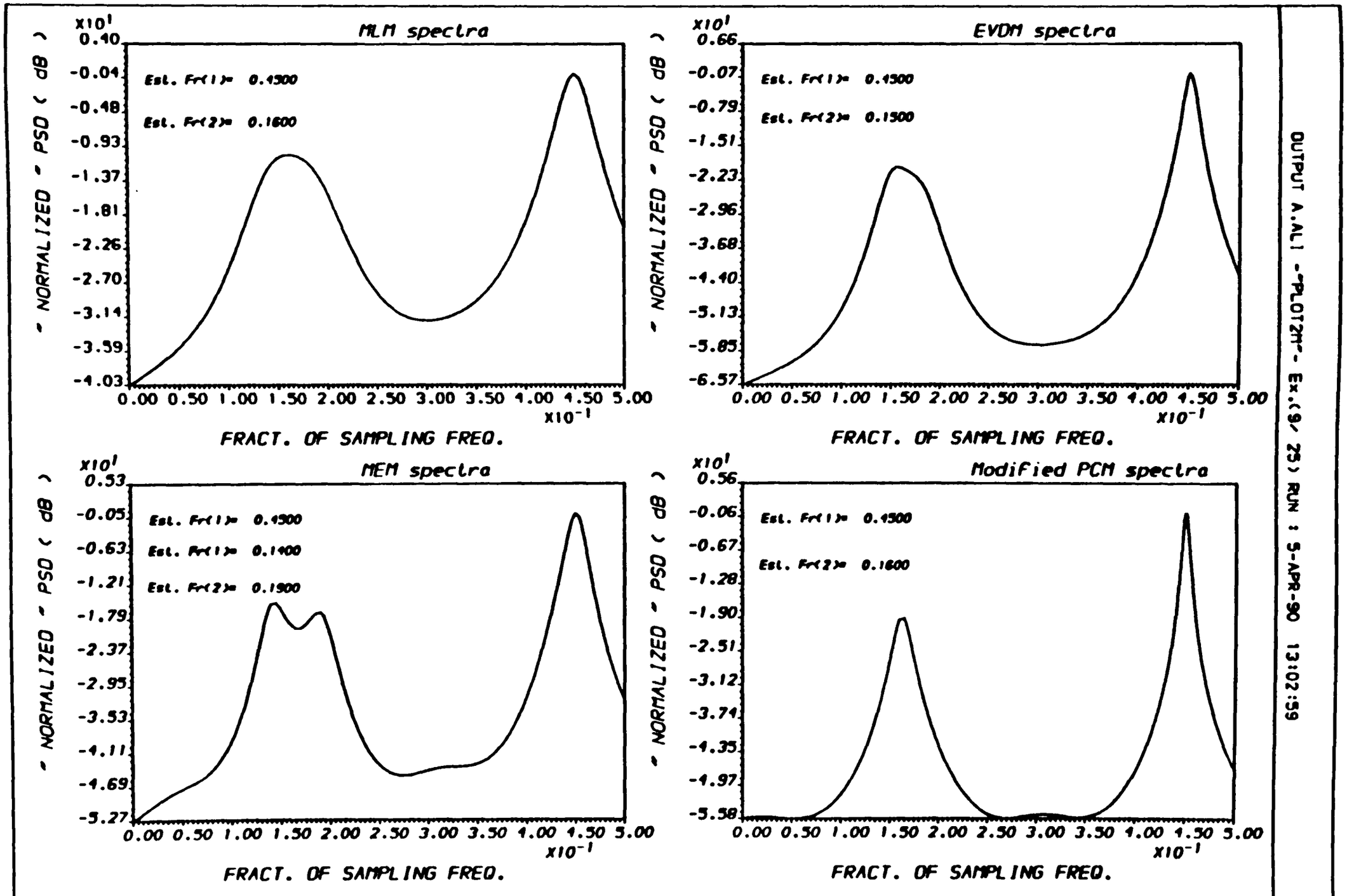

FIG.(5.55) POWER SPECTRAL DENSITY ESTIMATE
* For different PSDE methods *

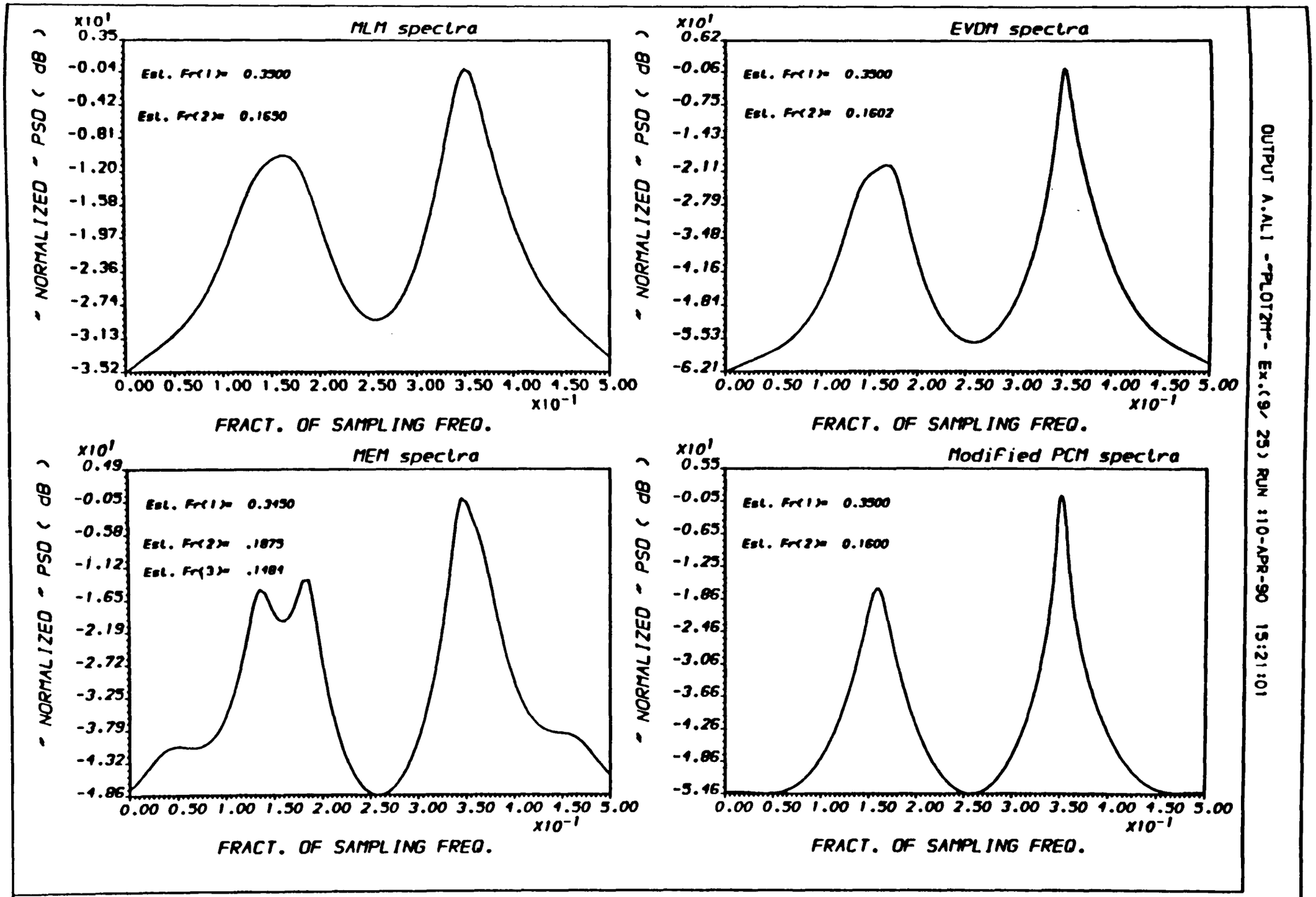

FIG.(5.56) POWER SPECTRAL DENSITY ESTIMATE
* For different PSDE methods *

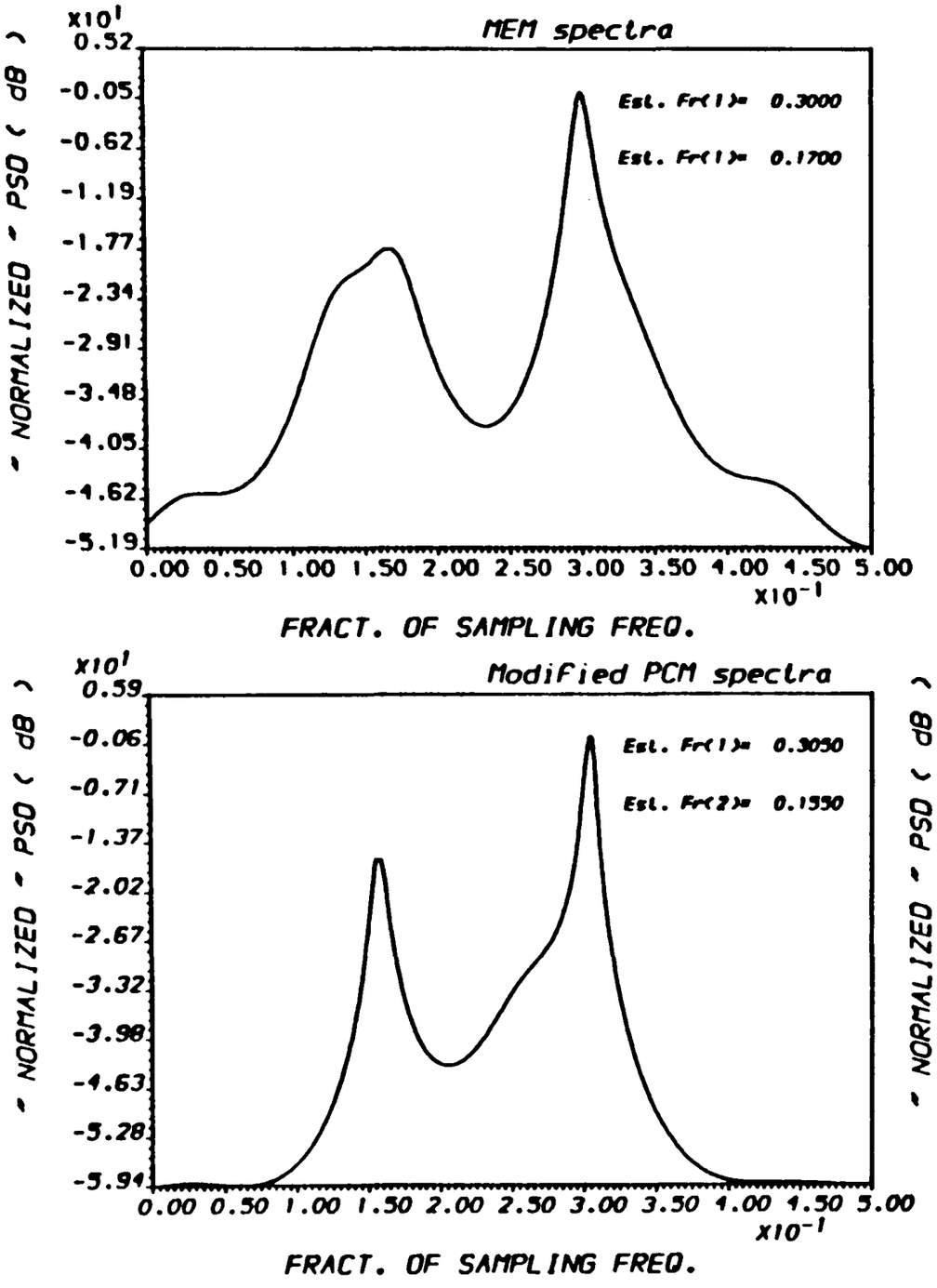


```
/////: Noisy sinusoid
NMAX        :  25
SAMP.FR.    :  1.000
AMPLITUDS   :  1.00   1.00   2.00
FREQS.      :  0.1500  0.1800  0.3000
Init.Phase  :   0.00    0.00    0.00
SNRs ( dB ):  40.000   40.000   46.021
STAND.DEV.  :        0.0100000000000000
RESOL.LIMIT :0.0400
SIMULATED Coverience Matrix
```

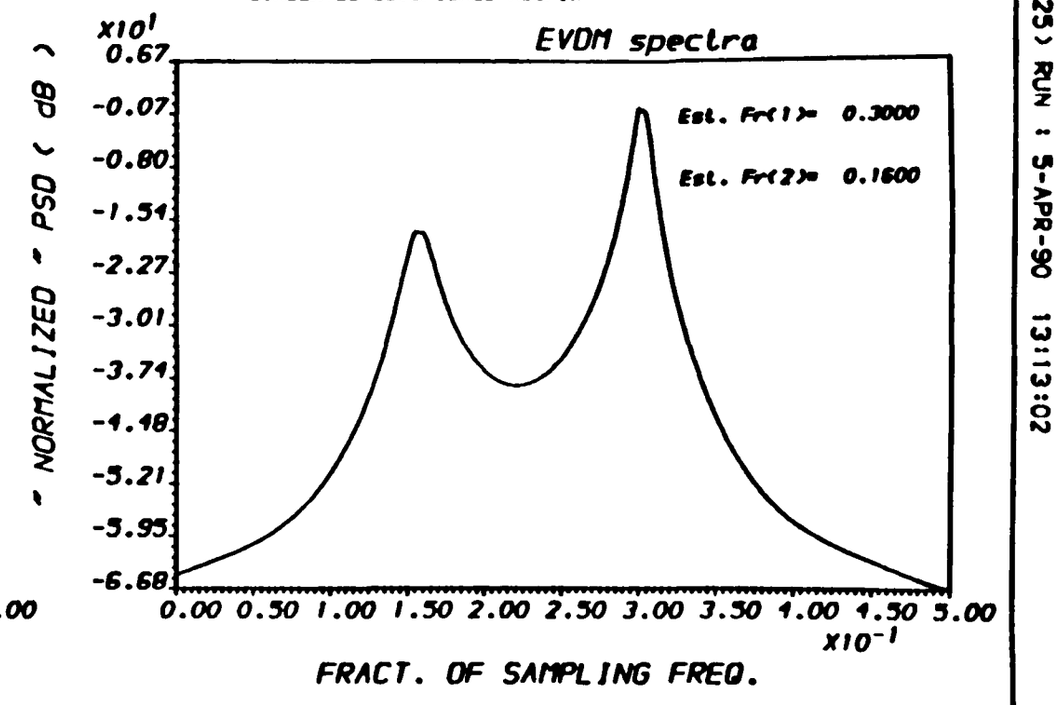

OUTPUT A.ALI -"PLOT2M"- Ex.(9/25) RUN : 5-APR-90 13:13:02

FIG.(5.57) POWER SPECTRAL DENSITY ESTIMATE
* For different PSDE methods *

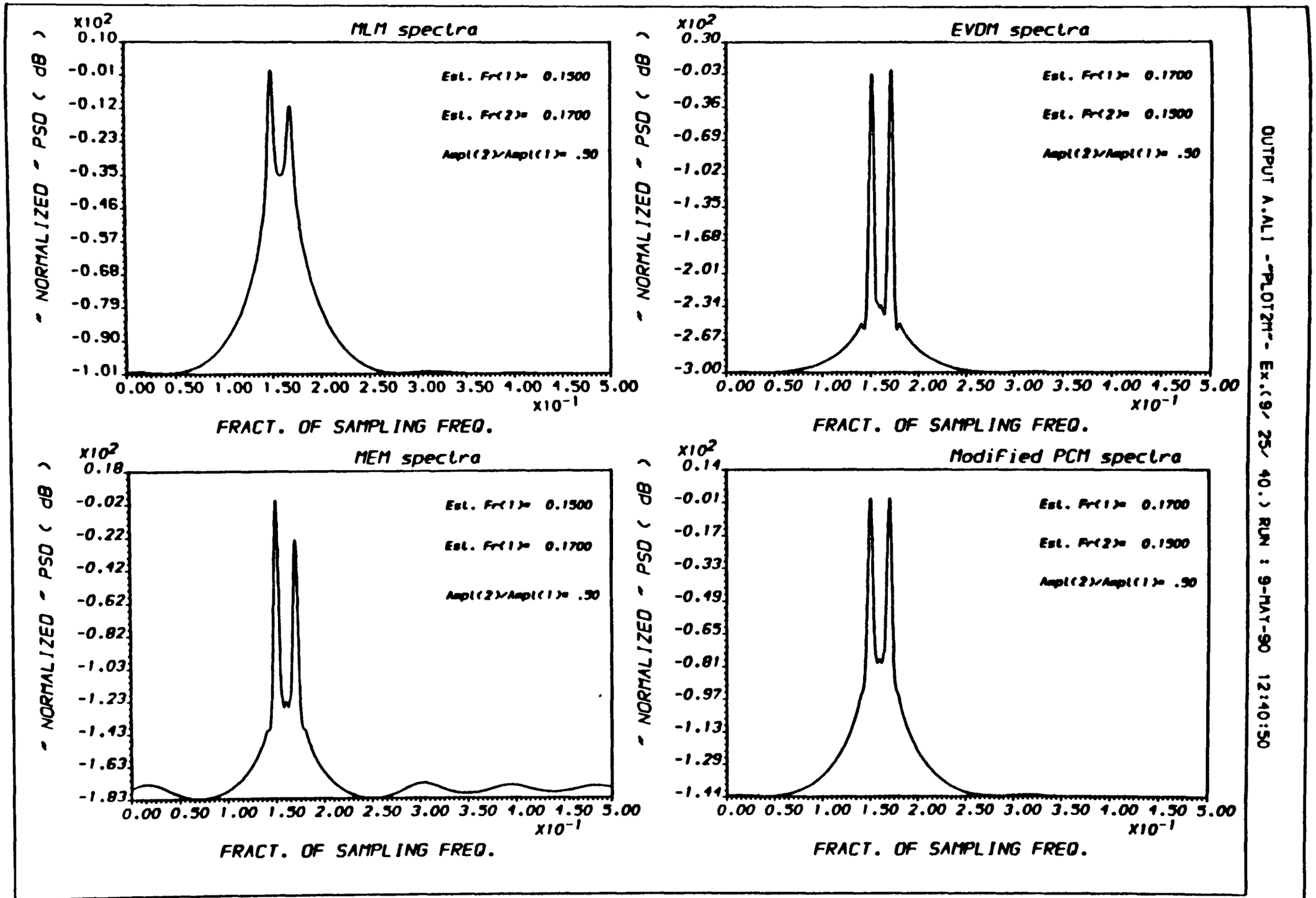

FIG.(5.58) POWER SPECTRAL DENSITY ESTIMATE
* For different PSDE methods *

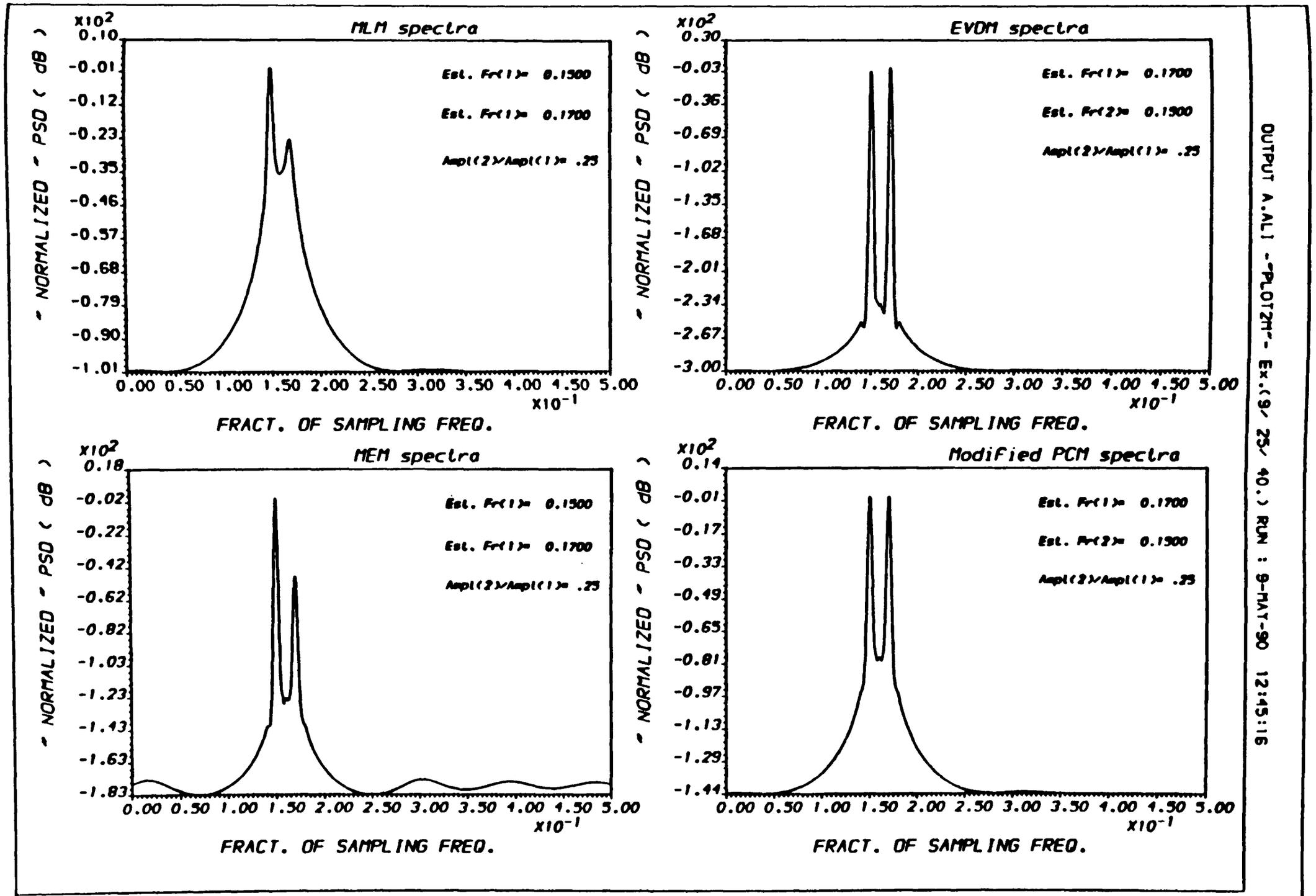

FIG.(5.59) POWER SPECTRAL DENSITY ESTIMATE
* For different PSDE methods *

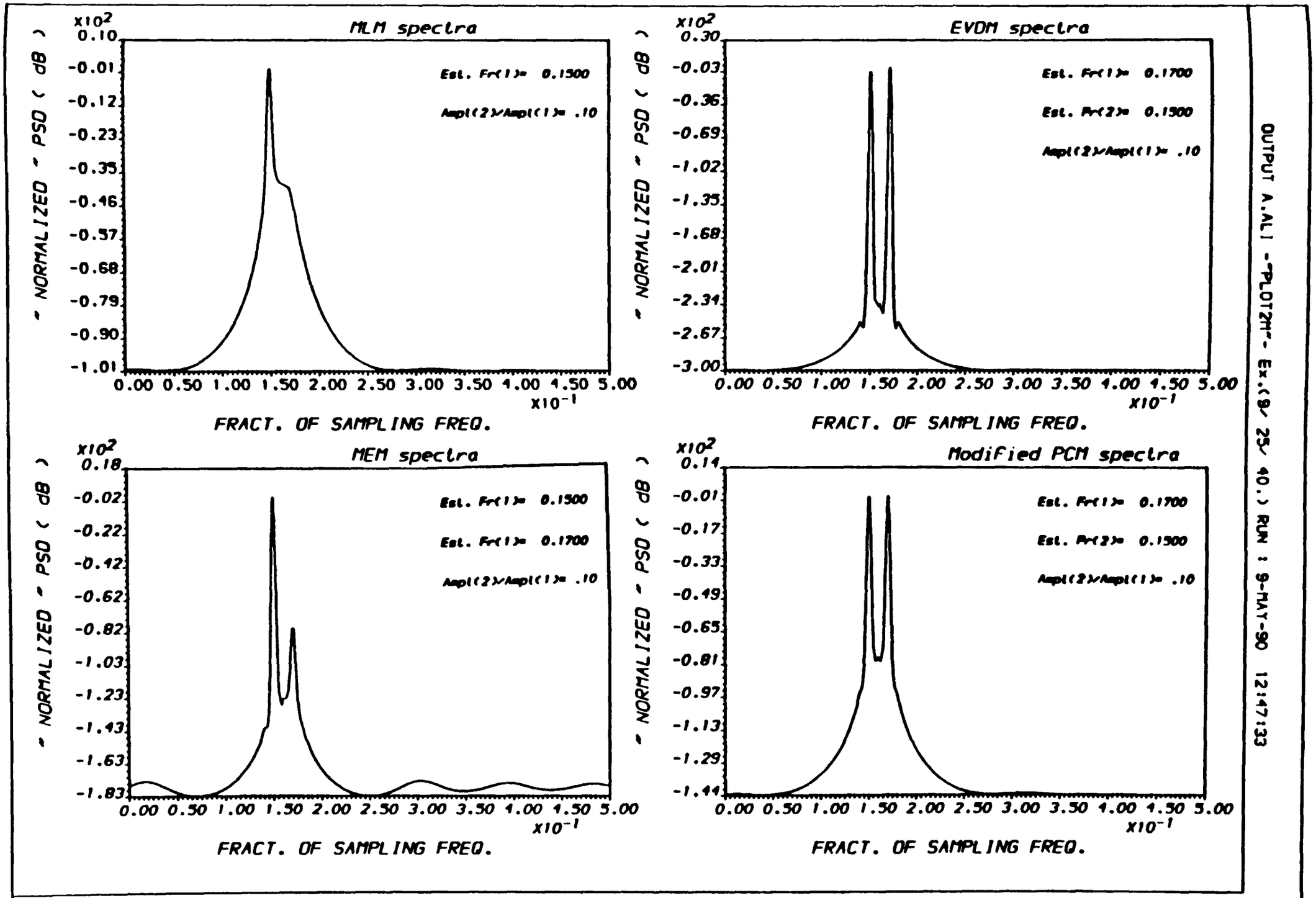

FIG.(5.60) POWER SPECTRAL DENSITY ESTIMATE
* For different PSDE methods *

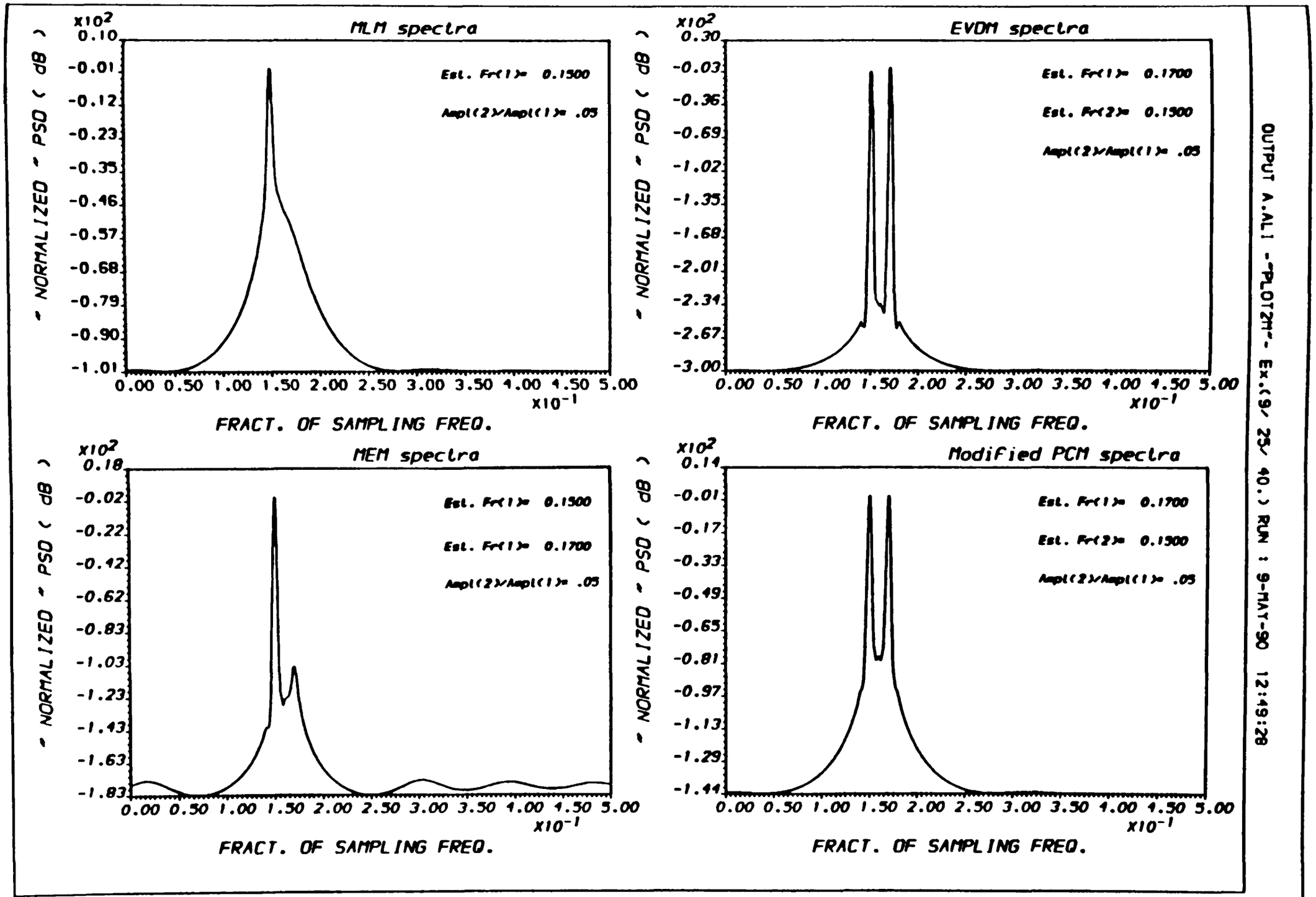

FIG.(5.61) POWER SPECTRAL DENSITY ESTIMATE
* For different PSDE methods *

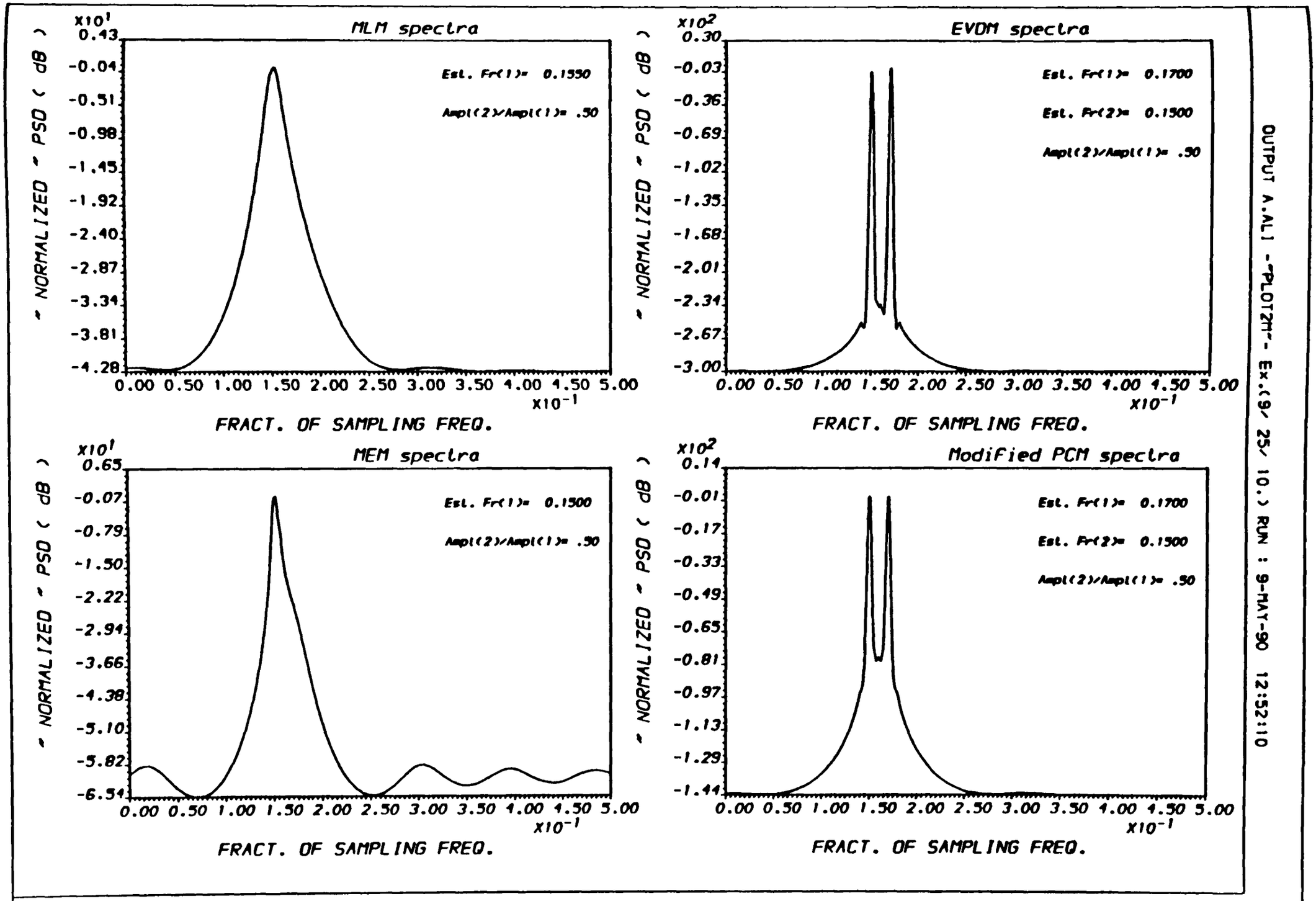

FIG.(5.62) POWER SPECTRAL DENSITY ESTIMATE
* For different PSDE methods *

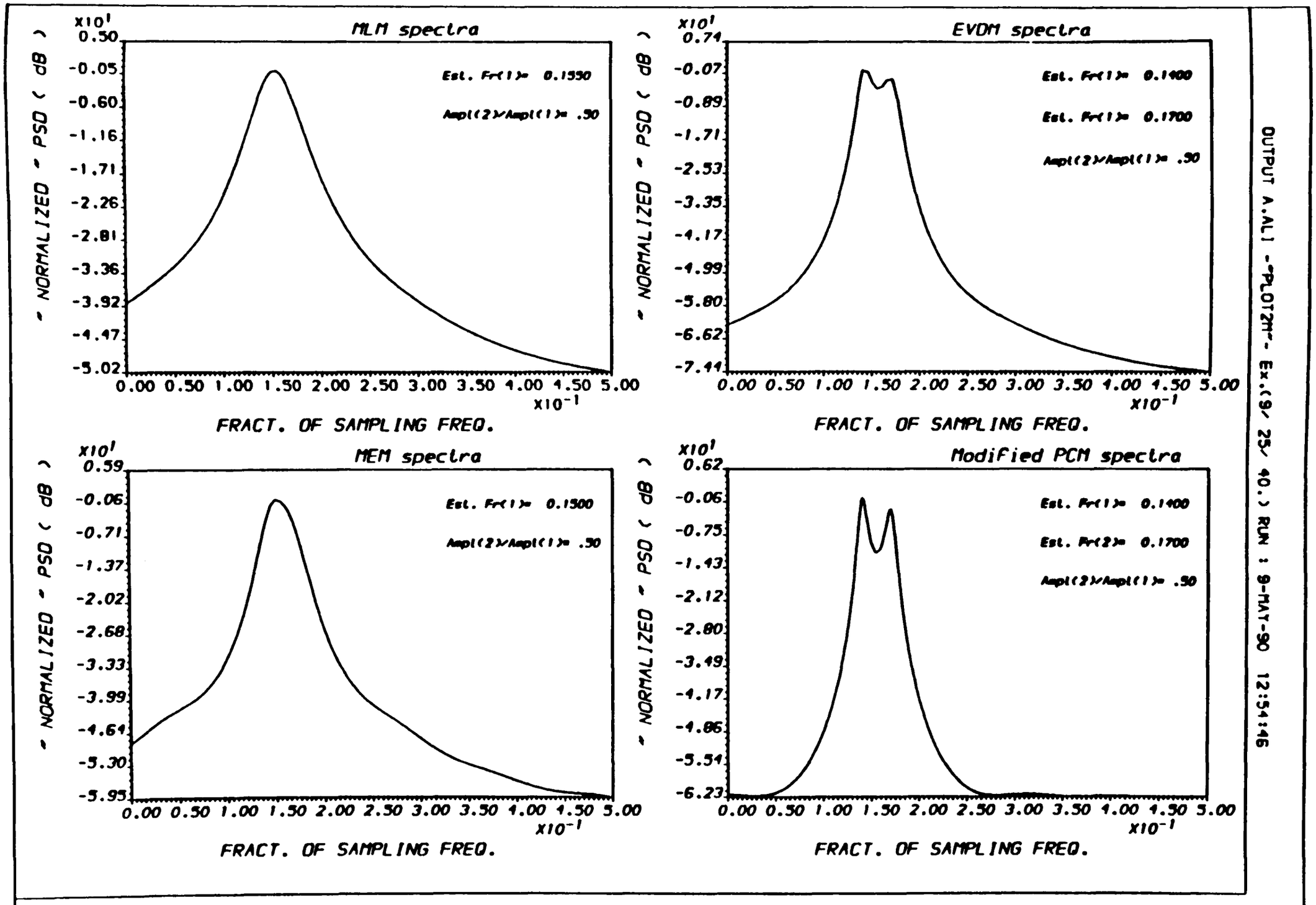

FIG.(5.63) POWER SPECTRAL DENSITY ESTIMATE
* For different PSDE methods *

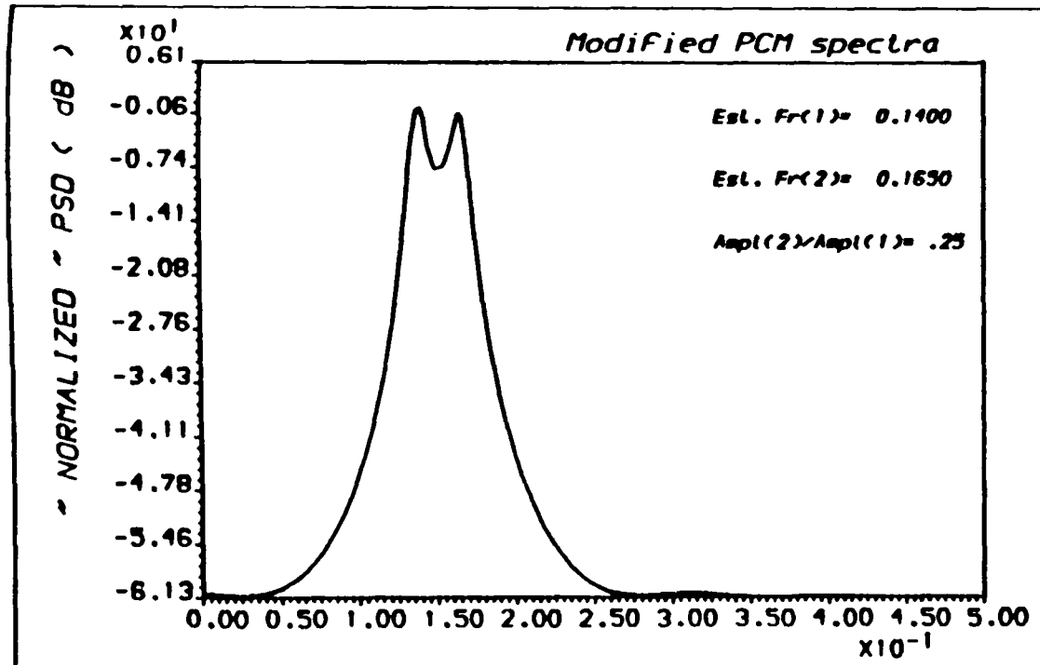

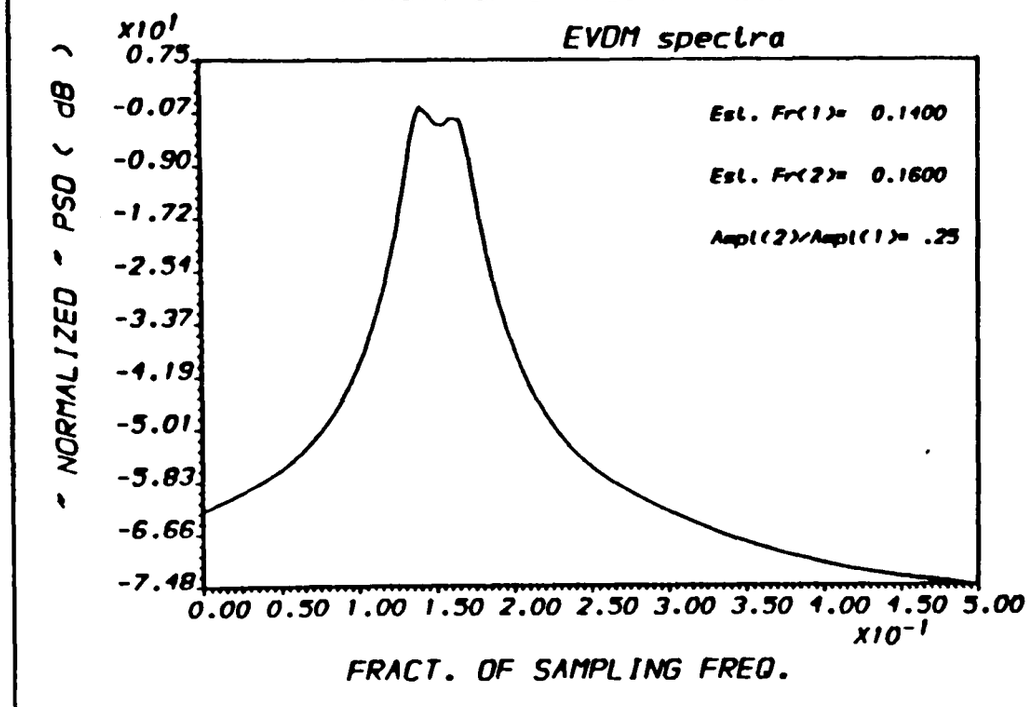

///// Noisy sinusoid

NMAX : 25

SAMP.FR. : 1.000

AMPLITUDS : 1.00 0.25

FREQS. : 0.1500 0.1700

Init.Phase : 0.00 0.00

SNRs (dB): 40.000 27.959

STAND.DEV. : 0.0100000000000000

RESOL.LIMIT :0.0400

SIMULATED Coverlance Matrix

OUTPUT A.ALI -"PLOT2MT- Ex.(9/ 25/ 40.) RUN : 9-MAY-90 12:57:16

FIG.(5.64) POWER SPECTRAL DENSITY ESTIMATE
* For different PSDE methods *

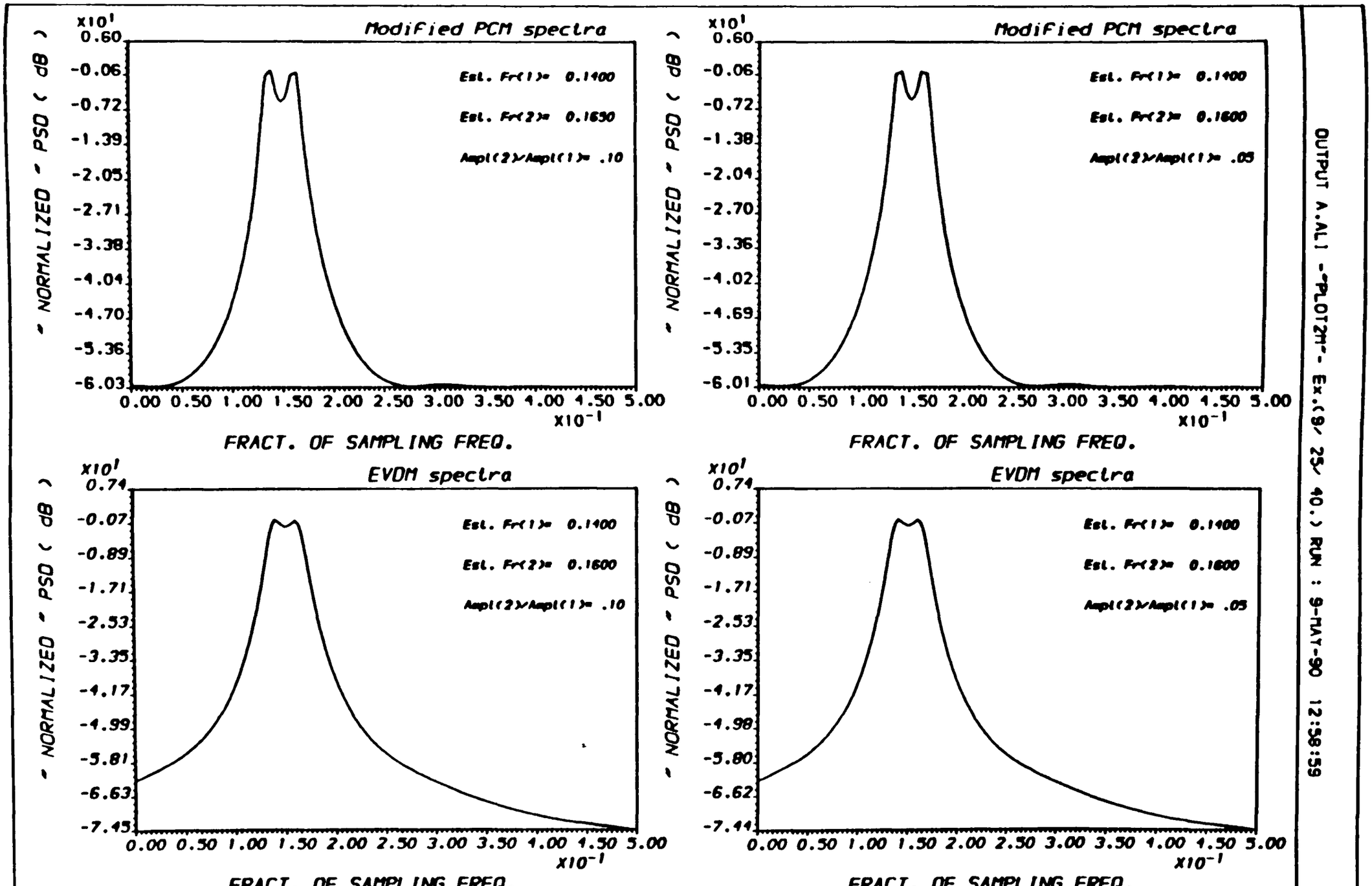

FIG.(5.65) POWER SPECTRAL DENSITY ESTIMATE
* For different PSDE methods *

Chapter Six

THE PREDICTION OF THE EVDT PERFORMANCE FROM THE BEHAVIOUR OF THE EIGEN VALUES OF THE COVARIANCE MATRIX

CHAPTER SIX

THE PREDICTION OF THE EVDT PERFORMANCE
FROM
THE BEHAVIOUR OF THE EIGEN VALUES
OF THE COVARIANCE MATRIX

6.1. INTRODUCTION

Eigen vector decomposition techniques gave excellent performance in terms of detection and frequency resolution of the two closely separated signals in white Gaussian noise which formed the basis of investigation. The key to this excellent performance was the estimated number of signals, which depends to a large extent on the multiplicity of the smallest eigen value of the random process covariance matrix, which is not always obvious as was demonstrated in chapter 4.

In this chapter, the effect of the different parameters mentioned in chapter five on the behaviour of the eigen values will be studied from which we can predict the way in which these parameters will affect the detection and resolution of the *EVDT* approaches. For the purpose of comprehension, this chapter will deal with the exact as well as the estimated covariance matrix.

6.2. TEST PROCEDURE :

Fig(6.1) shows the flow chart of the Fortran 77 program written to test the effect of these parameters on the behaviour of the signal and the noise eigen values of the covariance matrix. The parameter under study is changed in steps so that the random process data samples or their

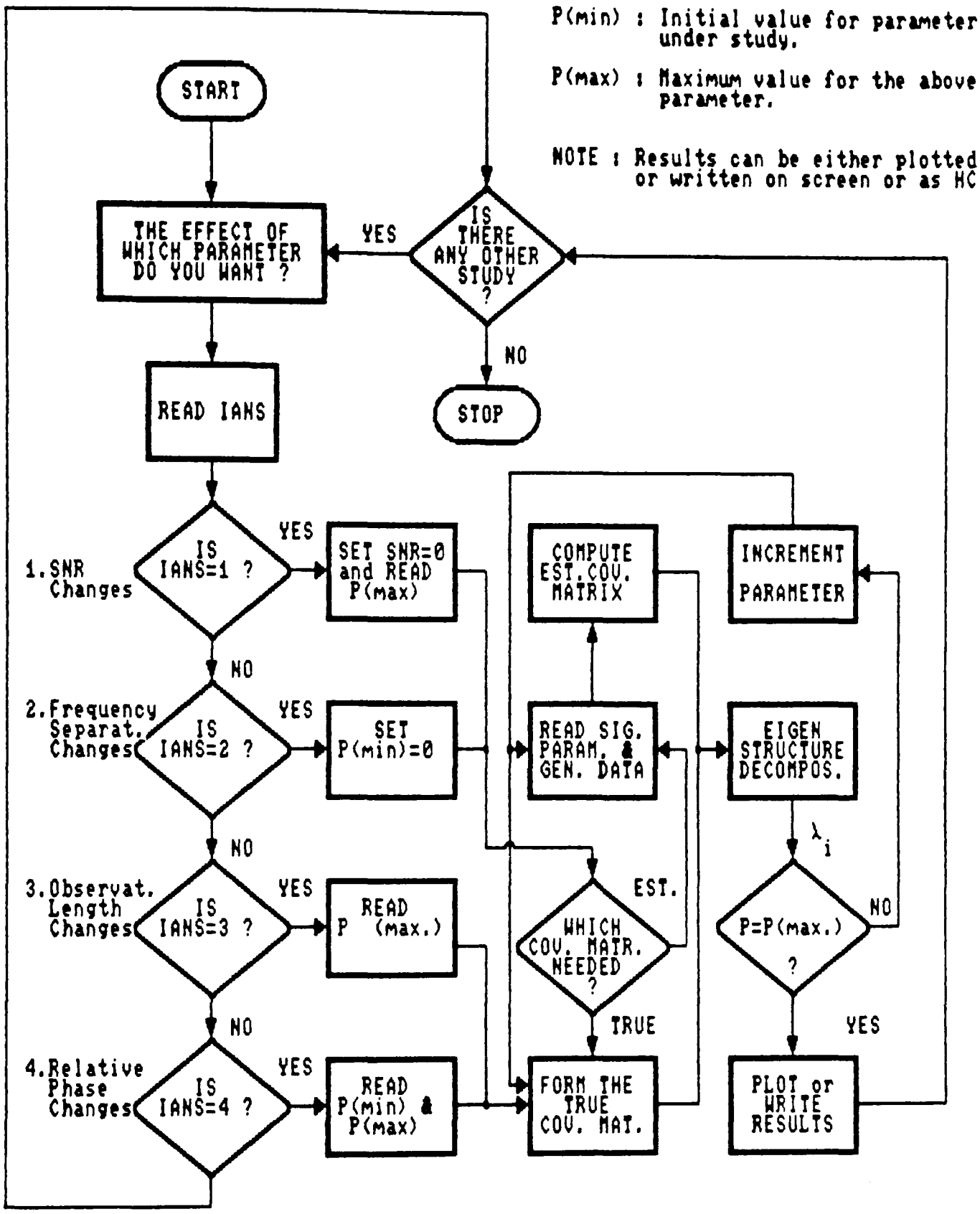

Fig.(6.1) FLOW CHART FOR PROGRAM RAGAD WHICH SIMULATES THE EFFECTS OF THE DIFFERENT PARAMETERS ON THE EIGEN VALUES BEHAVIOUR

covariance matrix is generated, which is then decomposed into its eigen values and the associated eigen vectors using the standard methods. Plots for these eigen values are obtained at the end of the process. The other parameters are kept constant at values well above their critical values in order not to affect the behaviour of the eigen values.

6.3. THE EFFECT OF OBSERVATION LENGTH VARIATIONS :

As was mentioned in chapter five section *(5.2.2.1)*, the detection and resolution capabilities of the eigen vector decomposition approaches are highly affected by data length variations, especially when the data length is short. In this section the behaviour of the signal and noise eigen values with the data length variations are studied for the cases of single and multiple sinusoids in white Gaussian noise.

6.3.1. SINGLE SINUSOID CASE :

In chapter three section *(3.1.1)* the detection capabilities of the different power spectral density estimators were studied, from which we saw that nearly all the estimators were capable of detecting easily the single sinusoid in white noise though the data length was short. However, the eigen vector decomposition technique was always the best technique in detecting signals corrupted by noise, the effect of this corruption can be severe when the data length is very short.

Fig(6.2) shows the eigen values of a random process consisting of a single sinusoid of unit amplitude and a normalized frequency of $0.25f_s$ in white Gaussian noise having a signal-to-noise ratio of *10dB, -this is the same test example used earlier in chapter three-*. From this

figure we can see that the signal eigen value level, *i.e eigen value No. 12,* was very high compared with the noise eigen values levels. Hence we can expect that the wavenumber and the frequency estimations will be perfect even at short data length. *Fig(6.3)* shows the *EVM* and *MPCM* estimates for the *PSD* of the above random process for sample length of *4* and *11* points from which we can see that these two algorithms were able to detect the signal *(with some bias)* at a data length of as short as four samples , so in this case we can consider that the data length variations has no effect on the signal and noise eigen values of the random process which in turn means that it will not affect the detection capability of the eigen vector decomposition technique.

6.3.2. MULTIPLE SINUSOIDS CASE :

Fig(6.4) and *Fig(6.5)* represent the behaviour of the signal and noise eigen values of the random process used in testing the resolution capabilities of the different algorithms in chapter three. These figures show that the signal eigen values have a damped oscillation around a constant value as the data length increases and they reached their steady state values as the data length became high where we can expect the resolution to be perfect. This oscillation was caused by many factors such as the correlation between the two sinusoids, which decreases as the frequency separation increases causing less oscillations to the signal eigen values and hence improving the resolution, *-see Fig(6.6)-*, and the fact that the covariance matrix estimated from a short data record is too far from the true one, and that is why these eigen values became nearly constant at long data records.

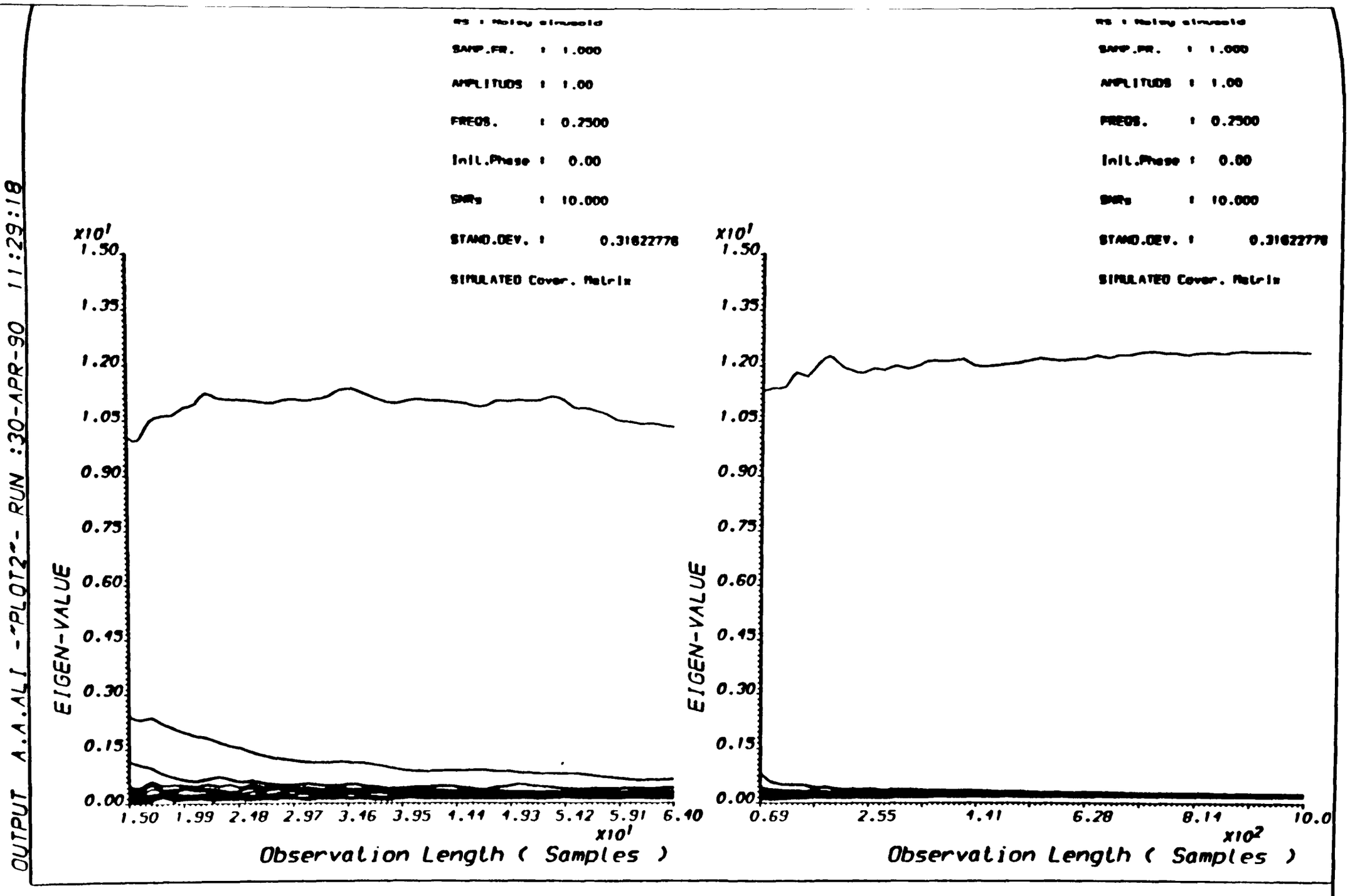

EIGEN-VALUES No. : 1, 2, 3, 4, 5, 6, 7, 8, 9,10

EIGEN-VALUES No. : 11,12,

FIG. (6.2) THE EFFECT OF OBSERVATION LENGTH ON EIGEN-VALUES

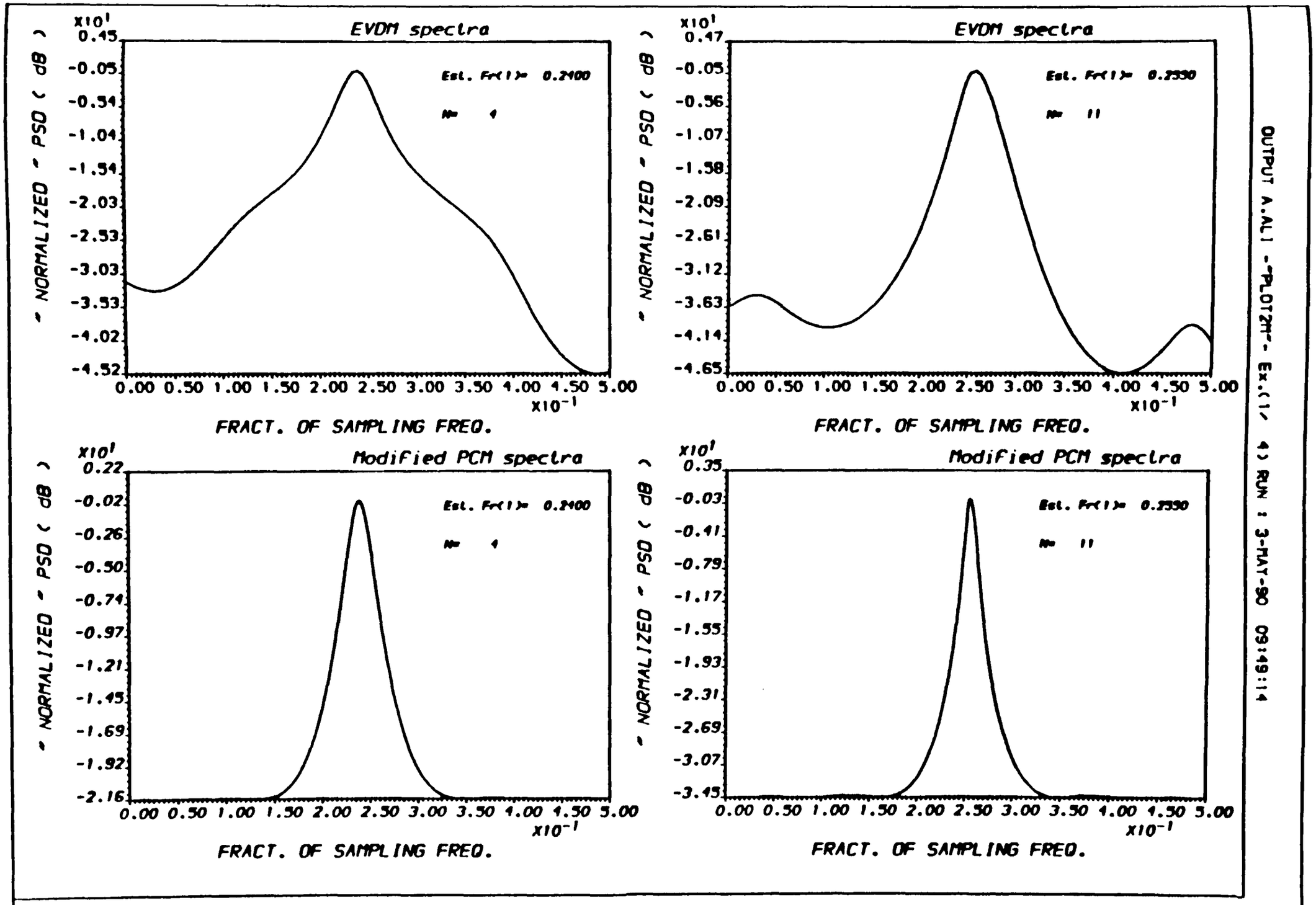

FIG.(6.3) POWER SPECTRAL DENSITY ESTIMATE
* For different PSDE methods *

Fig(6.5) shows the signal eigen values behaviour as the data length varies from *69* to *1000* samples, from which we can say that these eigen values remain nearly constant at their higher values and the noise eigen values remain constant at their lower values which indicates that the detection and resolution capabilities of the eigen vector decomposition approaches are very slightly affected by the data length variations when it is long and these capabilities tend to be perfect *(ideal)* when the observation length approaches infinity where on the other hand we can expect no estimation bias will exist.

It is obvious that these sets of eigen values curves are function of frequency separation between the two signals, *-i.e we can get another set of curves as the frequency separation changes-*. *Fig(6.6)* shows the eigen values as a function of observation length for two different sets of signal frequencies, $(0.15f_s,\ 0.2f_s)$ and $(0.15f_s,\ 0.35f_s)$ from which we can see that the difference between the two signal eigen values levels became less as the frequency separation increased allowing the second *(lower)* signal eigen value to be increased and to move away from the noise eigen values levels which in turn means an improvement in the detection and resolution capabilities of the eigen vector decomposition technique.

6.4. THE EFFECT OF SNR VARIATIONS :

6.4.1. SINGLE SINUSOID CASE :

The signal and noise eigen values of the single sinusoidal signal in white Gaussian noise random process mentioned in section *(6.3.1)* for both the true and estimated covariance matrix cases are shown in *Fig(6.7)*. In both of these cases the signal eigen value level was well above the noise eigen values levels even at low values of *SNR* which

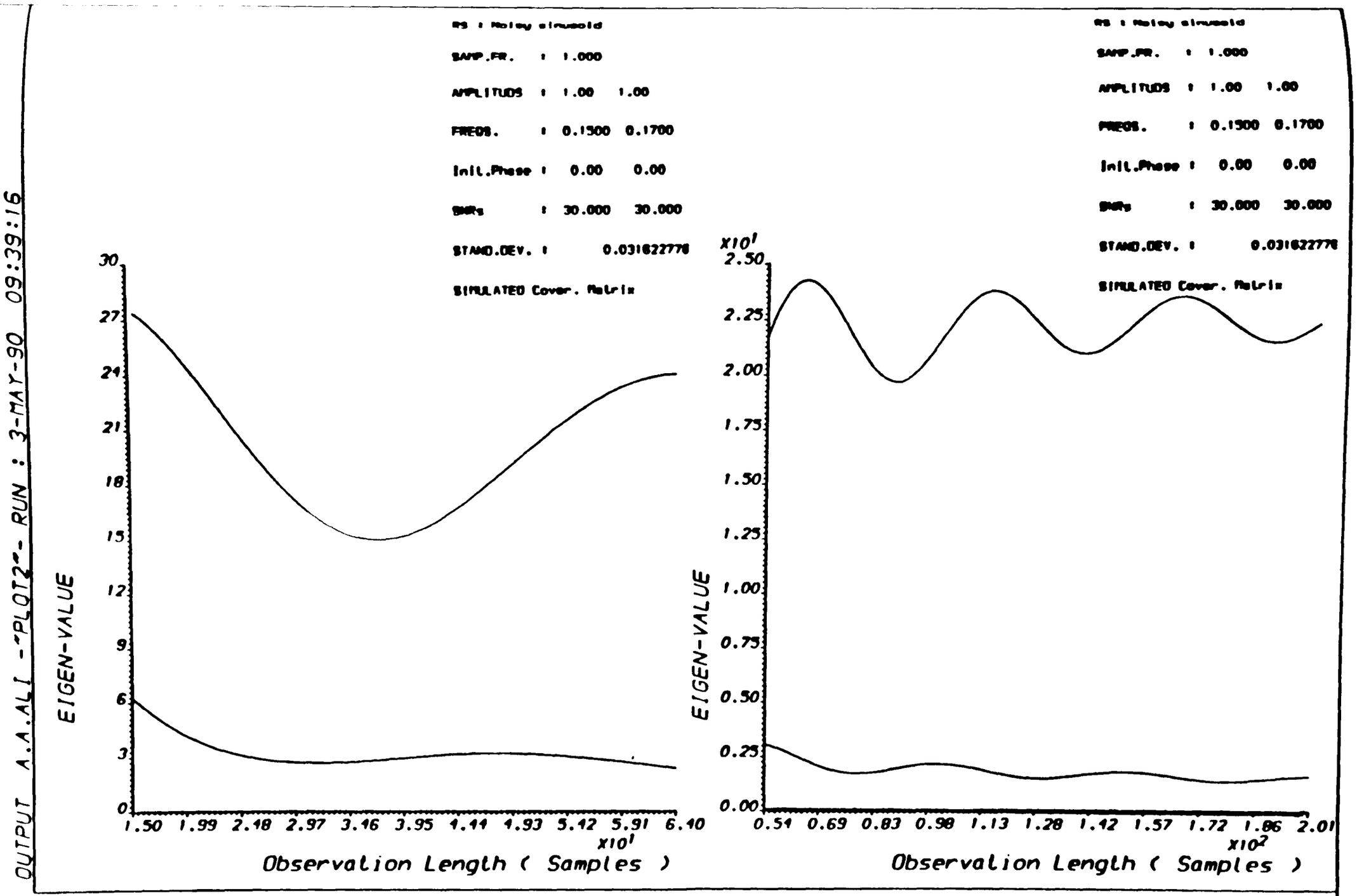

FIG. (6.4) THE EFFECT OF OBSERVATION LENGTH ON EIGEN-VALUES

EIGEN-VALUES No. : 11,12,

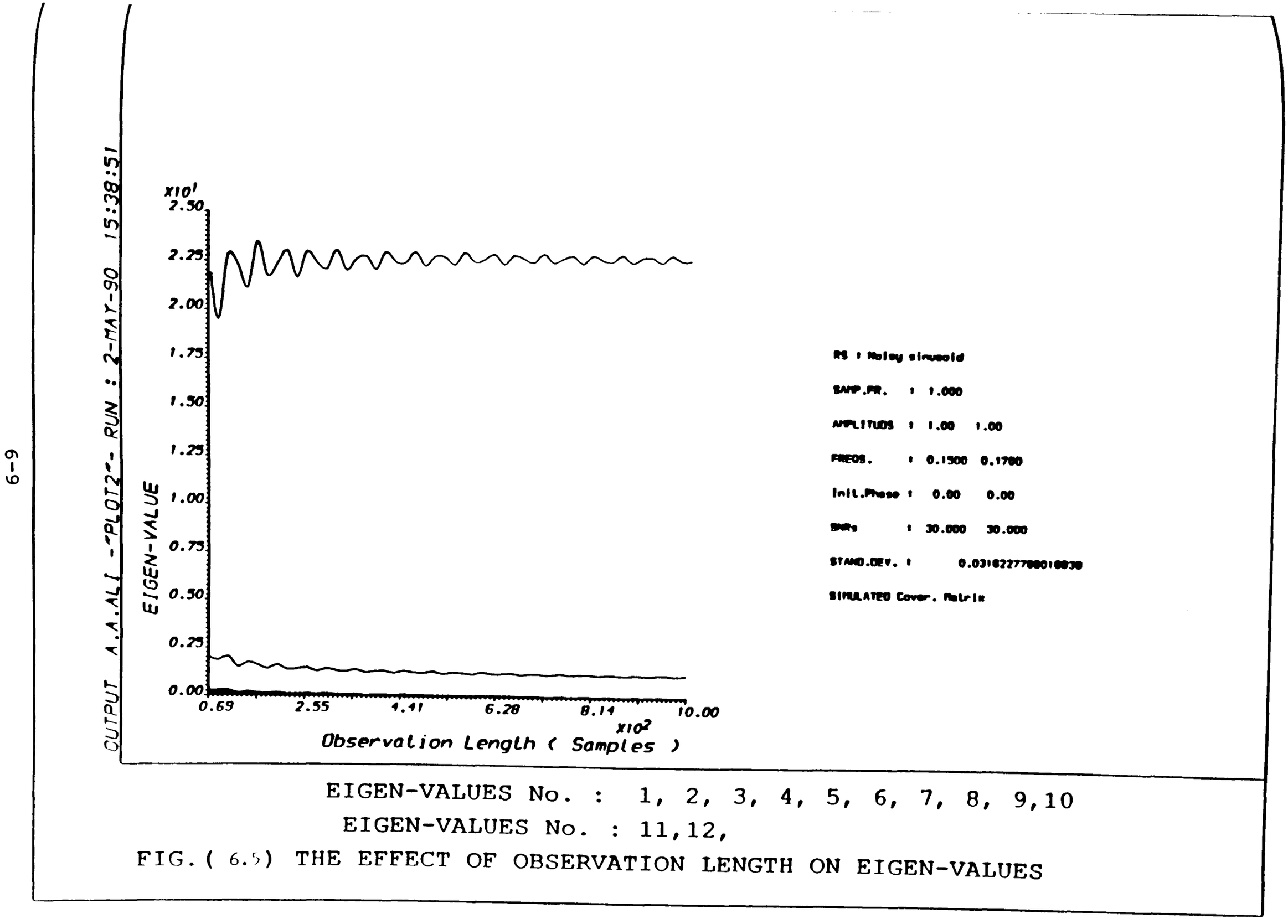

EIGEN-VALUES No. : 1, 2, 3, 4, 5, 6, 7, 8, 9,10

EIGEN-VALUES No. : 11,12,

FIG. (6.5) THE EFFECT OF OBSERVATION LENGTH ON EIGEN-VALUES

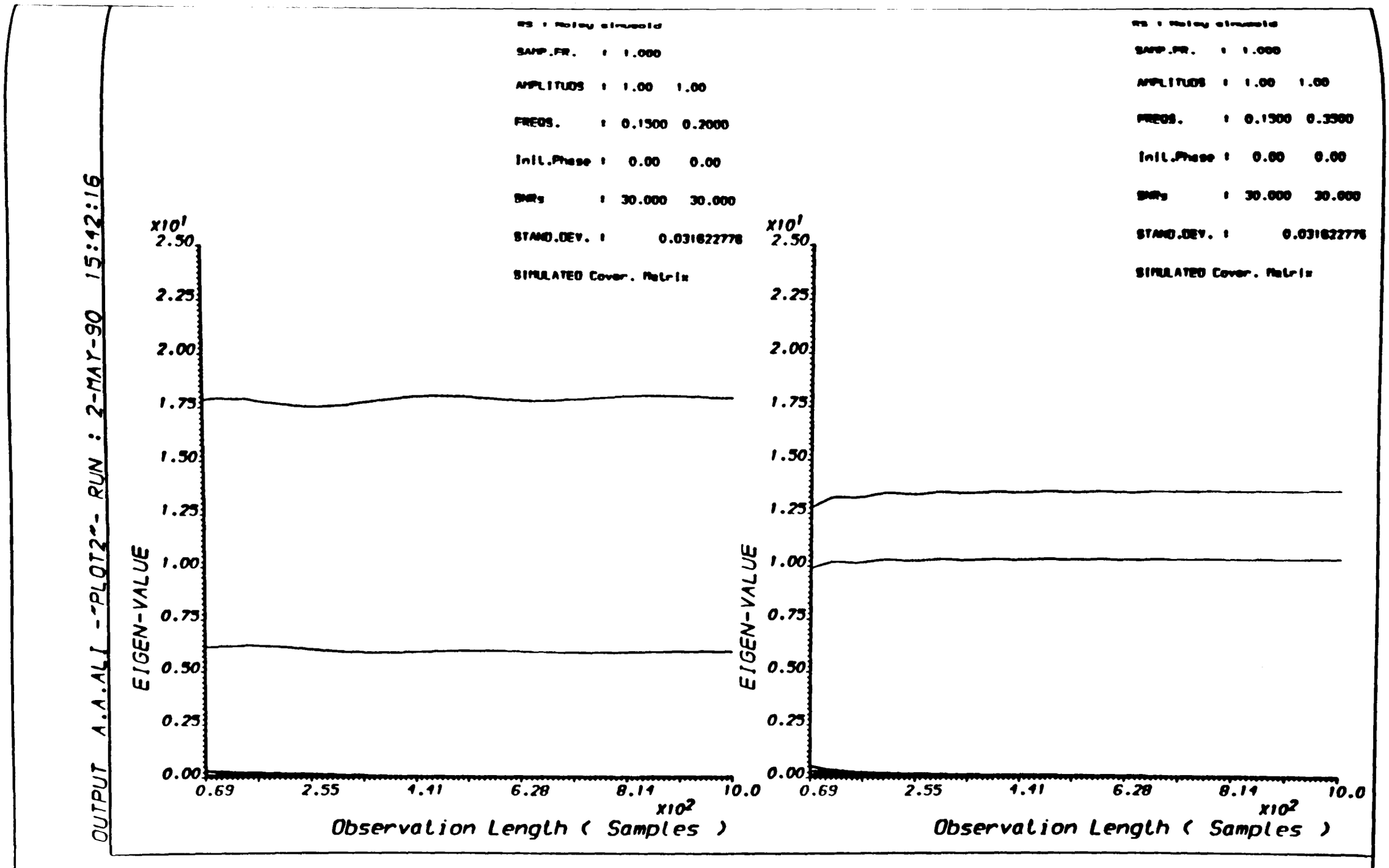

EIGEN-VALUES No. : 1, 2, 3, 4, 5, 6, 7, 8, 9,10

EIGEN-VALUES No. : 11,12,

FIG. (6.6) THE EFFECT OF OBSERVATION LENGTH ON EIGEN-VALUES

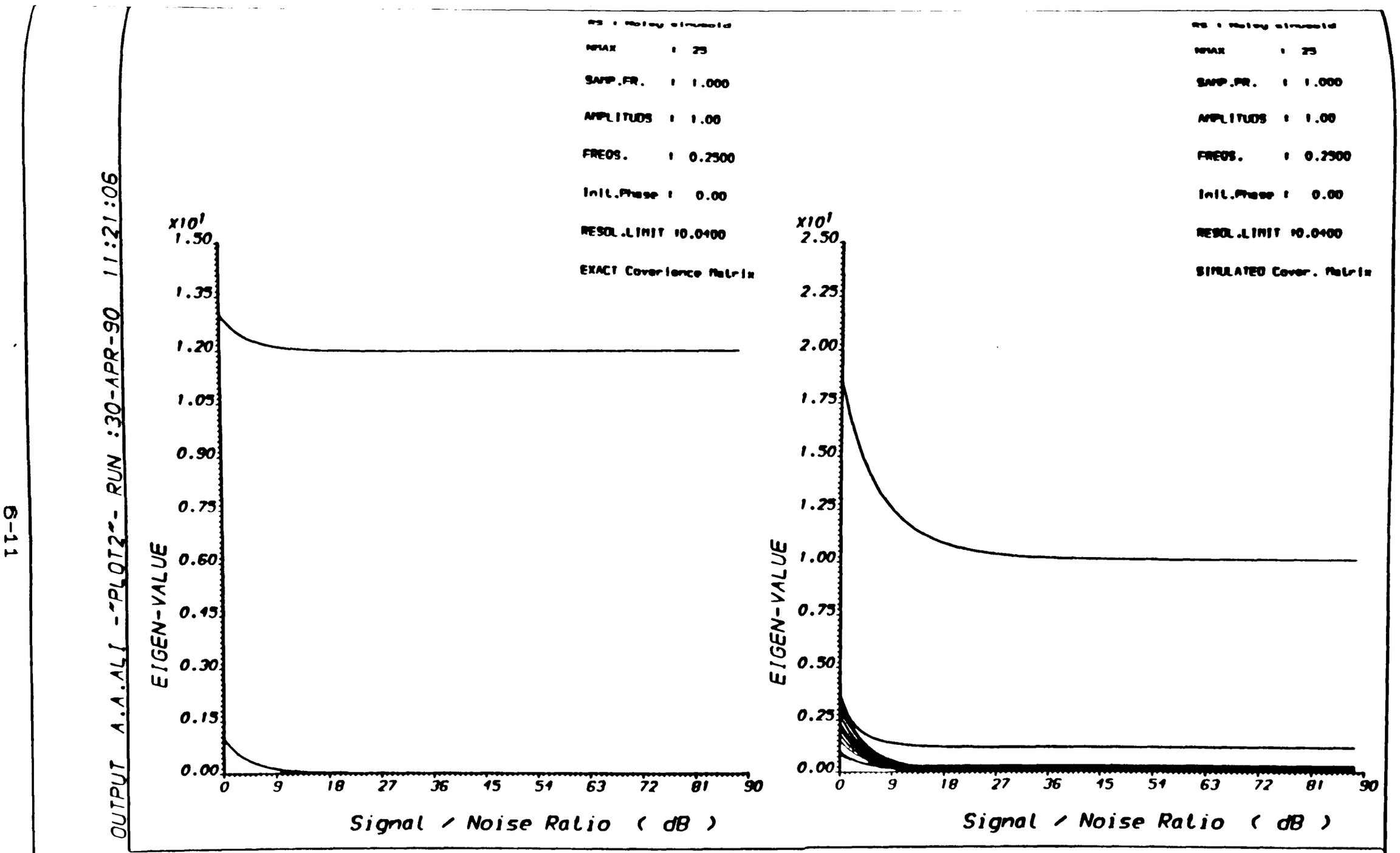

EIGEN-VALUES No. : 1, 2, 3, 4, 5, 6, 7, 8, 9,10

EIGEN-VALUES No. : 11,12,

FIG. (6.7) THE EFFECT OF Signal/Noise Ratio ON EIGEN-VALUES

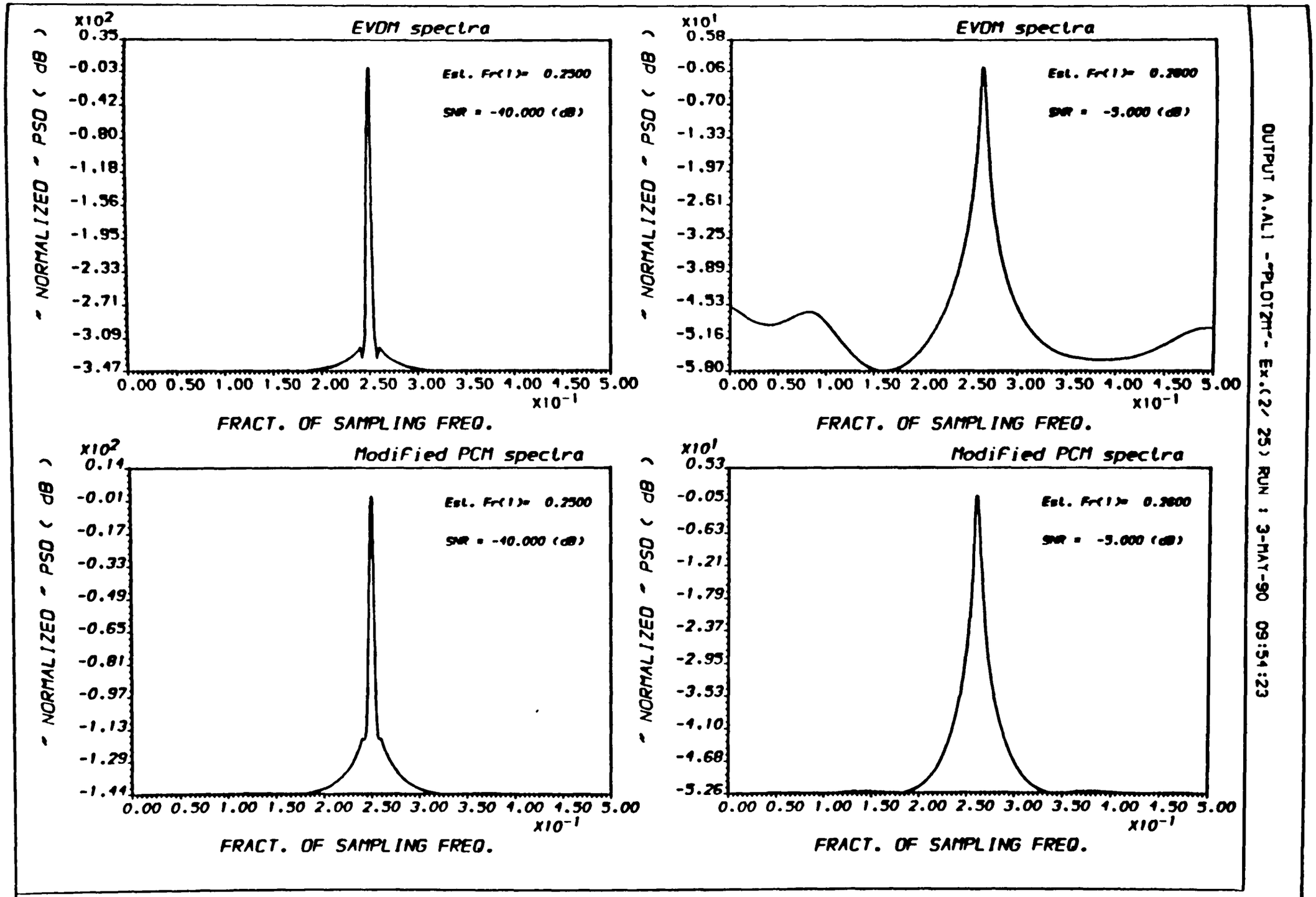

FIG.(6.8) POWER SPECTRAL DENSITY ESTIMATE
* For different PSDE methods *

indicates that the eigen vector decomposition technique will be able to detect this signal however small the *SNR* value is. *Fig(6.8)* shows the power spectral density estimates of this random process using the eigen vector method *(EVM)* and the new proposed method *(MPCM)* at low values of *SNR*, for the case of true and estimated covariance matrix *-40dB* and *-5dB* respectively, from which we can say that these two methods can easily estimate the exact signal frequency *(i.e without any estimation bias)* and they can estimate it with small amount of bias when the estimated covariance matrix is employed.

It is obvious that due to the influence of the noise upon the signal, the steady state level of the signal eigen value for the estimated covariance matrix is lower than that for the true covariance matrix, whereas the steady state levels of the noise eigen values for the case of estimated covariance matrix are higher than those obtained for the true covariance matrix case.

6.4.2. MULTIPLE SINUSOIDS CASE :

The signal-to-noise ratio of the two equipower signals was varied from *0dB* to *87dB*. The signal and noise eigen values as a function of this range of *SNR* variations are depicted in *Fig(6.9)* for the case of estimated and true covariance matrices. The figure shows that all the eigen values of the random process were gradually decreasing as the *SNR* increasing and after a certain limit of *SNR* values the eigen values remain constant. This *SNR* value *(limit)* when calculated from the graphs, *-see Fig(6.10)-*, appeared to be equal the threshold *SNR* value below which the noise eigen values levels were comparatively high when compared with the second *(low)* signal eigen value and that is why

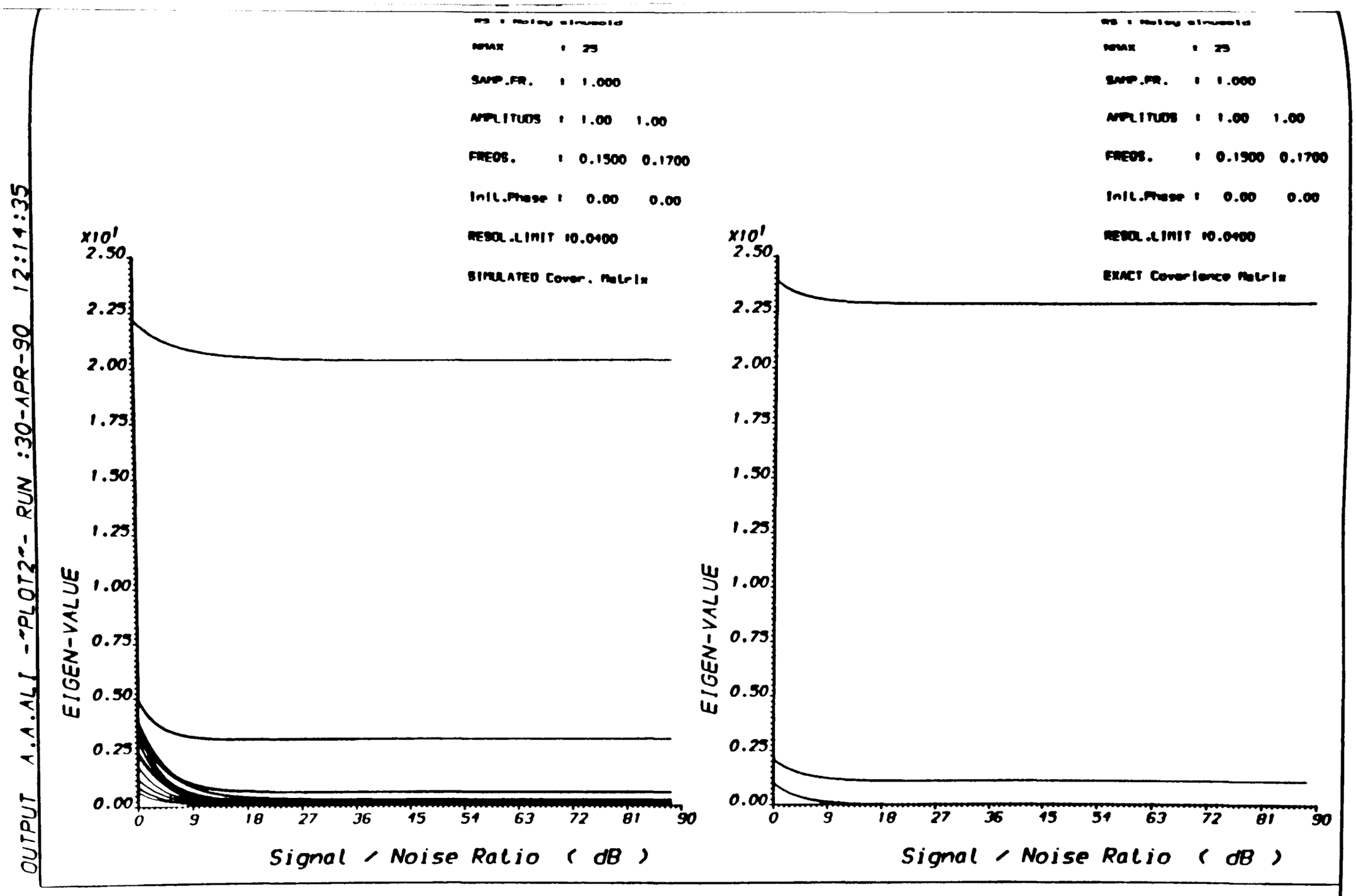

EIGEN-VALUES No. : 1, 2, 3, 4, 5, 6, 7, 8, 9,10

EIGEN-VALUES No. : 11,12,

FIG. (6.9) THE EFFECT OF Signal/Noise Ratio ON EIGEN-VALUES

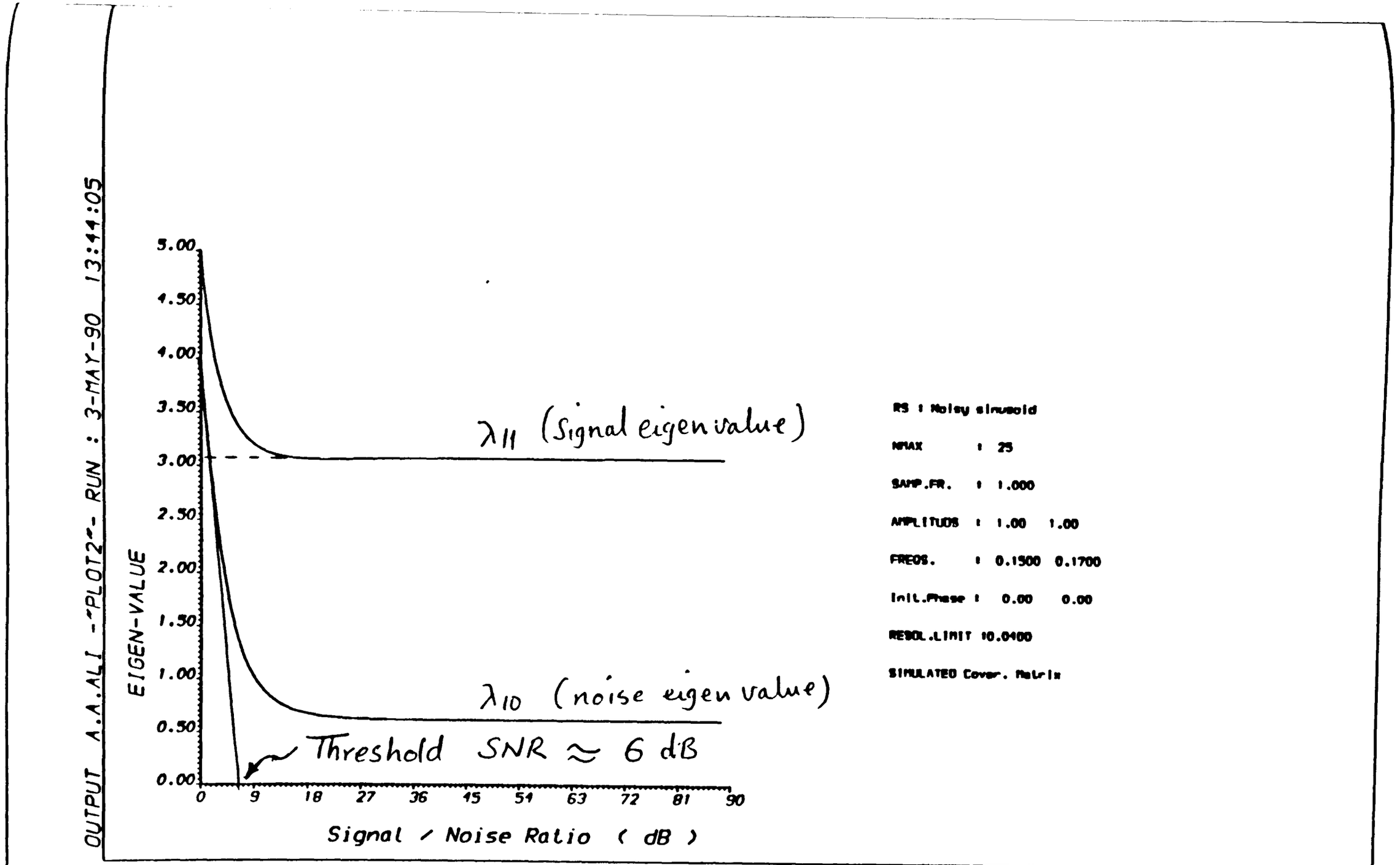

FIG. (6.10) THE EFFECT OF Signal/Noise Ratio ON EIGEN-VALUES
EIGEN-VALUES No. : 10,11,

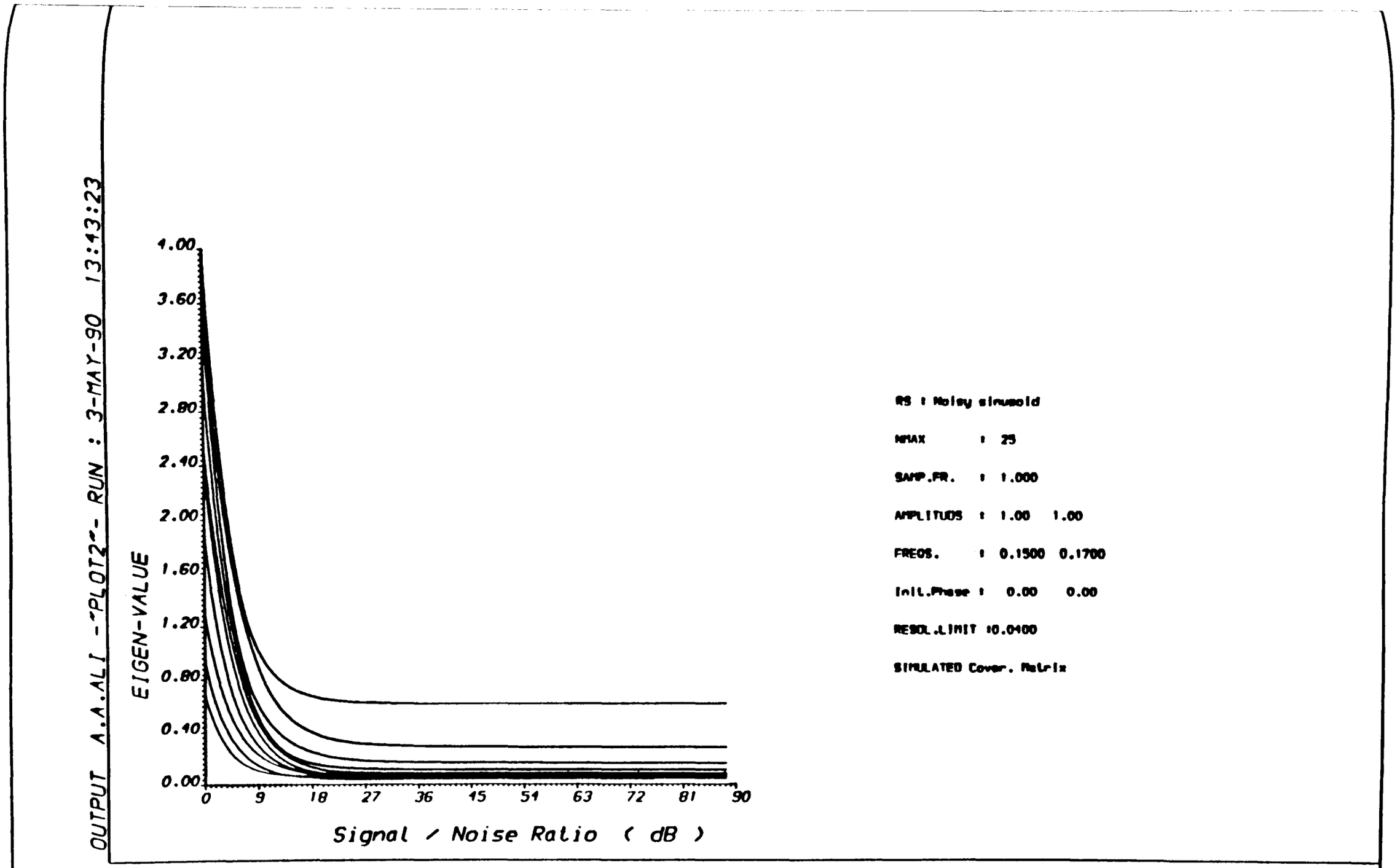

FIG.(6.11) THE EFFECT OF Signal/Noise Ratio ON EIGEN-VALUES
EIGEN-VALUES No. : 1, 2, 3, 4, 5, 6, 7, 8, 9,10

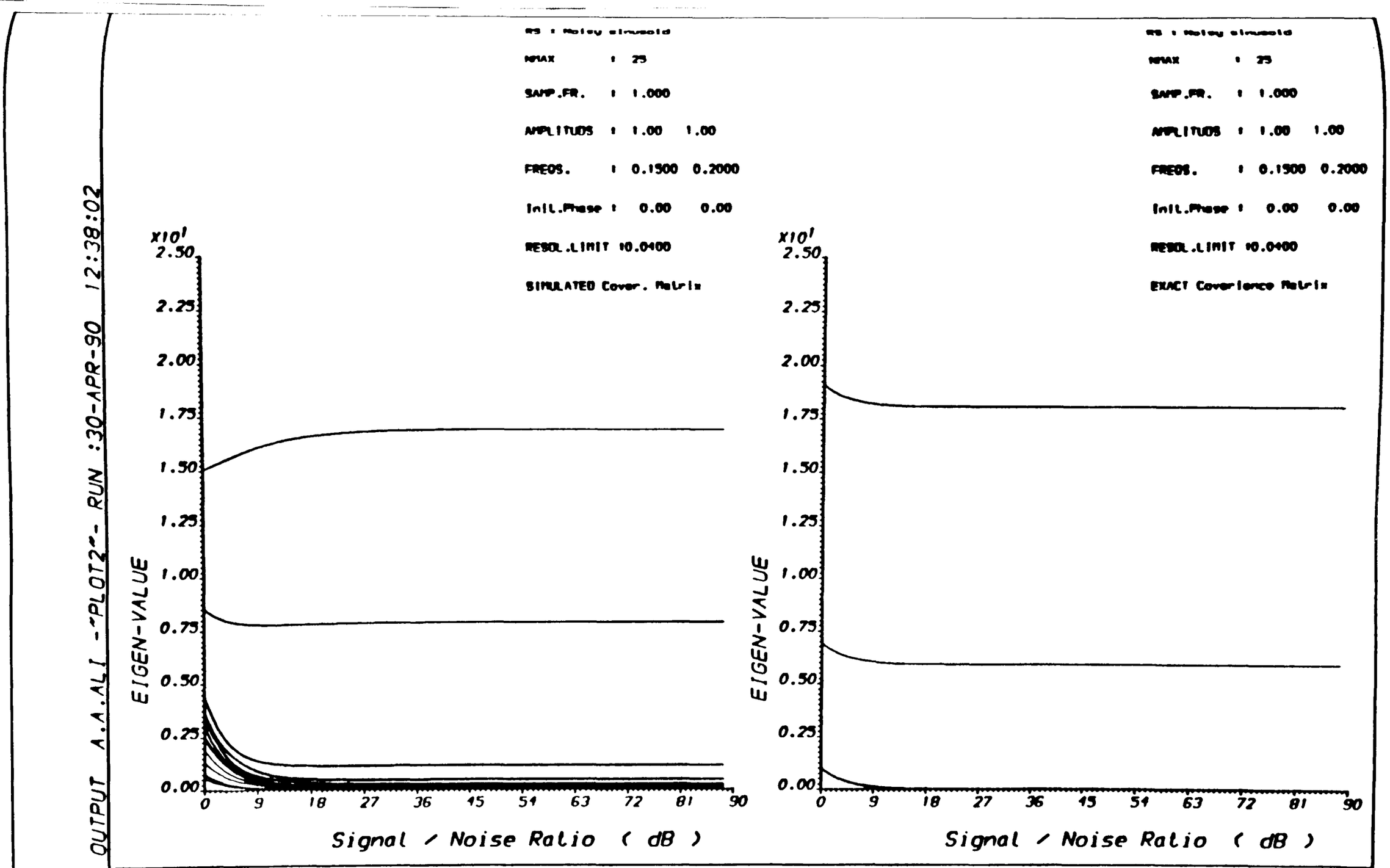

EIGEN-VALUES No. : 1, 2, 3, 4, 5, 6, 7, 8, 9,10

EIGEN-VALUES No. : 11,12,

FIG. (6.12) THE EFFECT OF Signal/Noise Ratio ON EIGEN-VALUES

there was no resolution achieved when the *SNR* value was below the threshold value of this technique, -*see Fig.(6.11)*-.

Fig(6.9) also shows the signal eigen values of the same random process for the case of true covariance matrix. Since the noise eigen values remained constant what ever low the *SNR* value was, then this means that this technique is capable of resolving the two closely separated signals at the worst situation, where lower *SNR* values are assigned.

Again these sets of curves are function of the frequency separation between the two signals to be resolved, so another sets of eigen values curves can be obtained when other values are assigned to the frequency separation, *see Fig(6.12) for the case of* $0.05f_s$ *frequency separation.*

6.5. THE EFFECT OF FREQUENCY SEPARATION VARIATIONS :

The plots for the signal and noise eigen values for the different values of frequency separation between the two signals are presented in *Fig(6.13)* and *Fig(6.15)* for the estimated and true covariance matrices cases respectively.

Fig(6.13) shows the first signal eigen value decreases sharply and the second signal eigen value increases until they reach the same level and then continue to be nearly constant at this level. The value of frequency separation at which they first met is called the discrimination frequency separation value at and above which the two signals have no effect on each other and the estimates become bias free. *Fig(6.15)* shows these two eigen values for the case of the true covariance matrix from which it can be seen that the second signal eigen value curve is exactly the reciprocal of the first signal eigen value curve and the decoupling or

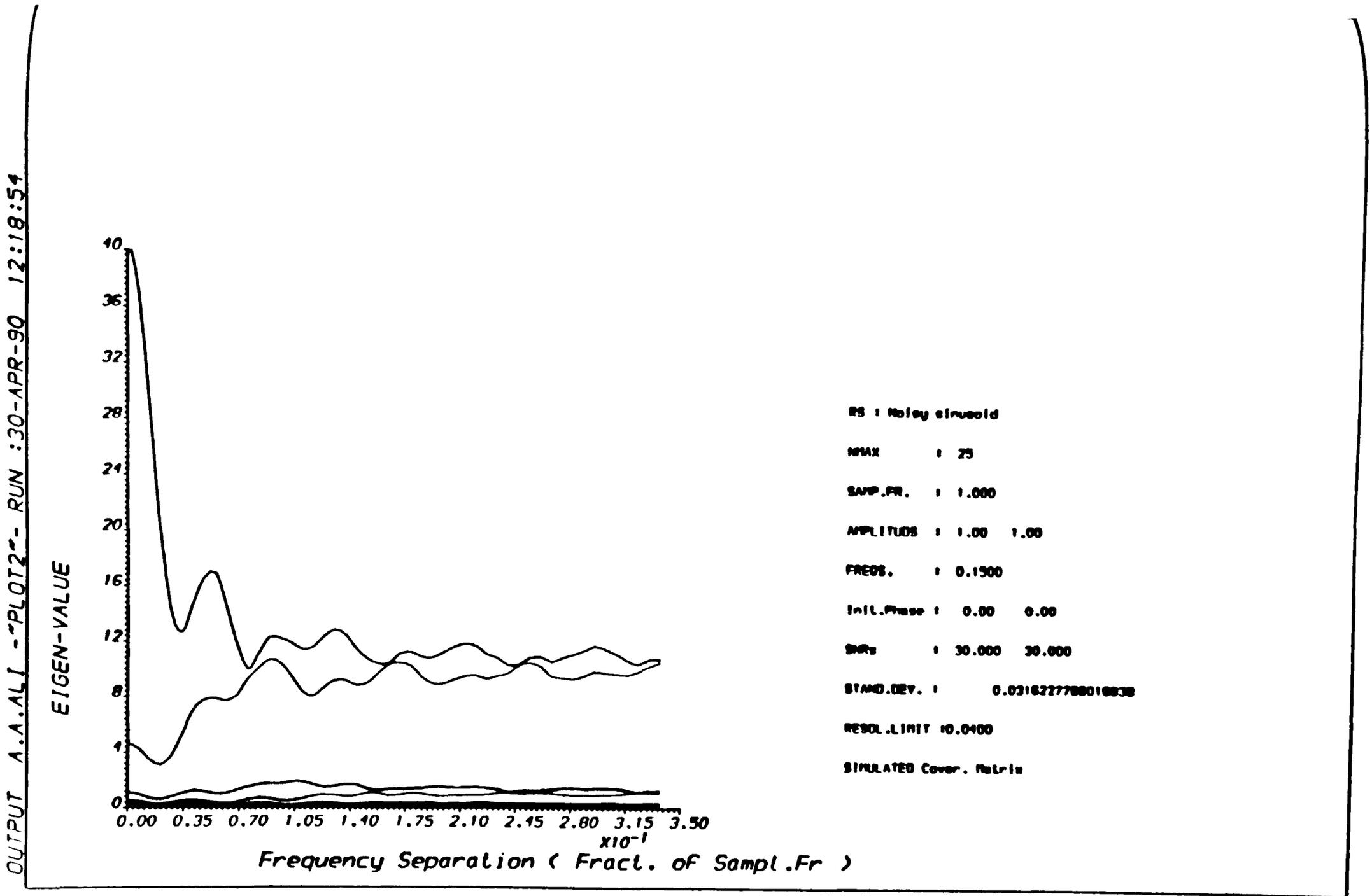

EIGEN-VALUES No. : 1, 2, 3, 4, 5, 6, 7, 8, 9,10

EIGEN-VALUES No. : 11,12,

FIG. (6.13) THE EFFECT OF FREQUENCY SEPARAT. ON EIGEN-VALUES

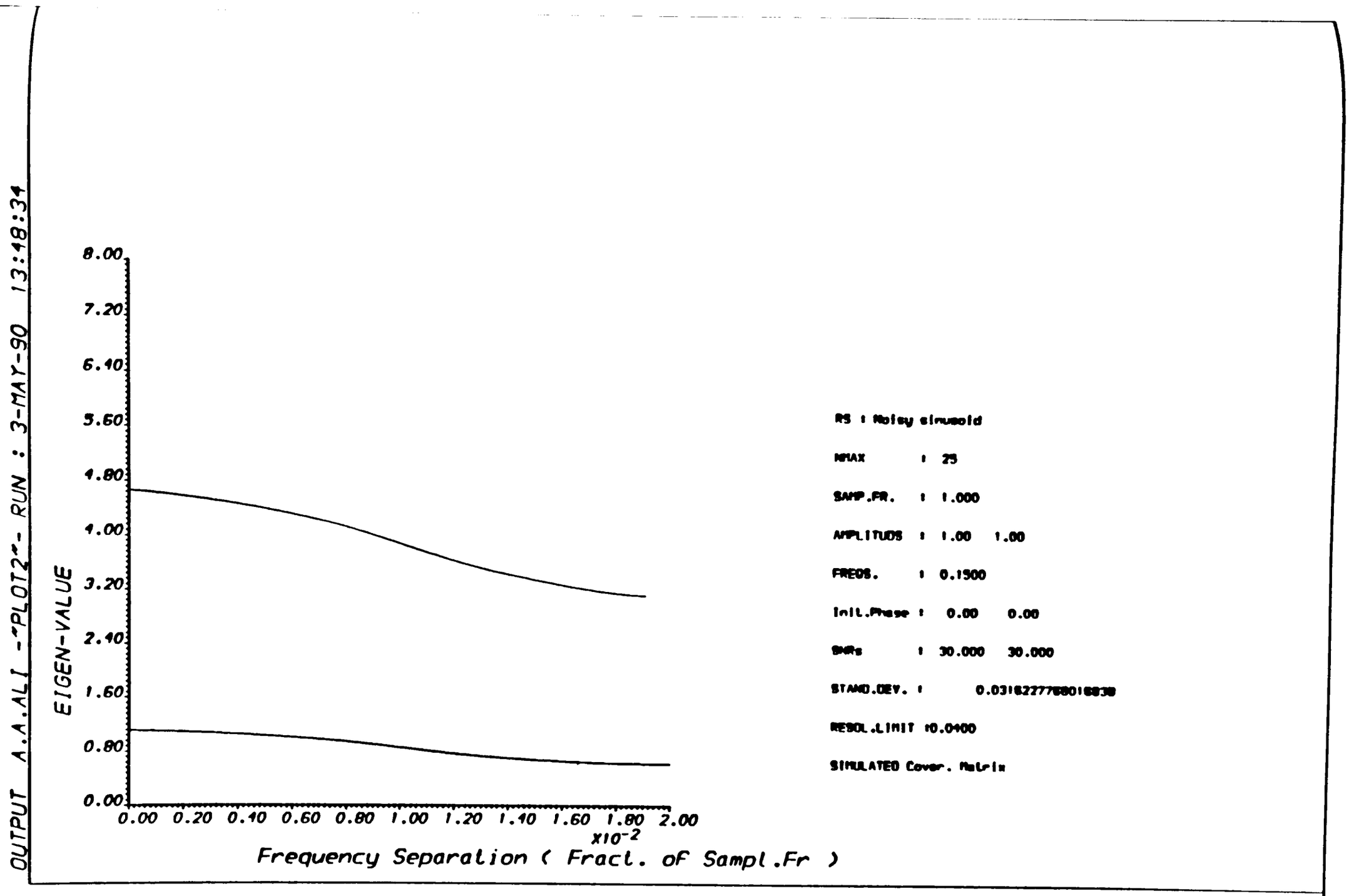

FIG. (6.14) THE EFFECT OF FREQUENCY SEPARAT. ON EIGEN-VALUES
EIGEN-VALUES No. : 10,11,

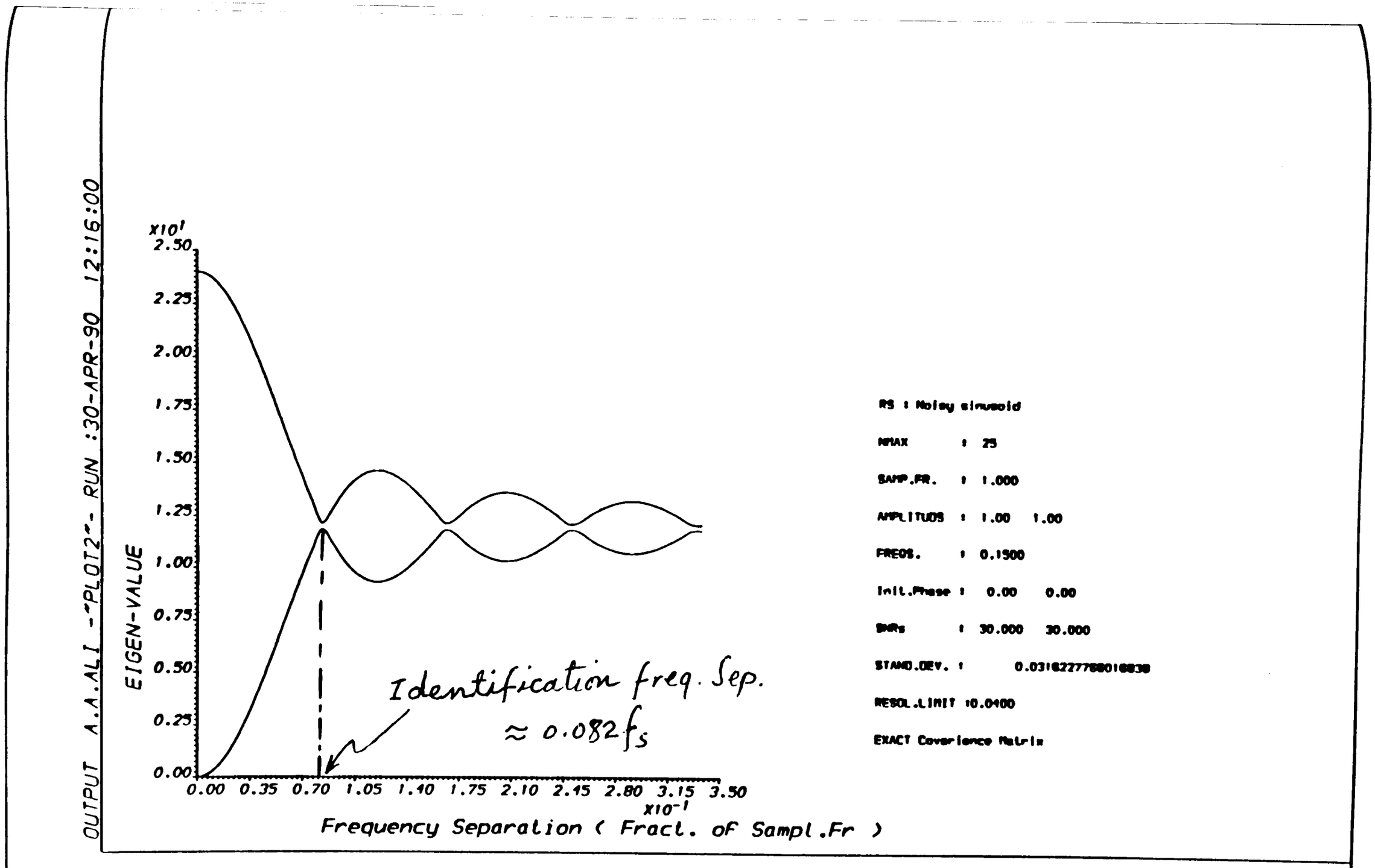

FIG. (6.15) THE EFFECT OF FREQUENCY SEPARAT. ON EIGEN-VALUES
EIGEN-VALUES No. : 12,11,

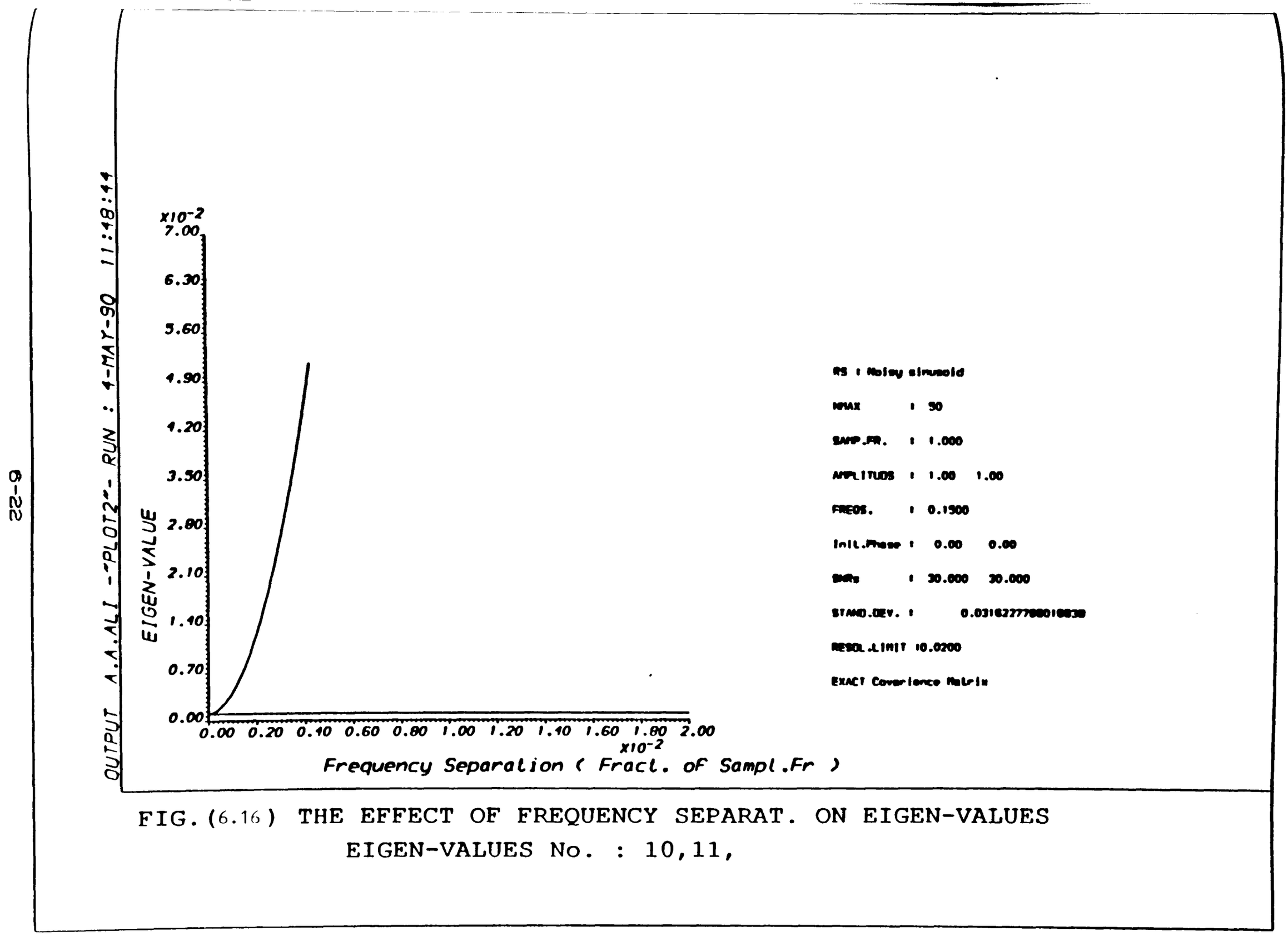

FIG. (6.16) THE EFFECT OF FREQUENCY SEPARAT. ON EIGEN-VALUES
EIGEN-VALUES No. : 10,11,

decorrelation time is clear to be equal to $1/0.08f_s$.

Another point which can be pointed out from these two figures, is that when the two signals had nearly the same frequency, $(0.15f_s)$, *-i.e for approximately zero frequency separation value-*, and for the case of true covariance matrix, the second signal eigen value had a very small value which was equal to the noise eigen values *(0.001dB), -see Fig(6.16)-*. So, in this case, we had only one very large signal eigen value giving rise to one signal to be detected and that confirms what has been said in chapter five, whereas for the estimated covariance matrix case this signal eigen value had a significantly high level *(4.65dB)* when compared with the noise eigen values at zero separation *(1.04dB)* and hence it is expected that two signals will be obtained from the estimates of these approaches which again confirm what has been obtained in chapter five.

6.6. THE EFFECT OF THE RELATIVE PHASE VARIATIONS :

The initial phase of the second signal was changed in steps from *(0 degrees)* to *(360 degrees)* and the signal and noise eigen values were plotted for the case of estimated covariance matrix only, since as was mentioned in chapter five, when the true covariance matrix is used the initial phases and so the relative phase between the two signals have no effects on the estimates.

Fig(6.17) shows the two signal eigen values behaviour, from which the corresponding eigen value reached its minimum level at an initial phase of *90* degrees in which case the two signals were orthogonal. Hence they had no effect upon each other and we can expect that they have the best resolution. As the relative phase increased, this eigen value reached its maximum level at relative phase of *270 degrees* and that explain why the worst resolution have been

obtained, *-see chapter five section (5.2.2.4)-.*

When the first signal was given an initial phase of *60* degrees and *180* degrees the sets of eigen values curves were shifted by those amounts as shown in *Fig(6.18)* and *Fig(6.19)* from which we can decide whether or not the first signal has been assigned an initial phase shift. The amount of phase shift assigned to the first signal can also be calculated from these plots by plotting two horizontal lines, one through the mid-level point of its eigen value curve, and another line at the value on the same eigen value curve corresponding to *180* degrees phase shift. Now, if the two lines coincide, then there must be an initial phase of *0* or *180* degrees being assigned to the first signal, depending upon wheather the eigen value curve is a negative going or positive going sine shape as shown in *Fig(6.17)* and *Fig(6.19)*. On the other hand, if the two lines do not coincide, *see Fig(6.18),* then we read the phase angle corresponding to the intersection between the first line and the eigen value curve, $\Phi_{intersec.}$, and the phase shift of the first signal is calculated as follows;

$$\Phi_1 = 180 - \Phi_{intersec.} \qquad (6.6.1)$$

$$= 180 - 224.8 = 64.8 \text{ degrees}$$

where Φ_1 is the initial phase of the first signal with respect to the observation window.

Other sets of frequencies were used to study the effect of the relative phase variations on the behaviour of the eigen values. *Fig(6.20)* shows that the swing of the eigen values was almost always less when the frequency separation

was increased, *-i.e the amplitude of the swing in the eigen value curve is inversely proportional to the frequency separation between the two signals-*, and that again confirms the effect of the correlation between the two signals which decreases as the frequency separation increases.

PAGE MISSING

Min. Value = 5

Max. Value = 35

Mid. point value = 20.

Calculated phase = 64.8 ≃ 60°

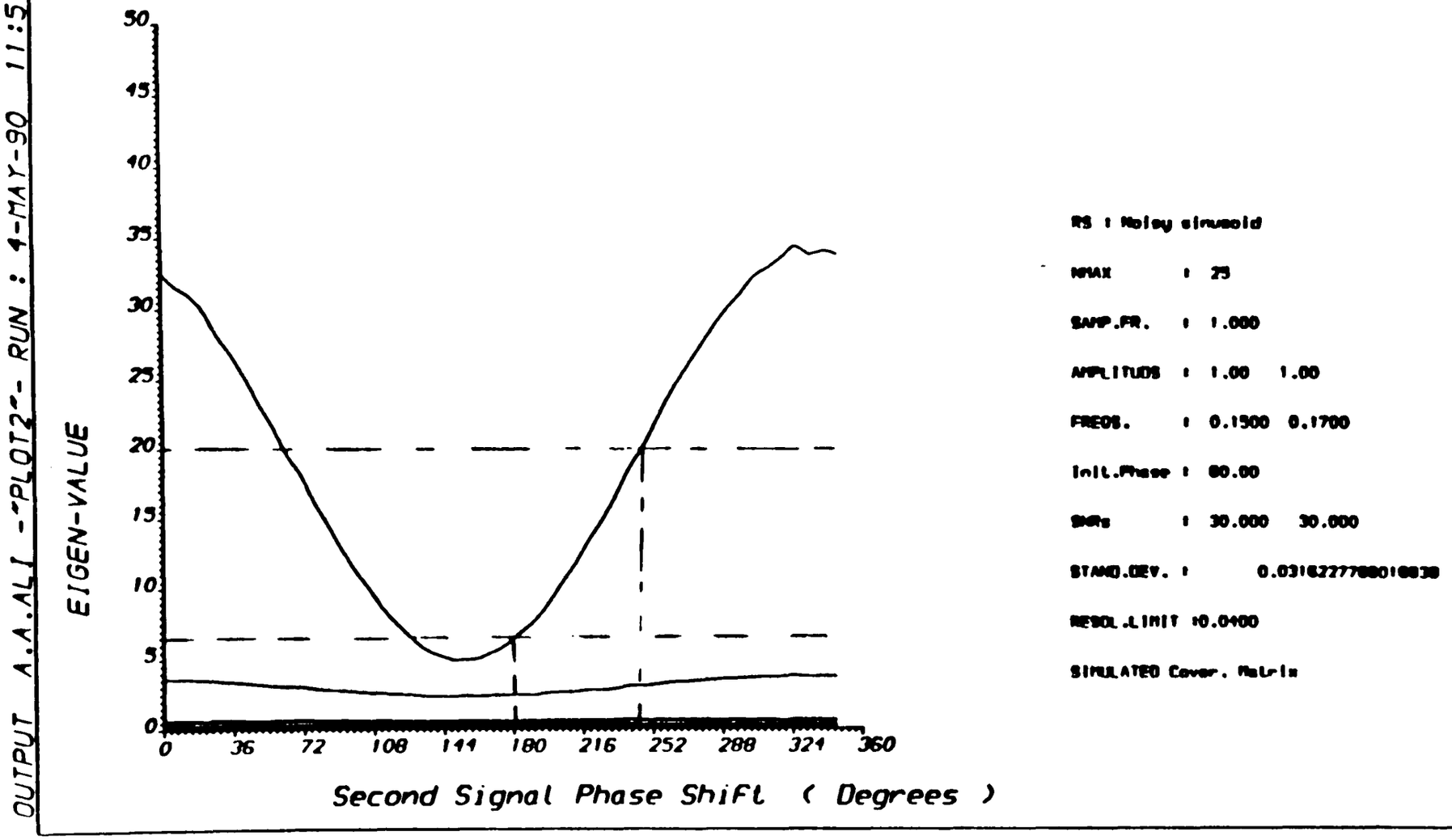

EIGEN-VALUES No. : 1, 2, 3, 4, 5, 6, 7, 8, 9,10

EIGEN-VALUES No. : 11,12,

FIG. (6.18) THE EFFECT OF 2nd SIGNAL PHASE SHIFT ON EIGEN-VALUES

Min. Value = 5.5
Max. Value = 34.5
Mid. Value point = 20
Calculated phase = 180°

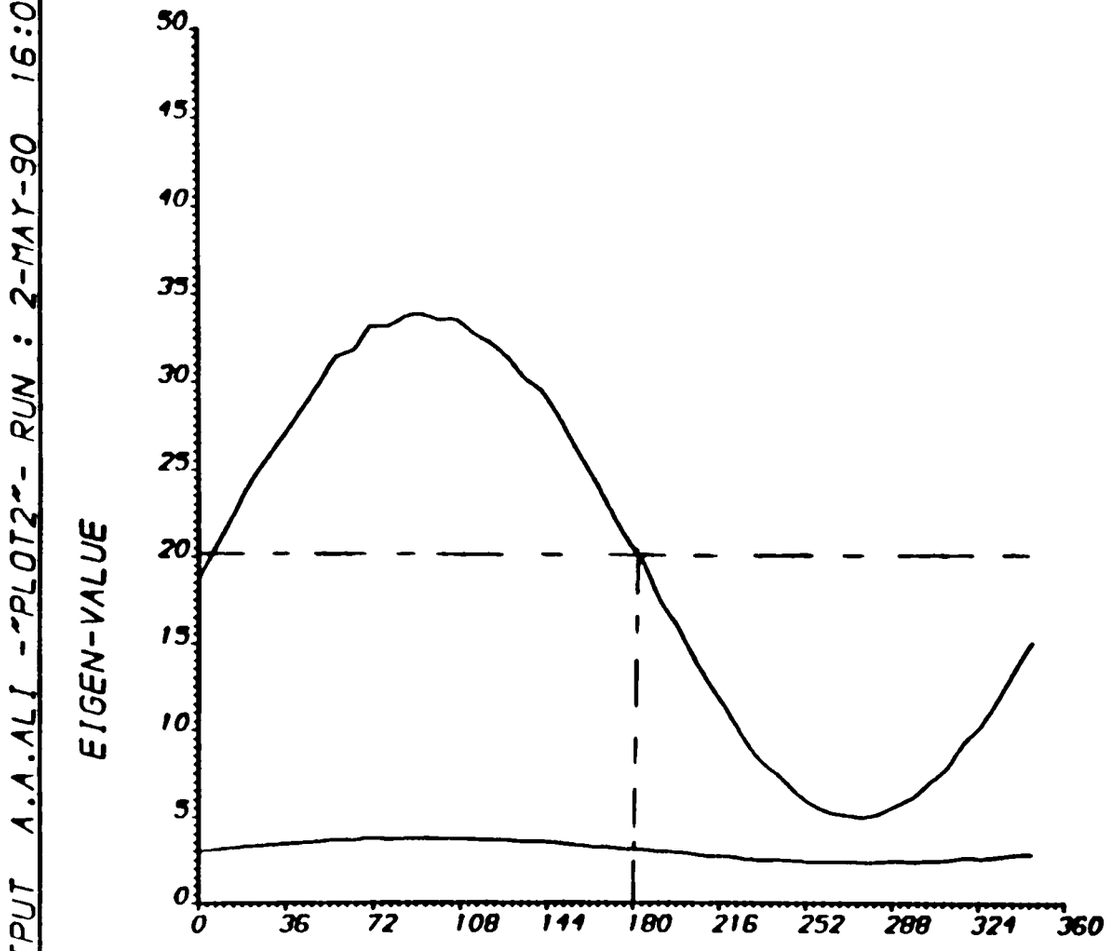

RS : Noisy sinusoid
NMAX : 25
SAMP.FR. : 1.000
AMPLITUDS : 1.00 1.00
FREQS. : 0.1500 0.1700
Init.Phase : 180.00
SNRs : 30.000 30.000
STAND.DEV. : 0.031622776601683
RESOL.LIMIT =0.0400
SIMULATED Cover. Matrix

FIG. (6.19) THE EFFECT OF 2nd SIGNAL PHASE SHIFT ON EIGEN-VALUES
EIGEN-VALUES No. : 11,12,

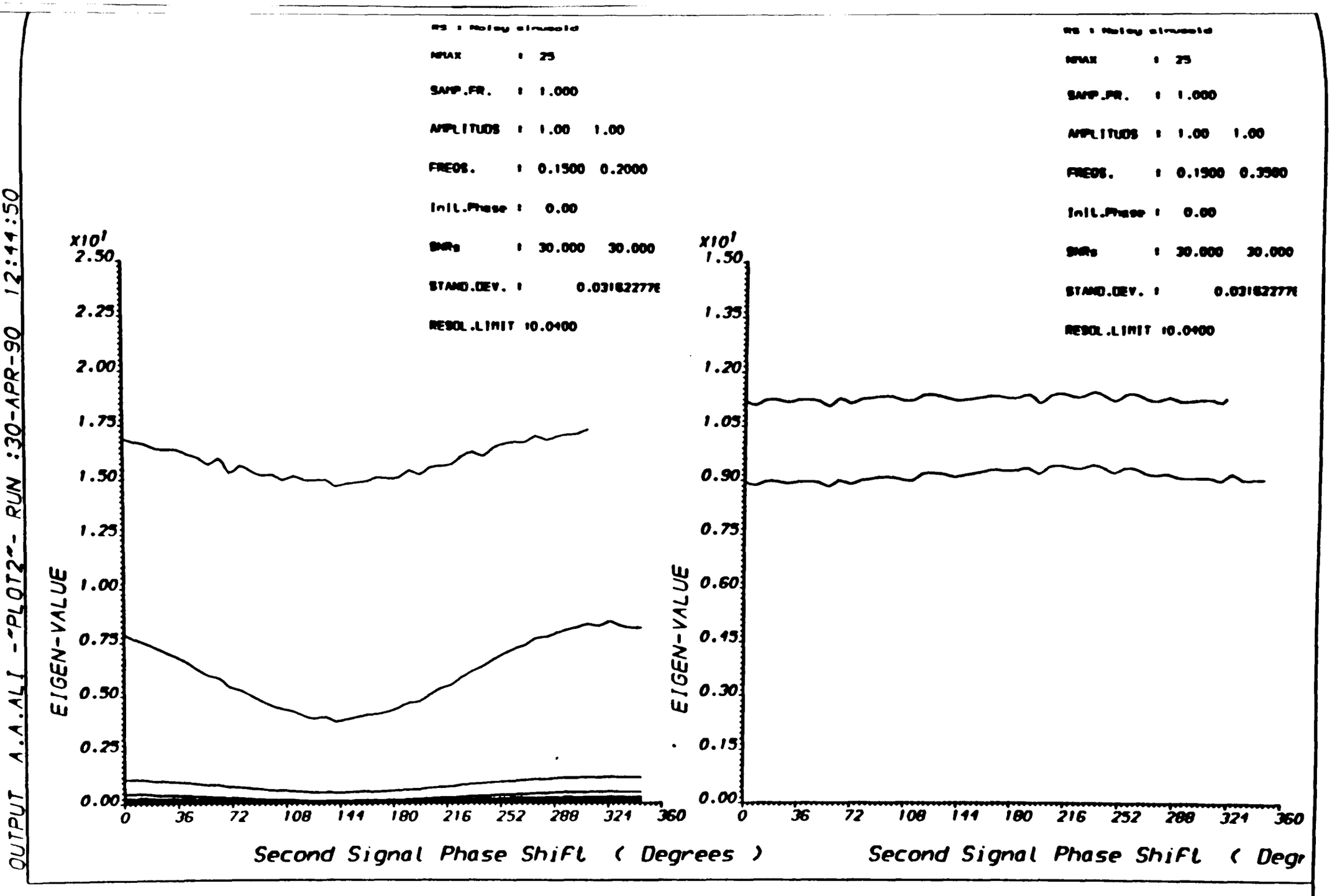

EIGEN-VALUES No. : 1, 2, 3, 4, 5, 6, 7, 8, 9,10

EIGEN-VALUES No. : 11,12,

FIG. (6.20) THE EFFECT OF 2nd SIGNAL PHASE SHIFT ON EIGEN-VALUES

Chapter Seven

CONCLUSIONS AND SUGGESTIONS FOR FURTHER WORK

CHAPTER SEVEN

CONCLUSIONS
AND
SUGGESTION FOR FURTHER WORK

7.1. CONCLUSIONS :

Most of the power spectral density estimates approaches have been examined using computer simulated data during this study. Emphasis has been given to so-called high resolution methods among which the Eigen Vector Decomposition Technique has superior resolution capabilites. A new eigen vector decomposition method has been proposed whose detection and resolution capabilities have been tested for the different circumstances and it proved to have superior performance. Another area where a new method has been suggested as well is the Partitioning of the random process covariance matrix into Signal Subspace and Noise Subspace by separating the signal eigen values from the noise eigen values.

As a result of the intensive computer simulation performed during this study, the following conclusions can be drawn :

1. All the PSD estimators are capable of correctly estimating the frequency of a single signal in white Gaussian noise without any bias and are capable of detecting and resolving multiple signal frequencies with different amounts of bias when a sufficiently long data record is employed.

2. Conventional PSDE methods became computationally efficient with FFT, but they suffer from ambiguities due to the side lobe leakage and their poor resolution capabilities.

3. Parametric PSDE methods have higher detection abilities with better side lobe supression and they possess higher resolution capabilities with significantly small estimation biases when compared with conventional approaches.

4. Non parametric approaches to PSDE, and Eigen Vector Decomposition Technique in particular, possess the highest detectability and resolution capability.

5. In spite of the resolution capabilities of the Modelling approaches and Burg algorithm, they suffer from some practical difficulties such as the order of the filter is not known a priori. Another major problem associated with AR modelling is that it exhibits Spontaneous Line Splitting which is more likely to occur when the SNR is high, the number of coefficients is a large percentage of the data samples, the data length includes some odd number of quarter cycles and the initial phase is an odd multiple of p/4.

6. The Maximum Likelihood Method (MLM) provides direct power estimation but it is unable to resolve two closely separated signals, whereas Maximum Entropy Method (MEM) gives no indication about the actual power of the signal but on the other hand it possesses higher resolution ability than MLM.

7. Methods with best performance are often based on the idea of decomposition of the covariance matrix into its

eigen values and their associated eigen vectors.

8. Intensive study was performed upon MLM, MEM, EVM, and MPCM which proves that EVDT has superior performance due to the lowest SNR threshold value it possesses (>-90dB), the shortest data length -6 or even 4 data samples on condition that the number of signals is known a priori-, with which it can still give a resonable estimate and the minumum frequency separation ($0.002f_s$) between the two signals to be resolved when compared with other approaches to PSDE.

9. Eigen Vector Decomposition Approaches pioneered by Pisarenko suffer from a number of disadvantages such as the number of computations required by the full eigen vector analysis and the evaluation of spectrum using the noise eigen vectors, -except MPCM which uses the signal eigen vectors-, In addition it shares with Pisarenko Harmonic Decomposition (PHD) the practical difficulty related to the actual number of signals, upon which the detection and resolution capabilitites are highly dependent, and which is not normally known a priori. This number, if overestimated, will give spurious frequencies -except in the case of EVM-, and if underestimated it will give highly smoothed spectra.

10. The new proposed method for separating the signal eigen values from the noise eigen values proves its effectivness especially when the true covariance matrix is used.

11. EVDT is capable of resolving the two closely separated signals with no limits to their relative amplitudes ratio when the true covariance matrix is known. on the other hand it is highly affected by the lower ratios

when the estimated covariance matrix is used.

12. Again when the true covariance matrix is used, the detection and resolution capabilities of Eigen Vector decomposition Technique (EVDT) are not affected by the presence of a third strong nearby signal whereas MLM and MEM capabilities are highly affected. On the other hand when the estimated covariance matrix is used, MEM is the less affected estimator.

13. The new proposed method -Modified Principal Components Method (MPCM)- has the best resolution capability among the EVDT approaches especially at low SNR values and short data records.

14. Intensive study was conducted upon the different parameters affecting the behaviour of the eigen values of the covariance matrix from which the following observations can be drawn :

14.1. It is possible to predict the performance of the EVDT from the behaviour of the eigen values of the covariance matrix.

14.2. Data length has a very slight effect on the detection and resolution capabilities of the EVDT and this effect vanishes as the signals become sufficiently separated in frequency.

14.3. The threshold SNR value for the EVDT can be calculated from the Eigen Values vs SNR curves which show that above this SNR value the SNR variation has no effect on the detection and resolution capabilities of the EVDT.

14.4. Eigen Values vs. Frequency Separation curves show exactly how the detection and resolution capabilities of the EVDT improve as the two signals become more and more apart from each other. EVDT reaches its superiority in resolving the two signals when they are separated by more than $Df=1/T_d$, where T_d is the decorrelation time which can be calculated from these curves.

14.5. Finally the initial phase given to one signal can be calculated from the curves of the Eigen Values vs. the Second Signal's Initial Phase Variation. These curves show that the amplitude of the swing associated with the second signal curve is a function of the frequency separation between the two signals.

7.2. SUGGESTION FOR FURTHER WORK :

Since it is the first time that the Space Domain Signal Processing Approaches are being used in the Time Domain Processing, it is of importance to :

A. Implement these algorithms to provide efficient tools in time domain signal processing in terms of computations and implementations especially as we are now facing a revolution in VLSI design and manufacturing and these algorithms have already been implemented in the space domain.

B. Extend the study of the behaviour of the eigen values of the covariance matrix from which we can have more possible prediction and further understanding of the EVDT performance and limitations.

APPENDICES

APPENDIX ONE :

REPRESENTATION OF THE COVARIANCE MATRIX IN TERMS OF ITS EIGEN DATA

Any matrix R can be analysed into its eigen data, and computations involving matrices may be largely simplified by using the two sets of parameters known as eigen values and eigen vectors of the matrix.

Let R be the covariance matrix with dimensions $M \times M$, and V an eigen vector corresponding to the eigen value λ, i.e.

$$\text{for} \quad V \neq 0$$

$$RV = \lambda V \qquad (A1.1)$$

For a typical $M \times M$ matrix R, there will be M such vectors. Equation *(A1.1)* can be rewritten as follows :

$$(R-\lambda I)V = 0 \qquad (A1.2)$$

where I is the Identity matrix. Equation *(A1.2)* has a non zero solution in vector V if and only if the characteristic equation is satisfied;

$$i.e \quad det(R-\lambda I) = 0 \qquad (A1.3)$$

The polynomial equation generated from this characteristic equation written as :

$$f(\lambda) = det(R-\lambda I) \qquad (A1.4)$$

has M roots (λ's) and hence there are M eigen vectors corresponding to these eigen values all satisfying *Equ(A1.1)*, or in other words,

$$RV_i = \lambda_i V_i \qquad \text{for } i=1,2,.....,M \qquad (A1.5)$$

Since the covariance matrix of a stationary time series is almost always positive definite *[23]*, then its eigen values are both real and positive.

Let U be an $M \times M$ matrix formed from the M eigen vectors of R as follows :

$$U = [V_1 \ |V_2 \ |..... \ |V_M] \qquad (A1.6)$$

and Λ be an $M \times M$ diagonal matrix formed by the M eigen values of R as follows :

$$\Lambda = diag[\lambda_1 \ \lambda_2 \ ..... \ \lambda_M] \qquad (A1.7)$$

Now rewrite the set of equations *(A1.4)* in a single matrix form as follows,*[48]* and *[53]* :

$$RU = U\Lambda \qquad (A1.8)$$

and when the eigen values of R are distinct, the corresponding eigen vectors will be orthogonal and hence matrix U, *-formed from these eigen vectors-* is non singular *[23]*.

Multiply both sides of *Equ(A1.8)* by U^{-1}, we get :

$$U^{-1}RU = \Lambda \qquad (A1.9)$$

Now, if U is a unitary similarity matrix, then :

$$\left.\begin{aligned} U^{-1} &= U^{H} \\ U^{H}U &= I \end{aligned}\right\} \quad (A1.10)$$

$$i.e \quad V_i^H V_k = \begin{cases} 1 & for\ i=k \\ 0 & other\ wise \end{cases} \quad (A1.11)$$

and so equation *(A1.9)* can be rewritten as :

$$U^{H}RU = \Lambda \quad (A1.12)$$

Now, since R is hermetian and Λ is diagonal matrix, then *Equ(A1.12)* can be rewritten as :

$$R = U\Lambda U^{H} \quad (A1.13)$$

OR

$$R = \sum_{i=1}^{M} \lambda_i V_i V_i^H \quad (A1.14)$$

APPENDIX TWO :

DERIVATION OF THE OPTIMUM WEIGHT FOR CAPON FILTER

We have the average power output P given by;

$$P = W^H R W \qquad (A2.1)$$

and we wish to minimize this power subject to the constraint;

$$W^T C = 1 \qquad (A2.2)$$

Using *Lagrange's* method, we can perform this minimization subject to the above constraint by defining a cost function as follows :

$$H(W) = P + \lambda(1 - W^T C) \qquad (A2.3)$$

where λ is an arbitrary constant. The minimization can be achieved by differentiating the cost function with respect to W and equating the derivative to zero, but before that let us assume, for generality, that W and C are complex vectors.

$$\left.\begin{aligned} i.e \quad & W = W_r + jW_j \\ and \quad & C = C_r + jC_j \end{aligned}\right\} \qquad (A2.4)$$

which implies two constraints as follows :

$$\left.\begin{aligned} Re[W^T C] &= 1 \\ Im[W^T C] &= 0 \end{aligned}\right\} \qquad (A2.5)$$

and $W^T C = (W_r^T + jW_j^T)(C_r + jC_j)$

$$= [(W_r^T C_r - W_j^T C_j) + j(W_r^T C_j + W_j^T C_j)] \qquad (A2.6)$$

Substituting this result in equation *(A2.3)* gives :

$$H(W) = P + \lambda[(1 - W_r^T C_r + W_j^T C_j) + j(W_r^T C_j + W_j^T C_r)] \qquad (A2.7)$$

The derivatives of P with respect to W_r and W_j are given by, *[48];*

$$\left.\begin{aligned} -\frac{\partial P}{\partial W_r} &= 2RW_r \\ -\frac{\partial P}{\partial W_j} &= 2RW_j \end{aligned}\right\} \qquad (A2.8)$$

So

$$\frac{\partial H(W_r)}{\partial W_r} = 2RW_r - \lambda(C_r - jC_j)$$

Equating the derivative to zero will give :

$$RW_r = \beta C^* \qquad (A2.9)$$

whre $\beta = \lambda/2$, is a constant.

and

$$\frac{\partial H(W_j)}{\partial W_j} = 2RW_j + \lambda(C_j + jC_r) = 0$$

$$Or \qquad RW_j = -\beta(C_j + jC_r) \qquad (A2.10)$$

Multiply both sides of *Equ(A2.10)* by the operator j will give :

$$jRW_j = \beta(C_r - jC_j) = \beta C^* \qquad (A2.11)$$

Combining equation *(A2.9)* and *(A2.11)* yields;

$$R(W_r + jW_j) = 2\beta C^*$$

$$or \qquad W_0 = \lambda R^{-1} C^* \qquad (A2.12)$$

$$and \qquad \lambda = constant = \frac{W_0}{R^{-1}C^*} \qquad (A2.13)$$

Multiply numerator and denominator of equation *(A2.13)* by C^T gives :

$$\lambda = \frac{C^T W_0}{C^T R^{-1} C^*} = \frac{1}{C^T R^{-1} C^*} \qquad (A2.14)$$

Substituting this value of λ in equation *(A2.12)* gives us the expression for the optimum weight as follows :

$$W_0 = \frac{R^{-1} C^*}{C^T R^{-1} C^*} \qquad (A2.15)$$

APPENDIX THREE :

1. LIST (3A.1) DATA RECORD OF ONE OF THE EXAMPLES USED IN TESTING THE DIFFERENT PSD ESTIMATION APPROACHES

```
NMAX         :  25
AMPLITUDS    :  1.00
FREQS.       :  0.2500
Init.Phase   :  0.00
SNRs ( dB ):  10.000
STAND.DEV.   :  0.3162277660168379
```

THE RANDOM PROCESS DATA SAMPLES :

```
Y(  0)=    0.1169593901160930D+01     0.6840502296968759D+00
Y(  1)=    0.4088306096275958D+00     0.1120480466941184D+01
Y(  2)=   -0.5003481413754939D+00     0.1318681167934090D+00
Y(  3)=   -0.8397240154769703D-02    -0.8477784492382966D+00
Y(  4)=    0.1479623355257666D+01     0.8753906370500357D-01
Y(  5)=   -0.1363086228548691D+00     0.1110139547023519D+01
Y(  6)=   -0.1243574940667354D+01     0.4836430175256730D+00
Y(  7)=    0.7414422010868044D-01    -0.8909489328601006D+00
Y(  8)=    0.1064621103096803D+01    -0.3016755283664857D+00
Y(  9)=   -0.4586941320239497D+00     0.1009639590877976D+01
Y( 10)=   -0.9810290259229588D+00     0.5057804559784573D+00
Y( 11)=    0.4891349243872809D+00    -0.1397039850903806D+01
Y( 12)=    0.1869861322366330D+01    -0.3861102031574317D+00
Y( 13)=    0.1917264741266617D+00     0.1058091967040075D+01
Y( 14)=   -0.1186377284318899D+01    -0.4895825204484141D+00
Y( 15)=   -0.5019215499138587D-01    -0.8397691370132612D+00
Y( 16)=    0.1441402331510620D+01     0.1129023447591659D+00
Y( 17)=   -0.2723283750898396D+00     0.1043549397963129D+01
Y( 18)=   -0.8710588596937930D+00    -0.4927149606409684D+00
Y( 19)=    0.1042464774287496D+00    -0.1029957891621009D+01
Y( 20)=    0.1028242218859698D+01    -0.4230550455120892D+00
Y( 21)=   -0.3666542008460105D+00     0.9550033681737977D+00
Y( 22)=   -0.6629669576514922D+00    -0.2861423056190439D+00
Y( 23)=    0.1982934152625639D+00    -0.1115733180063233D+01
Y( 24)=    0.8957972011246392D+00     0.4403240312434403D+00
```

2. LIST (A3.2) DATA RECORD OF ONE OF THE EXAMPLES USED IN TESTING THE DIFFERENT PSD ESTIMATION APPROACHES.

```
NMAX         :  64
AMPLITUDS    :  1.00    1.00
FREQS.       :  0.1500  0.1700
Init.Phase   :  0.00    0.00
SNRs ( dB ):  30.000    30.000
STAND.DEV.   :  0.03162277660168 38
```

THE RANDOM PROCESS DATA SAMPLES :

```
Y(  0)=    0.2016959390116093D+01     0.4868845916827514D-02
Y(  1)=    0.1110421944463016D+01     0.1639862940921318D+01
Y(  2)=   -0.7948787035710714D+00     0.1757589602762366D+01
Y(  3)=   -0.1949923000566816D+01     0.2140648611807693D+00
Y(  4)=   -0.1186833781171865D+01    -0.1515327503957802D+01
Y(  5)=    0.5741546632319198D+00    -0.1784167100773452D+01
Y(  6)=    0.1776774271764900D+01    -0.4846469417340772D+00
Y(  7)=    0.1326595210205865D+01     0.1259429011374204D+01
Y(  8)=   -0.3219452678299701D+00     0.1745522365790193D+01
Y(  9)=   -0.1615942017717774D+01     0.5773803518917667D+00
Y( 10)=   -0.1307119614277589D+01    -0.9822210833550901D+00
Y( 11)=    0.1456757697343562D+00    -0.1523190764133853D+01
Y( 12)=    0.1364586498354627D+01    -0.6723307245186435D+00
Y( 13)=    0.1218918838787446D+01     0.6635445774717297D+00
Y( 14)=    0.6141013783893589D-01     0.1311926618118088D+01
Y( 15)=   -0.9560760529866569D+00     0.7262144521861759D+00
Y( 16)=   -0.9522578553053381D+00    -0.4706355187748880D+00
Y( 17)=   -0.2077755768491726D+00    -0.9448276874761083D+00
Y( 18)=    0.6336538575646932D+00    -0.5931474488194823D+00
Y( 19)=    0.7235428933911255D+00     0.1688200963725736D+00
Y( 20)=    0.1938068780874848D+00     0.6026679018640262D+00
Y( 21)=   -0.3537073082703259D+00     0.4141531487162449D+00
Y( 22)=   -0.3381041057877947D+00    -0.1594102677560550D-01
Y( 23)=   -0.8689916989154436D-01    -0.2111371414181077D+00
Y( 24)=    0.5686943209071950D-01    -0.7118425285088646D-01
Y( 25)=    0.6840493554690848D-01    -0.7309643150080884D-02
Y( 26)=   -0.5524161047293137D-01    -0.1144852483453694D+00
Y( 27)=    0.1199156224153166D+00    -0.2211910897750290D+00
Y( 28)=    0.3870298011932669D+00    -0.1459772938039198D-01
Y( 29)=    0.3257954407555460D+00     0.3834992643548132D+00
Y( 30)=   -0.1799695750580820D+00     0.6163854711596512D+00
Y( 31)=   -0.6647544142908430D+00     0.1770033678532650D+00
Y( 32)=   -0.6098539367618552D+00    -0.5511129165291451D+00
Y( 33)=    0.1503765784020853D+00    -0.9101769234062238D+00
Y( 34)=    0.9973627366193897D+00    -0.3757572271763690D+00
Y( 35)=    0.1001634009144668D+01     0.7366112594188643D+00
Y( 36)=   -0.1197536395137847D+00     0.1264744693875607D+01
Y( 37)=   -0.1238358241587942D+01     0.6181013097480524D+00
Y( 38)=   -0.1271790291852934D+01    -0.6690850013025907D+00
Y( 39)=   -0.1457183719453044D+00    -0.1568904111950104D+01
Y( 40)=    0.1325041211431293D+01    -0.9698313663087803D+00
Y( 41)=    0.1581362025978306D+01     0.6005573046462739D+00
Y( 42)=    0.3327599256486645D+00     0.1765873459981662D+01
Y( 43)=   -0.1368454023224522D+01     0.1261971955938591D+01
```

```
Y( 44)=   -0.1804126970473755D+01    -0.4299200430336004D+00
Y( 45)=   -0.6300885819427308D+00    -0.1838808402227356D+01
Y( 46)=    0.1230298569043825D+01    -0.1511253238302535D+01
Y( 47)=    0.1920468817130985D+01     0.1962136253022328D+00
Y( 48)=    0.8332680694368833D+00     0.1817676114194283D+01
Y( 49)=   -0.1025508944164658D+01     0.1689347069969490D+01
Y( 50)=   -0.1985093169166847D+01    -0.2483149482723509D-01
Y( 51)=   -0.1087447923549667D+01    -0.1686464246947114D+01
Y( 52)=    0.8745455172469823D+00    -0.1814609169021447D+01
Y( 53)=    0.1894206357175859D+01    -0.2909216638835036D+00
Y( 54)=    0.1347501829000117D+01     0.1439679111186081D+01
Y( 55)=   -0.5534832606437060D+00     0.1814421222204194D+01
Y( 56)=   -0.1831266268875273D+01     0.4633049700921898D+00
Y( 57)=   -0.1336551877809709D+01    -0.1286318973352527D+01
Y( 58)=    0.4125064776845405D+00    -0.1696169806285736D+01
Y( 59)=    0.1572242683432001D+01    -0.6356809988250748D+00
Y( 60)=    0.1294660647399386D+01     0.9756929399937595D+00
Y( 61)=   -0.1340252583405900D+00     0.1560779111380152D+01
Y( 62)=   -0.1246737313560013D+01     0.7298868314670107D+00
Y( 63)=   -0.1208851859441751D+01    -0.6535904428276002D+00
```

REFERENCES

REFERENCES

[1] *AKAIKE, H.* "A New Look at the Statistical Model Identification". IEEE Transaction on Automatic Control, Vol.19, pp.716-723, 1974.

[2] --------- "Information Theory and an Extension of the Maximum Likelihood Principles". Proceeding 2nd Int. Symp. Inform. Thy. Supp. to problems of Control and Inform. Thy, pp.267-281, 1973.

[3] *BAYGIN, B. and YALCIN, T.* "Performance Analysis of MUSIC Algorithm in Direction Finding Systems". ICASP 1989 Glasgow, CH2673-2/89/0000-2298 IEEE.

[4] *BLACKMAN, R.B. and TUKEY, J.W.* "The Measurement of Power Spectra from the Point of view of Communication Engineering". New York, Dover 1959.

[5] *BRIGHAM, O.* "The Fast Fourier Transform". Englewood Cliffs, NJ: Prentice-Hall, 1974.

[6] *BURG, J.P.* "Maximum Entropy Spectral Analysis". PhD dissertation, Dept. Geophysics, Stanford univ., Stanford, CA, May 1975.

[7] *CADZOW, J.A.* "Spectral Estimation : An Overdetermined Rational Model Equation Approach". Proceeding of the IEEE, vol.70, No.9, Sept. 1982.

[8] --------- "ARMA Spectral Estimation; An Efficient Closed Form Procedure". Proceeding of RADC spectum estimation workshop, pp.81-97, Oct. 1979.

[9] *CAPON, J.* "High Resolution Frequency - Wavenumber - Spectrum Analysis". Proc. of the IEEE, vol.57, pp.1408-1418, Aug. 1969.

[10] *CHOW, J.C.* "On the Estimation of the Order of the Moving-Average Process". IEEE Trans. on Automatic Control, vol. AC-17, pp.386-387, June 1872.

[11] *DAREL, A.L. and RONALD, D.D.* "A Statistical Measure of Resolution for Modern Direction Finding Methods" ICASP 1989 Glasgow, CH2673-2/89/0000-2121 1989 IEEE.

[12] *DeGRAAF, S.R. and JOHNSON, D.H.* "Capability of Array Processing Algorithms to Estimate Source Bearings". IEEE Trans. on ASSP, vol.ASSP-33, No.6, Dec. 1985.

[13] *DURBIN, J.* "The Fitting of Time Series Models". Rev.Inst. Int. de state, vol.28, pp.233-244, 1960.

[14] *DURRANI, T.S. and SHARMASN, K.C.* "Eigenfilter Approaches to Adaptive Array Processing". IEE Proc., vol.130, pt. F and H, No.1, Feb. 1983.

[15] *FOUGERE, P.F., ZAWALICH, E.J. and RADOSKI, H.R.* "Spontaneous Line Splitting in Maximum Entropy Power Spectral Analysis". Physics Earth Planetary Interiour, vol.12, pp.201-207, Aug. 1976.

[16] *FOUGERE, P.F.* "A Solution to the Problem of Spontaneous Line Splitting in maximum Entropy Power Spectrum analysis". J. Geophysical Res., vol.82, pp.1051-1054, Mar. 1977.

[17] *FRIEDLANDER, B.* "Efficient Algorithms for ARMA Spectral Estimation". Proc.of the IEEE, vol.130, pt.f, pp.195-201, Apr. 1983.

[18] *GABRIEL, W.F.* "Spectral Analysis and Adaptive Array Super resolution Techniques". Proc. of the IEEE, vol.6, pp.661-175, 1968.

[19] *GRAY, D.A.* "Theoretical and Experimental Comparison of Optimum Elements, Beam and Eigen Space Array Processors". NATO ASIS on underwater signal processing in 1984.

[20] *GRIFFITHS, J.W.R.* "Adaptive Array Processing A tutorial" IEE proc., vol.130, pts F and H, No.1, Feb. 1983.

[21] *GROUPE, D., KRAUSE, D.J. and MOOR, J.B.* "Identification of Autoregressive Moving Average Parameters of Time Series". IEEE Trans. on Automat. Cont., vol. AC-20, pp.104-107, Feb. 1975.

[22] *HARRIS, F.J.* "On the Use Of Windows for Harmonic Analysis with Discrete Fourier Transform". Proc. of the IEEE, vol.66, pp.51-83, Jan. 1978.

[23] *HAYKIN, S.* "Introduction to Adaptive Filters". MacMillan Publishing Company, New York.

[24] *IBRAHIM, M.K.* "Improvement in the Speed of the Data-Adaptive Weigted Burg Technique". IEEE Trans. on ASSP, vol. ASSP-35, No.10, pp.1474-1476, Oct. 1987.

[25] -------- "On Line Splitting in the Tapered Burg Algorithm". Same Ref. above, pp.1476-1479.

[26] *JENKINS, G.M. and WATTS, D.G.* "Spectral Analysis and its Applications". San francisco, CA, Holden-Day 1968.

[27] *JOHNSON, D.H. and DeGRAAF, S.R.* "Improving Resolution of Bearings in Passive Sonar Arrays". IEEE Trans. on ASSP, vol. ASSP-30, No.4, Aug. 1982.

[28] *JONES, D.L. and PARKS, T.W.* "A Resolution Comparison of Several Time Frequency Representations". ICASP-1989 Glasgow, CH22673-2/89/0000-2222, IEEE.

[29] *KARHUNEN, J.* "Recursive Estimation of Eigen Vector of Correlation Type Matrices for Signal Processing Applications". Doctor of Technology thesis, Helsinki Univ. of Technology, Dept. of Tech. physics, ESP00,

Finland.

[30] *KAVEH, M.* "High Resolution Spectral Estimation of noisy Signal". IEEE Trans. on ASSP, vol. ASSP-27, No.3, June 1979.

[31] *KAVEH, M. and LIPPERT, G.A.* "An Optimum Tapered Burg Algorithm For Linear Prediction And Spectral Analysis". IEEE Trans. on ASSP, vol. ASSP-31, pp.438-444, Apr. 1983.

[32] *KAY, S.M.* "The Effect Of Noise On The Autoregressive Spectral Estimate". IEEE Trans. on ASSP, vol ASSP-27, No.5, Oct. 1979.

[33] *KAY, S.M. and MARPLE, S.L.* "Spectum Analysis - A Modern Perspective". Proceedings of the IEEE, vol.69, No.11, Nov. 1981.

[34] *LACOSS, R.T.* "Data Adaptive Spectral Analysis Methods".Geophysics, vol.36, No.4, pp.661-675, Aug. 1971.

[35] *MARPLE, S.L.* "A New Autoregressive Spectrum Analysis Algorithm". IEEE Trans. on ASSP, vol. ASSP-28, No.4, August 1980.

[36] -------- "Conventional, Fourier, Autoregressive and Special ARMA Methods of Spectral Analysis". Stanford Univ., Stanford, CA, Dept. Elect. Eng., Dec. 1976.

[37] -------- "Frequency Resolution of High Resolution Spectrum Analysis Techniques". Proc. of RADC Spectrum Estimation Workshop, pp.19-35,

1978.

[38], *McCLELLAN, J.H.* "Multidimentional Spectral Estimation". Proc. of the IEEE, vol.70, No.9, Sept.1982.

[39] *McDONOGH, R.N. and HUGGINS, W.H.* "Best Least-Square Representations of Signals by Exponentials". IEEE Trans. on Automatic control, vol. AC-13, pp.408-412, Aug. 1968.

[40] *NIKIAS, C.L. and RUGHUVEER, M.R.* "Bispectrum Estimation; A Digital Signal Processing Framework". Proc. of the IEEE, vol.75, No.7, July 1987.

[41] *NUTTAL, A.H.* "Spectral Estimation of a Univariate Process with Bad Data Points, via Maximum Entropy and Linear Prediction". Naval Underwater System Center, Tech. Rep. 5303, New London CT, Mar.26, 1976.

[42] *PARZEN, E.* "Mathematcical Considerations in the Estimation of Spectra". Technometrics, vol.3, pp.167-190, May 1961.

[43] ------- "Statistical Spectral Analysis - Single Channel Case in 1968". Dept. Statistics, stanford Univ., stanford, CA, Tech. rep. 11, Jun. 10, 1968.

[44] *PEYTON, Z. and PEEBLES, Jr.* "Probability, Random Variables, and Random Signal Principles". Sec. Edition, CH.6, pp.152-154, McGraw-Hill Book Company.

[45] *PISARENKO, V.F.* "The Retrieval of Harmonics from a Covariance Function". Geophysics J. R. Astr. Soc. (1973), 33, pp.347-366.

[46] -------- "On the Estimation of Spectra by Means of Non-Linear Functions of the Covariance Matrix". Geophys. J. R. Astr. Soc. (1972), 28, pp.511-531.

[47] *RISSANEN, J.* "Modelling by Shortest Data Description". Automatica, vol.14, pp.465-471, 1978.

[48] *SABBAR, B.M.* "High Resolution Array Signal Processing". Doctoral thesis, 1987, Dept. of Electronic and Electrical Engineering, Loughborough Univ., U.K.

[49] *SCHWARTZ, G.* "Estimating the Dimension of the Model". Ann. of State, vol.6, pp.461-464, 1978.

[50] *SHARMAN, K.C. and DURRANI, T.S.* "Spatial Lattice Filter for High Resolution Spectral Analysis". Proc. of the IEE, vol.130, pt. F, No.3, Apr. 1983.

[51] *SCHMIDT, R.* "Multiple Emitter Location and Signal parameter Estimation". Proc. RADC Spectral Estimation Workshop, pp.243-258, Rome, NY, 1979.

[52] *SRINAVSAN T., SWANSON, D.C. and SYMONS, F.W.* "ARMA Model Order/Data Length Tradoff For Specified Frequency Resolution". Proc. of

the IEEE ICASP 1984,ASSP, CH1945-5/84/0000-0413.

[53] *STEPHENSON G.* "An Introduction to Matrices, Sets and Groups for Science Students". Longman Group ltd., London and Harlow ISBN 0582 44426 6, 1974.

[54] *ULRYCH, T.J. and CLAYTON, R.W.* "Time Series Modelling and Maximum Entropy". Phys. Earth Planetary Interiours, vol.12, pp.188-200, Aug. 1978.

[55] *WAX, M. and KAILATH, T.* "Determination of the Number of Signals by Information Theoretic Criteria". Proc. of the ASSP Spectral Estimation Workshop pp.192-196, Nov. 1983.

[56] *WHITMAN, E.C.* "The Spectral Analysis of Discrete Time Series in Terms of Linear Regressive Models". Naval Ordnance Labs. Rep. NOLR-70-109, White Oak, MD, June 23, 1974.

[57] *ZOHAR, S.* "FORTRAN Subroutines for the Solution of Toeplitz Sets of Linear Equations". IEEE Trans. on ASSP, vol. ASSP-27, pp.656-658, Dec. 1979.